REGULATION OF SYNAPTIC VESICLE TRAFFICKING AT CENTRAL SYNAPSES

APPROVED BY SUPERVISORY COMMITTEE

Ege T. Kavalali, Ph.D.

Ilya Bezprozvanny, Ph.D.

Donald W. Hilgemann , Ph.D.

Jose Rizo-Rey , Ph.D.

To my dear family
for their endless support and unwavering trust

REGULATION OF SYNAPTIC VESICLE TRAFFICKING AT CENTRAL SYNAPSES

By

CHIHYE CHUNG

DISSERTATION

Presented to the Faculty of the Graduate School of Biomedical Sciences

The University of Texas Southwestern Medical Center at Dallas

In Partial Fulfillment of the Requirements

For the Degree of

DOCTOR OF PHILOSOPHY

The University of Texas Southwestern Medical Center at Dallas

Dallas, Texas

July, 2009

In the search for new laws, you always have the psychological excitement of feeling that possibly nobody has yet thought of the crazy possibility you are looking at right now.

Richard P. Feynman (1918-1988)

REGULATION OF SYNAPTIC VESICLE TRAFFICKING AT CENTRAL SYNAPSES

Publication No._____

CHIHYE CHUNG, Ph.D.

The University of Texas Southwestern Medical Center at Dallas, 2009

Supervising Professor:
EGE T. KAVALALI, Ph.D.

Synapses are where electrical information is converted to chemical signaling, allowing for careful regulation of inter-neuronal communication in the brain. At presynaptic terminals, synaptic vesicles fuse with plasma membrane in response to electrical stimulation, followed by rapid retrieval to the terminal and re-organization for reuse. Thus, synaptic vesicle trafficking is of interest as to where presynaptic regulations of synaptic transmission begins to occur.

The first two chapters explored a novel secretagogue, lanthanum (La^{3+}), and its potential usage as a probe to study vesicle recycling at central synapses. Chapter two describes the characteristics of La^{3+} -evoked transmission at hippocampal synapses. La^{3+} has two separate actions on transmission, with a different time course and underlying mechanism of action. This newly characterized rapid action of La^{3+} is intracellular Ca^{2+} –independent, in contrast to its delayed action, yet requires functional SNARE complex formation. Therefore, chapter three took advantage of La^{3+}-evoked transmission as a tool to investigate the coupling between exo- and endocytosis in SNARE-dependent fusion. Using multifaceted approaches, I propose that La^{3+} induces transmitter release via narrow fusion pore opening and closure, or a 'kiss-and-run' mode of exo- and endocytosis.

Chapter four investigates the molecular requirement for the synaptic vesicle recycling pathway. I analyzed the impact of one of main players in endocytosis, dynamin in different forms of release. Acute inhibition of dynamin in central synapses impairs activity-dependent synaptic vesicle recycling while leaves spontaneous recycling intact, suggesting the operation of two parallel recycling pathways in central synapses as well as proposing the molecular signature between spontaneously and activity-dependently recycling pathways.

In chapter five, I further investigated the origins of spontaneously recycling synaptic vesicles by simultaneous monitoring of spectrally separable

FM dyes, as chapter suggested four that they are originated from an isolated pool. This chapter includes comprehensive analysis of the endocytic pathway operating at rest and its molecular participants –specifically dynamin, which was implicated to play a role in the endocytic pathway from observations I made in chapter four.

Chapter six expands the investigation as to how presynaptic signaling regulates synaptic vesicle trafficking in glutamatergic synapses. I focused on the impact of ambient glutamate concentration on vesicle recycling as a feedback signal to rapid synaptic reuse to impact short-term synaptic plasticity.

Taken together, these results suggest that synaptic vesicle trafficking is an actively regulated process, impacting various aspects of information cascades between neurons.

ACKNOWLEDGEMENT

I would like to thank a number of people, without whom this work would not have been possible. First and foremost, I would like to thank my doctoral studies mentor Ege Kavalali, who I can not respect enough. His contribution to my growth and training requires no elaboration. He has held the highest expectations for me from the first day we met and his expectation has been my best motivation. To describe all of what I have learned from him is beyond my ability. Ege, who cites Eliot drinking morning coffee, is not afraid of opening new doors with his keen insight into surmises and dogmas. His contagious enthusiasm and faith in science inspired me and helped me to shape my future. I am extremely grateful to have him as a mentor and share all the literature and music, as well as good times and less good times.

My dissertation committee has also contributed to my achievement. Drs. Ilya Bezprozvanny, Don Hilgemann and Jose Rizo-Rey have been constructively critical and generously supportive to my work, and thus my committee meetings were always enjoyable events which I was looking forward to.

I remember several professors who have changed the direction of my life: Dr. Bong-Kiun Kaang introduced me the exciting realm of neuroscience and Dr. Hee Byung Park inspired me in many ways, especially when I was lost between literature and biology. I am also very thankful to have encountered Dr. Min Whan Jung and Sungchil Yang, who opened my eyes to the beauty and charm of electrophysiology.

I am indebted to former and present members of the Kavalali Lab for their help and support over the years. They certainly contributed a lot to my development. Besides their support and care, Tuhin and Mert taught me how to do patch clamp recordings and Catherine trained me in making cultures. Deniz Atasoy, Waseem Aktar, Jesica Raingo, Elena Nosyreva and Mikhail Khvochtchev deserve my great appreciation for their invaluable sage advice and many stimulating discussions. A lot of people helped me to develop my research. Jeremy constantly provided cultures and Dr. Xinran Liu provided his expertise on electron micrography. I borrowed the expertise of Dr. Barbara Barylko on dynamin activity assay. Drs. Megumi Adachi and Lisa Monteggia greatly helped me with taking care of transgenic mice. I would like to thank Amy Arguello for taking the time to critically read this manuscript.

I have met great friends during my graduate school, who made me relish days in Dallas. I owe my deepest gratitude to Amy, Emin, Euiseok, Melissa, Umar and Junghwan for sharing all my excitement and more importantly, all the frustration throughout my graduate school. Without their support and encouragement, I would not have been able to get through everything. I am also thinking of my friends in Korea and over the US who I know have always supported me.

Last but not the least, I would like to thank to my family, especially my mom, dad, Heenae and Jihoon for their constant encouragement and unconditional love. They have been showed enormous support to whatever I do. If I have achieved anything, it is all thanks to unwavering trust and devoted support from my family.

TABLE OF CONTENTS

PRIOR PUBLICATIONS

Chung C, Kavalali ET., Synaptic vesicle endocytosis: Get two for the price of one? *Neuron*. 2009 Feb;61(3):333-334.

Atasoy D, Ertunc M, Moulder KL, Blackwell J, **Chung C**, Su J, Kavalali ET., Spontaneous and evoked glutamate release activates two populations of NMDA receptors with limited overlap., *J Neurosci.* 2008 Oct 1;28(40):10151-66.

Chung C, Deák F, Kavalali ET., Molecular substrates mediating lanthanide-evoked neurotransmitter release in central synapses., *J Neurophysiol.* 2008 Oct;100(4):2089-100.

Ertunc M, Sara Y, **Chung C**, Atasoy D, Virmani T, Kavalali ET., Fast synaptic vesicle reuse slows the rate of synaptic depression in the CA1 region of hippocampus. *J Neurosci*. 2007 Jan 10;27(2):341-54.

Chung C, Kavalali ET., Seeking a function for spontaneous neurotransmission. *Nat Neurosci*. 2006 Aug;9(8):989-90.

Yang S, Lee DS, **Chung CH**, Cheong MY, Lee CJ, Jung MW., Long-term synaptic plasticity in deep layer-originated associational projections to superficial layers of rat entorhinal cortex. *Neuroscience.* 2004;127(4):805-12.

LIST OF FIGURES

CHAPTER ONE: INTRODUCTION

CHAPTER TWO: La^{3+} AS A PROBE TO STUDY SYNAPTIC VESICLE EXOCYTOSIS

CHAPTER THREE: La^{3+} AS A PROBE TO STUDY SYNPATIC VESICLE ENDOCYTOSIS

CHAPTER FOUR: THE RELATIONSHIP BETWEEN EVOKED AND SPONTANEOUS SYNAPTIC VESICLE TRAFFICKING

CHAPTER FIVE: DISTINCT MODES OF SYNAPTIC VESICLE RETRIEVAL AT REST

CHAPTER SIX: GLUTAMATERGIC REGULATION OF SYNAPTIC VESICLE REUSE

LIST OF ABBREVIATION

AMPA	α-amino-3-hydroxyl-5-methyl-4-isoxazole-propionate
A.U.	arbitrary unit
AP	action potential
AP5	D-2-amino-5-phosphonopentanoate
AP-2	adaptor protein 2
AP-180	adaptor protein 180
AZ	active zone
BAR	Bin/Amphiphysin/RVS
Ca^{2+}	calcium ions
CB_1R	cannabinoid receptor type 1
CdK	cyclin-dependent kinase
CNQX	6-cyano-7-nitroquinoxaline-2,3-dione
CNS	central nervous system
DAB	3,3-Diaminobenzidine
DHPG	3,5-dihydroxyphenylglycine
DIV	days *in vitro*
eCB	endocannabinoid
EGTA	ethylene glycol tetraacetic acid
EM	electronmicrographs
EPSC	excitatory post synaptic current
fCdK5	floxed cyclin-dependent kinase 5
GED	GTPase effector domain
GFP	green fluorescent protein
HRP	horseradish peroxidase
Hz	hertz
IPSC	inhibitory post synaptic current
K^+	potassium ions
mEPSC	miniature excitatory post synaptic current

mGluR	metabotrophic glutamate receptor
mIPSC	miniature inhibitory post synaptic current
NMDA	N-methyl-D-aspartic acid
NMJ	neuromuscular junction
PH	pleckstrin homology
PI3K	phosphatidyl inositol-3-kinase
PKC	protein kinase C
PPR	paired-pulse ratio
Pr	release probability
PRD	proline-rich domain
PSD	post-synaptic density
PTX	picrotoxin
RP	reserve pool
RRP	readily releasable pool
SEM	standard error of the mean
SH3	Src homology 3 domain
sIPSC	spontaneous inhibitory post synaptic current
SNARE	soluble N-ethylmaleimide-sensitive factor attachment protein receptors
SpH	synaptobrevin-pHluorin
STP	short term plasticity
SV	synaptic vesicle
Syb2 –/–	synaptobrevin-2-deficient
SypHy	synaptophysin-pHluorin
Syt1 –/–	synaptotagmin-1-deficient
TTX	tetrodotoxin
vGAT	vesicular GABA Transporter
VGCC	voltage gated Ca^{2+} channel
vGlut	vesiclular Glutamate Transporter
WT	wild-type

CHAPTER ONE
INTRODUCTION

The architecture of the presynaptic terminal of chemical synapses

Information processing and storage in the brain takes place between neurons, which communicate through specialized intracellular junctions. Charles Sherrington proposed that there is a membranous separation between neurons and named the narrow space as "synapse" (meaning "to clasp" in Greek), which is currently articulated as a chemical synapse. Chemical synapsesare are built by juxtaposed yet spaced compartments–with presynaptic and postsynaptic specialization, whereas electrical synapses occur between neurons that are connected to each other via gap junction and communicate by nearly simultaneous electrical coupling,

Presynaptic terminals contain a number of vacuolar organelles called synaptic vesicles (~45 nm in diameter), which securely store neurotransmitters (Figure 1.1). The active zone is a specialized structure, which is enriched with scaffolding molecules to anchor synaptic vesicles, and is dedicated for synaptic vesicle fusion. Once released onto the synaptic cleft, a narrow space where two neurons are juxtaposed (~ 20 nm in width), neurotransmitters activate postsynaptic receptors residing in the postsynaptic density (PSD), thus inducing depolarization as well as signaling cascades (Figure 1.1). Therefore, information flow via chemical synapses is mainly uni-directional although retrograde messengers have been identified (Wilson and Nicoll, 2001, 2002).

Postsynaptic specializations triggers diverse signaling pathways upon neurotransmitter release and thus are generally considered to be in charge of regulation and modulation of synaptic transmission. However postsynaptic activity can wax and wane depending on presynaptic changes. Therefore, the

presynaptic terminal is implicated to be where tight regulation and modification in information propagation begins to occur.

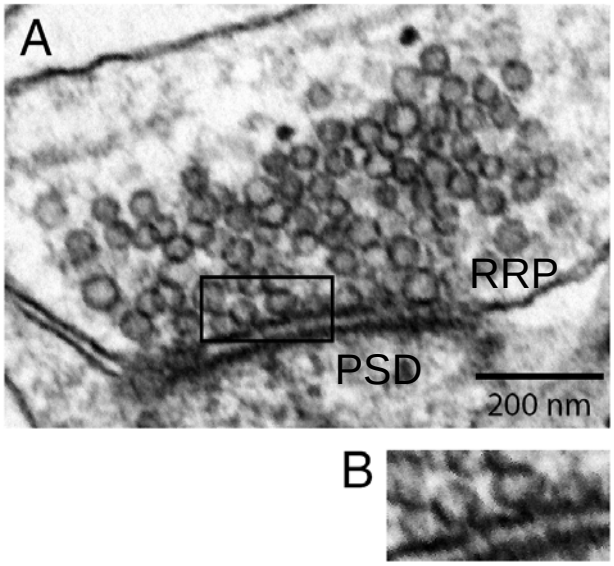

FIGURE 1. 1. Synaptic architecture analyzed at EM level.
(A) Presynaptic terminal contains synaptic vesicles homogeneous in size. A set of vesicles are very close to the presynaptic active zone (RRP). Due to their high density, presynaptic active zone (AZ) and postsynaptic density (PSD) can be readily appreciated. The narrow space between AZ and PSD is synaptic cleft. (B) A magnified view of synaptic vesicles connected to plasma membrane, presumably undergoing fusion or endocytosis. The neck of synaptic vesicles can be appreciated.

Synaptic vesicles, the translators of synaptic transmission

Synaptic vesicles contain chemical neurotransmitters such as glutamate or GABA, and respond to increases in Ca^{2+} induced by action potentials, thereby transforming electrical information to chemical information. According to ultrastructural analysis of small central synapses, synaptic vesicles seem to be morphologically uniform and ubiquitous in the synaptic terminal (Figure 1.1.). These terminals contain hundreds of synaptic vesicles, however, most of them are

known to be "dormant" because they do not seem to be involved in synaptic transmission (Harata et al., 2001; Rizzoli and Betz, 2005; Sudhof, 2000).

Only a small fraction (5-10%) of synaptic vesicles is set for fusion, collectively called the readily releasable pool (RRP) (Rizzoli and Betz, 2005). Morphologically, synaptic vesicles belonging to the RRP are located in close proximity to the release site, although the close location of synaptic vesicles to active zone does not necessarily guarantee their fusion potency at a given time (Rizzoli and Betz, 2004). Functionally, these vesicles readily respond to Ca^{2+}-independent hypertonic stimulation (Rosenmund and Stevens, 1996) as well as to rapid Ca^{2+}-dependent stimulation or increases in intrasynaptic Ca^{2+} (Murthy and Stevens, 1999; Schneggenburger et al., 1999; Wu and Borst, 1999).

Another fraction of synaptic vesicles serve as a reservoir for the RRP, thus often referred as the reserve pool or recycling pool (RP) (Rizzoli and Betz, 2005). This pool of vesicles is proposed to be responsible for replenishing the RRP on demand in a Ca^{2+} –dependent manner because once the RRP is depleted, slower release kinetics are observed, presumably mediated by synaptic vesicles mobilized from the RP (Stevens and Wesseling, 1998; Wang and Kaczmarek, 1998).

Besides these three pools of synaptic vesicles, other types of synaptic vesicle pools have been defined such as a reluctant pool or a spontaneously recycling pool. Reluctant synaptic vesicles are documented when some synaptic vesicles which do not respond to Ca^{2+} –dependent action potentials yet are drawn out by mechanistic secretagogues such as hypertonicity (Moulder and Mennerick, 2005) (Figure 4.5).

Previously, our group proposed another pool of synaptic vesicles, which selectively carry out spontaneous release but not action-potential –driven release (Sara et al., 2005). Similar observations were made in cortical inhibitory synapses (Hablitz et al., 2009; Mathew et al., 2008) and in asynchronously released vesicles

(Wolfel et al., 2007). Although synaptic vesicles are known to be homogeneous in terms of morphology (Mundigl and De Camilli, 1994), this functional diversity in synaptic vesicle pools is expected to be achieved by heterogeneity in molecular compositions (Takamori et al., 2000), therefore in release probability (Wolfel et al., 2007), or alternatively their position relative to voltage –gated Ca^{2+} channels (VGCC) (Wadel et al., 2007).

Life cycle of synaptic vesicles: fusion, retrieval and recycling

Synaptic vesicles undergo three trafficking steps during their life cycle: vesicle fusion or exocytosis, vesicle retrieval or endocytosis, and local recycling for reuse (Kavalali, 2006; Sudhof, 1995, 2004). Upon the arrival of an action potential and following Ca^{2+} influx, synaptic vesicles fuse with the plasma membrane and release their chemical contents onto a narrow cleft and thereby relay the information focally to the postsynaptic neurons. However, the conversion of electrical signals to chemical signals is fairly selective rather than faithful. Only 10–20% of action potentials trigger release of neurotransmitter (Goda and Sudhof, 1997). Once a fusion event is completed, vesicles are rapidly retrieved back to the synaptic terminal and undergo maintenance routines including neurotransmitter refilling in order to accommodate multiple rounds of synaptic transmission. Given that small synapses possess limited synaptic vesicles and only a small fraction of them actually serves as the workhorses of neurotransmission (Harata et al., 2001; Zucker and Regehr, 2002). Efficient synaptic vesicle endocytosis and recycling is an important task for small yet active central synapses to accomplish.

Modes of synaptic vesicle release: synchronous, asynchronous and spontaneous release

Synapses sustain three forms of neurotransmitter release with distinct Ca^{2+}–dependence and time course (Neher and Sakaba, 2008). Presynaptic action potentials and ensuing Ca^{2+}–influx causes rapid (generally within a millisecond and as fast as within 50 μs) synchronous vesicle fusion, which is tightly coupled to excitation to achieve temporal precision of given signaling (Sabatini and Regehr, 1996).

Synchronous synaptic fusion can be followed by asynchronous fusion, which persists for even tens of milliseconds after the invasion of an action potential. This loosely coupled fusion is largely driven by residual Ca^{2+} at the microenvironment, presumably due to the brief lag between Ca^{2+} influx and buffering (Hefft and Jonas, 2005; Lu and Trussell, 2000; Maximov and Sudhof, 2005; Sun et al., 2007).

In addition, neurotransmitter release can occur spontaneously in the absence of presynaptic action potentials albeit at a rate that can be modulated by intracellular Ca^{2+} levels (Fatt and Katz, 1952; Lou et al., 2005; Wasser and Kavalali, 2008; Xu et al., 2009). Spontaneous neurotransmitter release (also known as “miniature release” or “minis”) is a common feature of synapses throughout the nervous system yet had been dismissed, until recently, as a synaptic noise or accidental release escaped from tight regulation of fusion machinery. Recently, a consensus is emerging that spontaneous neurotransmitter release is not so accidental after all, and might serve a list of several important roles in neuronal communication. This list includes contributing to maturation of synapses (Murphy et al., 1994), providing continuous background inhibition (Otis et al., 1991) or setting the inhibitory tone of postsynaptic neurons (Lu and Trussell, 2000), regulating receptor clustering (Saitoe et al., 2001), even

triggering action potential firing in cells with high membrane resistance (Carter and Regehr, 2002; Sharma and Vijayaraghavan, 2003). Furthermore, it has been shown that "minis" participate in regulating postsynaptic receptor trafficking and excitability (Pare et al., 1998) and suppressing the dendritic protein translation machinery locally, thereby keeping receptor composition at synapses in check (Sutton et al., 2006; Sutton et al., 2007; Sutton et al., 2004). More surprisingly, a subset of NMDA receptors seems to be assigned for this particular mode of release, presumably by which it impacts various aspects of neuronal communication (Atasoy et al., 2008).

These three forms of release largely differ in Ca^{2+}–dependence (Lou et al., 2005; Neher and Sakaba, 2008; Sun et al., 2007; Xu et al., 2009) and probably in the extent to which their maintenance relies on synaptic vesicle recycling (Ertunc et al., 2007; Groemer and Klingauf, 2007; Li et al., 2005; Lin et al., 2005). Chapter four investigates whether all forms of synaptic vesicle release also shares the same recycling pathway for maintenance.

Fusion machinery

As expected, synaptic vesicle fusion, or exocytosis is a highly regulated process, carried out by a group of coordinated presynaptic proteins (Sudhof, 2004). Three proteins, synaptobrevin (also known as vesicle-associated membrane protein) on synaptic vesicles, syntaxin 1 and SNAP-25 on the presynaptic membranes, collectively called SNAREs mediate vesicle fusion. The fusion process is controlled and regulated by other proteins such as complexins, synaptophysin and Sec1/Munc18-like proteins (Becher et al., 1999; Edelmann et al., 1995; Jahn et al., 2003; McMahon et al., 1995). Synaptotagmin 1 serves as a bona fide Ca^{2+} sensor (Geppert et al., 1994).

Modes of synaptic vesicle endocytosis and recycling

Upon fusion, synaptic vesicles undergo either full collapse with the plasma membrane and retrieval by clathrin-dependent endocytosis (Heuser, 1989; Heuser and Reese, 1973) or narrow fusion pore opening and closure at the site of fusion, often referred as the 'kiss-and-run' mode of recycling (Ceccarelli et al., 1972, 1973) (Figure 1.2).

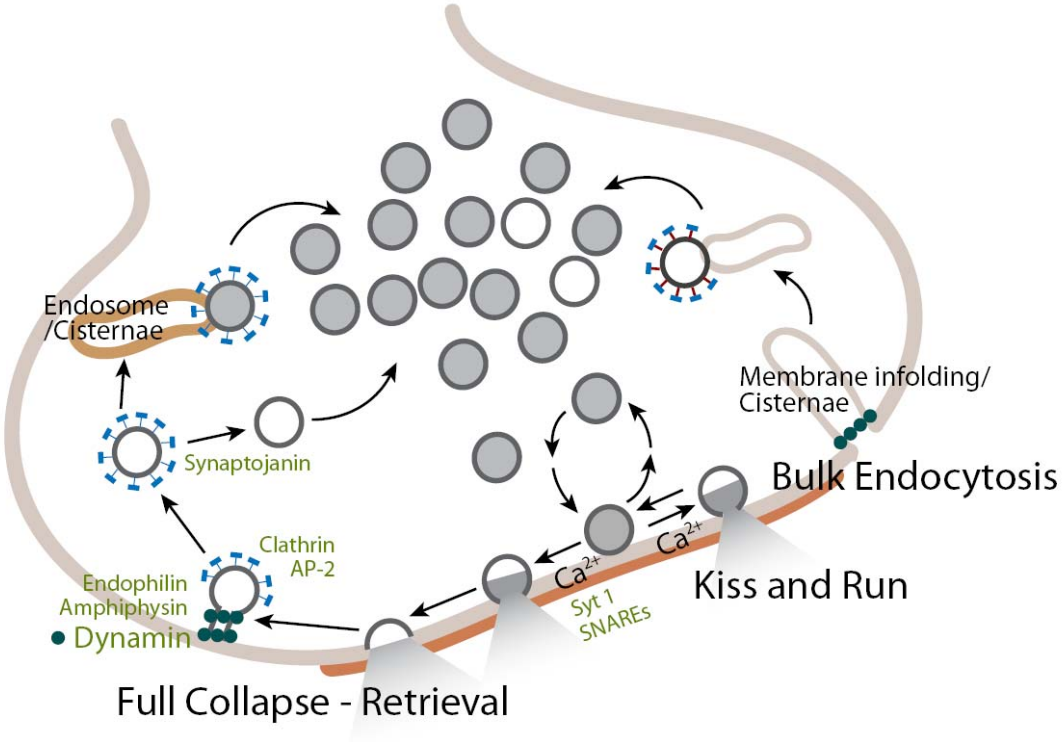

FIGURE 1. 2. Three modes of synaptic vesicle endocytosis and recycling.

Although the physiological relevance of the 'kiss-and-run' mode of recycling is still in doubt (reviewed in (He and Wu, 2007; Wu et al., 2007), this hypothesis seems to have several conceptual benefits over the full-collapse and

retrieval mode of recycling (Fesce et al., 1994; He and Wu, 2007; He et al., 2006; Wu et al., 2007). First, it allows for very rapid endocytosis, thereby providing an efficient way to replenish synaptic vesicles at small synapses. Second, it achieves synaptic vesicle retrieval at the site of fusion, thus carrying out a simple re-organization of vesicular proteins before leaving the plasma membrane. Less mixture between vesicular proteins and the membrane proteins is expected to shorten the amount to time to 'refresh' vesicles even further. Third, it can control the amount as well as the rate of neurotransmitter release by regulating the size of the fusion pore as well as the duration of opening. Regulation of fusion-pore opening has been proposed to contribute to plastic changes in hippocampal synapses by regulating the concentration and duration of neurotransmitter in the cleft (Choi et al., 2000).

However, a recently proposed model argues against the conceptual convenience of partial collapse and retrieval for faster vesicle reuse (Rizzoli and Jahn, 2007). A modified model has been proposed, where "ready-for-endocytosis" spots exist, which are fully equipped with all the endocytic machineries in apart from the fusion site, therefore allowing for synaptic vesicles to be "readily retrievable". This model is intriguing yet requires several validations to the following questions. This model assumes that vesicles can be regenerated from the separate vicinity of the active zone upon vesicle fusion at the active zone, suggesting that the newly endocytosed vesicle is different from the vesicle undergone fusion event. However, synaptic vesicle fusion and retrieval has been shown to occur without losing its original identity at central synapses (Aravanis et al., 2003), thereby supporting the hypothesis of the 'kiss-and-run' mode of vesicle use. Further studies are needed to delineate the synaptic vesicle mode of operation, which may be elucidated by examining the vesicle fusion cycle. Another complication is how the synaptic membrane initiates endocytosis upon fusion which occurs at several nanometers away from the fusion site. Are there any

molecular sensors to recognize fusion events and thus trigger endocytosis with great temporal precision? Which molecules regulate the quantity of vesicles being generated and how? Putative "linker" molecules need to be identified to fully support this model.

An alternative pathway has been proposed, which is designed to compensate for the increase in the surface area of the plasma membrane during strong stimulation when the rate of endocytosis can not catch up with the rate of exocytosis (Royle and Lagnado, 2003; Smith et al., 2008). This endocytic pathway, termed as "slow" or bulk endocytosis is different from fast endocytosis which is tightly coupled to fusion events. The bilk endocytosis operates in central synapses –even suggested to be primary (Jarousse and Kelly, 2001), including hippocampal synapses (Clayton et al., 2007; Cousin, 2009) and ribbon synapses (Jockusch et al., 2005). Relevant to this mode of vesicle retrieval, chapter five discovers that at resting conditions, a putative endocytosis pathway operation is influenced by the history of activity in local synaptic circuits.

Chapter four dissects the different molecular requirements for maintenance of synaptic vesicle recycling in evoked and spontaneous transmission, providing further evidence for operation of parallel recycling pathways.

Endocytic machinery

In contrast to the spatial limitation of exocytosis, endocytosis is thought to occur at the vicinity of active zone (Gundelfinger et al., 2003). It remains controversial when and which mode of endocytosis prevails at synaptic terminals. Furthermore, it remains unclear whether there different modes of endocytosis shares one master endocytic paradigm or require different machineries to achieve

their specificity (Aravanis et al., 2003; Granseth et al., 2007). By definition, the 'kiss-and-run' mode of recycling initiates endocytosis by immediate abortion of exocytosis thus seemingly independently of the conventional endocytic machinery (Aravanis et al., 2003; Gandhi and Stevens, 2003; Jarousse and Kelly, 2001; Klingauf et al., 1998; Neves and Lagnado, 1999). Classical clathrin-mediated endocytosis has gained most knowledge at the molecular level since it is largely shared within internalization processes critical for cell survival (Hirst and Robinson, 1998; Mellman, 1996).

Clathrin-mediated endocytosis

A number of protein-protein or protein-lipid interactions are known to mediate the classical clathrin-mediated endocytosis (Cremona and De Camilli, 1997; Takei and Haucke, 2001). The sequences for endocytic machinery assembly are the following. Synaptotagmin acts as a docking spot for adaptor protein-2 (AP-2). AP-2, which binds phospholipids as well as the C2B domain of synaptotagmin and recruits AP-180, another accessory protein suggested to regulate the size of the synaptic vesicles (Ye and Lafer, 1995). AP-180 binds to phospholipids as well as clathrin, and thus forms chathrin coats around the invaginated membrane structure. The scaffolding proteins, amphiphysin and endophilin, recruit dynamin 1 and synaptojanin to the AP-2 clathrin coat (de Heuvel et al., 1997; Ringstad et al., 1997). Dynamin 1, a large GTPase, then pinches the vesicle off,, whereas synaptojanin, a poly-phosphoinositide phosphatase (Cremona et al., 1999) participates in synaptic vesicle uncoating after endocytosis.

Dephosphins

Most of the players in clathrin –mediated endocytosis have been identified as dephosphins including AP-180, amphiphysin 1 and 2, dynamin 1 and

synaptojanin (Cousin and Robinson, 2001). These proteins are not structurally-related at all but uniquely, functionally related and participate in synaptic vesicle endocytosis. Upon depolarization, dephospins are promptly dephosphorylated by the calcium-dependent phosphatase, calcineurin, triggering endocytosis (Cousin and Robinson, 2001). To accommodate multiple rounds of endocytosis, dephosphins requires rephosphorylation, which could serve as a mechanism to regulate endocytic efficacy at given synaptic terminals.

Dynamin

Dynamin is a large GTPase, which forms rings and spirals along the neck of nascent synaptic vesicles or invaginating clathrin coated pits and mediates scission events, thereby freeing synaptic vesicles (Cremona and De Camilli, 1997). Dynamin was identified as the locus mutated in temperature-sensitive *drosophila shibire* mutants (citation). Dynamin contains an N-terminal GTPase domain, a pleckstrin homology (PH) domain, a GTPase effector domain (GED) and a C-terminal proline-rich domain (PRD) (Praefcke and McMahon, 2004). The PH domain interacts with phosphoinositides and is important for clathrin mediated endocytosis together with the GTPase domain (Achiriloaie et al., 1999; Barylko et al., 2001; Marks et al., 2001). The GED domain is suggested to mediate self-assembly of dynamin (Song et al., 2004). A number of binding motifs for the src-3 homology (SH3) domain have been found in the PRD domain (Ringstad et al., 1997) which mediates its interactions with Bin/Amphiphysin/RVS (BAR) domain-containing proteins such as amphiphysin 1 (Grabs et al., 1997), endophilin 1(Ringstad et al., 1999) and syndapin 1 (Itoh et al., 2005; Qualmann et al., 1999). These interactions are implicated to be critical in vesicle endocytosis (Anggono et al., 2006; Gad et al., 2000; Shupliakov et al., 1997).

The BAR domain contains a curvature-sensitive module, thus driving regeneration of sphere-shaped organelles (Farsad et al., 2001; Peter et al., 2004).

Amphiphyin and endophilin have been suggested to participate in either slow or fast endocytosis, respectively (Jockusch et al., 2005; Verstreken et al., 2003). In addition, endophilin 1 shares its binding sites for PRD domain in dynamin 1 with syndapin 1 (Anggono and Robinson, 2007). These findings implicate that the interactions between dynamin 1 and different BAR domain-containing proteins may contribute selectively to distinct modes of endocytosis. This idea gains further support from a recent study which has shown that bulk endocytosis requires the interaction of syndapin 1 with dynamin 1 (Clayton et al., 2009).

As described earlier, dynamin is one of dephosphins, and thus requires rephosphorylation. Two protein kinases are known to phosphorylate dynamin: protein kinase C (PKC) phosphorylates dynamin at Ser 795 and Cyclin-dependent kinase 5 (CdK5) at Ser 774 and Ser 778. The multiple phosphorylation sites upon different kinases may contribute to further regulation in synaptic vesicle recycling.

CdK5

Cyclin-dependent kinase 5 (CdK5) is a proline-directed serine/threonine kinase, which is presynaptically abundant in mature synapses (Tomizawa et al., 2002). It has been shown that CdK5 has a number of substrates that mediate or regulate exo- and endocytosis including synapsin 1 (Matsubara et al., 1996; Shuang et al., 1998), Munc-18 (Shuang et al., 1998) and P/Q type VDCC (Tomizawa et al., 2002) as well as dynamin 1 (Tomizawa et al., 2003). Interestingly, CdK5 activity has been suggested to be regulated by depolarization via an unknown mechanism (Schuman and Murase, 2003), as well as by activation of mGluR1 (Liu et al., 2001). More recently, CdK5 has been shown to regulate activity-dependent bulk membrane retrieval at small synapses (Evans and Cousin, 2007). The possible contribution of CdK5 in slow endocytosis as well as endocytosis at rest is examined in chapter five.

Studying synaptic transmission in cultured synapses

My work largely relies on electrophysiological recordings in a whole-cell voltage clamp configuration, which directly measures current across the membrane. Since the main communication between neurons is electrical, the electrophysiological recording provides most, thus employed throughout the studies presented here, except chapter five. Most of work was done in dissociated cultures, a widely –used *in vitro* system, where a variety of manipulations is possible.

Electrophysiological readout of synaptic activity was accompanied by optical analysis for a more comprehensive understanding of synaptic transmission. Several fluorescent probes are beneficial for my studies, including FM dye and pHluorin.

FM dyes are modified styryl dyes, which fluoresce when inserted into lipid membranes and are quenched in polar environments such as water (Gaffield and Betz, 2006; Grinvald et al., 1988). A lipophilic tail group allows FM dye to be incorporated into the plasma membrane. The length of the carbon tail varies among different types of commercially available FM dyes and determines the incorporation and departition rate from the plasma membrane. The head group is positively charged, thereby determining the orientation of dye on the synaptic vesicles. The carbon tail and head group are connected by two aromatic rings and the number of double bonds between aromatic rings determines the fluorophore properties of FM dye such as emission spectrum. FM1-43 has longer carbon tails and is thus more hydrophobic compared to FM2-10. FM2-10 and FM5-95 have similar structures including the same number of carbons in the tail region except that FM5-95 has three double bonds and thus exhibits a shift in its emission spectrum (see Figure 5.1). Chapter five mostly relies on this particular optical probe, providing further insight of how to take advantage of FM dyes for studying functional synapses.

Another probe employed to study synaptic transmission is modified synaptic proteins conjugated to pH-sensitive GFP, collectively termed pHluorin (Miesenbock et al., 1998). Monitoring of pHluorin –tagged synaptic protein trafficking has several advantages. First, unlike FM dyes, no wash time is required prior to stimulation. Second, pHluorin signal can detect both exocytosis and endocytosis with the aid of pharmacological tools, while only fusion events of vesicles can be detected with FM dye. The comparison analysis between FM dye and pHluorin provides a very specific and valuable tool to discover 'kiss-and-run' type of synaptic vesicle exo- and endocytosis in chapter three.

Taken together, the presynaptic terminal is a very dynamic cellular compartment with heavy trafficking of synaptic vesicles. The proceeding chapters will address the various questions raised in this introduction pertaining to the synaptic vesicle cycle.

CHAPTER TWO
La^{3+} AS A PROBE TO STUDY SYNAPTIC VESICLE EXOCYTOSIS

Background

Non-canonical secretagogues such as hypertonicity or α-latrotoxin have been valuable tools in studying the mechanisms underlying neurotransmission. For example, hypertonicity is widely used to estimate the size of readily releasable pool (Rosenmund and Stevens, 1996) and trigger neurotransmitter release independent of Ca^{2+} to assess selective defects in Ca^{2+} regulation of neurotransmission (Geppert et al., 1994). α-latrotoxin, on the other hand, helps to analyze the properties of unitary release events (Auger and Marty, 1997; Bevan and Wendon, 1984; Fesce et al., 1986) and has also been an extremely informative molecular bait to uncover several key components of synaptic junctions (Ushkaryov et al., 1992).

Lanthanum (La^{3+}) and other rare earth metals, collectively referred to as lanthanides, can also trigger neurotransmitter release but the mechanisms underlying their action is unknown. La^{3+} initially attracted investigators because of its ionic radius similar to Ca^{2+} (Lettvin et al., 1964) thus their expected role as Ca^{2+} in synaptic transmission. Previous studies in neuromuscular junction (NMJ) synapses showed that La^{3+} blocks the action potential evoked end plate potentials (Heuser and Miledi, 1971; Miledi, 1971), whereas increasing the frequency of miniature end plate potentials at the neuromuscular synapses of frog and goldfish (Bowen, 1972; Curtis et al., 1986; Dekhuijzen et al., 1989; Heuser and Miledi, 1971). These actions were shared with other lanthanides, including praseodymium (Pr^{3+}), gadolinium (Gd^{3+}), ytterbium (Yb^{3+}), europium (Er^{3+}), erbium (Eb^{3+}) and

yttrium (Y^{3+}) (Alnaes and Rahamimoff, 1974; Bowen, 1972; Metral et al., 1978; Molgo et al., 1991) Because these two consequences of La^{3+} treatment seemed inconsistent, La^{3+} and other lanthanides were often called to have dual action. Inhibition of evoked neurotransmission by La^{3+} is attributed to its potent ability to block voltage-gated Ca^{2+} channels (VGCCs) (Lansman, 1990; Lansman et al., 1986; Reichling and MacDermott, 1991).

In addition, La^{3+} can also inhibit Ca^{2+} uptake by mitochondria (Mela, 1969a, b), as well as by the plasma membrane Ca^{2+}-ATPase (PMCA) (Herrington et al., 1996). However, it remains unclear how La^{3+} increases spontaneous neurotransmission in synapses. Moreover, the impact of La^{3+} treatment on synaptic transmission in central synapses remains to be characterized. Increasing use of $LaCl_3$ as a therapeutic agent such as in treatment for hyperphosphatemia, further necessitates a better understanding of its impact on neurotransmission (Finn, 2006). Therefore, here La^{3+}'s potential was evaluated as a tool to pinpoint unconventional signaling pathways regulating central synapses, which are inaccessible to canonical secretagogues. This is not only important to better understand one of the longest standing enigmas of synaptic transmission, namely the mechanism of action of rare earth metals on neurotransmission, but also is a critical element to examine the properties of exocytosis-endocytosis coupling under physiological circumstances.

In this study, I found that La^{3+} application onto dissociated hippocampal cultures caused immediate neurotransmitter release (rapid effect) in a concentration-dependent manner. Interestingly, upon La^{3+} wash out, the frequency of spontaneous neurotransmission was increased and this delayed release (delayed effect) was only slowly reversible. Other lanthanides such as Eu^{3+}, Pr^{3+}, Yt^{3+} and Gd^{3+}, could mimic La^{3+} effect in central synapses, implying these two actions (rapid effect vs. delayed effect) are common features of all

lanthanides. Rapid effect of La^{3+} was independent of both extracellular and intracellular Ca^{2+} as well as activation of PLCβ. In addition, the rapid action of La^{3+} was insensitive to heavy metal chelators thus it does not require La^{3+} entry into the cell. In hippocampal cultures obtained from mice deficient in the synaptic vesicle soluble N-ethylmaleimide-sensitive factor attachment protein receptor (SNARE) protein synaptobrevin-2, the rapid effect of La^{3+} was abolished while the delayed effect was still detectable. In contrast, lowering internal $[Ca^{2+}]$ using Ca^{2+} chelators significantly attenuated the delayed effect while leaving the rapid La^{3+}-triggered neurotransmission intact. Therefore, I propose that La^{3+} has two separate effects on synaptic transmission. For its rapid action, La^{3+} appear to interact with a target on the surface membrane, triggering a SNARE dependent fusion while La^{3+} and/or $[Ca^{2+}]_i$ is required for the delayed action. These multiple effects of La^{3+} on neurotransmitter release in central synapses might mediate neurotoxic consequences of chronic exposure to La^{3+} (Feng et al., 2006a; Feng et al., 2006b).

Materials and Methods

Cell culture

Dissociated hippocampal cultures were prepared from Sprague-Dawley rats or synaptotagmin-1 deficient mice pups (gift of Dr. T. C. Sudhof) as previously described (Kavalali et al., 1999a). Synaptobrevin-2 deficient mice cultures were prepared at embryonic day 18, as previously described (Deak et al., 2004). Briefly, rats and mice were rapidly killed by decapitation after sedation by chilling on an ice-cold metal plate. Whole hippocampi were dissected from animal on postnatal days 0–2, trypsinized for 10 min at 37°C, and mechanically dissociated with siliconized glass pipettes prior to plating onto Matrigel-coated glass coverslips. 24 hours after plating, 4 μM cytosine arabinoside (Sigma) was added to prevent outgrowth of glia and exchanged with media containing 2 μM cytosine arabinoside at 4 days *in vitro* (DIV). All experiments with hippocampal cultures were performed during 14–21DIV, the time period already known as by that synapses become fully mature and represent the mature connections as *in vivo* (Mozhayeva et al., 2002).

Electrophysiology

Pyramidal neurons were voltage-clamped to −70 mV using whole-cell patch-clamp technique, using an Axopatch 200B amplifier and Clampex 8.0 software (Molecular Devices, Sunnyvale, CA), filtered at 2 kHz and sampled at 5 kHz. All recordings were performed at room temperature. The pipette solution contained the following (in mM): 115 Cs-$MeSO_3$, 10 CsCl, 5 NaCl, 10 HEPES, 0.6 EGTA, 20 tetraethylammonium chloride, 4 Mg-ATP, 0.3 Na_2GTP, 10 QX-314 (lidocaine N-ethyl bromide), pH 7.35, 300 mOsm (Sigma, St. Louis, MO). A modified Tyrode solution used as the extracellular solution with 2 mM Ca^{2+} and 1 μM tetrodotoxin (TTX). It contained the following (in mM): 150 NaCl, 4 KCl, 2 $MgCl_2$, 10 glucose, 10 HEPES, and 2 $CaCl_2$, pH 7.4, 310 mOsm. 0 mM Ca^{2+}

solution had same ionic composition except Ca^{2+} concentration and contained 1 mM EGTA. High K^+ solutions contained equimolar substitution of KCl (90 mM) for NaCl. The recordings were not corrected for the liquid junction potential (~12 mV).

To record and isolate miniature EPSCs, picrotoxin (PTX; 50 μM; Sigma) and TTX were added to the bath solution. In the experiments at which miniature IPSCs aimed to be isolated and recorded, ionotropic glutamate receptor antagonist, 6-cyano-7-nitroquinoxaline-2,3-dione (CNQX; 10 μM; Sigma), and aminophosphonopentanoic acid (AP-5; 50 μM; Sigma) were added to the bath solution in addition to 1 μM TTX.

The detection threshold amplitude of mEPSC and mIPSC was 4pA and the standard deviation of the baseline noise was 1.46±0.2 pA. To chelate intracellular Ca^{2+}, neurons were pre-treated with either 2 μM BAPTA-AM (Molecular Probes, Eugene, OR) for 30 minutes or 100 μM EGTA-AM (Molecular Probes) for 10 minutes. The exchange between extracellular solutions such as challenge with 2 mM La^{3+}-containing solution was achieved by direct perfusion of solutions onto the field of interest by gravity.

Lentivirus production

12 amino acids-inserted synaptobrevin 2 mutant (12-ins syb 2) construct was generated as described before (Deak et al., 2006a). HEK 293 cells were transfected with the Fugene 6 transfection system (Roche Molecular Biochemicals) with the expression plasmid and two helper plasmids, which are delta 8.9 and vesicular stomatitis virus G protein (3 μg of each DNA per 75 cm^2 flask of HEK cells) (Dittgen et al., 2004). After incubation of HEK cells at 37 °C for 48 hr, lentivirus containing culture medium was harvested and filtered at a 0.45 μm pore size prior to use for infection. Synaptobrevin 2 deficient mice cultures were infected with 12-ins syb 2 at 4 DIV by adding 400 μl of viral

suspension to each well. Patch clamp recording was carried out during 14-21 DIV.

Ca^{2+} Imaging

10 µl of 4% pluronic F-127 (low UV absorbance, Molecular Probes, Eugene, OR) and 3 µM Fura-2-AM (Invitrogen, Eugene, OR) were added to growth media of 18-19 DIV hippocampal cultures and cells were incubated for 45 min at 37°C. Cells were transferred to the chamber and washed with Tyrode's solution, containing nominal Ca^{2+} and 1mM EGTA for a couple of minutes. Images were obtained using DeltaRAM illuminator (Photon Technology International, Birmingham, NJ) and IC-300 camera (Photon Technology International) at the frequency of 0.5 Hz. Baseline was recorded for 1 minute before stimulation. 2 mM and 20 mM of Ca^{2+} or La^{3+} were used as ways of stimulation. Data analysis was performed using ImageMaster Pro software (Photon Technology International).

Statistical Analysis

Values are given as mean ± SEM. Two-tailed unpaired t-test was employed for statistical comparisons. ANOVA was used for statistical analysis of all multiple comparison experiments.

Results

Two components of La^{3+}- triggered neurotransmitter release at central synapses

La^{3+} triggers rapid neurotransmitter release (rapid effect)

To investigate the effect of La^{3+} on neurotransmitter release from central synapses, I used whole-cell patch clamp technique in rat dissociated hippocampal cultures and examined the basic properties of synaptic transmission. Bath application of 2 mM La^{3+} caused rapid neurotransmitter release (Figure 2.1.A-B). This rapid effect of La^{3+} has not been detected earlier because in previous studies of the neuromuscular junction preparations, the La^{3+} effect was monitored and analyzed not in real time but after incubation for a certain period. In these earlier experiments, the incubation times ranged between 1 and 4 minutes and in some cases synapses were incubated with La^{3+} for 45 minutes up to hours (Curtis et al., 1986; Heuser and Miledi, 1971). In contrast, here, the change of synaptic responses was monitored while bath-applying La^{3+}. As a result, I could observe prompt neurotransmitter release, referred as the rapid effect, both in excitatory and inhibitory synapses (see Figure 2.2). With sustained La^{3+} application, the neurotransmitter release was decreased presumably due to depletion of available vesicles akin to synaptic responses seen after hypertonic sucrose application (Moulder and Mennerick, 2005; Rosenmund and Stevens, 1996).

Next, the kinetics of La^{3+}-evoked release was compared to release evoked by hypertonic sucrose perfusion. Here, 2 mM La^{3+} solution was applied for 30 seconds followed by a +500 mOsm hypertonic sucrose solution for 30 seconds after a 3-minute wash period to compare La^{3+} effect to the effect of hypertonicity on release (Figure 2.1.A-C). The postsynaptic responses, quantified as average cumulative charge transfer induced by 2 mM La^{3+} during the first 10 seconds of

application, were almost half of the postsynaptic charge transfer caused by hypertonic sucrose solution (n = 20, Figure 2.1.D and G).

La^{3+} triggers rapid transmission by mobilizing synaptic vesicles largely from RRP in a concentration-dependent manner

The following sets of experiments were aimed to test the origin of vesicles mobilized by La^{3+}. To study whether La^{3+} mobilizes the same readily releasable pool (RRP) of synaptic vesicles that fuse in response to hypertonic sucrose application, \2 mM La^{3+} was applied 20 s after initial application of hypertonic sucrose in the continued presence of hypertonic solution. If La^{3+} induced the fusion of RRP vesicles, no additional release is anticipated. However, if La^{3+} mobilizes a separate set of synaptic vesicles, La^{3+} application on top of hypertonicity would be expected to trigger a comparable amount of neurotransmitter release regardless of hypertonic sucrose application. In these experiments, prior exposure to +500 mOsm hypertonic sucrose solution resulted in a 70% reduction in La^{3+}-induced neurotransmitter release compared with cells that were challenged with 2 mM La^{3+} alone (compare gray bars in Figure 2.1.D and F; P<0.001). Perfusion of 2 mM La^{3+} on top of +500 mOsm hypertonic sucrose solution was able to augment release by an additional 17% (n = 6), whereas 2 mM La^{3+} typically triggered 53% of release induced by hypertonicity alone (n = 20; Figure 2.1.G). Taken together, these findings suggest that the pools of vesicles mobilized by La^{3+} and hypertonic sucrose are largely overlapping but not completely identical.

As briefly mentioned earlier, the rapid effect of La^{3+} was observed both in excitatory and inhibitory synapses (Figure 2.2.A-B). When the La^{3+} concentrations were varied from 2 μM to 2 mM, the rapid effect of La^{3+} was detectable at 2 μM and showed a concentration-dependent increase in rate and magnitude (Figure. 2.2). The half rise time of release (t1/2) at 2 μM was 11.59 ±

2.43 nC/s and reached a maximum of 1.92 ± 0.4 nC/s at 2 mM La^{3+} (Figure 2.2.D).

La^{3+} has been shown to activate TRPC4 and 5 channels specifically through an unknown mechanism (Jung et al., 2003), and these transient receptor potential (TRP) channels are expressed in hippocampal neurons (Chung et al., 2006). To verify that La^{3+} acts by releasing neurotransmitters presynaptically and does not have a direct postsynaptic effect, La^{3+} was applied in the presence of TTX, PTX, and CNQX to block voltage-gated Na^{+} channels, GABA receptors, and postsynaptic AMPA receptors, respectively. If La^{3+} response was caused by direct activation of postsynaptic TRP channels, a similar pattern of activity is expected to be observed in the absence of neurotransmitter receptor activation. However, TTX, PTX, and CNQX completely eliminate La^{3+} response, and thus rule out the possibility that postsynaptic TRP channels were responsible for the neurotransmitter release induced by La^{3+} (Figure 2.2.E).

La^{3+} application does not alter the properties of unitary synaptic responses

To further evaluate the specificity of La^{3+} action on neurotransmitter release, I probed the properties of unitary transmission triggering by low concentrations of La^{3+}. Here, 2 μM La^{3+} was applied because higher concentrations of La^{3+} caused several overlapping quantal events, which were hard to assess individually. Unitary release events (miniature excitatory postsynaptic activity, mEPSC) activating a specific type of receptor were recorded with the aid of pharmacological blockers. In this way, a large number of AMPA-mEPSCs, *N*-methyl-D-aspartate (NMDA)-mEPSCs, and mIPSCs was measured, before and during La^{3+} application in isolation. This analysis showed no significant changes in the 10–90% rise times and amplitudes of individual events before and after La^{3+} application (Figure 2.3). These results indicate that the neurotransmitter release triggered by La^{3+} is quantal in nature and not likely caused by a nonspecific disruption of presynaptic terminals or postsynaptic

responsiveness and may share the same neurotransmitter release mechanism with physiological forms of synaptic transmission.

Other lanthanides mimic the action of La^{3+}

Other earth rare metals such as Pr^{3+}, Gd^{3+}, ytterbium (Yb^{3+}), Er^{3+}, and Y^{3+} have been reported to show La^{3+}-like dual action on synaptic transmission at the neuromuscular junction (Alnaes and Rahamimoff, 1974; Bowen, 1972; Metral et al., 1978; Molgo et al., 1991). To test whether the stimulatory action of La^{3+} on neurotransmitter release from hippocampal synapses is shared by other lanthanides, 2 mM of europium (Eu^{3+}), Pr^{3+}, Gd^{3+}, and Yb^{3+} was applied for 30 s and examined resulting neurotransmission. In these experiments, all lanthanides tested triggered a similar effect on neurotransmission (Figure 2.4.A), although the amount of release was typically smaller than that of La^{3+} (Figure 2.4.B). The average charge transfer triggered by 2 mM Gd^{3+}, Eu^{3+}, Yb^{3+}, and Pr^{3+} for 10 s was 0.33 ± 0.13, 0.37 ± 0.09, 0.43 ± 0.09, and 0.60 ± 0.12 nC, respectively ($n = 4$ each). Among these lanthanides, Pr^{3+} was the most potent, reaching 80% of the La^{3+} effect. These observations suggest that the ability to trigger neurotransmitter release is shared by all lanthanides.

La^{3+} increases spontaneous neurotransmission (delayed effect)

After La^{3+} washout, the frequency of mEPSCs or mIPSCs was highly increased, which referred as the "delayed effect", and the increased level of mPSCs was maintained for ≥10 min (Figure 2.5). The ability of La^{3+} to cause a sustained increase in the frequency of mPSCs has been already documented in neuromuscular junction preparations (Curtis et al., 1986; Heuser and Miledi, 1971). I could also consistently observe this effect in central synapses as a delayed consequence on withdrawal of La^{3+}, distinct from the rapid effect observed during La^{3+} application. Delayed effect was also concentration dependent in both

mEPSCs and mIPSCs (Figure 2.5.A–C). Removal of 2 μM La^{3+} solution caused a 1.74 ± 0.16-fold increase in mEPSC frequency compared with rest, whereas at 2 mM, this increase was 9.91 ± 1.53-fold (n = 5–9). Interestingly, the fold increase in the frequency of mEPSCs was greater than the change in mIPSCs (Figure 2.5.C). The fold increase in mIPSC frequencies after 2 μM La^{3+} was 1.11 ± 0.2 and reached a maximum of 4.48 ± 0.17-fold at 200 μM (n = 5–9). In contrast, no significant difference was observed in amplitudes of mEPSCs and mIPSCs (Figure 2.5.D).

Characteristics of rapid component of La^{3+}- triggered neurotransmission

Rapid effect of La^{3+} is independent of both extracellular and intracellular Ca^{2+}

What is the underlying mechanism of lanthanide-evoked neurotransmission at central synapses? The data suggest that La^{3+} can stimulate a releasable pool of vesicles presumably shared by the hypertonic sucrose stimulation, and La^{3+} application has no detectable direct postsynaptic effect (e.g., activation of TRP channels; Figure 2.1.H). In the next set of experiments, I pursued how La^{3+} may mobilize the RRP at central synapses. La^{3+} may trigger neurotransmitter release by one of three possible scenarios. First, La^{3+} might trigger Ca^{2+} entry presynaptically (e.g., via presynaptic TRP channels) or cause intracellular Ca^{2+} release and augment Ca^{2+}-dependent neurotransmission. In this case, La^{3+} would require Ca^{2+} as a mediator for its action. Second, La^{3+} might enter into a cell and cause neurotransmitter release by substituting Ca^{2+}. This scenario predicts that the action of La^{3+} does not require Ca^{2+} but requires its entry to a cell to surrogate Ca^{2+}. La^{3+} has a roughly similar ionic radius (3.1 Å) to Ca^{2+} (2.8 Å) (Lettvin et al., 1964); thus VGCCs can be a possible entryway of La^{3+} into a cell (Lansman, 1990; Lansman et al., 1986). In addition, several lines of evidence including electron micrographs (Pecot-Dechavassine, 1983) showed that La^{3+} could also enter a cell via the Na^{+}/Ca^{2+} exchanger (Powis et al., 1994; Reeves and Condrescu,

2003; Shimizu et al., 1997). Finally, if La^{3+} neither stimulates Ca^{2+} signaling nor enters into a cell for its rapid action, La^{3+} might act at the surface of membrane and interact with surface receptors, which can eventually evoke neurotransmission. An earlier study suggested that La^{3+} might act at superficial side of sartorius muscle (Weiss, 1970). More recently, another study in synaptosomes also proposed that La^{3+} may act extracellularly (Lopatina et al., 2005), possibly by modifying membrane lipid packing (Verstraeten et al., 1997).

To elucidate the underlying mechanism of prompt La^{3+}-evoked neurotransmission, I tested the first scenario that La^{3+} may act by increasing Ca^{2+}-evoked transmission. Experiments were carried out similar to above with extracellular solution containing 1 mM EGTA and nominal Ca^{2+}, which is expected to remove extracellular Ca^{2+} that can enter a cell on La^{3+} stimulation. In addition, to test whether increase in intracellular Ca^{2+} mediates rapid action of La^{3+} either by release from internal stores or by attenuated uptake by mitochondria, cells were treated with 100 μM EGTA-AM for 10 min or 2 μM BAPTA-AM for 30 min before La^{3+} stimulation. The effect of 2 mM La^{3+} was examined in the presence of 1 mM EGTA and nominal extracellular Ca^{2+}. Chelating extracellular Ca^{2+} as well as buffering intracellular Ca^{2+} could not antagonize the rapid action of La^{3+} (Figure 2.6.A). La^{3+} could still cause a similar amount of release independent of intracellular or extracellular Ca^{2+}. In the presence of EGTA, the cumulative charge transfer by 2 mM La^{3+} was 1.34 ± 0.39 nC, which is comparable to the control experiments shown in Figure 2.1. The release induced by La^{3+} after incubation with EGTA-AM or BAPTA-AM was 0.94 ± 0.14 and 1.18 ± 0.22 nC, respectively. These findings suggest that the neurotransmitter release by La^{3+} is not likely caused by its potential effects on Ca^{2+} signaling pathways. In agreement with these observations, depletion of Ca^{2+} from internal Ca^{2+} stores by for 30-min treatment of neurons with 1 μM

thapsigargin did not impair release induced by subsequent application of 2 mM La^{3+} (Figure 2.7).

These experiments using plasma membrane-permeable heavy metal chelators partly argue against the second possibility because EGTA-AM or BAPTA-AM is not only able to chelate Ca^{2+} but also La^{3+}. In fact, EGTA can effectively chelate heavy metals including La^{3+} even with higher affinity than it has for Ca^{2+} (Sillren and Martell, 1971), implying that pre-treatment with EGTA-AM or BAPTA-AM could significantly eliminate intracellular La^{3+} and block its action. For that reason, although 2 mM La^{3+} was applied under these conditions shown in Figure 2.6.A, the actual concentration of La^{3+} in the solution is estimated to be lower than 2 mM. Previous studies showed that La^{3+} could enter into a cell through Na^{+}/Ca^{2+} exchanger albeit with a slow time course around 30 seconds (Powis et al., 1994; Reeves and Condrescu, 2003). Therefore, Na^{+}/Ca^{2+} exchanger is not a likely mediator of La^{3+} entry for its rapid action because 30 seconds is longer than the typical response time to La^{3+} application (< 5 seconds).

Nevertheless, to examine the second possibility more directly, cells were incubated with 200 μM Cd^{2+}, a potent pore blocker of voltage-gated Ca^{2+} channels for 10 minutes prior to application of 2 mM La^{3+} and hypertonic solution to examine whether La^{3+} entry through VGCCs is responsible for rapid action of La^{3+}. If the rapid action of La^{3+} requires its entry through Ca^{2+} channels, pre-incubation with 200 μM Cd^{2+} would be expected to impede the rapid effect of La^{3+}. However, 200 μM Cd^{2+} did not interrupt the rapid action of La^{3+} as La^{3+} could trigger substantial release (1.35±0.19 nC) in its presence (Figure 2.6.B). This finding indicates that the possible entry of La^{3+} through voltage gated Ca^{2+} channels is not required for its rapid effect.

In addition to Ca^{2+} influx through VGCCs, presynaptic Ca^{2+} can be regulated by several mechanisms such as Na^{+}/Ca^{2+} exchanger, Ca^{2+} uptake and

release from mitochondria, and by the plasma membrane Ca^{2+}-ATPase (PMCA). La^{3+} is also known as a strong inhibitor of Ca^{2+} uptake by mitochondria (Mela, 1969a, b) and as an inhibitor of PMCA (Herrington et al., 1996), indicating that La^{3+} might interfere with Ca^{2+} homeostasis in presynaptic terminals in multiple ways leading to augmentation of neurotransmitter release. Besides the activation of channels or their permeation into cells, lanthanides can also bind to Ca^{2+} receptors, which are found in central nerve terminals (Smith et al., 2004), and these receptors are typically coupled to the activation of the PLCβ pathway (Breitwieser et al., 2004). To test the possibility that binding of La^{3+} to Ca^{2+} receptors and consequent activation of PLCβ pathway is responsible for its rapid action, hippocampal neurons were treated with U73122, a PLCβ inhibitor for 10 minutes prior to 2mM La^{3+} stimulation. After U73122 treatment, 2 mM La^{3+} still caused neurotransmitter release (1.34±0.28 nC) comparable to its effect on untreated cells, indicating that U73122 treatment failed to disrupt the rapid effect of La^{3+} (Figure 2.6.B). Figure 2.6.C summarizes the results of these experiments using 2 mM La^{3+} under different conditions as a fraction of La^{3+} responses in untreated cells. La^{3+} evoked response with nominal Ca^{2+} and 1 mM EGTA containing extracellular solution, after EGTA-AM and BAPTA-AM treatment, were 1.19 ± 0.35 nC (n = 5), 0.84 ± 0.13 nC (n = 4), and 1.06 ± 0.20 nC (n = 6), respectively. Average postsynaptic charge transfer values after 200 μM Cd^{2+} treatment or U73122 application were similar to controls (Cd^{2+}: 1.21 ± 0.17 nC (n = 7) and U73122: 1.19 ± 0.25 nC (n = 6)).

In the next set of experiments, I evaluated the effectiveness of EGTA-AM treatment to inhibit rapid action potential–evoked release in response to 10-Hz stimulation (Figure 2.8). For this purpose, IPSCs (eIPSCs) was evoked for 1 s in 8 mM Ca^{2+} before and after treatment with 100 μM EGTA-AM (Figure 2.8.A). These experiments showed that brief treatment with EGTA-AM is sufficient to

lower the concentration of intracellular Ca^{2+} and inhibit release (Figure 2.8.B and C). This finding further supports the premise that, if La^{3+}-evoked release was caused by a rise in intracellular Ca^{2+}, it should have been susceptible to EGTA-AM treatment.

Taken together, two possibilities can be ruled out. First, the action of La^{3+} does not seem to require rises in intracellular Ca^{2+}. Second, La^{3+} entry through VGCCs or activation of PLCβ is unlikely to mediate rapid effect of La^{3+}.

La^{3+} entry proceeds with a slow time course and cannot account for the rapid release induced by La^{3+}

La^{3+} might be able to enter into a cell via several poorly characterized pathways. Therefore, next set of experiments aimed to monitor La^{3+} entry optically using Fura-2-AM, a membrane-permeable derivative of the ratiometric Ca^{2+}-selective fluorescent dye Fura-2. Fura-2's affinity to La^{3+} is a thousand-fold higher than to its affinity to Ca^{2+} (Reeves and Condrescu, 2003). In addition, in response to La^{3+} binding Fura-2 displays a spectral shift (increase in fluorescence emission ratio in response to excitation at 340 *vs*. 380 nm wavelengths) similar to the shift seen after its Ca^{2+} binding (Reeves and Condrescu, 2003).

In these experiments, Fura-2-AM was added in growth media for 45 min at 37°C [final concentration = 3 μM] and cells were transferred to the recording chamber and briefly washed with Tyrode's solution, containing nominal Ca^{2+} and 1 mM EGTA. The fluorescence baseline was measured in Tyrode's solution in the presence of 1mM EGTA for 1 minute, and applied 2 mM La^{3+} or Ca^{2+} to monitor the entry of each ion for 30 seconds. As a very small increase of 340/380 ratio was detected with 2 mM La^{3+} application, cells were challenged again with higher concentrations of La^{3+} or Ca^{2+} (20 mM) as a positive control. In this setting only a small increase of 340/380 ratio was observed when 2 mM La^{3+} was applied, in contrast to the rapid and robust increase of 340/380 ratio by 2 mM Ca^{2+} (Figure 2.9). This suggests that there is small, if any, entry of La^{3+} into a cell upon its bath

application. Second, the rise in 340/380 ratio after La^{3+} application started slower than in after Ca^{2+}. The initiation of rise in 340/380 ratio by La^{3+} indicated as the black dotted line in Figure 2.9.B. Compared to the grey dotted line which indicates the rise in 340/380 ratio by Ca^{2+}, there is a delay between two lines, which is approximately 15 seconds (Figure 2.9.B). No significant difference was observed between the baseline fluorescence ratios in cells treated with La^{3+} or Ca^{2+} (0.4458 for La^{3+}, $n = 55$ from 6 coverslips and 0.434 for Ca^{2+}, $n = 30$ from 3 coverslips). Thus, it takes longer for La^{3+} to enter into a cell and the entry occurs slower compared to the entry of Ca^{2+} (Figure 2.9). This result strongly argues against the possibility that the rapid effect of La^{3+} is mediated by intracellular action of La^{3+}.

After 20 mM La^{3+} application, the 340/380 ratio increased gradually but the fluorescence signal was not decreased upon La^{3+} removal (Figure 2.9.A), which is consistent with the earlier observations in CHO cells (Reeves and Condrescu, 2003). This finding suggests that La^{3+} is not readily extruded from cells and it is buffered rather ineffectively, once it is introduced. This observation may explain the hardly reversible nature of the delayed effect of La^{3+}on neurotransmitter release.

The rapid effect of La^{3+} is strictly dependent on the vesicular SNARE protein synaptobrevin-2 but not on synaptotagmin-1

The results so far indicate that La^{3+} triggers rapid neurotransmitter release independent of its entry into cells. Thus, it is likely that La^{3+} acts at an extracellular site presumably by binding to a putative receptor or by direct modification of plasma membrane lipids to trigger neurotransmitter release (Andjus et al., 1997; Cheng et al., 1999). In order to test whether the form of release triggered by La^{3+} shares the same molecular machinery as the physiological action potential driven release, I took advantage of mice deficient in the synaptic vesicle protein synaptobrevin-2. Synaptobrevin-2 (also called

VAMP-2) is a synaptic vesicle associated soluble NSF receptor binding protein (SNARE), which interacts with the plasma membrane bound syntaxin and SNAP-25 to trigger neurotransmitter release (Sollner et al., 1993). Together, these proteins form a four-helix bundle (Otto et al., 1997; Sutton et al., 1998). Analysis of cultured hippocampal neurons from synaptobrevin-2 (syb2) knockout mice revealed a less severe impairment of spontaneous and hypertonic sucrose-induced release compared to evoked neurotransmitter release (Schoch et al., 2001). In addition, loss of synaptobrevin leads to a facilitation of release during high frequency stimulation and a defect in fast endocytosis (Deak et al., 2004).

To test whether SNARE complex-mediated fusion mechanism involving synaptobrevin-2 (syb2) mediates the rapid action of La^{3+}, 2 mM La^{3+} was applied onto cortical or hippocampal cultures obtained syb2 knock out mice. Synapses in cultures obtained from wild type mice showed the same sensitivity to La^{3+} as responses from wild type rat cultures. Interestingly, rapid effect of La^{3+} was completely abolished in syb2 deficient cultures (Figure 2.10.B, *middle*), supporting the premise that rapid action of La^{3+} requires functional SNARE proteins. The average amount of neurotransmitter release triggered by 2 mM La^{3+} in syb2 deficient cultures was 0.05 ± 0.01 nC (n = 14), which was indistinguishable from the baseline level of activity (0.03 ± 0.01 nC; n = 4). In contrast, parallel control experiments in wild type cultures displayed normal release in response to La^{3+} (0.86 ± 0.11 nC, n = 6) (Figure 2.10.B and C). In the same set of experiments, application of 2 mM Gd^{3+} was also ineffective in triggering rapid neurotransmitter release in syb2 deficient cultures. A separate set of experiments tested whether the loss of La^{3+} response in syb2 deficient synapses was indeed due to the absence of syb2 by reintroducing syb2. In syb2 deficient cultures infected with syb2 the charge transfer during 30 seconds of 250 μM La^{3+} was 1.11 ± 0.11 nC (n = 3), nearly 60% of neurotransmitter release compared to

wild type controls. This indicates that the defect shown in syb2 deficient culture was a specific consequence of the loss of syb2.

In a recent study, the ability of several synaptobrevin mutants to rescue synaptic transmission was tested in cultures from synaptobrevin knockout mice (Deak et al., 2006a). Mutants with insertion of 12 and 24 amino acids between the SNARE motif and the transmembrane domain (TMD) of synaptobrevin-2 revealed that the physical distance between the two regions of synaptobrevin is indeed critical for the rescue of evoked fusion. Surprisingly, in contrast to the mutant with insertion of 24 amino acids, the 12 amino acids insertion mutant syb2 (12-ins syb2, shown in Figure 2.10.A) completely rescued spontaneous release, suggesting that constraints on SNARE function during spontaneous fusion are more flexible than for evoked fusion. Interestingly, the La^{3+} effect on neurotransmission was also strictly dependent on the distance between the SNARE motif and the transmembrane domain of synaptobrevin-2, because La^{3+} application on synaptobrevin-2 deficient cultures infected with the lentivirus expressing 12-ins syb2 could not evoke any release (Figure 2.10.B, *bottom*). This result strongly suggests that La^{3+} triggered transmission shares the same strict molecular constraints as rapid action potential-evoked fusion. This is in striking contrast to spontaneous fusion or hypertonic sucrose evoked fusion, which both persists at a reduced but readily detectable level in synaptobrevin-2 deficient synapses (Deak et al., 2004; Schoch et al., 2001).

To probe the molecular machinery underlying the rapid effect of La^{3+} further, I next took advantage of synaptotagmin-1 (syt-1) deficient mice to examine whether La^{3+} may utilize the same pathway as rapid Ca^{2+}-dependent synchronous release. Cortical cultures obtained from syt-1 -/- mice were stimulated to confirm the genotype electrophysiologically prior to application of 2 mM La^{3+} for 30 sec (Figure 2.11.A). Neurons obtained from Syt-1 +/- were used as controls. The absence of syt-1 failed to block the rapid effect of La^{3+} (Figure

2.11.B). The cumulative charge transfer triggered during the first 10 seconds of La^{3+} application was 1.87 ± 0.49 nC in syt-1 +/- (n = 4) and 1.94 ± 0.22 nC in syt-1 -/- (n = 6) cultures (Figure 2.11). This result suggests that although the La^{3+}-triggered release is strictly dependent on synaptobrevin-2, it does not require the function of synaptotagmin-1 as a sensor. This finding also argues against the possibility that the rapid effect of La^{3+} requires La^{3+} entry as intracellular La^{3+} could readily interact with synaptotagmin-1 and trigger release.

Characteristics of delayed component of La^{3+}- triggered neurotransmission

Delayed action of La^{3+} is maintained in the absence of functional SNARE protein

In contrast to its rapid action, the delayed action of La^{3+} was still detectable in cultures from synaptobrevin-2 deficient mice where the baseline rate of spontaneous release was typically ten-fold lower than in wild type cultures (Figure 2.12). The delayed effect could also be elicited by Gd^{3+}, which also manifested a rapid synaptobrevin-2 dependent stimulation of neurotransmitter release. However, rapid application and wash out of 2 mM La^{3+} or Gd^{3+} caused significant increase in the frequency of mPSCs in syb2 deficient as well as wild type hippocampal cultures, suggesting that lanthanides have two distinct effects on central synapses. The frequencies of mPSCs after 2 mM La^{3+} application showed more than five-fold increase after 2 mM La^{3+} application (before La^{3+}, 0.34 ± 0.05 Hz and after La^{3+}, 1.97 ± 0.32 Hz, n = 14, P<0.01) and a two-fold increase after 2 mM Gd^{3+} application (before Gd^{3+}, 0.46 ±0.08 Hz and after Gd^{3+}, 1.01 ± 0.14 Hz, n = 8, P<0.02) (Figure 2.12.C). The change in the amplitude of mPSCs was not statistically significant under all conditions (Figure 2.12.D). Thus, in contrast to their rapid effects on neurotransmission, delayed effect of La^{3+} and Gd^{3+} on synaptic transmission in central synapses is only partially dependent on SNARE interactions.

Intracellular chelation of Ca^{2+} and La^{3+} abolishes the delayed release evoked by La^{3+}

To further characterize the delayed effect of La^{3+}, the mPSC frequency was quantified before and after application of 2 mM La^{3+} after treatment of cultures with Ca^{2+} chelators such as EGTA-AM or BAPTA-AM (Figure 2.13.A-B). These treatments substantially attenuated the delayed release while leaving the rapid effect intact (compare to Figure 2.6.A). Following incubation with 100 μM EGTA-AM for 10 minutes, the frequency of spontaneous release was largely unchanged compared to baseline after La^{3+} wash out (before La^{3+}, 3.84 ± 0.73 Hz and after La^{3+}, 4.64 ± 1.01 Hz, $n = 4$). Incubation with 2 μM BAPTA-AM for 30 min also significantly diminished the delayed effect of La^{3+} (before La^{3+}, 1.94 ± 0.61 Hz vs. after La^{3+}, 3.58 ± 0.81 Hz, $n = 6$). In the presence of 1 mM EGTA and nominal Ca^{2+} in the extracellular environment, La^{3+} application caused an eleven-fold increase in the frequency of mPSCs (from 2.96 ± 0.49 Hz to 34.28 ± 1.36 Hz, $n = 5$, $P<0.001$) (Figure 2.13.C). This finding suggests that either intracellular Ca^{2+} or delayed entry of La^{3+} (e.g. Figure 2.10) but not extracellular Ca^{2+} is responsible for the delayed release seen after removal of La^{3+} (Figure 2.13.D). In agreement with this premise, Cd^{2+} was ineffective in blocking the delayed effect, which suggests that Ca^{2+}/La^{3+} entry through voltage gated Ca^{2+} channels was not required (Figure 2.13.D). The delayed effect was also insensitive to a specific inhibitor of PLCβ (U73122) (Figure 2.13.D), which suggests that Ca^{2+} mobilization from internal stores that could be triggered by La^{3+} binding to the Ca^{2+} receptor is an unlikely source for this effect (Smith et al., 2004).

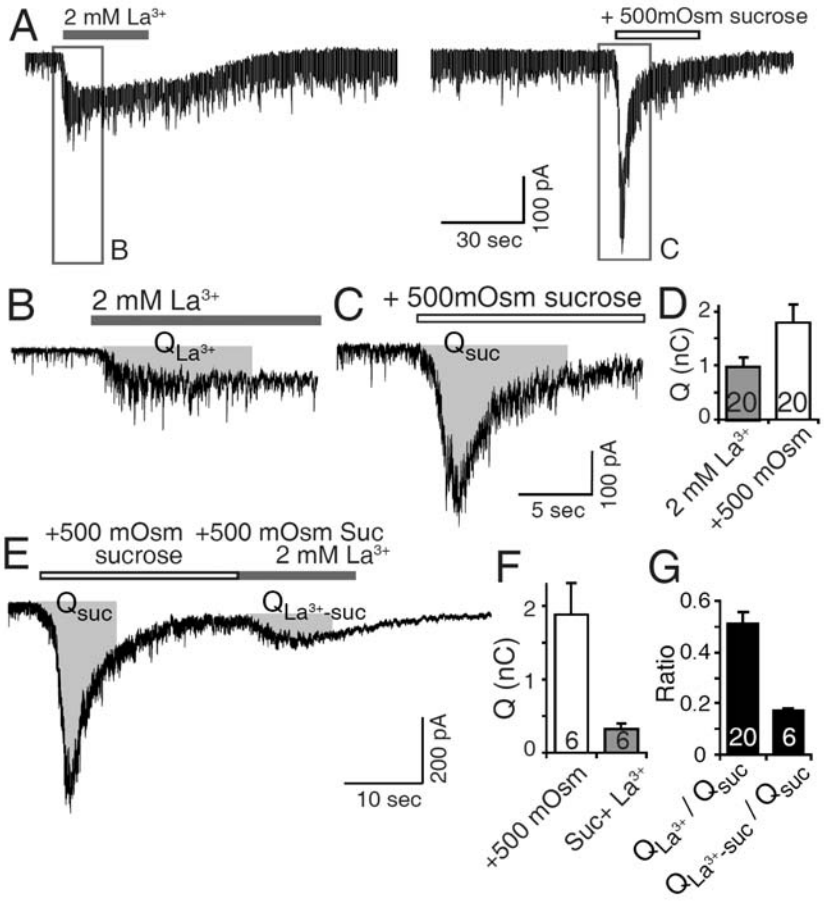

FIGURE 2. 1. La^{3+} application can trigger robust neurotransmitter release.
(A) 2 mM La^{3+} application results in a rapid neurotransmitter release, which is compared with response to hypertonic sucrose application on the same cell. 2 mM La^{3+} was applied for 30 s and hypertonic sucrose application for 30 s after 3 min of La^{3+} washout. (B and C) Response to 2 mM La^{3+} or hypertonic sucrose application following 2 mM La^{3+} is shown at an expanded time scale. (D) The average postsynaptic charge transfer triggered by 2 mM La^{3+} (for 10 s) was 53% of the amount triggered by subsequent hypertonic sucrose application (n = 20). (E and F) 2 mM La^{3+} followed by +500 mOsm hypertonic sucrose application induced additional release, which is 17% of release by hypertonicity alone and 30% of release by 2 mM La^{3+} alone (n = 6). (G) The fractional release triggered by 2 mM La^{3+} to +500 mOsm hypertonic sucrose before and after exposure to hypertonicity was 0.53 ± 0.08 and 0.17 ± 0.01, respectively.

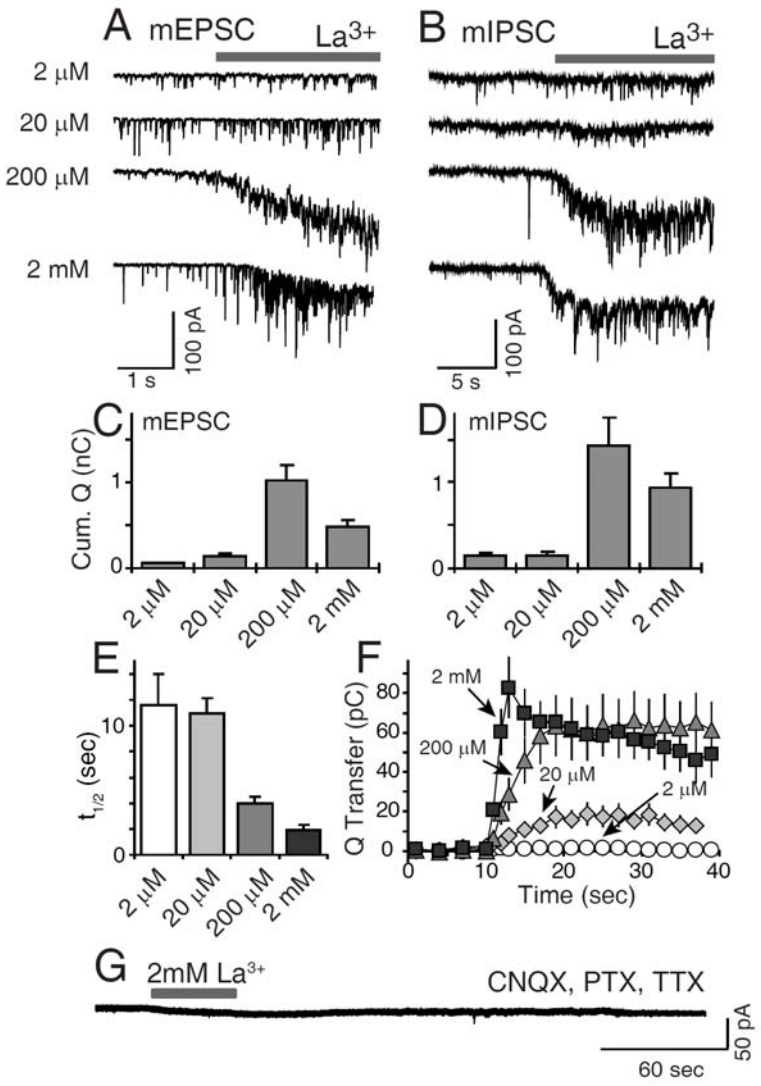

FIGURE 2. 2. Rapid effect of La^{3+} is concentration dependent in both excitatory and inhibitory synapses.

(A and B) Increasing concentrations of La^{3+} results in rapid neurotransmitter release both in excitatory and inhibitory synapses (n = 9–14). (C) Bar graphs show the cumulative amount of charge transfer triggered by each La^{3+} concentration within 10 s. (D) The charge transfer per second by La^{3+} plotted as a function of time. t1/2 denotes the half-maximal rise time at each concentration. (E) La^{3+} responses can be completely blocked in the presence of 6-cyano-7-nitroquinoxaline-2,3-dione (CNQX), picrotoxin (PTX), and TTX, suggesting that activation of transient receptor potential (TRP) channels are not responsible for the rapid effect of La^{3+}.

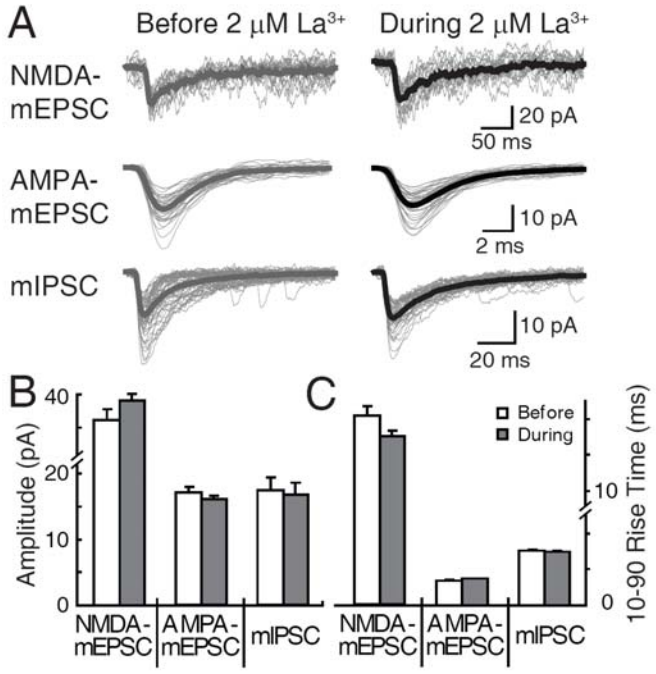

FIGURE 2. 3. The kinetics of individual unitary events was not altered during 2 μM La^{3+} application.

(A) The averaged traces of N-methyl-D-aspartate (NMDA)-miniature excitatory postsynaptic currents (mEPSCs), AMPA-mEPSCs, and mIPSCs during La^{3+} application (black trace) were not different from before (gray trace). (B) The 10–90% rise times and the amplitudes of NMDA-mEPSC (n > 120 responses from 5 cells, P>0.3), AMPA-mEPSC (n > 1,200 responses from 10 cells, P>0.5), and mIPSC (n > 2,000 responses from 12 cells, P>0.8) before and during La^{3+} application were not different. This indicates that the neurotransmitter release triggered by La^{3+} is quantal in nature and not likely caused by a nonspecific disruption of presynaptic terminals or postsynaptic responsiveness and may share the same neurotransmitter release mechanism with physiological forms of synaptic transmission.

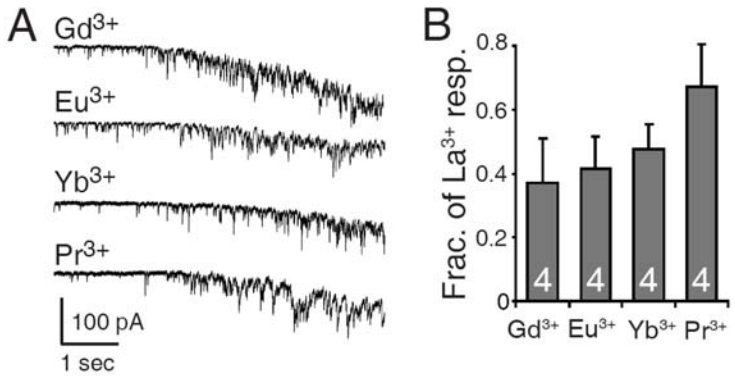

FIGURE 2. 4. Other lanthanides mimic the effect of La^{3+} on neurotransmitter release.
(A) 2 mM gadolinium (Gd^{3+}), europium (Eu^{3+}), ytterbium (Yb^{3+}), and praseodymium (Pr^{3+}) were also able to trigger neurotransmitter release. (B) The relative amount of average charge transfer triggered by 2 mM Gd^{3+}, Eu^{3+}, Yb^{3+}, and Pr^{3+} ($n = 4$, each) is plotted as a fraction of the cumulative charge transfer induced by 2 mM La^{3+}. Among these lanthanides, Pr^{3+} was the most potent, reaching 80% of the La^{3+} effect. These observations suggest that the ability to trigger neurotransmitter release is shared by all lanthanides.

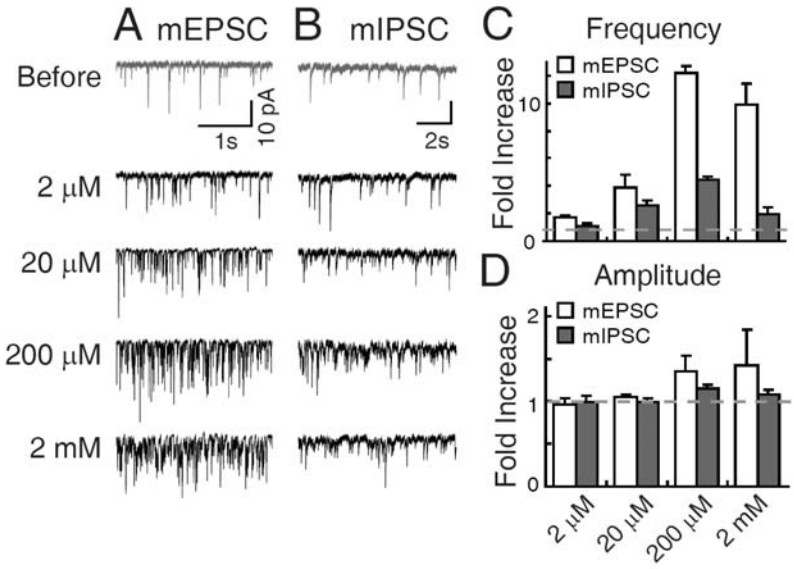

FIGURE 2. 5. La^{3+} induces delayed release after its removal from the extracellular solution.

(A and B) Sample traces of mEPSC and miniature inhibitory postsynaptic current (mIPSC) before and after increasing concentrations of La^{3+} application. (C) The fold increase in mEPSC and mIPSC frequencies after La^{3+} application compared with baseline at each concentration (n = 5–9). Except after 2 μM La^{3+} in mIPSC, all changes were significant (P<0.005). (D) The differences in the amplitudes of miniature responses before and after La^{3+} application were not statistically significant (P>0.1).

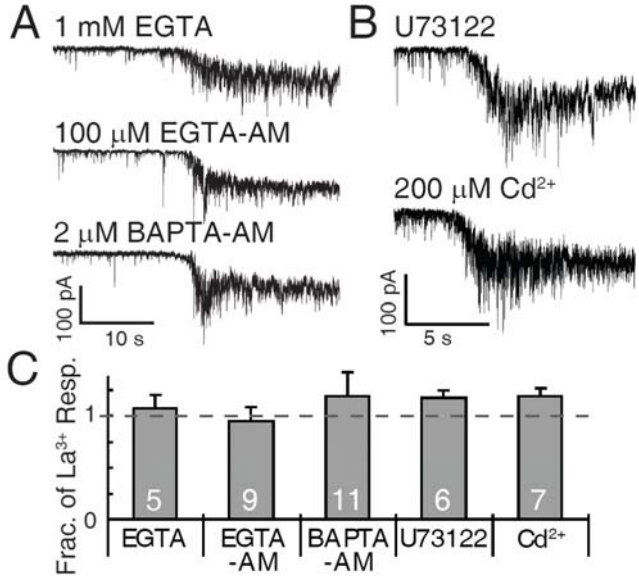

FIGURE 2. 6. Rapid effect of La^{3+} remains intact after inhibition of Ca^{2+} entry or intracellular Ca^{2+} signaling.
(A) Rapid action of La^{3+} is independent of internal or extracellular Ca^{2+}. Extracellular solution containing 1 mM EGTA and 0 mM Ca^{2+} (EGTA, $n = 5$, *top*) or preincubation with 100 μM EGTA-AM for 10 min (EGTA-AM, $n = 9$, *middle*) or 2 μM BAPTA-AM for 30 min (BAPTA-AM, $n = 11$, *bottom*) did not block rapid action of 2 mM La^{3+}. (B) Rapid effect of 2 mM La^{3+} was not interrupted in neurons pretreated with U73122 for 10 min ($n = 6$, *top*) or 200 μM Cd^{2+} for 10 min ($n = 7$, *bottom*). (C) The averages of cumulative charge transfer induced by 2 mM La^{3+} in each condition are shown here as a relative fraction of 2 mM La^{3+} response in the presence of 2 mM Ca^{2+} and TTX. Gray dotted line indicates the amount of release under control conditions. No significant difference was observed with any treatment (1-way ANOVA test, $P>0.5$).

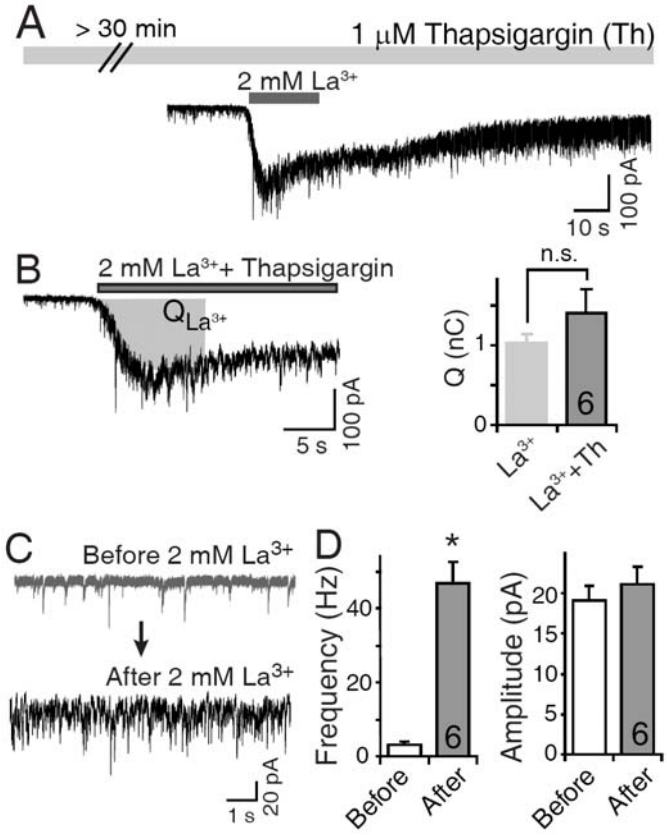

FIGURE 2. 7. Depletion of Ca^{2+} from internal Ca^{2+} stores failed to inhibit both rapid and delayed release triggered by 2 mM La^{3+}.
(A) To deplete Ca^{2+} from internal sources, cells were incubated with 1 μM thapsigargin for 30 min prior to 2 mM La^{3+} application. 2 mM La^{3+} stimulation was performed in the presence of 1 μM thapsigargin. (B) Rapid release triggered by La^{3+} after thapsigargin treatment did not show significant difference compared to release triggered by La^{3+} alone (n = 6, P>0.2, light grey bar represents the same data shown in Figure 2.1.D). (C and D) Delayed release after application of La^{3+} is not affected by thapsigargin treatment, suggesting that Ca^{2+} release from internal stores is not a major contributor to this release. Similar to the data presented in Figure 2.13, after thapsigargin treatment, the frequency of mPSCs increased upon removal of La^{3+} (n = 6, P>0.001) while their amplitudes were not changed (P>0.5).

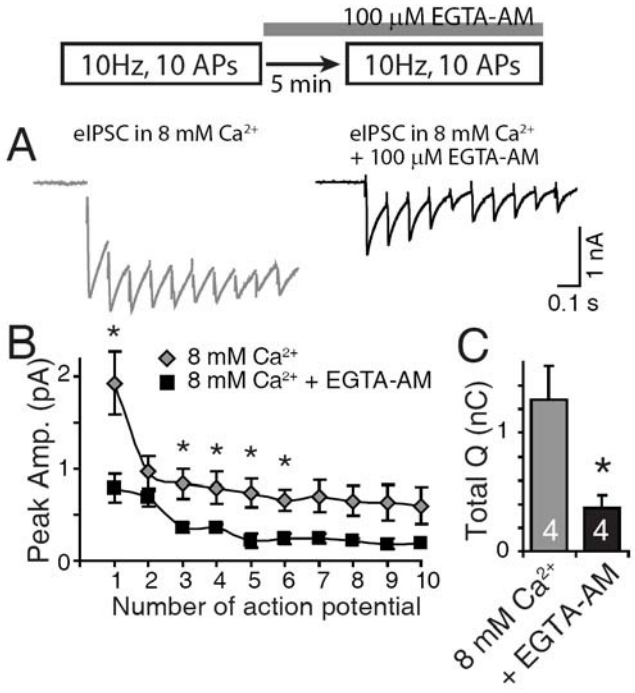

FIGURE 2. 8. EGTA-AM treatment in dissociated hippocampal synapses efficiently lowers concentration of intracellular Ca^{2+}.

Evoked IPSCs (eIPSCs) were measured for 1 s in 8 mM Ca^{2+} before and after treatment with 100 μM EGTA-AM. (A) Representative traces of evoked IPSCs (eIPSCs) at 10 Hz for 1 s in 8 mM Ca^{2+} before perfusion of EGTA-AM (*left*) and after 5 min in 100 μM EGTA-AM (*right*). (B) The amplitudes of the eIPSCs after EGTA-AM treatment showed a 50% reduction after treatment, suggesting that 100 μM EGTA-AM was sufficient to lower the concentration of intracellular Ca^{2+} to trigger release (**P*<0.05, *n* = 4). (C) The graph depicts the decrease in total charge transfer activated by 10-Hz stimulation after EGTA-AM treatment (**P*<0.05, *n* = 4), indicating that brief treatment with EGTA-AM is sufficient to lower the concentration of intracellular Ca^{2+} and inhibit release, thus, if La^{3+}-evoked release was caused by a rise in intracellular Ca^{2+}, it should have been susceptible to EGTA-AM treatment.

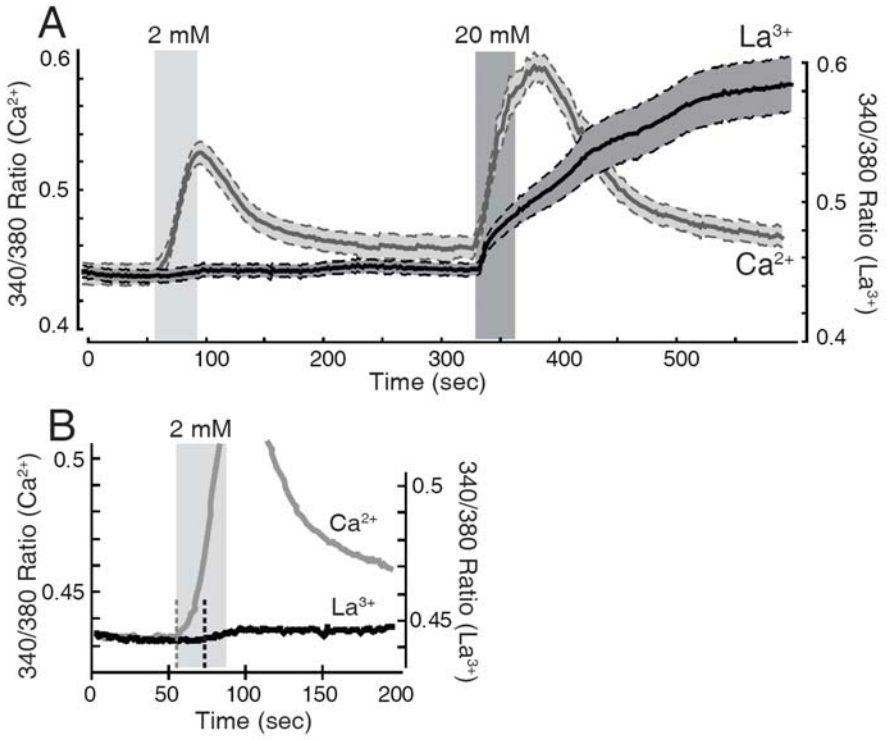

FIGURE 2. 9. Fura-2 imaging showed limited La^{3+} entry after bath application of 2 mM La^{3+}.

(A) The ratio of Fura-2 emission (at 510 nm) after excitation at 340 *vs*. 380 nm is plotted as a function of time. Gray boxes indicate the application of La^{3+} or Ca^{2+} (n = 30 cells from 3 coverslips for Ca^{2+} and n = 55 cells from 6 coverslips for La^{3+}). (B) Magnified plot at the onset of first stimulation depicts the delay (15 s) in rise of 340/380 ratio by Ca^{2+} (gray dotted line) with respect to the rise of La^{3+} signal (black dotted line). Thus, the rapid effect of La^{3+} is not likely to be mediated by intracellular action of La^{3+}.

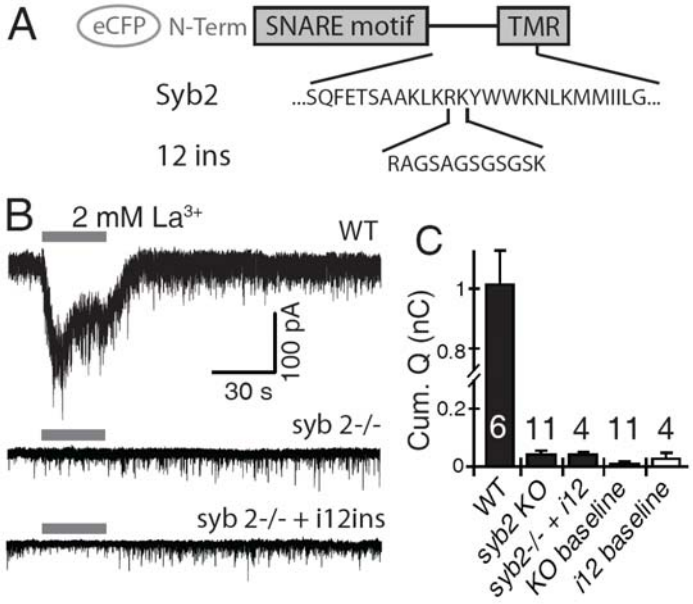

FIGURE 2. 10. Rapid effect of La^{3+} is strictly soluble N-ethylmaleimide-sensitive factor attachment protein receptor (SNARE) dependent.
(A) The construct of syb-2 and modified syb2 with 12 amino acid insertion (*i*12ins as in from Deak et al. 2006a). (B) Hippocampal neurons from wild type (WT) mice showed the same response to La^{3+} as rat hippocampal neurons (*top*). In syb2-deficient (syb2$^{-/-}$) neurons, rapid effect of La^{3+} is completely abolished (*middle*). The infection with lentivirus expressing the *i*12ins syb2 construct failed to rescue the rapid effect of La^{3+}, whereas it successfully rescued spontaneous synaptic transmission (*bottom*). (C) The average charge transfer triggered by 2 mM La^{3+} in WT (n = 6), syb-2$^{-/-}$ (n = 14), and syb-2$^{-/-}$ infected with *i*12ins syb2 (n = 4). The lack of fully functional syb2 reduced the rapid effect of La^{3+} (P<0.001).

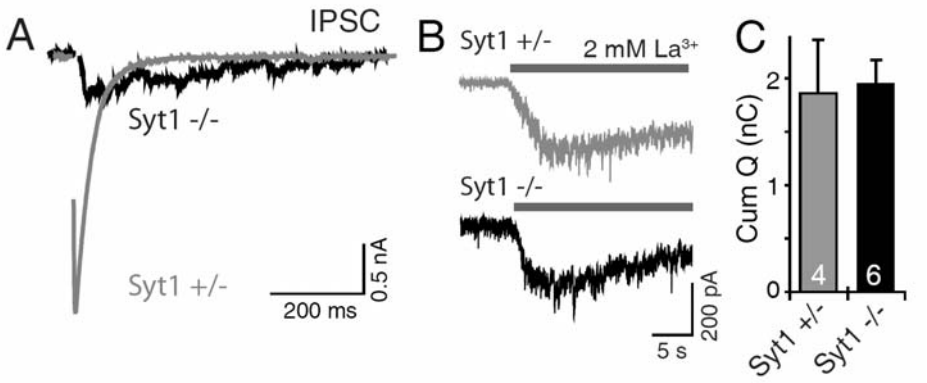

FIGURE 2. 11. The rapid effect of La^{3+} remains intact in synaptotagmin-1 deficient (syt1–/–) mice.

(A) As previously characterized, the synchronized evoked release is disrupted in cultures from syt1$^{-/-}$ mice. (B) The rapid effect of La^{3+} was still observed in the absence of syt1. *C*: the bar graph shows that the postsynaptic charge transfer during 2 mM La^{3+} application in syt1$^{-/-}$ cultures (n = 6), which was not different from the response in its heterozygote littermates (n = 4; P>0.8).

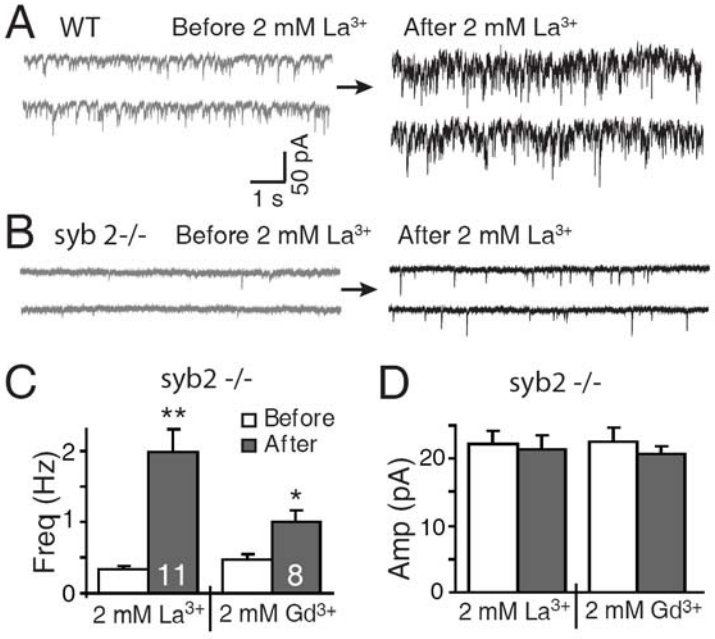

FIGURE 2. 12. In contrast to strict requirement of functional SNARE to mediate rapid action La^{3+}, delayed effect of La^{3+} is only partly SNARE independent.

(A and B) Representative traces of WT and syb-$2^{-/-}$ hippocampal neurons before and after 2 mM La^{3+} application. (C and D) The bar graphs show the changes in the frequency and amplitude of spontaneous synaptic events before and after application of 2 mM La^{3+} or Gd^{3+}. The changes in the frequency of mPSCs by La^{3+} or Gd^{3+} were statistically significant (**P<0.01, n = 14 for 2 mM La^{3+}; *P<0.05, n = 8 for 2 mM Gd^{3+}). The change in the amplitudes of mPSCs was not significant (P>0.9).

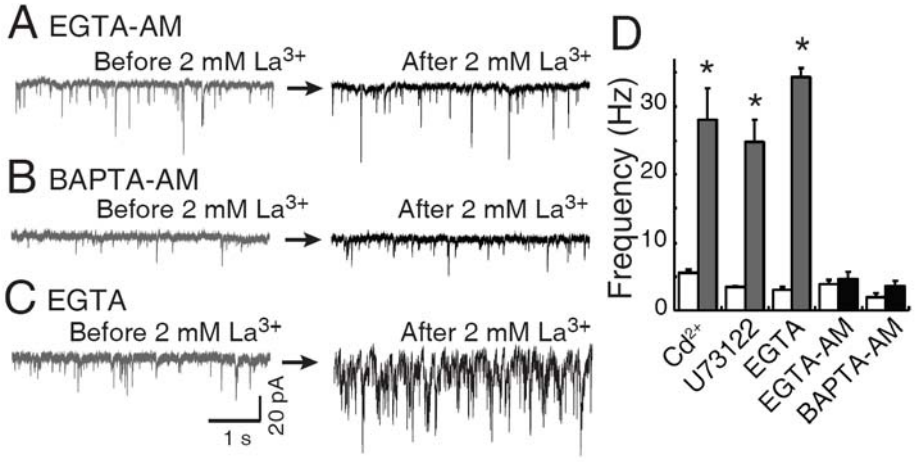

FIGURE 2. 13. Delayed action of La^{3+} requires internal Ca^{2+} or possibly La^{3+} entry. (A-C) Representative traces before and after 2 mM La^{3+} application under each condition. Incubation with 100 μM EGTA-AM for 10 min or with 2 μM BAPTA-AM for 30 min before 2 mM La^{3+} application suppressed the increase of mPSCs frequency (n = 4–6). In contrast, extracellular EGTA (below La^{3+} concentration) did not hinder the delayed effect of La^{3+}. (D) The delayed effect of La^{3+} after each treatment (Cd^{2+}, U73122, EGTA, EGTA-AM, and BAPTA-AM) is quantified as the frequency of mPSCs. After incubation with Cd^{2+}, U73122, or in the presence of 1 mM EGTA, the frequency of mPSCs were still increased in response to 2 mM La^{3+} application (n = 5–9, ***P<0.001). In contrast, treatment with EGTA-AM or BAPTA-AM completely blocked the delayed effect of La^{3+} (P>0.7).

Discussion

Two components of neurotransmitter release triggered by La^{3+}

This study examined the effect of La^{3+} and other lanthanides, in particular Gd^{3+}, on neurotransmitter release in dissociated hippocampal cultures and found that they triggered release in a rapid phase, which occurred within seconds, followed by a slow phase of release detectable after washout, which was hardly reversible. These data demonstrate that the rapid effect of La^{3+} is not mediated by augmenting existing Ca^{2+}-dependent release, by increasing internal Ca^{2+} or by La^{3+} entry through various putative pathways. Instead, these findings suggest that La^{3+} acts extracellularly and mediates rapid neurotransmitter release, which requires the SNARE-dependent fusion machinery. The most salient feature of rapid La^{3+} triggered release is its strict dependence on synaptobrevin-2. The rapid effect of La^{3+} was abolished in the absence of synaptobrevin-2 but not synaptotagmin-1. This is surprising because other forms of Ca^{2+}-dependent and independent release including release driven by hypertonic sucrose are not fully eliminated in synaptobrevin-2 deficient synapses. Synaptobrevin-2 mutant with 12 amino acid insertion was also ineffective to rescue the rapid effect of La^{3+}, suggesting that La^{3+}-triggered fusion events are mechanistically closely related to fast evoked release. In addition, the properties of unitary synaptic responses during La^{3+} application were not different from events detected during normal spontaneous neurotransmission, providing further support that La^{3+} triggers neurotransmitter release by activating the conventional fusion machinery.

A delayed effect of La^{3+} is detect, which is characterized as an increase in the frequency of mPSCs seen after removal of La^{3+} as previously shown in neuromuscular junction studies (Heuser and Miledi, 1971). Delayed effect of La^{3+} is hardly reversible and persistent even in the absence of La^{3+}, leading to conclude that the entry of La^{3+} might mediate this delayed effect. I showed that pre-

treatment with well-known Ca^{2+} chelators, such as EGTA-AM or BAPTA-AM significantly attenuate the delayed effect of La^{3+}. As mentioned earlier, EGTA and BAPTA are effective chelators of La^{3+} as well as Ca^{2+}. The absolute stability constants of EGTA:Ca^{2+} and EGTA:La^{3+} complexes indicate that EGTA can bind to La^{3+} with about 10,000-fold higher affinity than Ca^{2+} (Sillren and Martell, 1971). In cells pre-treated with Ca^{2+} chelators, I assume that internal Ca^{2+} is effectively chelated before application of La^{3+}. However, once La^{3+} was applied, EGTA inside of a cell is expected to dissociate from internal Ca^{2+} and bind to La^{3+} because of its higher affinity to La^{3+}. Thus, for its delayed effect, La^{3+} entry through sources other than VGCCs might be required and internalized La^{3+} itself might mediate neurotransmitter release. Alternatively, La^{3+} might use Ca^{2+} as a mediator for its delayed action. In this case, La^{3+} contributes indirectly to delayed effect by increasing internal Ca^{2+} concentration, presumably through its ability to inhibit Ca^{2+} uptake by mitochondria (Mela, 1969a, b) or the function of PMCA (Herrington et al., 1996). Therefore, both internal Ca^{2+} and La^{3+} uptake can be responsible for the delayed effect. In the absence of specific tools to clearly distinguish between Ca^{2+} and La^{3+} it is difficult to conclusively pinpoint whether the delayed release triggered by La^{3+} is a direct and indirect effect of La^{3+}. However, this data strongly bolsters the hypothesis that the rapid effect of La^{3+} does not require intracellular Ca^{2+} or La^{3+} because it is not susceptible to the same intracellular chelators.

La^{3+} as a specific tool to study synaptobrevin–2–dependent neurotransmitter release

As indicated above, rapid neurotransmitter release triggered by La^{3+} strictly required synaptobrevin-2, which argues for a strong specificity of La^{3+}, mechanism of action beyond any other means to trigger neurotransmission. Most forms of release can persist in the absence of synaptobrevin-2 albeit at severely

reduced levels (Deitcher et al., 1998; Schoch et al., 2001). This remaining release is thought to be triggered by an alternative vesicular SNARE(s) (Borisovska et al., 2005; Deak et al., 2006b). However, the results presented here indicate that in the case of La^{3+}-mediated release these non-cognate SNAREs may not be able to substitute synaptobrevin-2 functionally. This finding raises two possibilities. First, different vesicular SNAREs may manifest high functional specificity for different secretagogues. Or alternatively, these non-cognate vesicular SNAREs are located in a distinct population of vesicles that are not mobilized in response to La^{3+}. The strong specificity of La^{3+} evoked fusion, compared to other means to trigger release, makes it a powerful tool to probe synaptobrevin-2 function in central synapses. Another advantage of La^{3+} as a tool to probe release machinery stems from the fact that most other secretagogues can cause morphological distortion of cell membranes either by inducing shrinkage (e.g. hypertonicity) or forming Ca^{2+} permeable channels (α-latrotoxin). In contrast, in the current setting, the concentrations of La^{3+} used to trigger release did not have any negative impact on membrane integrity. Another key feature of La^{3+} triggered rapid release is its persistence in the absence of synaptotagmin-1, which is consistent with the observation that rapid release triggered by La^{3+} is independent of Ca^{2+} or La^{3+} entry and may provide a useful probe to examine release independent of the fast Ca^{2+} sensing machinery.

Possible mechanisms of La^{3+}–driven synaptic vesicle fusion

What is the transduction mechanism that link La^{3+} to SNARE-mediated fusion machinery? As indicated above, these results suggest that La^{3+} appears to act at an extracellular site to trigger rapid SNARE-mediated neurotransmitter release. Whereas the delayed release seems either to be a consequence of La^{3+}'s slow entry into the cell or an indirect effect of Ca^{2+} signaling initiated by La^{3+} binding to an extracellular receptor (or both). There are several earlier studies

which suggest that neurotransmitters or neuromodulators acting on presynaptic G-protein coupled seven transmembrane domain receptors may directly regulate neurotransmission in a SNARE-dependent manner. For instance, in lamprey central synapses interaction of Gβγ subunits with SNAP-25 during serotonergic stimulation results in kiss-and-run type fusion events (Gerachshenko et al., 2005; Photowala et al., 2006) and restricts glutamate release suggesting a direct interaction between a G protein coupled receptor and the fusion machinery. In addition, recent studies propose that the time-course of acetylcholine release is regulated by the voltage-sensitive muscarinic autoreceptors (Parnas and Parnas, 2007). These findings suggest that muscarinic acetylcholine receptors tonically inhibit the release machinery and this inhibition is relieved by membrane depolarization. Thus, acting through a voltage driven conformational change in muscarinic receptors, membrane voltage can exert tight control on the timing of neurotransmitter release (Slutsky et al., 2003). Furthermore, several G-protein coupled receptors such as the Ca^{2+} receptor (Smith et al., 2004) and group I metabotropic glutamate receptors (Abe et al., 2003) are present in central nerve terminals and possess binding sites for lanthanides. Therefore, La^{3+} as well as other lanthanides may act on these presynaptic receptors which directly impact the release machinery.

Taken together, these results suggest that lanthanides act as powerful secretagogues to induce neurotransmitter release in a Ca^{2+}-independent manner taking advantage of the conventional SNARE-mediated release machinery. Further investigation of the mechanism underlying this process will not only help us better understand Ca^{2+} independent mechanisms that mediate neurotransmission but also provide insight into how extracellular heavy metals

impact synaptic transmission under physiological as well as pathological circumstances.

CHAPTER THREE
La^{3+} AS A PROBE TO STUDY SYNPATIC VESICLE ENDOCYTOSIS

Background

Presynaptic terminals in typical central synapses contain hundreds or so of synaptic vesicles. Given that the number of available synaptic vesicles at the nerve terminal is limited, exo- and endocytosis coupling and fast replenishment of fusion-potent vesicles are essential steps for central synapses with high network activity. Therefore, the regulatory mechanisms underlying the tight coupling of exo- and endocytosis has been of great interest.

A transient fusion pore opening or so-called 'kiss and run' type of exo- and endocytosis was proposed several decades ago (Ceccarelli et al., 1973; Fesce et al., 1994). The 'kiss-and-run' type of fusion could be conceptually advantageous because if accounts for the rapid re-use of synaptic vesicles with relatively small numbers of functional vesicles in central synapses (de Lange et al., 2003; Klingauf et al., 1998). The existence of this particular mode of fusion has not obtained full agreement in the field, though the hypothesis has been around for decades (for review see; (He and Wu, 2007; Wu et al., 2007)), due to inconsistent optical observations and controversial interpretations (For example, (Aravanis et al., 2003; Fernandez-Alfonso and Ryan, 2004; Klingauf et al., 1998; Stevens and Williams, 2000) with little direct evidence supporting the presence of this particular type of neurotransmitter release in central synapses (But see; (He et al., 2006; Zhang et al., 2009)

In the previous chapter, it was shown that lanthanum (La^{3+}), a rare earth metals, can induce a substantial amount of neurotransmitter release as well as

other lanthanides (Chung et al., 2008). I thoroughly characterized La^{3+}-evoked neurotransmission and proposed La^{3+} as a novel secretagogue in central synapses. This chapter took advantage of La^{3+} as a tool to examine questions in exo- and endocytosis coupling and vesicle recycling during and after stimulation in central synapses. Exo- and endocytosis coupling was detected with whole-cell patch clamping recordings and synaptopHluorin signals but not with FM dyes or HRP, suggesting that La^{3+} triggers release through the fusion pore which allows exchange of protons and neurotransmitters but not of bulky molecules such as FM dyes or HRP. Therefore, I propose La^{3+} as a valuable secretagogue to probe exo- and endocytosis coupling during the 'kiss-and-run' mode of synaptic vesicle trafficking in central synapses.

Materials and Methods

Dissociated hippocampal culture

Dissociated hippocampal cultures were prepared from postnatal Sprague-Dawley rats or from postnatal day mice pups expressing synaptopHlourin selectively in excitatory synapses (spH21, gift of Dr. Venkatesh Murthy, Harvard University) as previously described (Kavalali et al., 1999a). Unless stated otherwise, all experiments were carried out after 14 days *in vitro* (DIV) when synapses are known to represent mature synapses *in vivo* (Mozhayeva et al., 2002).

Lentivirus production

The synaptophysin-pHluorin (sypHy) construct contained two pHluorins and was a generous gift of Drs. Y. Zhu and C.F. Stevens (The Salk Institute, La Jolla, CA). HEK 293 cells were transfected with the Fugene 6 transfection system (Roche Molecular Biochemicals) with the expression plasmid, two helper plasmids, which are delta 8.9 and vesicular stomatitis virus G protein, and either pFUGW-sypHy or 12-ins syb 2 mutant construct, (3 μg of each DNA per 75 cm^2 flask of HEK cells). After incubation of HEK cells at 37 °C for 48 hr, lentivirus containing culture medium was harvested and filtered at a 0.45 μm pore size prior to use for infection. Hippocampal cultures were infected with sypHy at 4 DIV by adding 300 μl of viral suspension to each well, and imaging experiments were carried out during14-21 DIV.

Electron microscopy

For horseradish peroxidase (HRP) uptake experiments, hippocampal cultures were stimulated with either 47 mM K^+-containing or 2 mM La^{3+} containing Tyrode solution in the presence of 25 mg ml^{-1} HRP (Sigma) for 90 seconds in 10 μM CNQX and 50 μM AP5. After brief wash of excess HRP with buffer, cells were immediately fixed with 2% glutaraldehyde in 0.1 M sodium phosphate buffer, pH 7.4 at 37°C and washed with Tris-Cl (100 mM, pH 7.4) buffer. Then, cells were

incubated with 3,3'-diaminobenzidine (0.1% DAB, Sigma) in Tris-Cl buffer and H_2O_2 (0.02%) for 15 min (DAB reaction), and washed with Tris-Cl buffer. At this point cells were incubated in 1% OsO_4 for 30 min at room temperature and stained *en bloc* with 2% aqueous uranyl acetate for 15 min, dehydrated in ethanol, embedded in Poly/Bed 812, (Polysciences Inc, and Warrington, PA, USA) for 24 hrs. 60 nm thick sections were post-stained with uranyl acetate and lead citrate. Images were obtained with a JEOL 1200 EX transmission microscope.

For depletion experiments, hippocampal cultures were incubated with either 2 mM Ca^{2+} or 2 mM La^{3+} for 10 minutes before fixation. 1 μM TTX, 10 μM CNQX and 50 μM AP5 were added to inhibit the network activity during the stimulation. All analyses were performed by an individual blind to the treatment conditions of the samples.

Electrophysiology

Pyramidal neurons were voltage-clamped to −70 mV using an Axopatch 200B amplifier and Clampex 8.0 software (Molecular Devices, Sunnyvale, CA), filtered at 2 kHz and sampled at 5 kHz at room temperature. The pipette solution contained (in mM): 115 Cs-$MeSO_3$, 10 CsCl, 5 NaCl, 10 HEPES, 0.6 EGTA, 20 tetraethylammonium chloride, 4 Mg-ATP, 0.3 Na_2GTP, 10 QX-314 (lidocaine N-ethyl bromide), pH 7.35, 300 mOsm (Sigma, St. Louis, MO). A modified Tyrode solution used as the extracellular solution contained (in mM): 150 NaCl, 4 KCl, 2 $MgCl_2$, 10 glucose, 10 HEPES, and 2 $CaCl_2$, pH 7.4, 310 mOsm. High K^+ solutions contained equimolar substitution of KCl (90 mM) for NaCl. To chelate intracellular Ca^{2+}, neurons were pretreated with either 2 μM BAPTA-AM for 30 minutes or 100 μM EGTA-AM for 10 minutes and washed for at least 5 minutes before recording. Folimycin (Calbiochem, La Jolla, CA) was dissolved in DMSO under dark. The exchange between extracellular solutions was achieved by direct perfusion of solutions onto the field of interest by gravity.

Fluorescence imaging

Hippocampal cultures were infected with lentivirus expressing the synaptophysin-pHluorin construct at 4 DIV or obtained from transgenic mice expressing synaptopHluorin exclusively at excitatory synapses. All imaging experiments were carried out after 14 DIV at room temperature. A Modified Tyrode's solution containing 2 mM Ca^{2+}, 10 μM CNQX and 50 μM AP-5 was used in all experiments. Baseline images were obtained every second for 30 s and cultures were challenged by direct perfusion of La^{3+}-containing or 47 mM K^{+}- containing Tyrode solutions onto the field of interest by gravity. To chelate intracellular heavy metals, cultures were incubated in the 10 μM BAPTA-AM for 15 min, or 100 μM EGTA-AM for 10 min. After 5 min wash, cells were challenged by bath application of 2 mM La^{3+}-containing Tyrode solution in the presence of 1 mM EGTA. Images were obtained by a cooled-intensified digital CCD camera (Roper Scientific, Trenton, NJ) during illumination at 480 ± 20 nm (505 DCLP, 535 ± 25 BP) via an optical switch (Sutter Instruments, Novato, CA). Images were acquired and analyzed using Metafluor Software (Universal Imaging, Auburn Hills, MI).

Data analysis

Two-tailed unpaired t-test was used for all statistical comparisons and values are given as mean ± SEM.

Results

Intact coupling of exo-endocytosis during La^{3+}-triggered neurotransmission at central synapses

Rapid action of La^{3+} does not interrupt synaptic vesicle recycling

Prior to employing La^{3+} -induced transmission as a tool to study the coupling of exo- and endocytosis, I evaluated whether synaptic vesicle recycling machinery is intact during La^{3+}-induced transmission. In order to examine vesicle recycling during La^{3+}-triggered rapid transmission, cultured neurons were incubated with EGTA-AM for 10 min prior to repeated applications of La^{3+}, to selectively prevent delayed action of La^{3+} on synaptic vesicle exocytosis (Chung et al., 2008). The extracellular solution contains 1 mM EGTA to chelate any heavy metals including Ca^{2+}. 2 mM La^{3+} was bath applied for 30 seconds for 4 times and removed from the extracellular solution for 1 min in between La^{3+} application (Figure 3.1).

A previous study suggested that La^{3+} selectively interrupts the endocytosis process at larval *Drosophila* neuromuscular junctions (Kuromi et al., 2004). If La^{3+} selectively blocks endocytosis while causing exocytosis at hippocampal synapses as reported at *Drosophila* neuromuscular junctions, attenuated synaptic responses are anticipated as La^{3+} application repeated, presumably due to depletion of functional synaptic vesicles. However, repeated applications of 2 mM La^{3+} were not observed to decrease the size of synaptic responses (Figure 3.1A-C). 2 mM La^{3+} could repeatedly trigger a comparable amount of neurotransmitter release, quantified as charge transfer in the presence of La^{3+} (Figure 3.1.C, grey bars, $P>0.7$), suggesting that synaptic vesicle recycling operates during rapid transmission triggered by 2 mM La^{3+}.

Synaptic vesicle recycling is in operation during rapid as well as delayed La^{3+}-triggered transmission

Earlier studies did not dissociate the rapid action of La^{3+} from its delayed action. To examine whether delayed neurotransmitter release triggered by La^{3+} contributes to the depletion of synaptic vesicles as seen at *Drosophila* neuromuscular junction synapses, 2 mM La^{3+} was repeatedly applied in the presence 2 mM Ca^{2+} and TTX, which preserves the delayed action of La^{3+}. A comparable amount of neurotransmitter release was observed with repeated La^{3+} application (Figure 3.1.C, white bars, $P>0.7$). It is possible that brief application of La^{3+} might trigger fusion of only a small fraction of synaptic vesicles, thus eliminating the requirement of recycling large fractions of synaptic vesicles. When synaptic responses were measured upon repeated La^{3+} application in the presence of vacuolar type ATPase (v-ATPase) inhibitor, folimycin (Drose and Altendorf, 1997), a stepwise reduction in synaptic responses was observed, suggesting that synaptic vesicles undergo recycling during brief La^{3+} application (Figure 3.9).

Another possibility is that the inhibitory action of La^{3+} on synaptic vesicle endocytosis is reversible, thus a pool of releasable synaptic vesicles can be restored during 1 min-long wash between La^{3+} applications. To induce maximal release with La^{3+}, 2 mM La^{3+} was continuously bath-applied for a prolonged time (up to 10 min). As shown in Figure 3.1.D, the prolonged application of La^{3+} does not lead to attenuation of synaptic responses, suggesting that synaptic vesicles are still available after a prolonged challenge in La^{3+}-containing solution. These results suggest that synaptic vesicles recycle during La^{3+}-triggered transmission, implying that the responsiveness of synaptic vesicles towards La^{3+} stimulation in central synapses could be different from that in neuromuscular junctions.

Normal ultrastructure of synapses after prolonged exposure to La^{3+}

In the proceeding set of experiments, the ultrastructure of synaptic terminals was analyzed after exposure to La^{3+} for a prolonged period. Hippocampal cultures were incubated with 2 mM Ca^{2+} or 2 mM La^{3+} for 10 min in the presence of TTX and images were obtained by using electron micrography (EM). The number of synaptic vesicles (SVs) per synapse was quantified and the density of SVs at synapses was estimated by measuring the cross section area of synaptic terminal (number of total SV/ cross section area of synaptic terminal). 10 min exposure to 2 mM La^{3+} does not cause any decrease in the number of total SVs or the estimated density of SVs per synapse (Figure 3.2, n=90-125 synapses, $P>0.5$). This result is in contrast to the data from earlier work in neuromuscular junctions (Segal et al., 1985).

The ultrastructural analysis of synapses after prolonged incubation with 2 mM La^{3+} reveals that synaptic vesicles are not depleted after La^{3+}-evoked neurotransmitter release. The ultrastructural data further support the electrophysiological data (Figure 3.1), suggesting that La^{3+}-induced transmission could be a useful tool to probe exo-endocytosis coupling as well as vesicle recycling in central synapses.

Nominal FM dye uptake and release during rapid La^{3+}-triggered neurotransmission

Very little, if any, FM dye uptake was observed during rapid action of La^{3+}

In order to further examine the properties of exo-endocytosis coupling during La^{3+}-evoked transmission, I took advantage of optical imaging techniques by employing FM dye, a well-known ampiphilic dye. Hippocampal synapses were incubated with 8 μM FM1-43 or 400 μM FM2-10 in the presence or absence of 2 mM La^{3+} or under depolarization (47 mM K^{+}) for 90 seconds to specifically label a subset of synaptic vesicles or a pool of maximal recycling synaptic vesicles, respectively. In contrast to electrophysiological recordings, detection of FM dye

uptake was comparable to baseline (Figure 3.3). The amount of FM dye uptake during La^{3+} stimulation was not different from background dye uptake measured in the absence of La^{3+} (Figure 3.3, $P>0.3$).

These contradictory observations can be due to either problem in detection or FM dye uptake in contrast to electrophysiological recordings. First, La^{3+} might not allow for the release of synaptic vesicles above the number necessary for the threshold of detection. If this is the case, La^{3+}-evoked vesicles were capable of taking up FM dye but could not be detected simply because the amount of dye taken up is not within the detection resolution of CCD camera.

To examine this possibility, the summation of neurotransmitter release during 2 mM La^{3+} stimulation for 30 seconds was compared with the amount of release during depolarization measured in the whole cell voltage clamp configuration. The cumulative charge release triggered by 2 mM La^{3+} for 30 seconds was 14 % of charges transferred by 47 mM K^+ (13.7 ± 0.4 %, n=4). The FM fluorescence intensity was in non-linear relationship with the electrophysiologically measured charge transfer amount, largely due to the higher background level with FM dye. Baseline synaptic activity measured as charge transfer per second (Q nC/s) was 8% of activity during 2 mM La^{3+} application. Given that the charge transfer per second (Q nC/s) during La^{3+} application was approximately 17-fold higher than baseline activity, significantly increased FM dye uptake was expected with 2 mM La^{3+} from background.

Second, synaptic vesicles released during La^{3+} stimulation are endocytosed but during the wash step, these dye-containing vesicles are all released due to an increase in the frequency of miniature postsynaptic current resulting from the delayed action of La^{3+}. La^{3+} induced 10 fold increase in synaptic activity in a delayed manner and this delayed facilitation in mEPSC and mIPSC lasted for more than 10 min in the absence of La^{3+} (Chung et al., 2008).

Thus, the total charge transferred immediately after La^{3+} stimulation (delayed effect) for 10 minutes can be comparable to the charge integrals by La^{3+} stimulation (rapid effect, for 30 seconds).

Very little, if any, FM dye release was detected upon La^{3+} application

Another reason for no detectable FM dye uptake during La^{3+} -induced transmission is that La^{3+} might block following endocytosis while concurrently triggering exocytosis as proposed earlier. According to this scenario, all vesicles fused by La^{3+} stimulation will fail to be endocytosed, hence leading to no FM dye uptake. For FM dye uptake, both synaptic vesicle fusion and endocytosis should occur in the presence of FM dye whereas detecting departition of FM dye which loaded upon depolarization requires only exocytosis events to occur. If nominal dye uptake is due to impaired endocytosis or due to loss of FM dye by delayed action of La^{3+} during wash, La^{3+}-driven fusion events are expected be detected as the form of FM dye release or loss in the synapses with synaptic vesicles previously marked by FM dye during depolarization.

Therefore, it was examined whether FM dye can be released while it can not be loaded into synaptic vesicles upon La^{3+} stimulation or not. FM dyes labeled synaptic vesicles belonging to the recycling pool at given synaptic terminals by exposure to 47 mM K^{+}-containing solution for 90 seconds. After a 10 min-long washout, synapses were challenged by either depolarization or 2 mM La^{3+} application while changes in fluorescence were monitored. As shown in Fig. 4, fast FM dye release upon 2 mM La^{3+} application was hardly detected in either type of FM dyes (Figure 3.4.A-D). Instead La^{3+} caused only steady dye loss, suggesting that FM dyes are reliable markers to detect La^{3+} -induced synaptic vesicle fusions. The loss of FM 2-10 was detected upon hypertonicity and after fast destaining by hypertonicity, synapses could also release FM dye further in response to depolarization (Figure 3.4.E-F). This result also rules out the possibility regarding to detection threshold. The amount and kinetics of dye loss

upon hypertonic solution is comparable to previously published work (Pyle et al., 2000), indicating the detection threshold of the setup is not questionable (Pyle et al., 2000; Stevens and Williams, 2000).

FM dye appears to be able to track delayed action of La^{3+}

However, FM dye seems to detect delayed transmission induced by La^{3+}. After FM2-10 uptake during 47 mM K^+ –induced depolarization, dye loss kinetics was observed at resting conditions (2 mM Ca^{2+}) or upon 2 mM La^{3+} application (Figure 3.5). The release kinetics during La^{3+} stimulation appears to be faster than at rest, suggesting that more dye loss or more exocytosis occurs in response to La^{3+} compared to 2 mM Ca^{2+} (Figure 3.5.A). The size of released synaptic vesicles (ΔF) during 5 min in La^{3+} was larger than at rest (Figure 3.5.B, $P<0.05$). This result further supports that a separate mechanism may mediate the delayed action of La^{3+} (Chung et al., 2008).

Why was no FM dye uptake detected during rapid release upon La^{3+} application? Given the contrary observations between electrophysiological results and optical data obtained from FM dye experiments, I hypothesized that La^{3+} drives a syb2-dependent, 'kiss and run' type exo- and endocytosis at central synapses. FM dyes are styryl dyes and require certain temporal and spatial characteristics of the fusion pore for incorporation into cell membranes. If La^{3+} triggers the formation of a narrow fusion pore, this fusion pore opening is expected to detect an exchange of neurotransmitter but not incorporation or departition of FM dye.

To examine this hypothesis, two additional probes, synaptopHluorin (spH) and horse radish peroxidase (HRP), were utilized. SynaptopHluorin (spH) is a fusion protein of pH-sensitive EGFP and synaptic vesicle protein (in this case, syb-2) and senses pH change. On the other hand, HRP is relatively large in size

(44 kDa) and can be visualized under EM after DAB reaction. Given the size of HRP, it is reasonable to surmise that HRP can not be taken up through a narrow fusion pore, whereas partial exposure of synaptic vesicles to the cytoplasm should not hinder the detection of pH change.

Correlated pHluorin signal upon La^{3+} stimulation

Monitoring of pHluorin –tagged synaptic protein trafficking has several advantages. First, unlike FM dyes, the loading step is unnecessary and thus no delay due to wash time is required. This is more useful in this case because La^{3+} has a prolonged effect once applied. Second, pHluorin signal can detect multiple rounds of exo- and endocytosis because the fluorescence changes upon pH is reversible. Third, both exocytosis and endocytosis can be detected and isolated by pHluorin fluorescence with the aid of pharmacological tools, while only fusion events of vesicles can be detected with FM dye.

The rapid effect of La^{3+} can be estimated by the fractional increase of fluorescence. 2 mM La^{3+} or 90 mM K^{+} was applied onto cultures obtained from a transgenic mouse (spH21), expressing synaptopHluorin (spH) exclusively at excitatory synapses (Figure 3.6). Upon stimulation, a correlated increase in fluorescence upon both stimulations was observed, which is followed by a swift decay upon wash reflecting vesicle endocytosis after the end of stimulation (Figure 3.6.A-B). The size of the response upon La^{3+} stimulation was about 30% of the fluorescence change upon depolarization (Figure 3.6.B *left*). The amount of release (ΔF) was normalized to the amount of fluorescence increase in response to 100 mM NH_4Cl. Normalized ΔF during La^{3+} - induced transmission was 18 % of normalized ΔF upon depolarization (Figure 3.6.B *right*). Repeated applications of La^{3+} induced a comparable increase of pHluorin signal, in correlation with electrophysiological recordings (Figure 3.6.B). This observation was reiterated in

hippocampal cultures infected with synaptophysin-pHluorin (sypHy) (Figure 3.6.C). The fluorescence change upon La^{3+} application was approximately 23 % of the change upon depolarization (Figure 3.6.D).

Repeated application of La^{3+} resulted in repeated rise and decay of pHluorin signal with similar size in response (Figure 3.6.E-F), which resembles electrophysiological detection of release in response to La^{3+} application (Figure 3.1.A).

Less HRP uptake during La^{3+}-triggered transmission

To selectively visualize synaptic vesicles released by La^{3+} stimulation at the ultrastructural level, synaptic vesicles (SVs) containing horseradish peroxidase (HRP) were quantified using electron microscopy (Heuser and Reese, 1973). Hippocampal cultures were exposed to depolarized (90 mM K^{+}) solution or 2 mM La^{3+} -containing solution for 90 seconds in the presence of HRP (25 mg/ml) and immediately fixed after DAB reaction (Figure 3.7). After depolarization, the number of HRP-positive SVs per synapse was around seven and half, which is ~ 11% of total vesicle pool (7.5±0.6/synapse, 11.5±1.5%, 90 synapses). In La^{3+} treated synapses, the number of HRP-positive SVs per synapse was less than one per synapse, which is less than 1% of total vesicle pool (0.6±0.1/synapse, 0.07±0.01%, 85 synapses). The HRP-containing synaptic vesicles during La^{3+} application was approximately 7.5% of HRP-labeling during depolarization, which is only half of the neurotransmitter release measured by electrophysiological recording (14% of charge transfer by 2 mM La^{3+} compared to the release elicited by depolarization).

The number of total SVs was comparable in the two groups as well as the estimated density of SVs (P>0.6). The morphology or distribution of SVs was not different between the two groups. No significant distortion in estimated density was observed between synapses containing HRP-positive synaptic vesicles and

HRP-negative vesicles, although smaller synapses tend to have no HRP during depolarization (Figure 3.8).

Synaptic vesicle recycling during La^{3+} stimulation

What are the characteristics of endocytosis during La^{3+}-triggered transmission? Is there any fast reuse of synaptic vesicles during La^{3+}-triggered transmission? To characterize vesicle endocytosis during La^{3+} –triggered transmission, folimycin, a high-affinity inhibitor of vacuolar type ATPase was employed (Drose and Altendorf, 1997). Folimycin inhibits the refilling of neurotransmitters by trapping vesicles in an alkaline state, thus providing a cumulative measure of exocytosis without the caveat of a potential decrease in fluorescence due to ongoing endocytosis events. (Sankaranarayanan and Ryan, 2001).

Cultures expressing spH were exposed to 40 nM folimycin for 3 minutes prior to La^{3+} application. Then, pHluorin signal changes were analyzed before and after folimycin treatment from the same set of synapses (Figure 3.9.A). Inhibition of synaptic vesicle refilling revealed an additional increase of pHluorin upon La^{3+} application, suggesting that La^{3+}-induced transmission is dependent on rapid synaptic vesicle reuse (Figure 3.9.A). This observation lends further support to the idea that La^{3+} does not impair the exo- and endocytosis coupling in central synapses or constant vesicle recycling during La^{3+} stimulation.

Moreover, I found that dynasore, a small molecule inhibitor of GTPase activity in dynamin, interrupted synaptic vesicle endocytosis during La^{3+} application (Figure 3.9.B), suggesting that vesicle reuse during La^{3+} –induced transmission depends on a conventional endocytic machinery requiring dynamin activity.

Next, postsynaptic currents in whole –cell voltage clamp configuration were measured upon repeated stimulation in the presence of 40 nM folimycin

(Drose and Altendorf, 1997). As shown in Figure 3.9.C, inhibition of v-ATPase function during La^{3+} reduced the neurotransmitter release when repeated. When stimulated for the second time, 2 mM La^{3+} induced only 70% of neurotransmitter release compared to the first application. Stimulation for 3rd and 4th time with 2 mM La^{3+} applications also induced 70-80% of neurotransmitter release when compared to the previous stimulation (Figure 3.9.C-D). Repeated La^{3+} stimulation in the presence of 40 nM folimycin resulted in pHluorin signals that also correlate with electrophysiological measurements (Figure 3.9.E-F).

PHluorin fluorescence in the presence of folimycin provides a cumulative measure of non-recycled vesicle exocytosis since folimycin blocks re-acidification, internalized vesicles remain fluorescent, and their reuse does not result in increased fluorescence. In contrast, electrophysiological recordings report the summation of neurotransmitter release from recycled as well as non-recycled vesicles. Therefore, comparisons between the kinetics of sypHy fluorescence increase in the presence of folimycin and the cumulative neurotransmitter release at the same stimulation can provide a wealth of information on the time course of synaptic vesicle reuse. Therefore, I compared the cumulative neurotransmitter release amount during La^{3+} application (both exocytosis and endocytosis occur) to pHluorin fluorescence change in the presence of folimycin (endocytosis is impaired –pure exocytosis is measured). As presented in Figure 3.9.G, the estimated synaptic vesicle reuse from the difference in sypHy and electrophysiological recordings starts 14 seconds after La^{3+} application, meaning that synaptic vesicles undergone La^{3+} -dependent fusion are undergoing another round of exocytosis in 14 seconds.

Why do the two optical probes display seemingly opposing results? If both fluorescent probes detect synaptic vesicle fusions as they occur, then the kinetic changes in both probes upon same stimulations should be comparable. Therefore,

the kinetics of two optical probes, FM dyes and pHluorin upon La^{3+} or 90 mM K^{+} application was compared (Figure 3.10). FM dyes and pHluorin exhibited comparable kinetics upon depolarization when normalized and scaled, whereas during La^{3+} stimulation, both probes showed quite disperse behavior (Figure 3.10.C-D). These observations suggest that La^{3+} -driven release is not fully detected by FM dyes. Moreover, the comparison of the rise and decay kinetics between FM dyes and pHluorin fluorescence can be a valuable tool to examine the fidelity of both optical probes and to evaluate the size of fusion pores.

Physiological relevance of 'kiss-and-run' mode of fusion

Thus far, the present observations strongly suggest that La^{3+} induces the 'kiss-and-run' mode of neurotransmission. However, is this observation physiologically relevant? I explored whether there are fusion events which can be readily detected by pHluorin fluorescence but not by FM dyes. Electrical stimulation is a well established method to elicit synaptic responses within a few milliseconds in electrophysiological recordings. Thus, I acquired images at the frequency of 5 Hz during different frequencies of stimulations to detect fluorescence changes with higher resolution, and carefully monitored pHluorin fluorescence rise and the release of FM dyes during stimulation (Figure 3.11). Stimulation was elicited at a time point of 10 seconds. Furthermore, data from stimulation at a time point of 200 ms was analyzed but for better resolution, the axis for intervals is extended. In the case of 10Hz stimulation, cells received 2 action potentials between two arrows, and for 30 Hz stimulation, around 6 action potentials were given. As shown in Figure 3.11, pHluorin –tagged vesicle protein trafficking successfully reflects the changes induced by electrical stimulation at the onset of all frequencies of stimulation (grey triangle), whereas FM1-43 –taken up vesicle trafficking exhibited a delay before the fluorescence loss started in a frequency –dependent manner (Figure 3.11.A-C). FM2-10 –taken up vesicle

trafficking showed shorter delay only at the onset of 10 Hz stimulation but prompt dye loss at the onset of 20 -30Hz stimulation, presumably due to their faster departition rate (Figure 3.11.D-F). These observations strongly suggest that partial opening and closure of the fusion pore is the dominant mode of neurotransmitter release at the beginning of a stimuli train.

In addition, the kinetics between fluorescent probes upon concurrent stimulation was compared (Figure 3.12). For comparison purposes, the changes in pHluorin fluorescence, FM1-43 or FM2-10 during the first 20 seconds after the onset of 10Hz, 20Hz, or 30Hz stimulation was normalized and scaled (n=300-500 synapses). In contrast to La^{3+} application (Figure 3.10), 10Hz stimulation elicits similar kinetics of fluorescence changes in spH and FM2-10 whereas FM1-43 exhibited slower dye release compared to spH (Figure 3.12.A). However, in the case of higher frequency stimulation, spH tends to report a faster rise of fluorescence (Figure 3.12.B-C and E-F). This result indicates that ‘kiss-and-run’ exo- and endocytosis increases as stimulation intensity increases.

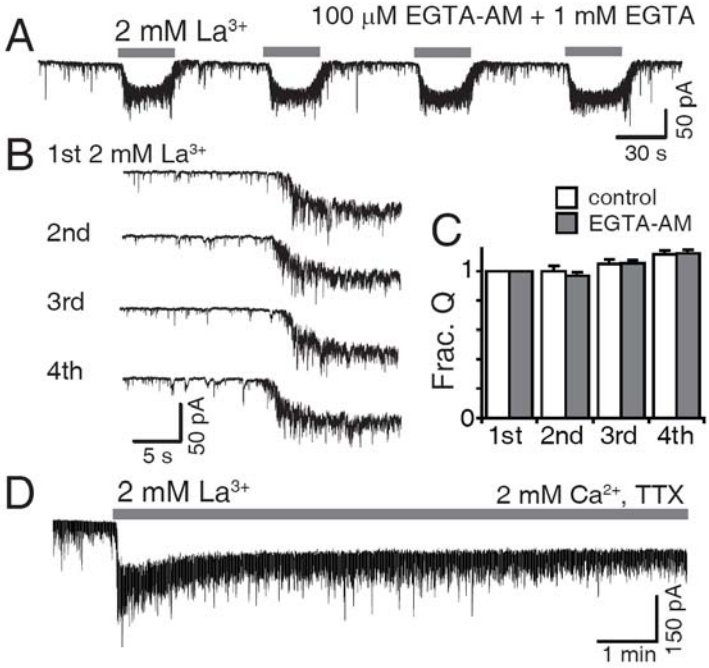

FIGURE 3. 1. Repeated La^{3+} application does not lead to depletion of available vesicles at hippocampal synaptic terminals.
(A) Cells were incubated with EGTA-AM for 10 min prior to repeated applications of La^{3+}, to prevent delayed action of La^{3+} on synaptic vesicle exocytosis. Extracellular solution contains 1 mM EGTA to chelate any heavy metals including Ca^{2+}. 2 mM La^{3+} was bath applied for 30 seconds for 4 times and removed from the extracellular solution for 1 min in between. (B) Synaptic responses during repeated La^{3+} application are shown in a magnified scale. (C) Fractional release by each application of 2 mM La^{3+} was quantified and no reduction in La^{3+} responses was observed (P>0.3). In the presence of Ca^{2+} , the fractional release by 2nd, 3rd and 4th La^{3+} was 1.0 ± 0.04, 1.05 ± 0.03, and 1.11 ± 0.03 (white bars), respectively. In the absence of Ca^{2+}, 0.97 ± 0.02, 1.06 ± 0.02, and 1.12 ± 0.02, respectively (grey bars, n=3), respectively. (D) Prolonged application of 2 mM La^{3+} for 10 min in the presence of Ca^{2+} and TTX also did not attenuate synaptic responses.

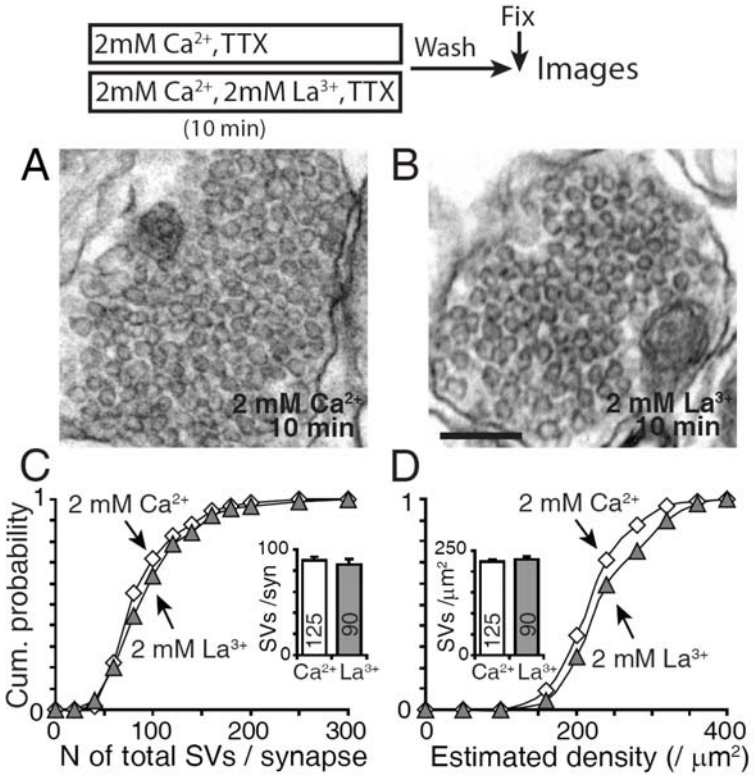

FIGURE 3. 2. Prolonged application of 2 mM La^{3+} does not decrease the number of synaptic vesicles at a given synaptic terminal.
(A, B) Sample EM images of synapses after 10 minutes in 2 mM La^{3+} or 2 mM Ca^{2+} (scale bar =200 nm). (C, D) Incubation in 2 mM La^{3+} has no effect on the distribution and average of total number of synaptic vesicles (SVs) per synapse as well as the estimated density of SVs. In control group, the number of total SVs per synapse was 89.5±3.4 and the estimated density was 224.1±5.2. When exposed to 2 mM La^{3+} for 10 min, the number of total SVs per synapse was 86 ± 4.6 and the estimated density was 228.9±6 (90-125 synapses, P>0.5).

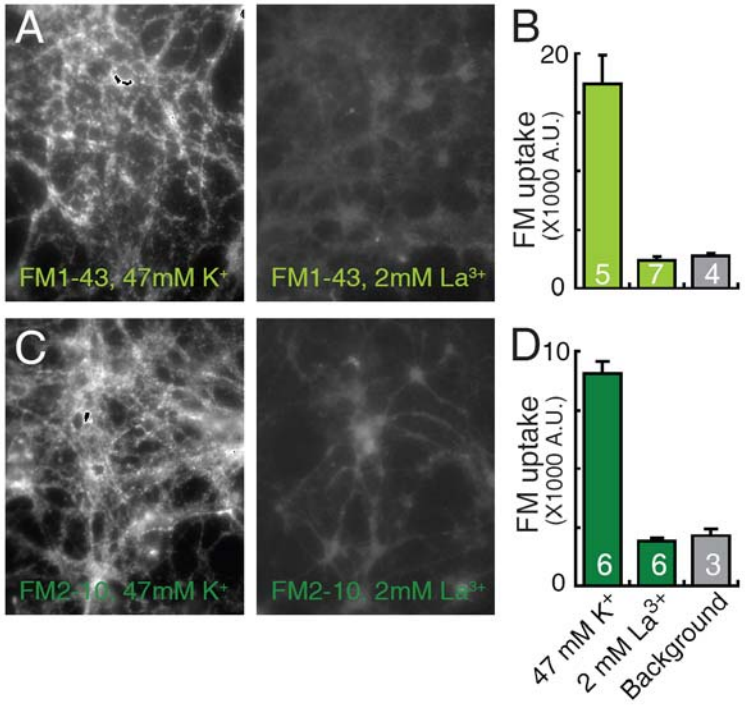

FIGURE 3. 3. There is minimal, if any, FM dye uptake upon 2 mM La^{3+} stimulation. (A, B) Neurons were stimulated with either 47 mM K^+ or 2 mM La^{3+} in the presence of 8 μM FM 1-43 for 90 seconds and excess dye was washed for 10 minutes. Images were taken at the end of wash. Fluorescence value for 47 mM K^+ and 2 mM La^{3+} loading were 17459±2362 (1065 synapses from 5 coverslips) and 2427±290 (900 synapses from 7 coverslips), respectively. La^{3+} loading was not more than background, which was 2761±244 (730 synapses from 4 coverslips, P>0.9). (C, D) The same loading protocol was used in the presence of 400 μM FM 2-10. Fluorescence value for 47 mM K^+ and 2 mM La^{3+} loading were 9029.03±520.12 (985 synapses from 6 coverslips) and 1905.08±120.86 (625 synapses from 6 coverslips), respectively. La^{3+} loading was not more than background, which was 2139.38±271.52 (520 synapses from 3 coverslips, P>0.3).

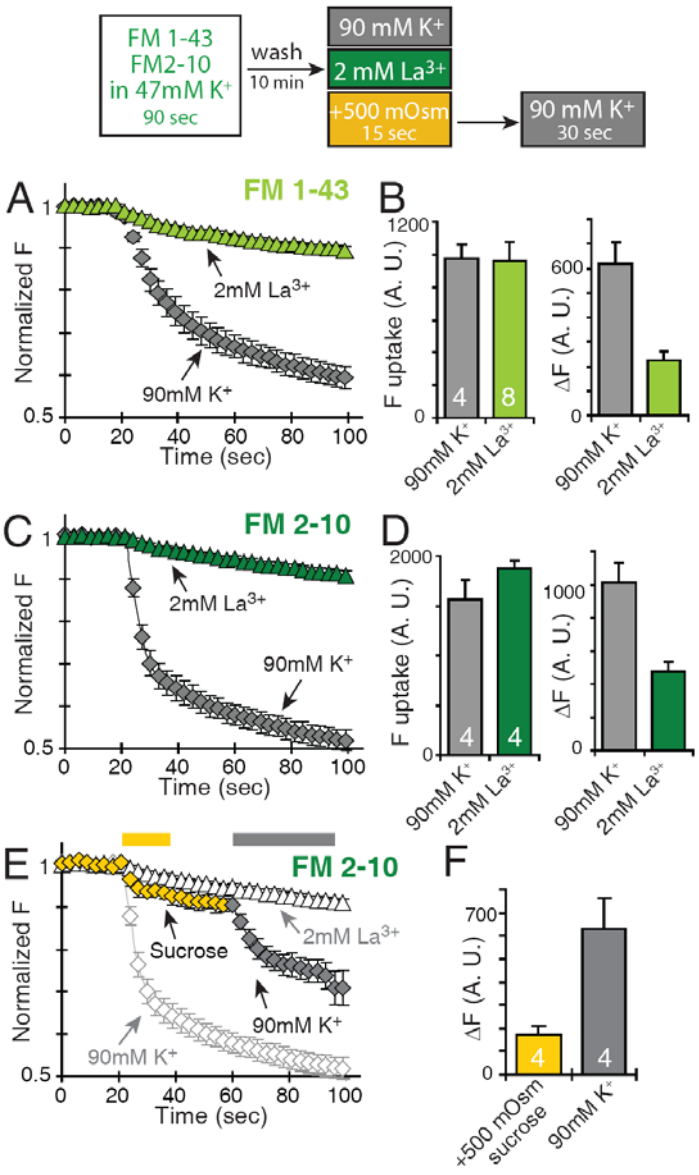

FIGURE 3. 4. There is very little, if any, FM dye loss upon 2 mM La^{3+} stimulation. After FM dyes maximally labeled synaptic vesicles belonging to recycling pool at given synaptic terminals, synapses were challenged by either depolarization as loaded, or 2 mM La^{3+} application while changes in fluorescence were monitored. (A, B) Kinetics of FM1-43 release upon 90 mM K^+ stimulation or 2 mM La^{3+} stimulation. 2 mM La^{3+} only caused a slower decrease in FM1-43 fluorescence level (n=4-8). After three rounds of 90 mM K^+

or 2 mM La^{3+} application for 90 seconds long each, total fluorescence amount released the during given stimulation (ΔF) was quantified. (C, D) FM2-10 also exhibited slower dye loss upon application of La^{3+} in contrast to depolarization (n=4, each). (F, G) FM2-10 could detect synaptic vesicle mobilization upon +500mOsm hypertonic sucrose stimulation, as previously reported (n=4, each).

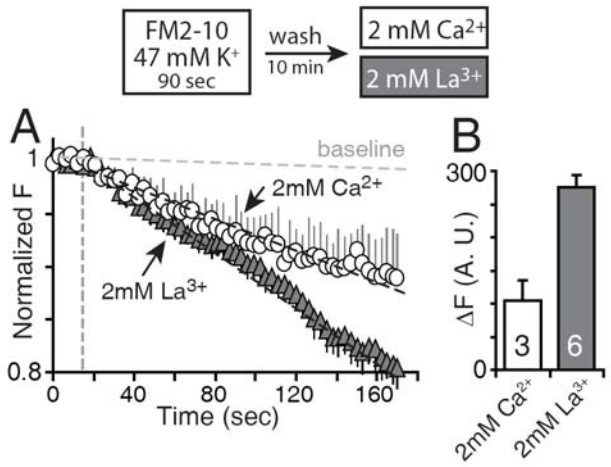

FIGURE 3. 5. FM dyes can detect delayed enhancement of synaptic activity during La^{3+}-triggered transmission.
(A) The release kinetics of FM2-10 upon 2 mM La^{3+} compared to resting condition showed slightly enhanced release although it was not significant (P>0.05 at all time points). (B) The amount of dye release during 3 min induced by La^{3+} was larger than spontaneous dye loss (P<0.05, n=3-6).

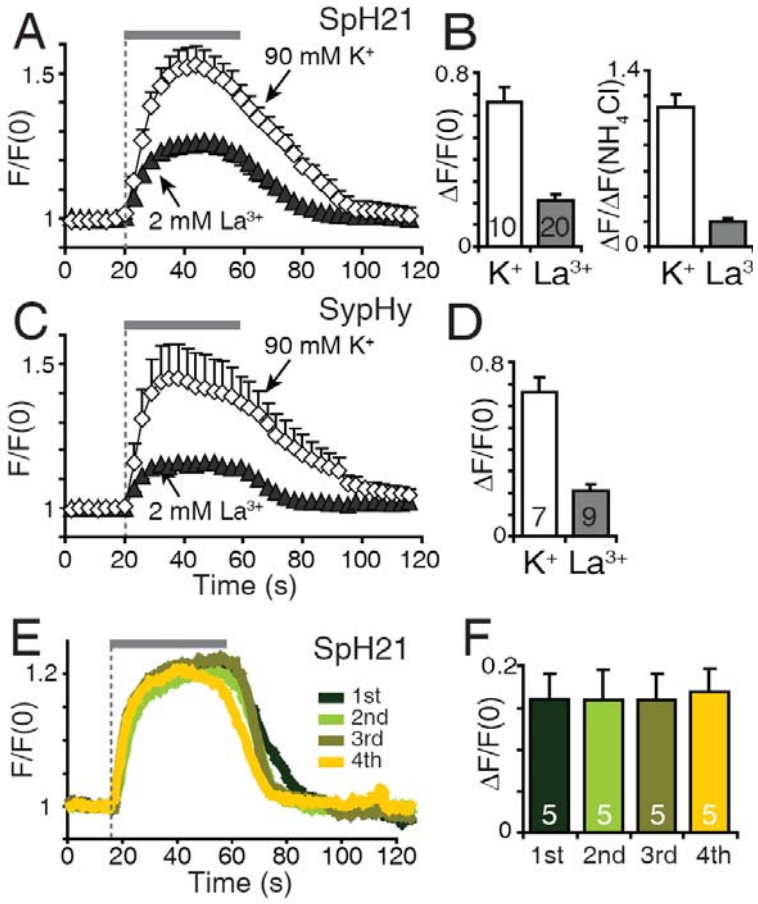

FIGURE 3. 6. SynaptopHluorin (spH) can detect robust exocytosis triggered by La^{3+}.

(A) Fluorescence changes were monitored during application of 2 mM La^{3+} in cultured hippocampal synapses expressing synaptopHluorin (spH) at excitatory synapses. Bath application of La^{3+} induced robust increase in fluorescence level (n=20), reflecting La^{3+}-triggered exocytosis. An increase in fluorescence was followed by a swift decay of pHluorin signal, presumably due to following endocytosis events. The behavior of spH upon depolarization is plotted for comparison (n=10). (B) Depolarization induced 66±7% increase of baseline fluorescence and 2 mM La^{3+} induced 21±3% increase. The size of ΔF in response to 100 mM NH_4Cl was used for normalization. The amount of increase in fluorescence ($\Delta F/\Delta F(NH_4Cl)$) induced during 2 mM La^{3+} application was 18 % of release during depolarization. (C, D) Hippocampal cultures infected with sypHy also exhibited a

prompt rise and decay of fluorescence upon La^{3+} application. Depolarization induced 68±10% increase of baseline fluorescence and 2 mM La^{3+} induced 16±2% increase (n=7-9). (E, F) Repeated application of 2 mM La^{3+} induced repeated increase of fluorescence as seen in electrophysiological recordings. The amount of release was comparable (n=5).

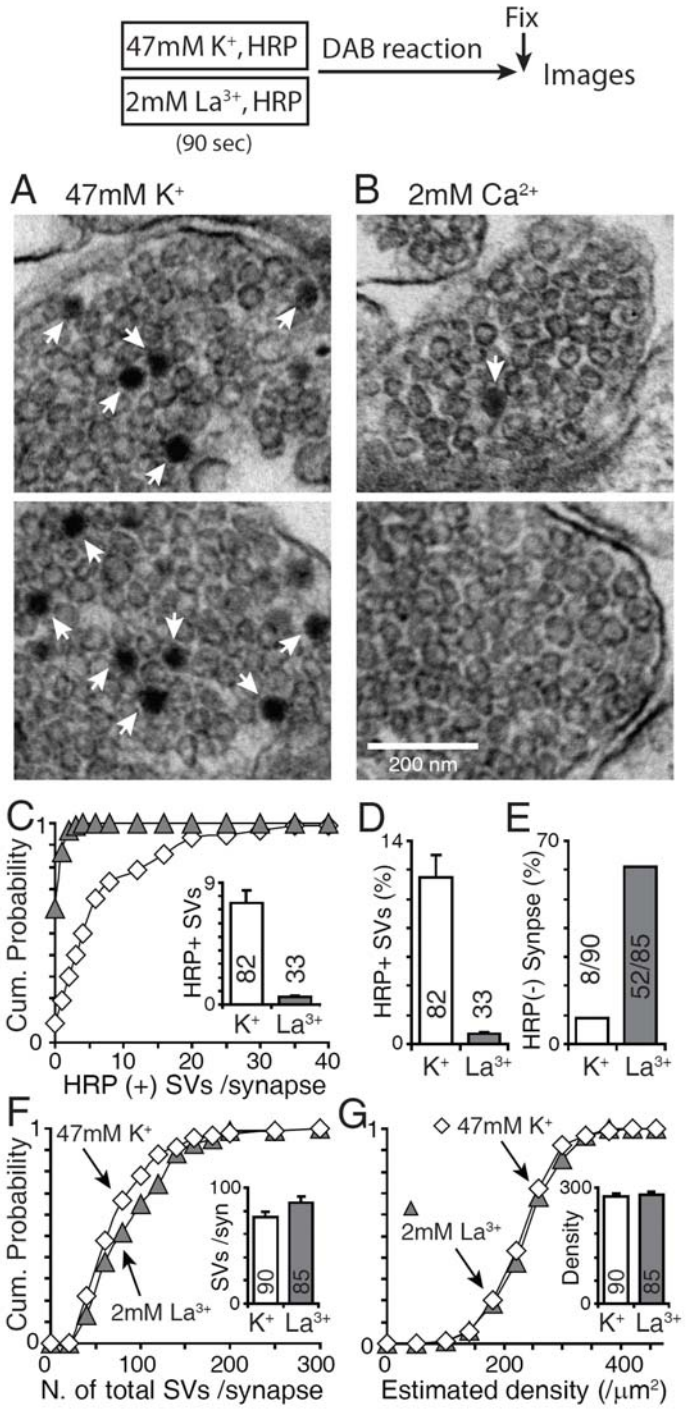
47mM K+, HRP
2mM La3+, HRP
(90 sec)
DAB reaction
Fix
Images
A 47mM K+
B 2mM Ca2+
200 nm
C
Cum. Probability
HRP (+) SVs /synapse
HRP+ SVs
82
33
K+ La3+
D
HRP+ SVs (%)
82
33
K+ La3+
E
HRP(-) Synpse (%)
8/90
52/85
K+ La3+
F
47mM K+
2mM La3+
Cum. Probability
N. of total SVs /synapse
SVs /syn
90
85
K+ La3+
G
47mM K+
2mM La3+
Estimated density (/μm2)
Density
90
85
K+ La3+

FIGURE 3. 7. Synaptic vesicles released upon La^{3+} take up less HRP than expected. Synapses were incubated with 25 mg/ml of HRP for 90 seconds during depolarization or in the presence of 2 mM La^{3+} prior to DAB reaction and fixation. (A-B) Sample EM images of synapses after 90 seconds in 47 mM K^+ or 2 mM La^{3+}, containing HRP-positive synaptic vesicles (Scale bar=200nm). (C) The distributions of HRP-positive SVs in both conditions are quantified. The average number of HRP-positive SVs was 7.5±0.9 and 0.6±0.1 in 47 mM K^+– and 2 mM La^{3+}– stimulated synapses, respectively. (D) The relative number of HRP-positive synaptic vesicles per synapse was quantified. In depolarized synapses, 12±1.5% of synaptic vesicles per synapse contained HRP while less than 1% of synaptic vesicles were HRP-positive in 2 mM La^{3+}-treated synapses (85-90 synapses, $P<0.001$). (E) Upon depolarization, 9% of synapses (8 out of 90 synapses) contain no HRP-positive synaptic vesicles while 61% of synapses (52 out of 85 synapses) do not have any HRP-positive synaptic vesicles. (F) The distributions of the number of total SVs per synapses in both conditions are plotted. The average of total SVs per synapse was 74.5±4.6 and 86.9±5.2 in 47 mM K^+– and 2 mM La^{3+}– stimulated synapses, respectively ($P>0.5$). (G) The distributions of the estimated density of SVs in both conditions were comparable. The average of estimated density of total SVs was 230±6.2 and 233.9±6.2 per mm^2 in 47 mM K^+– and 2 mM La^{3+}– stimulated synapses, respectively. (85-90 synapses, $P>0.6$)

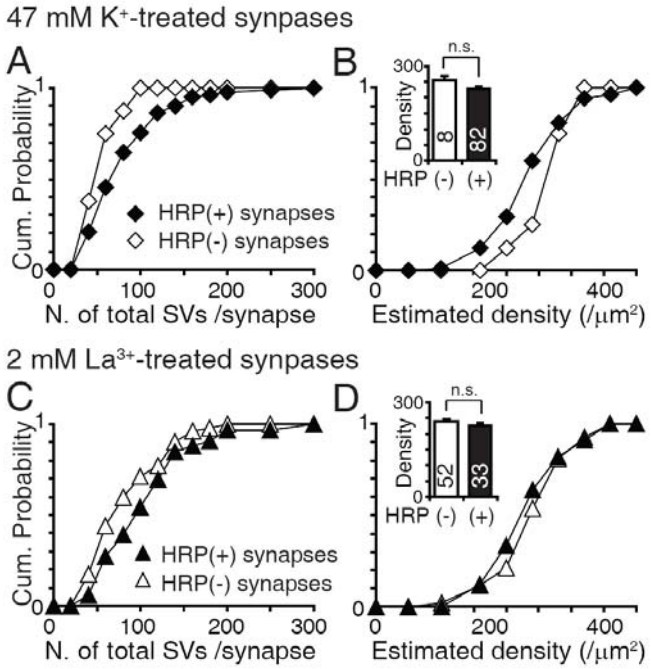

FIGURE 3. 8. Less HRP uptake is not due to synaptic abnormality induced by incubation with La^{3+} or depolarization challenge.
The total number of synaptic vesicles (SVs) per synapse as well as estimated density (/μm^2) was analyzed separately in synapses containing HRP-positive synaptic vesicles and in synapses without HRP-positive synaptic vesicles after depolarization (A, B) and La^{3+} application (C, D). No significant distortion in estimated density was observed between synapses (P>0.2 for 47 mM K^+ and P>0.3 for 2 mM La^{3+}) although smaller synapses tend to have no HRP (P=0.054 for 47 mM K^+, P=0.06 for 2 mM La^{3+}).

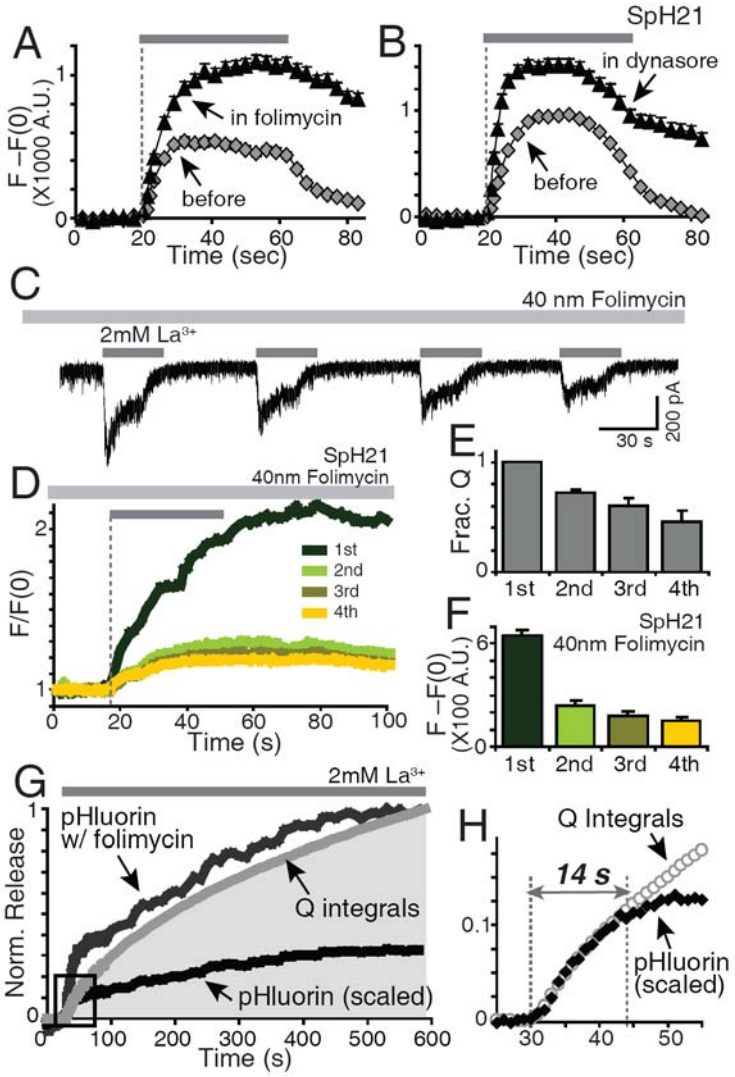

FIGURE 3. 9. SpH signals can successfully report endocytosis during La^{3+}-induced transmission.

(A) Incubation with 40 nM folimycin reveals additional increase in pHluorin signals by uncovering an endocytic component during La^{3+} bath application, suggesting synaptic vesicles recycle during La^{3+}-triggered transmission (n=6). (B) Synaptic vesicle recycling during La^{3+}-induced transmission is dependent on GTPase activity of dynamin. In the presence of 80 μM dynasore, an additional increase in pHluorin signals was observed

presumably due to impaired endocytosis (n=5). (C-F) Synaptic activity and pHluorin fluorescence changes are monitored during repeated application of 2 mM La^{3+} in the presence of 40 nM folimycin. (C, E) Neurotransmitter release measured as postsynaptic currents gradually decreases as repeatedly challenged with 2 mM La^{3+}, suggesting an operation of synaptic vesicle recycling during La^{3+}-evoked transmission. (D, F) pHluorin fluorescence is monitored during repeated application of 2 mM La^{3+} in the presence of 40 nM folimycin. ΔF (%) of increase in the presence of folimycin decreased with repeated La^{3+} stimulation. (G) The comparison of charge transfer (measuring both exo and endocytosis) and pHluorin signal in the presence of folimycin (measuring exocytosis only) for 10 min in 2 mM La^{3+}. The difference between these optical and electrophysiological measures provides an independent estimate of synaptic vesicle reuse. (H) When pHluorin signal in the presence of v-ATPase blocker is scaled, it starts to diverge from the normalized charge transfer at approximately 14 seconds, suggesting that during La^{3+}-evoked exocytosis, exocytosed synaptic vesicles are ready for re-use approximately after 14 seconds.

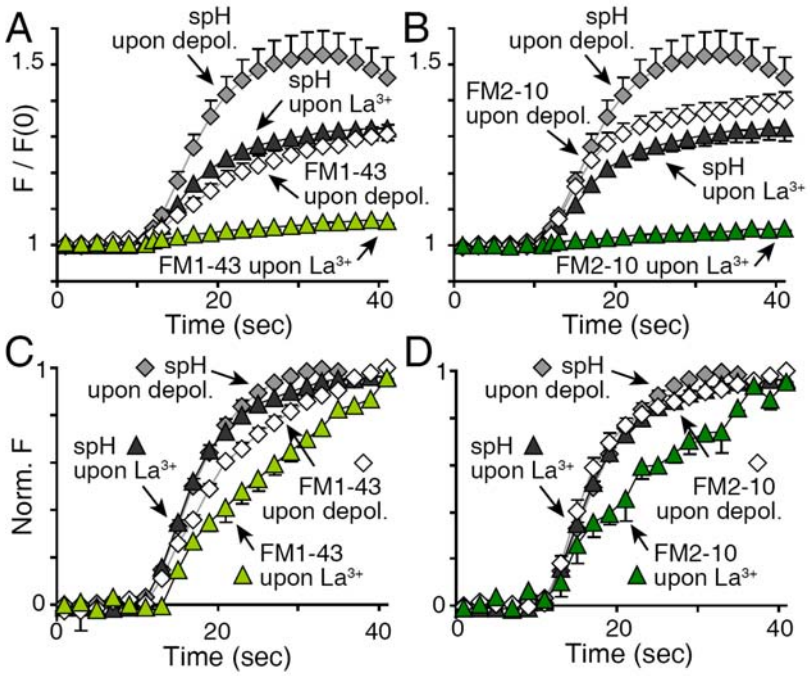

FIGURE 3. 10. The kinetics of fluorescence changes in FM dye and pHluorin upon depolarization or 2 mM La^{3+} application.

(A, B) The changes in pHluorin signal during the first 30 seconds in 47 mM K^{+} or 2 mM La^{3+} was compared to in FM1-43 or FM2-10 during corresponding time course (n=4-20). For the sake of comparison, fluorescence changes in FM dyes were inverted. (C, D) The change in fluorescence during 30 seconds of stimulation was normalized and scaled. The kinetics of fluorescence changes in both spH and FM dyes were robust upon depolarization, whereas the robust increase of fluorescence change upon La^{3+} application was only detected with spH but not with FM1-43 or FM2-10. Both FM dyes report linear or slower rate of increase in fluorescence upon La^{3+} application, in contrast to depolarization. Note that upon depolarization, FM1-43 reports synaptic vesicle fusion slower than pHluorin compared to FM2-10.

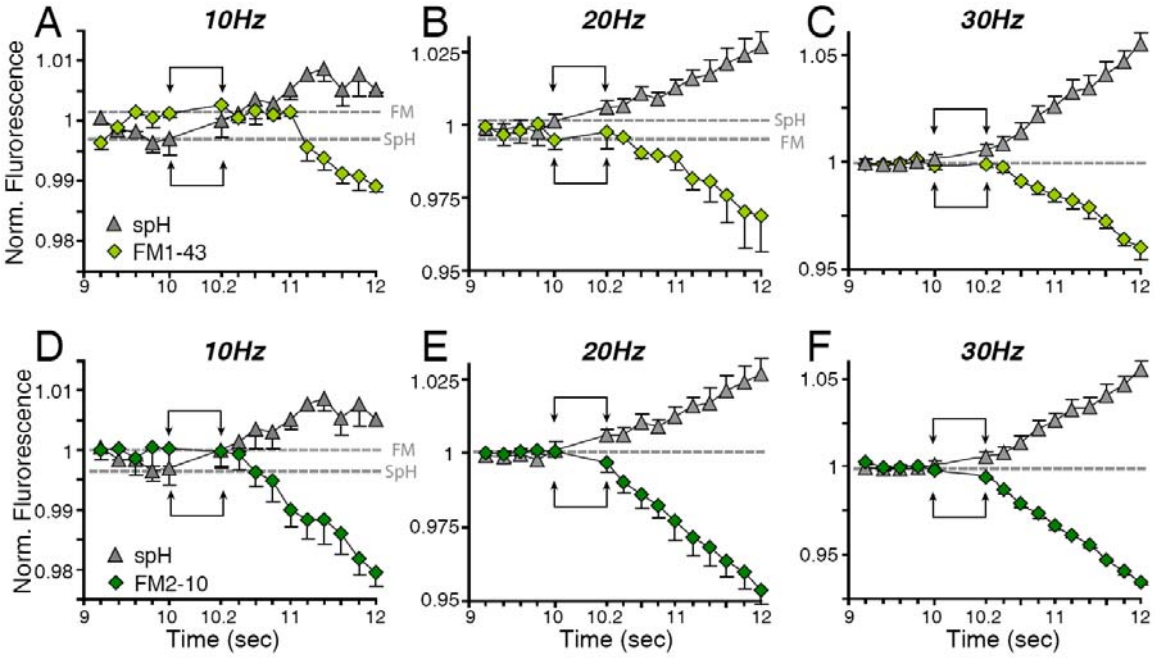

FIGURE 3. 11. At the onset of moderate stimulation, the synaptic activity is selectively detected by spH

Images were acquired every 200 ms to detect the behavior of spH and FM dyes at the onset of stimuli train. Stimulation elicited at the time point of 10 seconds, and for comparison purposes, the next 200 ms point is displayed with an extended interval. Stimulation was started at the 10 second time point. The duration indicated with a set of arrows is the first 200 ms after stimulation. (A) After 2 action potentials at 10Hz, spH successfully showed an increase in fluorescence but FM 1-43 release starts approximately 1 second after. (B) 4 action potentials at 20 Hz initiated the rise of spH fluorescence but not the release of FM 1-43. (C) 6 action potentials at 30 Hz still did not cause FM1-43 dye loss. FM dye loss was observed 400 ms after the onset of stimulation. (D) 2 action potentials at 10Hz did not induce the release of FM2-10 –taken up vesicles. (E, F) FM2-10 exhibited prompt dye loss at the onset of 20 -30Hz stimulation, presumably due to their faster departition rate compared to FM1-43.

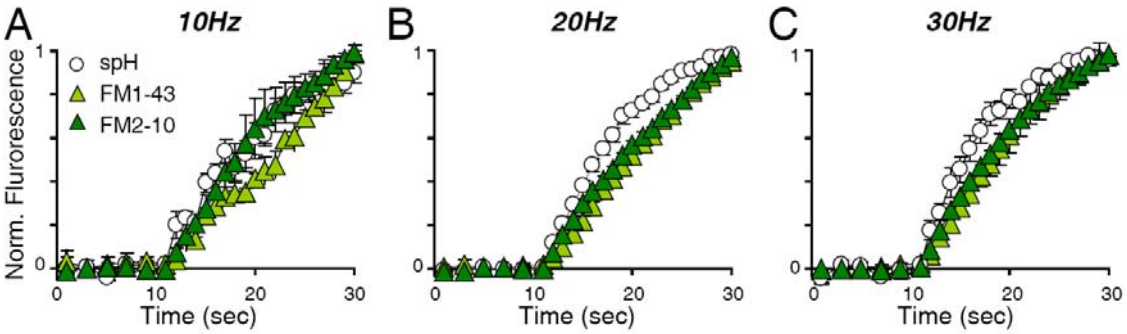

The kinetics of fluorescence changes in FM dye and pHluorin during electrical stimulation.

The changes in pHluorin fluorescence, FM1-43 or FM2-10 during first 20 seconds of 10Hz, 20Hz, or 30Hz stimulation was normalized and scaled during corresponding time course (n=300-500 synapses from 3-5 coverslips). (A) During 10Hz stimulation, the similar kinetics of fluorescence changes in spH and FM2-10 was observed whereas FM1-43 exhibited slower dye release compared to spH (P<0.05 during 13-16 second). (B) SpH tends to report a faster rise of fluorescence upon 20Hz stimulation (P<0.05 during 13-23 second for FM1-43, 15-25 second for FM2-10). (C) 30Hz stimuli train increased SpH fluorescence changes when compared to FM dyes. (P<0.05 during11-19 second for FM1-43 and during 15-25 second for FM2-10).

Discussion

'Kiss-and-run' mode of transmitter release during La^{3+} –triggered neurotransmission

La^{3+} triggers robust neurotransmitter release in a strictly SNARE-dependent manner, independent of both extracellular and intracellular Ca^{2+}, as shown in chapter 2. This is a very unique characteristic of La^{3+} as a secretagogue because other secretagogues depend on the functional SNARE assembly but do not necessarily mediates SNARE-dependent fusions only. For example, synaptobrevin 2-deficient synapses still respond to hypertonic challenge (Schoch et al., 2001) and α-latrotoxin-induced fusion is able to trigger exocytosis without the activation of the conventional SNARE-mediated fusion machinery (Deak et al., 2009).

In optical experiments, La^{3+}-induced fusion permits less uptake of HRP into synaptic vesicles as well as only nominal FM dye uptake or release, whereas the fluorescence of pHluorin-tagged synaptic vesicle proteins increased instantly upon La^{3+} stimulation, reflecting exocytosis triggered by La^{3+}. A reasonable explanation for this discrepancy is that the fusion induced by the rare earth metal, La^{3+}, is mediated through a transient fusion pore, which is not sufficient in size for FM dye to incorporate into or departition from the lipid membrane and not for HRP to be fully loaded into synaptic vesicles, while allowing proton and neurotransmitter diffusion. Therefore, I suggest that La^{3+} triggers a SNARE-dependent, so called 'kiss-and-run' type neurotransmitter release and propose La^{3+} as a valuable secretagogue to probe exo- and endocytosis coupling during narrow fusion pore opening events at central synapses. This is not only important to better understand one of the longest standing enigmas of synaptic transmission, namely the mechanism of action of rare earth metals on neurotransmission, but

also is a critical element to examine the properties of exocytosis-endocytosis coupling in isolation of other modes of fusion under physiological circumstances.

Properties of endocytosis during La^{3+} –triggered neurotransmission

Several lines of observations suggest that La^{3+} induces neurotransmitter release without impairing endocytic machinery in central synapses in contrast to neuromuscular junction synapses (NMJ) (Segal et al., 1985) or in *Drosophila* synapses (Kuromi et al., 2004). In central synapses, synaptic responses can be detected upon repeated application of La^{3+} without exhaustion (Figure 3.1) and increased pHluorin fluorescence upon La^{3+} application was followed by a rapid decay (Figure 3.6). Moreover, the decay of spH fluorescence after La^{3+} stimulation was sensitive to a v-ATPase blocker, folimycin and a dynamin inhibitor, dynasore (Figure 3.9), suggesting that endocytosis during and after La^{3+} application depends on similar molecular machinery widely used for vesicle reuse.

The opposing observations upon concurrent stimuli between central synapses are not surprising any more. Historically, synaptic stimuli such as 90mM –induced depolarization or α –latrotoxin have shown to deplete NMJ synaptic terminals but not central synaptic terminals (Gennaro et al., 1978; Sara et al., 2002), suggesting that the ruling of two synapses might be quite different. One of possible mechanisms that central synapses operate could be the fast synaptic re-use. The rapid re-use of synaptic vesicles which have undergone exocytosis for next round of fusion may contribute to prevent synaptic vesicle depletion in central synapses (Sara et al., 2002).

'Kiss-and-run' mode of transmitter release at the onset of stimulation as well as during intense stimulation

In addition, I improvised the analysis between two optical probes –FM dyes and pHluorin. For example, the detection disparity between FM dye release

and neurotransmitter release has been suggested as a powerful evidence of the 'kiss-and-run' mode of vesicle trafficking (Stevens and Williams, 2000). This hypothesis was further investigated with expanded probes, thus providing detailed and convincing evidence. The comparison of kinetics as well as the onset of fluorescence responses upon same stimulation serves as a useful analysis tool to evaluate the fusion pore size. Furthermore, the disparity between FM dyes and pHluorin is observed at the onset of stimulation and increases at intense stimulation. These observations share similar characteristics with a previous study (Zhang et al., 2009). The present study will significantly contribute to the field of synaptic transmission by proposing an instrumental tool to study the properties of 'kiss-and-run' type synaptic vesicle retrieval after SNARE-dependent fusion in central synapses.

CHAPTER FOUR
THE RELATIONSHIP BETWEEN EVOKED AND SPONTANEOUS SYNAPTIC VESICLE TRAFFICKING

Background

Synapses sustain three forms of neurotransmitter release with distinct Ca^{2+}-dependence and time course, mediated by synchronous, asynchronous and spontaneous vesicle fusion (Neher and Sakaba, 2008). Despite recent advances in understanding of the mechanisms that underlie the Ca^{2+}-dependence of these three forms of release (Lou et al., 2005; Neher and Sakaba, 2008; Sun et al., 2007; Xu et al., 2009), summarized in chapter one, the extent at which their maintenance relies on synaptic vesicle recycling remains unclear (Ertunc et al., 2007; Groemer and Klingauf, 2007; Li et al., 2005; Lin et al., 2005). In addition, to date it remains uncertain whether these three forms of neurotransmission originate from the same vesicle pool.

To address this question, I targeted dynamin, which is required to pinch synaptic vesicles off from the plasma membrane during endocytosis (Cremona and De Camilli, 1997). Dynamin belongs to a family of large GTPases, and forms rings and spirals along the neck of nascent synaptic vesicles and thereby generate constriction and mediate scission events (Cremona and De Camilli, 1997; Hinshaw, 2000; Marks et al., 2001; Praefcke and McMahon, 2004; Roux et al., 2006). In the mammalian brain, three isoforms of dynamin is expressed and among then, dynamin 1 is exclusively expressed in the brain (Cao et al., 1998).

Although dynamin has been implicated to play a major role in endocytosis (Kawasaki et al., 2000; Yamashita et al., 2005) by mediating clathrin-dependent endocytosis (Marks et al., 2001), dynamin 1 deficient mice exhibited little

phenotype in synaptic morphology (Ferguson et al., 2007). This might not be a big surprise to consider that a seemingly GTP-independent or clathrin-independent membrane retrieval has been reported in retinal bipolar cells (Heidelberger, 2001; Jockusch et al., 2005). Recently, GTP-independent form of endocytosis has been proposed at calyx of Held synapses (Kramer and Kavalali, 2008; Xu et al., 2008) as well as in dorsal root ganglion neurons (Zhang et al., 2004).

Dynamin ability to trigger vesicle scission requires GTP hydrolysis in a reaction that can be reversibly inhibited by dynasore, a selective small molecule inhibitor of dynamin1 and 2 GTPases (Kirchhausen et al., 2008; Macia et al., 2006). Dynasore is Previous work using synaptopHluorin-based monitoring of synaptic vesicle trafficking has shown that dynasore is a dose-dependent inhibitor of synaptic vesicle endocytosis (Newton et al., 2006). This acute inhibition strategy provided two particular advantages in assessing the impact of dynamin-dependent synaptic vesicle recycling on neurotransmission. First, acute dynamin inhibition does not provide sufficient time for homeostatic compensation of dynamin function. For instance, such compensation has been reported for mouse knockouts of P/Q-type voltage-gated calcium channels, which manifest a milder impairment of synaptic transmission compared to the one seen after acute inhibition of channel function (Piedras-Renteria et al., 2004). And this could be the reason why little abnormality is exhibited in dynamin 1 knockout mice (Ferguson et al., 2007). Second, reversible nature of dynasore-mediated dynamin inhibition allowed us to monitor the recovery kinetics of neurotransmission from inhibition.

These results suggest that the maintenance of evoked synchronous or asynchronous release strictly depends on dynamin function at a rapid time scale, whereas spontaneous release does not require dynamin activation for up to 1 hour. In contrast, spontaneous neurotransmission can be maintained at normal levels

even after complete depletion of vesicle pools that sustain Ca^{2+}-evoked neurotransmission. These findings imply that spontaneous recycling operates independent of evoked recycling machinery without a strict requirement for dynamin activation.

Materials and Methods

Dissociated and organotypic slice culture

Dissociated hippocampal cultures were prepared from postnatal Sprague-Dawley rats as previously described (Kavalali et al., 1999a). Unless stated otherwise, all experiments were carried out after 14 days *in vitro* (DIV) when synapses reach maturity comparable to mature brain (Mozhayeva et al., 2002).

For slice experiments 400 μm thick transverse hippocampal slices were prepared from postnatal day 6-8 mice pups expressing synaptopHlourin selectively in inhibitory synapses (spH64, gift of Dr. Venkatesh Murthy, Harvard University) using a McIlwain tissue chopper and maintained *in vitro* on Millicell-CM filter inserts (Millipore, Bedford, MA). Culture medium was composed of Minimum Essential Medium containing 20% Equine Serum (HyClone, Logan, UT), 0.0012% ascorbic acid, 1 mM L-glutamine, 1 mM $CaCl_2$, 2 mM $MgSO_4$•7 H_2O, 12.87 mM Dextrose, 5.25 mM $NaHCO_3$, 30 mM HEPES, and 0.17 mM Insulin. Culture media was replaced after 24 hrs with media containing 1 g/mL FUDR. After 24 hrs incubation in FUDR, culture media was replaced with media containing no FUDR and subsequently changed every 2 days. Experiments were carried out between 9-15 days *in vitro*.

Dynamin 1 GTPase activity assay

Dynamin 1 was expressed and purified from baculovirus-infected Sf9 cells following previously published procedures (Achiriloaie et al., 1999). GTPase activities of dynamin were measured by the release of ^{32}Pi from [G-^{32}P]GTP by charcoal-based method (Higashijima et al., 1987) after incubation at room temperature for 15 min in a buffer containing 20 mM HEPES, pH 7.5, 0.1 M NaCl, 4 mM $MgCl_2$ and 1 mM GTP. PIP_2- Phosphatidylcholine (1:9 molar ratio) vesicles were prepared in 20 mM HEPES, pH 7.5 as described previously (Barylko et al., 1998).

Electron microscopy

For horseradish peroxidase (HRP) uptake experiments, hippocampal cultures were depolarized with 90 mM K^+-containing Tyrode solution and after removal of 90 mM K^+ solution they were incubated with 25 mg ml^{-1} HRP (Sigma) for 15 min in 1 μM TTX, 10 μM CNQX and 50 μM AP5 either with 80 μM dynasore or 0.2% DMSO. After HRP incubation cells were washed twice with buffer and immediately fixed with 2% glutaraldehyde in 0.1 M sodium phosphate buffer, pH 7.4 at 37°C and washed with Tris-Cl (100 mM, pH 7.4) buffer. Then, cells were incubated with 3,3'-diaminobenzidine (0.1% DAB, Sigma) in Tris-Cl buffer and H_2O_2 (0.02%) for 15 min (DAB reaction), and washed with Tris-Cl buffer. At this point cells were incubated in 1% OsO_4 for 30 min at room temperature and stained *en bloc* with 2% aqueous uranyl acetate for 15 min, dehydrated in ethanol, embedded in Poly/Bed 812, (Polysciences Inc, Warrington, PA, USA) for 24 hrs. 60 nm thick sections were post-stained with uranyl acetate and lead citrate. Images were obtained with a JEOL 1200 EX transmission microscope. All analyses were performed by an individual blind to the treatment conditions of the samples.

Electrophysiology

Pyramidal neurons were voltage-clamped to −70 mV using an Axopatch 200B amplifier and Clampex 8.0 software (Molecular Devices, Sunnyvale, CA), filtered at 2 kHz and sampled at 5 kHz. The pipette solution contained (in mM): 115 Cs-$MeSO_3$, 10 CsCl, 5 NaCl, 10 HEPES, 0.6 EGTA, 20 tetraethylammonium chloride, 4 Mg-ATP, 0.3 Na_2GTP, 10 QX-314 (lidocaine N-ethyl bromide), pH 7.35, 300 mOsm (Sigma, St. Louis, MO). A modified Tyrode solution used as the extracellular solution contained (in mM): 150 NaCl, 4 KCl, 2 $MgCl_2$, 10 glucose, 10 HEPES, and 2 $CaCl_2$, pH 7.4, 310 mOsm. High K^+ solutions contained equimolar substitution of KCl (90 mM) for NaCl. The recordings were not corrected for the liquid junction potential (~12 mV). Under this recording

condition, the equilibrium potential for Cl^- was estimate at -40 mV, therefore inward inhibitory current was able to be recorded without altering the standard pipette solution. To record and isolate inhibitory postsynaptic currents (IPSCs) ionotropic glutamate receptor antagonist, 6-cyano-7-nitroquinoxaline-2,3-dione (CNQX; 10 μM; Sigma), and aminophosphonopentanoic acid (AP-5; 50 μM; Sigma) were added to the bath solution. Spontaneous IPSCs were recorded in the same condition without field stimulation and miniature IPSC (mIPSC, or minis) were recorded in the addition of 1 μM TTX. mIPSC events were analyzed manually to avoid false positive and false negative events. The detection threshold amplitude of mIPSC was 4pA and the standard deviation of the baseline noise was 1.46±0.2 pA. Dynasore (Sigma, St. Louis, MO) was dissolved in DMSO under dark. To elicit evoked responses, electrical stimulation was delivered through parallel platinum electrodes in modified Tyrode's solution (duration, 1 ms; amplitude, 20 mA). The exchange between extracellular solutions was achieved by direct perfusion of solutions onto the field of interest by gravity. All the experiments were performed at room temperature.

Fluorescence imaging

The synaptophysin-pHluorin construct contained two pHluorins and was a generous gift of Drs. Y. Zhu and C.F. Stevens (The Salk Institute, La Jolla, CA). Hippocampal cultures were infected with lentivirus expressing the synaptophysin-pHluorin construct at 5 DIV and imaging experiments were carried out after 14 DIV at room temperature. A Modified Tyrode's solution containing 2 mM Ca^{2+}, 10 μM CNQX and 50 μM AP-5 was used in all experiments. Baseline images were obtained every second for 30 s and cultures were stimulated with field stimulation. After incubation with 80 μM dynasore (Sigma, St Louis, MO) dissolved in DMSO (Sigma, St Louis, MO) stimulation was repeated on the same set of synaptic boutons. Images were obtained by a cooled-intensified digital CCD camera (Roper Scientific, Trenton, NJ) during

illumination at 480 ± 20 nm (505 DCLP, 535 ± 25 BP) via an optical switch (Sutter Instruments, Novato, CA). Images were acquired and analyzed using Metafluor Software (Universal Imaging, Auburn Hills, MI).

For experiments on organotypic slice cultures, slices were perfused with a modified Tyrode's solution and stimulated by application of a Tyrode's solution containing 47 mM K^+. Images were obtained using a Nikon D-Eclipse C1 confocal microscope and analyzed using EZ-C1 imaging software.

Data analysis

For kinetic analysis of asynchronous release, decay phase of last eIPSC was normalized and fitted to a single exponential decay function to calculate time constant (τ_{decay}). Two-tailed unpaired t-test was used for all statistical comparisons and values are given as mean ± SEM.

Results

Dynasore, a small molecule inhibitor of dynamin

Dynasore potently inhibits both the GTPase activity of dynamin 1

To investigate the role of dynamin-dependent synaptic vesicle recycling in maintenance of neurotransmission, I first tested whether the small molecule inhibitor, dynasore, suppresses GTPase activity of dynamin under these settings. For this purpose, an *in vitro* GTPase activity assay was used, which took advantage of the well-characterized interaction between dynamin and phosphatidylinositol (4,5)-bisphosphate ($PI(4,5)P_2$). This interaction plays a critical role in driving synaptic vesicle endocytosis under physiological conditions (Cremona and De Camilli, 1997; Takei et al., 2005). Initial experiments confirmed that the GTPase activity of dynamin 1 is stimulated as a function of dynamin concentration in the presence of $PI(4,5)P_2$ (Barylko et al., 1998; Higashijima et al., 1987). Under these conditions (0.1 M NaCl and 0.24 μM dynamin 1), GTPase activity was stimulated from a basal level of 0.9 min^{-1} in the absence of lipids, up to 86 min^{-1} in the presence of 4 μM $PI(4,5)P_2$. Dynasore inhibited $PI(4,5)P_2$-stimulated dynamin 1 activity in a dose–dependent manner, with 50% inhibition achieved at a dynasore concentration approximately 40 μM ($P<0.001$, Figure 4.1.B).

Dynasore inhibits the coupling between synaptic vesicle exocytosis and endocytosis

In order to examine whether dynasore is a functional inhibitor of endocytosis in central synapses, synaptophysin-pHluorin infected neurons were used and applied brief stimulation (10 Hz for 10 seconds) before and after dynasore application. Following the results of the *in vitro* assay, as well as a previous study (Newton et al., 2006), I opted to use 80 μM dynasore for the

experiments unless stated otherwise. As shown in Figure 4.1.C, dynasore treatment inhibited the decay of pHluorin signal after the stimulation, suggesting that synaptic vesicle endocytosis was impaired (Newton et al., 2006). Moreover, an additional increase of fluorescence was observed during the stimulation in the presence of dynasore, indicating inhibition of endocytosis during stimulation, which may impact short-term synaptic plasticity (Figure 4.1.C).

Impact of acute dynamin inhibition on neurotransmission

Acute dynamin inhibition results in rapid synaptic depression and complete depletion of evoked neurotransmission

To investigate the dependence of neurotransmission on dynamin-mediated synaptic vesicle trafficking, I focused on inhibitory neurotransmission because several inhibitory central synapses display salient features of synchronous and asynchronous as well as spontaneous release (Hefft and Jonas, 2005; Lu and Trussell, 2000; Maximov and Sudhof, 2005). In these experiments, hippocampal cultures were stimulated at 10 or 20 Hz either in the presence of 0.2 % DMSO (control) or after 2 minutes-long incubation in 80 or 160 μM dynasore (Figure 4.2). Dynasore treatment caused a marked depression of evoked inhibitory postsynaptic currents (eIPSCs) within 1 second, indicating that the degree of synaptic depression at these frequencies is determined by dynamin-dependent vesicle reuse (Figure 4.2.A-B and D). These findings are consistent with earlier observations that recycled vesicles contribute to neurotransmission within seconds (Delgado et al., 2000; Ertunc et al., 2007; Pyle et al., 2000; Sara et al., 2002). After the 10 or 20 Hz trains of action potentials, cells were stimulated at 1 Hz for 2 minutes to monitor rapid recovery of depressed synaptic activity. Under control conditions, synaptic responses rapidly recovered approximately 70% of their initial amplitude (Figures 4.2.A-B, open diamonds). In the presence of dynasore, however, synaptic responses failed to recover, indicating that the dynasore-

mediated inhibition of endocytosis impairs synaptic vesicle re-supply to the recycling synaptic vesicle pool (Figures 4.2.A-B, filled symbols). 3-minutes-long dynasore treatment prior to stimulation did not cause a significant decrease in the amplitudes of initial eIPSCs (Figure 4.2.C). The amplitude of first eIPSC in control was 2.6 ±0.2 nA and in 80 μM dynasore and 2.1 ± 0.3 nA in 160 μM dynasore compared to 2.4 ± 0.3 nA (n = 7-9, P>0.3) under control conditions. This observation is consistent with the expectation that dynasore effect on release is use-dependent and is not due to inhibition of exocytosis *per se*.

Acute dynamin inhibition results in no changes in spontaneous neurotransmission

In the same set of experiments, spontaneous miniature IPSCs (mIPSCs) was also monitored before and after stimulation to examine their susceptibility to dynamin inhibition (Figure 4.3). Surprisingly, extensive and unrecoverable synaptic depression induced by stimulation in the presence of dynasore did not significantly alter spontaneous neurotransmission. When mIPSCs were compared before and after stimulation in dynasore, only a small increase in the frequency of mIPSCs (P<0.05 in 80 μM, P>0.3 in 160 μM dynasore) was detected but no change in their amplitudes or other kinetic properties (P>0.8, Figure 4.3.A-B). Thus, inhibition of dynamin-dependent synaptic recycling appears to impair action potential driven neurotransmission without altering the properties of spontaneous neurotransmission.

Spontaneous transmission simultaneously occurs with evoked transmission at the same synapses

These findings rely on the assumption that spontaneous and evoked neurotransmission originate from the same set of synapses and activity-dependent depletion of vesicles giving rise to evoked release does not interfere with the maintenance of spontaneous release from individual synapses (Atasoy et al., 2008). In order to test this assumption, I took advantage of organotypic hippocampal cultures of spH64 transgenic mice, which express synaptopHluorin

selectively in inhibitory presynaptic terminals (Li et al., 2005) (Figure 4.4). In order to compare the rate of spontaneous and evoked release at individual synaptic boutons, slice cultures were incubated with folimycin (80 nM), a high-affinity blocker of vacuolar ATPase (Drose and Altendorf, 1997) to provide a cumulative measure of exocytosis (Sankaranarayanan and Ryan, 2001). In the absence of folimycin, little change in fluorescence was detected at rest suggesting that spontaneous exocytosis and endocytosis are in balance under resting conditions (Figure 4.4.A-B *left column,* and 4.4.C open triangle). In folimycin, however, synaptopHluorin labeled terminals showed a slow increase in fluorescence attributable to spontaneous release consistent with a previous report in dissociated hippocampal cultures (Figure 4.4.A-B *middle column* and 4.4.C grey diamond) (Atasoy et al., 2008). After monitoring the fluorescence for 10 minutes at rest, the slice was stimulated with bath application of 47 mM K^+ solution in order to visualize activity-dependent synaptic vesicle trafficking in all synaptic boutons within the field of view. Under these conditions, the majority of synaptic boutons (615/890, ~70%) that showed robust spontaneous release responded well to 47 mM K^+ application. The remaining population of synapses (275/ 890, ~30%), which did not show any detectable spontaneous release in the presence of folimycin, nevertheless showed robust response to 47 mM K^+ stimulation. Overall, these data suggest that spontaneous fusion co-exists with evoked release in majority (~70 %) of synapses in slices (Figure 4.4.C).

Next, I optically analyzed how acute inhibition of dynamin in the presence of 80 μM dynasore impacts spontaneous vesicle trafficking. In agreement with electrophysiological observations, dynasore application did not cause a significant fluorescence increase at rest compared to controls indicate that dynasore application does not alter the balance between exocytosis and endocytosis (Figure 4.4.A *right column* and 4.4.C black diamond). On average the rate of spontaneous fluorescence increase in the presence of folimycin was faster than the alterations

in resting fluorescence levels in control or dynasore incubated slices ($P<0.05$), while control and dynasore incubated slices did not show a significant difference in their fluorescence levels ($P>0.5$) (Figure 4.4.D) (968 synapses tested). Taken together, optical analysis in spH64 slice cultures suggests that acute inhibition of dynamin does not impair spontaneous synaptic vesicle recycling at individual synapses that show robust activity-dependent vesicle trafficking.

Induction of temporary depletion of presynaptic terminal in the presence of dynasore

Extensive depletion of recycling vesicles after dynamin inhibition leaves spontaneous neurotransmission intact

Even though majority of synapses simultaneously operate both spontaneous and evoked transmission, unstimulated synapses, thus protected from inhibition by dynasore, might still able to contribute to maintain spontaneous transmission. To ensure complete depletion of readily releasable pool (RRP) vesicles, therefore, stronger high potassium stimulation were used to mobilize most of the recycling synaptic vesicle pool in dynasore and tested whether this maneuver was sufficient to impair both evoked and spontaneous neurotransmission (Figure 4.5). Two rounds of 30-seconds long 90 mM K^+ application in the presence of dynasore ("depletion protocol") was employed to achieve complete depletion of synaptic vesicles belonging to RRP. If the spontaneous and evoked forms of release are originated from the same population of vesicles, equal suppression and similar time courses of recovery is expected for both forms of release after dynamin inhibition. However, in contrast to substantial inhibition of action potential evoked release and the marked reduction of hypertonicity-driven neurotransmission, 90 mM K^+ stimulation during dynamin inhibition did not reduce spontaneous neurotransmission below its baseline level (Figures 4.5.D-F). In these experiments, after temporary depletion by two consecutive applications

of 90 mM K^+ solution in the presence of dynasore, dynasore was removed from the extracellular solution and monitored the time course of recovery for the two forms neurotransmission (Figure 4.5). Removal of dynasore following 90 mM K^+ stimulation resulted in extremely slow recovery of evoked responses (Figures 4.5.A-C). eIPSCs recovered only 15% of their initial amplitudes 10 minutes after perfusion of dynasore-free solution, and on average 50% recovery was reached at 185 seconds (Figures 4.5.B-C). In contrast, the frequency and the amplitudes of spontaneous mIPSCs, monitored in the absence of TTX for a direct comparison to the recovery of eIPSCs, were unaltered throughout this period (Figure 4.5.F). These findings were also replicated using moderate stimulation (10 Hz for 60 sec) in the presence of 80 or 160 μM dynasore. In this case upon removal of dynasore, evoked IPSCs slowly recovered 43% or 13% of their original amplitudes (in 80 or 160 μM dynasore, respectively). I detected 80% recovery by 320 seconds after 80 μM dynasore-mediated inhibition, whereas mIPSCs were unaffected during as well as after the extensive suppression of evoked neurotransmission.

Reluctant synaptic vesicles, or synaptic vesicles belonging to reserve pool might selectively contribute to spontaneous transmission

Where synaptic vesicles contributing to spontaneous transmission come from? Are there any synaptic vesicles left after temporary depletion is induced by maximal depolarization in the presence of dynasore? To examine the source of synaptic vesicles responsible to maintain spontaneous transmission even after induction of temporary depletion, neurons were challenged with two rounds of 30-seconds long 90 mM K^+ application in the presence of dynasore ("depletion protocol", Figure 4.6). This indeed caused substantial suppression of neurotransmission as indicated by complete cessation of responses evoked at 20 Hz stimulation (Figure 4.6.A-B). The amplitude of the first eIPSC after 90 mM K^+ stimulation in the presence of dynasore application was only 5% of the

amplitude of the eIPSC recorded before the stimulation, suggesting that nearly all vesicles within the readily releasable pool were depleted. In contrast, the same stimulation when applied in the presence of DMSO temporarily depressed eIPSCs down to 70% of their original amplitudes. Under the same conditions, 90 mM K^+ stimulation in the presence of dynasore caused only partial depletion of the vesicles released in response to hypertonic (+500 mOsm) sucrose stimulation. The amount of charge transfer induced by hypertonic sucrose solution after 90 mM K^+/dynasore application was 40% of the charge transferred in the presence of DMSO (Figures 4.6.A and C, $P<0.001$), suggesting that a significant number of synaptic vesicles respond to hypertonicity but not to action potentials. This finding agrees with earlier reports that hypertonicity-driven release is partly mediated by a reluctant synaptic vesicle pool that is not mobilized during activity (Moulder et al., 2007; Moulder and Mennerick, 2005), and suggests that these synaptic vesicles might contribute to spontaneous transmission (Fredj and Burrone, 2009).

Ultrastructural investigation of synaptic terminal after acute dynamin inhibition

Acute inhibition of dynamin activity during depolarization decreases total synaptic vesicle number but leaves spontaneous synaptic vesicle trafficking intact.

In order to examine whether strong high K^+ stimulation in the presence of dynasore causes detectable changes in synaptic vesicle numbers at the ultrastructural level, the morphology of synaptic terminals was analyzed after depletion protocol using electron microscopy (EM). In the first set of experiments, cells were challenged with 90 mM K^+ stimulation two consecutive times (30 s each) in the presence of either 0.1% DMSO or 80 μM dynasore prior to fixation (Figure 4.7). Figure 4.7 summarizes the results of electron micrograph analysis by an observer blind to the treatment conditions. This analysis revealed that

incubation with dynasore during strong activity depletes a substantial number of synaptic vesicles despite the large size of the resting pool (Figure 4.7.C). This result suggests that synaptic vesicle reuse during strong depolarization requires dynamin activation.

Acute inhibition of dynamin activity during depolarization leaves spontaneous synaptic vesicle trafficking intact.

To investigate whether this strong synaptic vesicle depletion protocol affects spontaneous synaptic vesicle trafficking, I took advantage of HRP to selectively label recycling vesicles (Figure 4.8). In order to label spontaneously recycling vesicles after activity-dependent vesicle depletion, cells were incubated with HRP (25 mg/ml) for 15 min in the presence of TTX at the end of the high K^+-induced depletion protocol. Figure 4.8.A and B show sample electron micrographs of synaptic terminals after 90 mM K^+ application in either DMSO or dynasore. White arrows indicate spontaneously recycling synaptic vesicles that took up HRP after 90 mM K^+ depletion protocol. Under these conditions again a reduction in the total number of synaptic vesicles was observed after activity-dependent vesicle depletion (81.85±8.8 for DMSO, 58.44±3.14 for dynasore, $P<0.001$) (Figure 4.8.C, *left*), which was also reflected in a slight decrease in the number of HRP positive synaptic vesicles (Figure 4.8.C, *middle*). Nevertheless, given the decrease in the total number of synaptic vesicles, the fraction of HRP positive synaptic vesicles in a given synapse was not altered in the presence of dynasore (Figure 4.8.C, *right*). This finding suggests that after 90 mM K^+-mediated depletion of recycling synaptic vesicles, spontaneous uptake of HRP remains relatively intact consistent with the premise that at individual synapses spontaneous synaptic vesicle recycling is relatively unaffected by dynamin-inhibition and vesicle depletion.

Dynamin dependence of asynchronous neurotransmitter release

In the preceding set of experiments, removal of 90 mM K^+ stimulation under control conditions resulted in nearly two-fold increase in spontaneous mIPSC activity (Figure 4.5.E). This increase in spontaneous transmission could be attributed to asynchronous release typically observed after extensive stimulation (Lu and Trussell, 2000; Maximov and Sudhof, 2005; Otsu and Murphy, 2004; Otsu et al., 2004). Interestingly, co-application of dynasore and 90 mM K^+ solution completely inhibited this increase in neurotransmission (Figure 4.5.F). Therefore, next I investigated whether asynchronous neurotransmitter release also depended on dynamin-dependent synaptic vesicle recycling. To address this question, a round of 10 Hz stimulation was applied for 5 seconds in 8 mM Ca^{2+} to exacerbate the extent of asynchronous release, followed by a second round of 10 Hz stimulation in the presence of 80 μM dynasore (Figure 4.9). The amount of asynchronous neurotransmitter release was measured as the charge transfer (shaded area depicted in Figure 4.9.C) after the cessation of stimulation (Maximov and Sudhof, 2005).

Under these conditions, dynasore application did not only cause faster depression of release evoked during stimulation (Figure 4.9.B, *right*), but also a marked reduction in the amount of asynchronous release detected at the end of the stimulation train (Figure 4.9.A and C). The amplitudes of first eIPSCs were comparable in the presence of DMSO or dynasore, suggesting that exocytosis was not altered by dynamin inhibition (Figure 4.9.B, *left*). The loss of asynchronous component in the presence of dynasore was further quantified by decay kinetics of eIPSCs. The decay time course of the last eIPSC in the train was significantly faster in the presence of dynasore indicating loss of asynchronous release that follows the burst of action potentials (Figure 4.9.D). These results suggest that synaptic vesicles recycled in a dynamin-dependent manner drive asynchronous release that follows extensive activity. This finding is in agreement with the earlier proposal that the two forms neurotransmission originate from the same

pool of vesicles albeit with distinct Ca^{2+}-dependence (Otsu and Murphy, 2004; Otsu et al., 2004; Sun et al., 2007).

Maintenance of spontaneous neurotransmission in the absence of GTPase activity of dynamin

Results presented so far are consistent with the hypothesis that synchronous as well as asynchronous forms of neurotransmitter release originate from the same population of vesicles that rapidly recycle in a dynamin-dependent manner. In contrast, spontaneous neurotransmission appears to originate from a distinct vesicle pool that maintains its activity even after complete suppression of other forms of release. However, these findings do not exclude the possibility that spontaneous neurotransmission operates in a dynamin-dependent manner albeit at slower time scale. To test this premise, spontaneous neurotransmission was monitored up to 1 hour and examined whether sustained treatment with dynasore at rest (in the presence of TTX) altered the properties of mIPSCs as well as subsequent eIPSCs. In these experiments, initially the amplitudes of eIPSCs was measured followed by application of TTX. Once a stable baseline for mIPSCs was obtained (~3 min in DMSO), 80 μM dynasore was applied and monitored mIPSCs for 1-hour. At the end of the 1-hour recording period, TTX was cleared from the extracellular medium (~5 min) in the presence of 80 μM dynasore, and re-stimulated eIPSCs (Figure 4.10). As shown in Figure 4.10, a significant increase in the frequency of mIPSCs was detected ($P<0.001$ Figures 4.10.A-B). During this period, amplitudes of mIPSC also showed an increasing trend that did not reach significance ($P=0.056$, Figure 4.10.C), which is consistent with a postsynaptic effect of dynasore. These data show that spontaneous neurotransmission does not rely on dynamin-dependent synaptic vesicle recycling up to 1-hour. 1-hour treatment with dynasore at rest caused up to ~60% reduction in the amplitudes of subsequent eIPSCs (Figure 4.10.D), indicating that dynasore

is still capable of inhibiting trafficking at rest, although this inhibition spares spontaneous neurotransmission. Interestingly, the remaining amount of evoked release is comparable to the level of eIPSCs detected in mice deficient in dynamin 1 (Ferguson et al., 2007). Taken together, these observations are consistent with the possibility that vesicle pools maintaining spontaneous and evoked neurotransmission mix with a slow rate in the order of hours (Sara et al., 2005). Therefore, the observations made in the present study suggest that acute inhibition of dynamin function with dynasore selectively suppresses evoked but not spontaneous synaptic vesicle trafficking.

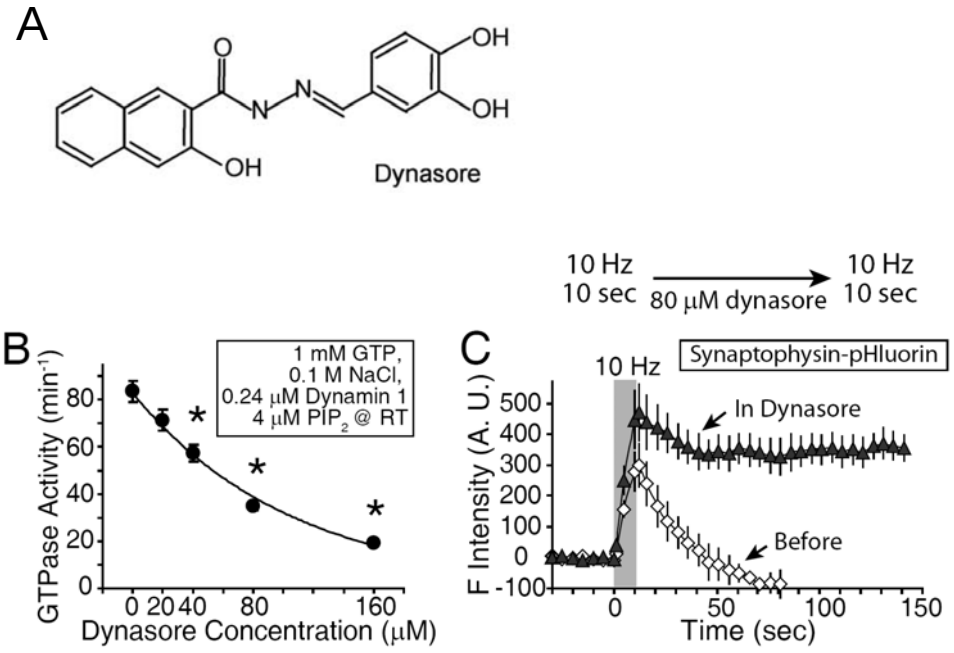

FIGURE 4. 1. Dynasore inhibits GTPase activity of dynamin 1 *in vitro* as well as endocytosis measured with pHluorin signal.
(A) Structure of a small molecule inhibitor of dynamin, dynasore (Macia et al., 2006) (B) Dynasore inhibits GTPase activity of $PI(4,5)P_2$-stimulated dynamin 1 *in vitro* in a concentration-dependent manner (n = 3-4). (C) Dynasore impairs endocytosis of synaptic vesicles upon stimulation.10 Hz stimulation in the presence of 80 μM dynasore showed little decay of pHluorin signal after stimulation as well as revealed additional rise of fluorescence during stimulation, suggesting that dynasore indeed impairs endocytosis in hippocampal synapses (n = 450 synapses from 4 coverslips).

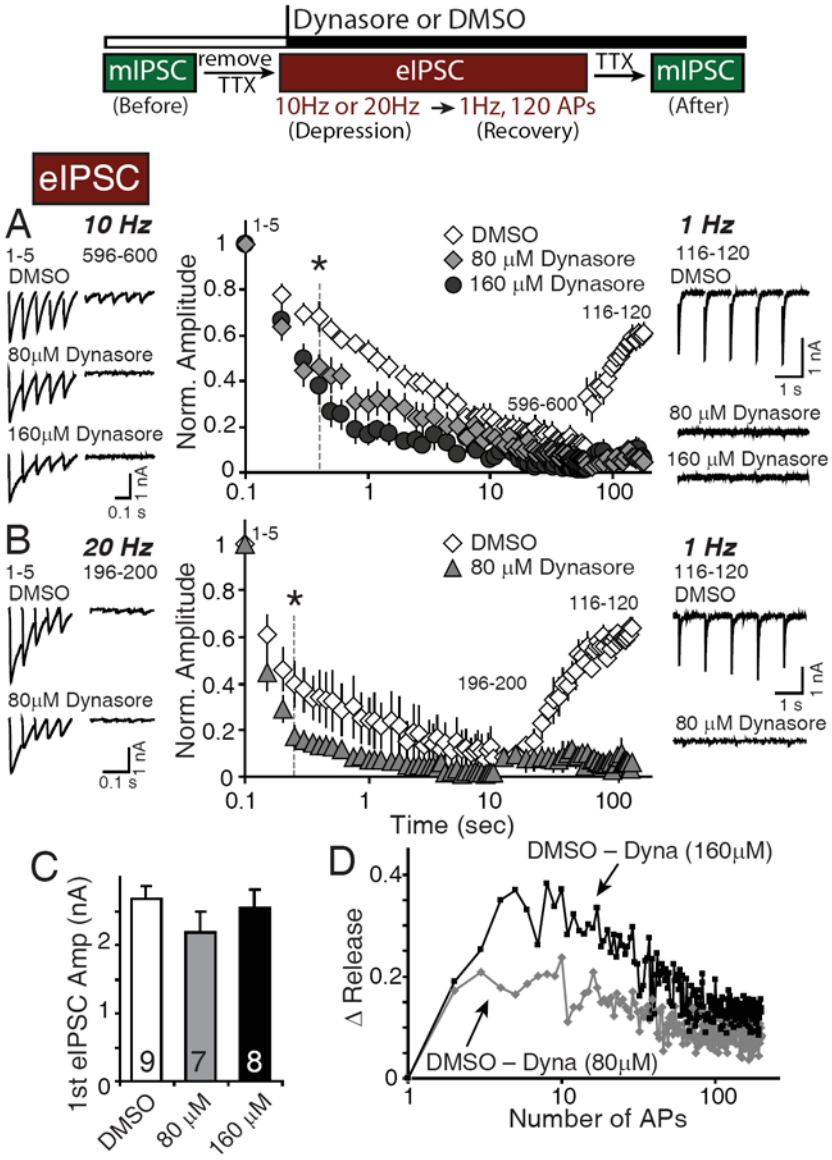

FIGURE 4. 2. Endocytosis of synaptic vesicles during and after sustained stimulation requires GTPase activity of dynamin.
Cells were stimulated at 10 Hz for 60 sec or 20Hz for 10 sec in the presence of either 0.2% DMSO (vehicle) or indicated concentrations of dynasore. mIPSCs were measured

before and after transient incubation with DMSO or dynasore in the presence of TTX. (A and B) After application of dynasore, synaptic responses elicited by field stimulation (eIPSCs) depressed faster during successive stimulation of 10 Hz for 1 min or 20 Hz for 10 sec, leading to temporary depletion of available synaptic vesicles at terminals. In addition, dynasore at the concentrations employed (80 μM and 160 μM), blocked the recovery of synaptic responses after depression (1 Hz, *right panels*). (C) The amplitude of first eIPSC was not changed by brief application of dynasore, suggesting that dynamin plays little role in exocytosis. ($P > 0.6$) (D) The amount of endocytosis during stimulation that is dynasore-sensitive was estimated by subtracting synaptic responses in the presence of dynasore from of DMSO.

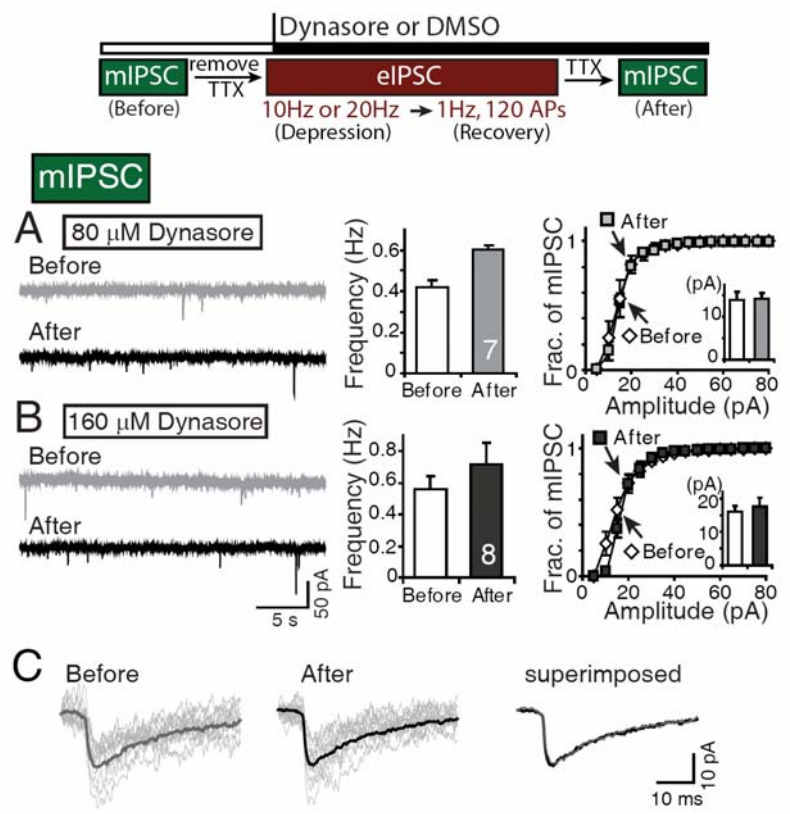

FIGURE 4. 3. Spontaneous transmission is not diminished by incubation with dynasore during trains of stimulation.
Cells were stimulated at 10 Hz for 60 sec or 20Hz for 10 sec in the presence of either 0.2% DMSO (vehicle) or indicated concentrations of dynasore. mIPSCs were measured before and after transient incubation with DMSO or dynasore in the presence of TTX. (A and B) Only the increase in the frequency of mIPSCs before and after 10 Hz stimulation in 80 μM dynasore was statistically significant (0.42±0.03 Hz before, 0.6±0.02 Hz after dynasore application, $P<0.05$). The frequency of mIPSCs in 160 μM dynasore (0.56±0.08 Hz before, 0.72±0.1Hz after dynasore application, $P>0.3$) and the amplitude of mIPSCs in both concentrations of dynasore remained unchanged (15.81±2.07 and 14.25±1.2 pA before and after 80 μM dynasore, $P>0.8$; 16.08±1.8 pA and 17.46±2.6 pA before and after 160 μM dynasore, $P>0.9$). (C) Averaged unitary responses before and after 80 μM dynasore application can be fully superimposed, suggesting that dynasore treatment does not alter the kinetics of individual mIPSCs.

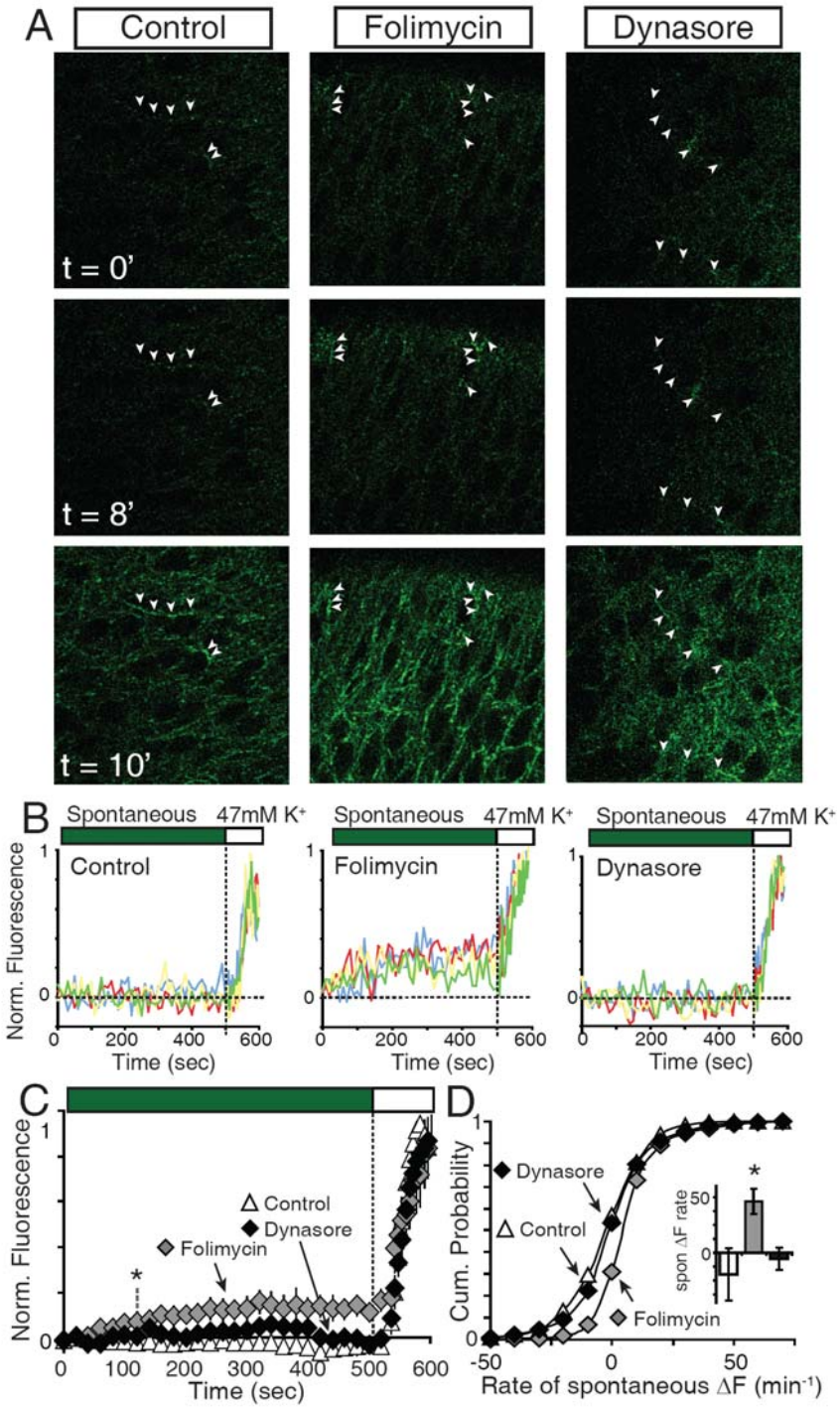
A
Control
Folimycin
Dynasore
t = 0'
t = 8'
t = 10'
B
Spontaneous
47mM K+
Control
Folimycin
Dynasore
Norm. Fluorescence
Time (sec)
C
Norm. Fluorescence
Control
Dynasore
Folimycin
Time (sec)
D
Cum. Probability
Dynasore
Control
Folimycin
spon ΔF rate
Rate of spontaneous ΔF (min-1)

FIGURE 4. 4. Majority of single synapses can operate both spontaneous and evoked transmission simultaneously and the inhibition of dynamin activity differentially affects both transmissions.
(A *top*) Sample images of spH64 slice cultures of control (*left*), in 80 nM folimycin (*middle*) and in 80 μM dynasore (*right*). Arrowheads indicate examples of selected individual boutons. (A *middle*) Same sample images after 10 minutes incubation depicting the changes in fluorescence at rest presumably due to spontaneous release (see Atasoy et al., 2008). The presence of folimycin caused a slight increase of fluorescence with a relatively constant rate over 10 min. In contrast the presence of dynasore did not trigger a comparable change in resting fluorescence levels suggesting that spontaneous synaptic vesicle recycling was not affected by dynamin inhibition. (A *bottom*) Robust increase in fluorescence was observed after application of 47 mM K^+ solution in all cases. (B) Sample traces depict the fluorescence change at the level of individual synapses. Note that, folimycin incubation (*middle*) alters the rate of fluorescence increase at rest and during depolarization at each selected synaptic bouton, indicating that spontaneous and evoked neurotransmission occurs at the same inhibitory synapses. (C) Averaged fluorescence changes at rest and during elevated K^+ application under each condition (n = 934, 890, 968 synapses from 6 slices each for control, folimycin, dynasore, respectively). Fluorescence values were normalized with respect to their highest respective levels during 47 mM K^+ application. Note that fluorescence changes at rest in the presence of dynasore were not different from control (P>0.5) while notable increases were detected in the presence of folimycin (P<0.05) suggesting that application of dynasore hardly interferes with spontaneous synaptic vesicle recycling. (D) Cumulative probability histogram of the rate of spontaneous fluorescence increase in individual synapses. The inset shows the average rate of spontaneous fluorescence increase (ΔF/min) under each condition. The spontaneous fluorescence increase rate (ΔF/min) in folimycin was faster than in dynasore or in control conditions, while no significant difference was observed between control and dynasore group (P<0.05).

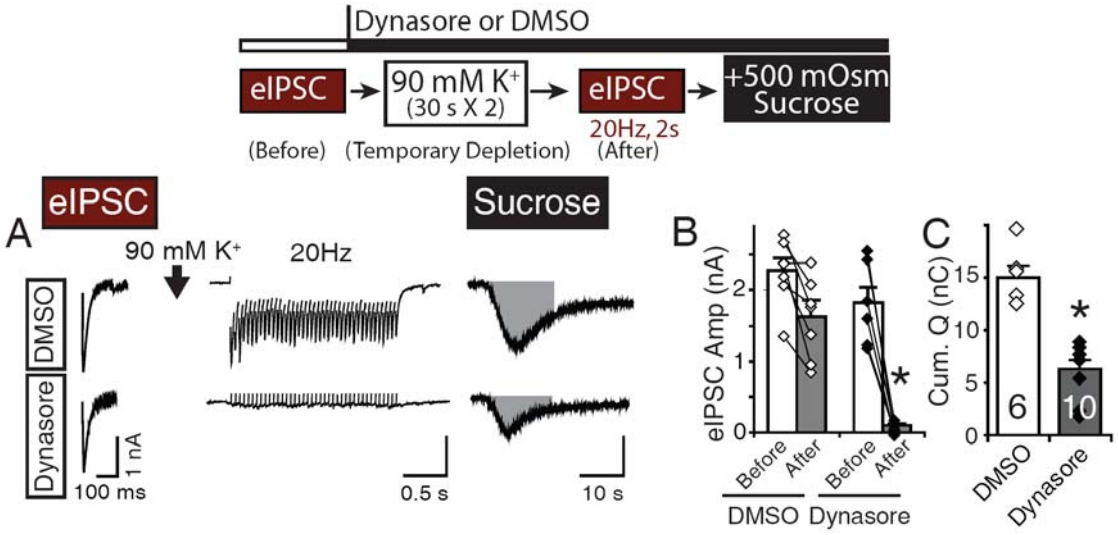

FIGURE 4. 5. Extensive depletion of recycling vesicles after dynamin inhibition leaves spontaneous neurotransmission intact.
Application of two rounds of 90 mM K^+ solution was used to exhaust synaptic terminals. The recovery of synaptic activity was monitored during very low frequency stimulation upon removal of dynasore from extracellular solution to monitor repopulation kinetics of synaptic vesicles after temporary depletion. (A) Sample recordings depicting recovery of eIPSCs after 90 mM K^+ stimulation (with or without dynasore). (B) Fractional recovery of synaptic responses after 90 mM K^+ stimulation (with or without dynasore) is plotted as a function of time. To illustrate the differences in the time courses of recovery plots are normalized with respect to the amplitude of final eIPSC after 10 min of perfusion. (C) Bar graphs depict the amplitudes of eIPSCs before application of 90 mM K^+ with either DMSO or dynasore and after 10 min wash of 90 mM K^+/DMSO or 90 mM K^+/dynasore (2.32±0.33 and 2.18±0.35 pA before and after 90 mM K^+/DMSO; 2.28±0.2 and 0.36±0.04 pA before and after 90 mM K^+/dynasore). (D) A sample recording after temporary depletion induced by two executive applications of 90 mM K^+ in the presence of dynasore. Arrows indicate the time points when stimulations were applied. Note that under these conditions spontaneous neurotransmission remains intact, while eIPSCs are abolished. (E and F) The levels of sIPSCs (spontaneous transmission measured in the absence of TTX) before and after application of 90 mM K^+/0.2 % DMSO or 90 mM K^+/80 μM dynasore were analyzed. The frequency of sIPSCs was not decreased after 90 mM K^+/dynasore (1.05±0.18 and 1.03±0.28 Hz before and after 90 mM K^+/80 μM dynasore, n = 6, P>0.9), suggesting that differential regulation of synaptic vesicles for action potential-driven release and spontaneous release (n = 3-6). The amplitude of sIPSCs was not altered (15.54±1.4 and 16.03±1.04 pA, n = 6, P>0.6). Challenge with 90

mM K^+ with DMSO increased the frequency (0.78±0.08 and 1.45±0.2 Hz before and after 90 mM K^+/0.2 % DMSO, $n = 3$, $P<0.01$) but not the amplitude of sIPSCs (14.55±2.26 and 15.93±0.84 pA, $n = 3$, $P>0.6$).

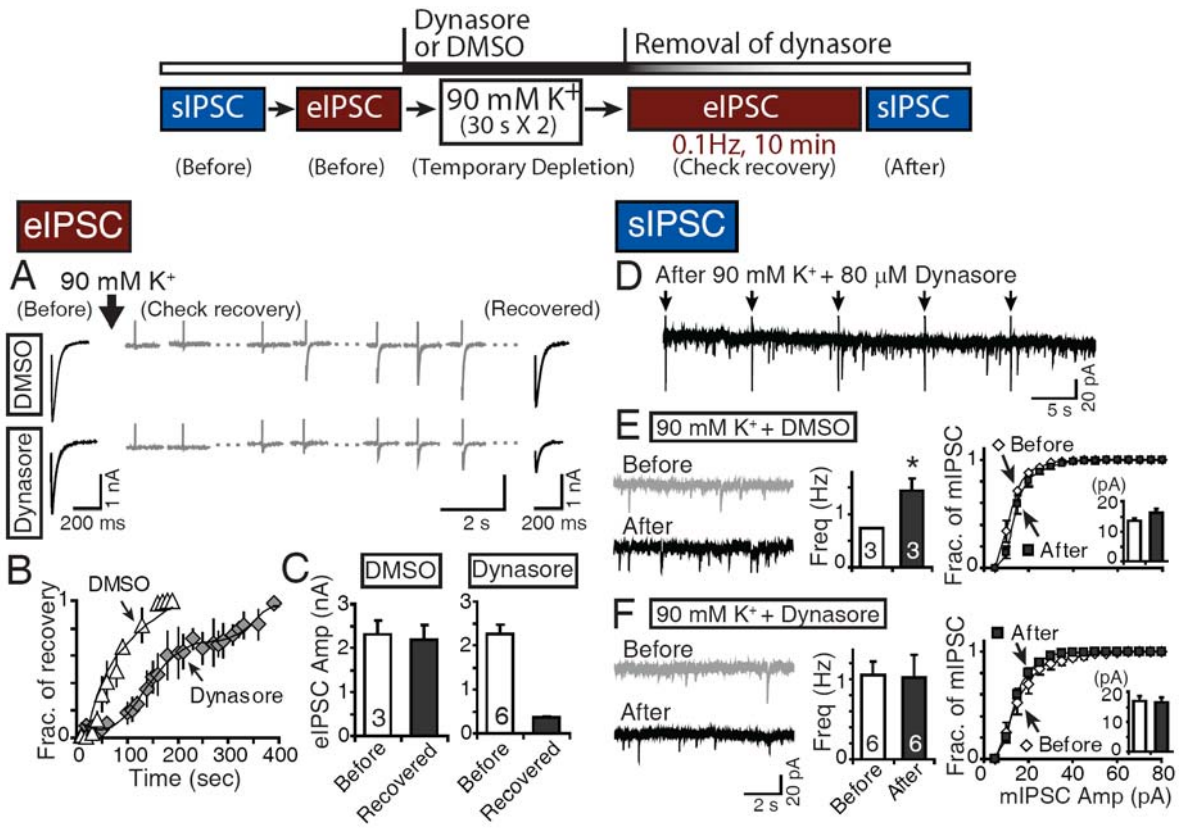

FIGURE 4. 6. Synaptic terminal contains synaptic vesicles after extensive depletion of recycling vesicles under dynamin inhibition.
90 mM K^+/dynasore application was used to deplete most of the recycling synaptic vesicle pool. (A) After repeated application of 90 mM K^+/dynasore, 20 Hz stimulation evoked synaptic responses were completely suppressed while hypertonic sucrose induced neurotransmitter release was decreased by 60%. (B) Comparison of the amplitudes of eIPSCs before 90 mM K^+ application and after 90 mM K^+ application in DMSO or dynasore. The amplitudes of eIPSC before and after 90 mM K^+ application in the presence of DMSO were not significantly different (2.2±0.2 and 1.6±0.2 nA, respectively, $n = 7$, $P>0.1$, *left*). However, the amplitudes of eIPSC after 90 mM K^+/dynasore were remarkably decreased to 5% of before, suggesting that 90 mM K^+ application in the presence of dynasore indeed depleted available vesicles that fuse in response to action potentials (1.8±0.2 and 0.09±0.03 nA, respectively, $n = 6$, $P<0.001$, *right*). (C) Plots depicting the amount of charge transfers for 15 sec of sucrose application. The charge transfer induced by sucrose application in the presence of dynasore was 40% of control (14.96±1.13 nC in the presence of DMSO and 6.31±0.8 nC in the presence of dynasore, $n = 6$-10, $P<0.001$), suggesting that hypertonicity mobilizes larger pool of synaptic vesicles than 20 Hz stimulation.

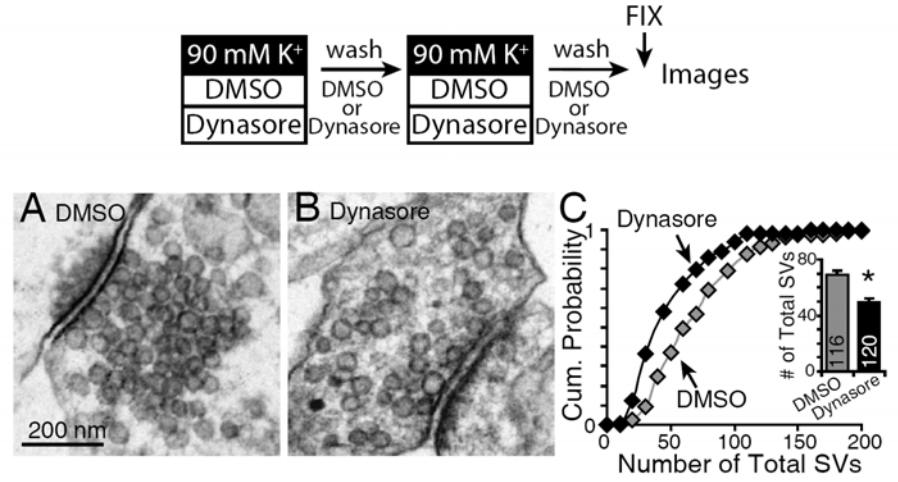

FIGURE 4. 7. Incubation with dynasore during stimulation causes vesicle depletion. Prior to fixation and visualization cells were challenged with 90 mM K^+ solution (2X for 30 s each) in the presence of either 0.1% DMSO or 80 μM dynasore. (A and B) Representative electron micrographs of synaptic terminals after 90 mM K^+/DMSO or 90 mM K^+/dynasore. (C) Application of 90 mM K^+/dynasore solution decreased the number of total synaptic vesicles (68.75±3.44 for DMSO, 48.94±3.52 for dynasore, $P<0.001$).

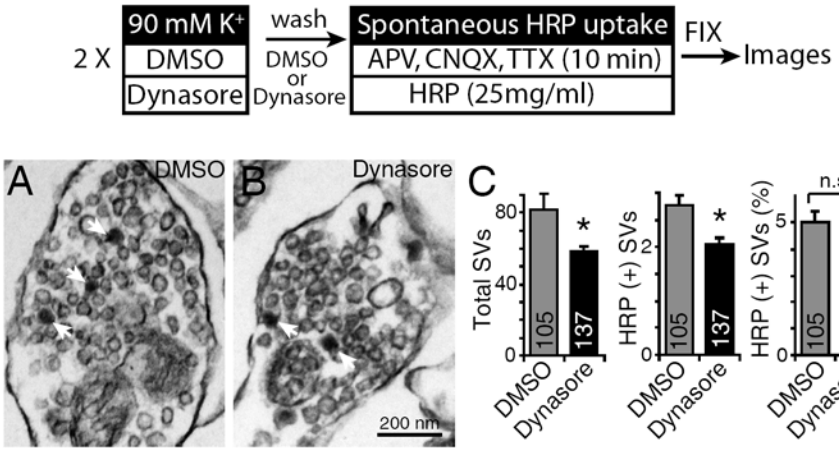

FIGURE 4. 8. Spontaneous transmission is intact after Incubation with dynasore during stimulation.
Cells were incubated with HRP (25 mg/ml) for 15 min in the presence of TTX after depletion protocol to assess the degree of spontaneous synaptic vesicle trafficking. (A and B) Representative electron micrographs of synaptic terminals. White arrows indicate synaptic vesicles that took up HRP under resting conditions following 90 mM K^+/dynasore induced depletion. (C) 90 mM K^+/dynasore- induced depletion decreased number of the total synaptic vesicles (81.85±8.8 for DMSO, 58.44±3.14 for dynasore, P<0.001). The number of HRP positive synaptic vesicles was slightly decreased in dynasore group (2.76±0.18 for DMSO, 2.06±0.12 for dynasore, P<0.01). However, the relative number of HRP positive synaptic vesicles per synapse remains unchanged (4.97±0.4 for DMSO, 2.73±0.35 for dynasore, P>0.6).

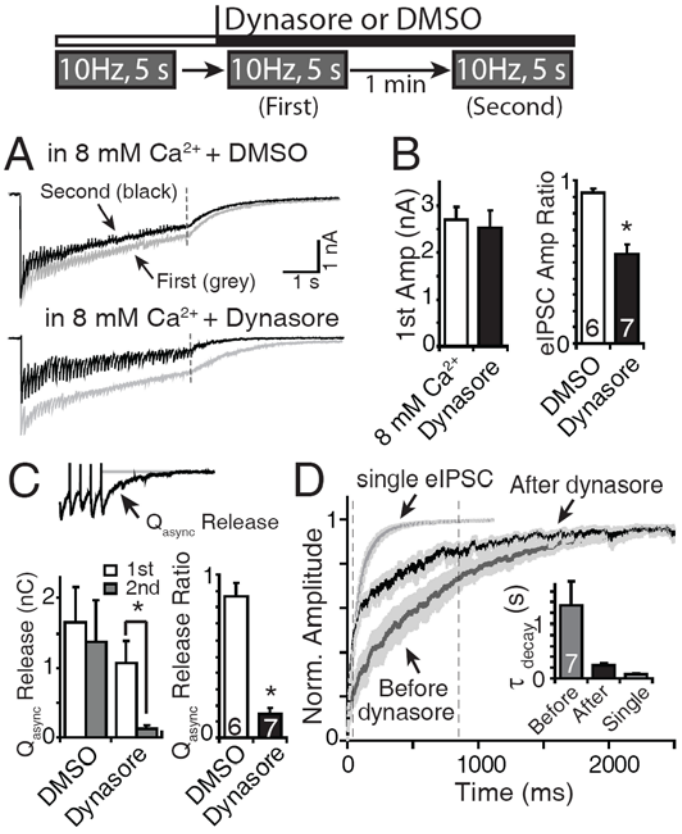

FIGURE 4. 9. Dynamin dependence of asynchronous neurotransmitter release. Cells were stimulated at a frequency of 10Hz for 50 action potentials. Then, after 2-minutes long application of dynasore (or DMSO control) cells were stimulated twice in 1 minute intervals. (A) Sample recordings in 8 mM Ca^{2+} before dynasore application and two rounds of stimulation in the presence of 8 mM Ca^{2+} and dynasore. (B) Brief application of dynasore does not affect the first eIPSC amplitude in 8 mM Ca^{2+} as similar to in 2 mM Ca^{2+} (2.7±0.27 nA in DMSO and 2.5±0.38 nA in dynasore, n = 7-13, P>0.8). However, the ratio of first eIPSC amplitude in the presence of dynasore was decreased, compared to controls recorded in the presence of DMSO. The amplitude of first eIPSC in 2nd round of stimulation in DMSO was 0.92±0.02% of in 1st round of stimulation and in dynasore was 0.55±0.06% (n = 6-7, P<0.001). (C) Total asynchronous release was quantified as the area from the onset of final stimulation to the baseline (Q_{async} release, grey area). Q_{async} release was decreased in the presence of dynasore (from 1.07±0.32 nC to 0.14±0.05 nC (15±4%), n = 7, P<0.001) but not in DMSO (from 1.65±0.5 nC to1.38±0.58 nC (87±4%), n = 6, P>0.5). First Q_{async} release in dynasore was not different from in 8 mM Ca^{2+} before dynasore application (P>0.4). (D) Decay phase of the last (50th) eIPSC was normalized and fitted with a single exponential function to extract the

time constant τ_{decay}. τ_{decay} of the 50 th eIPSC before dynasore application was 1242±420 ms, and after dynasore application it was reduced to 237±38 ms (n = 7, P<0.05 between the dotted time line). τ_{decay} of single eIPSCs were measured as 78±7 ms.

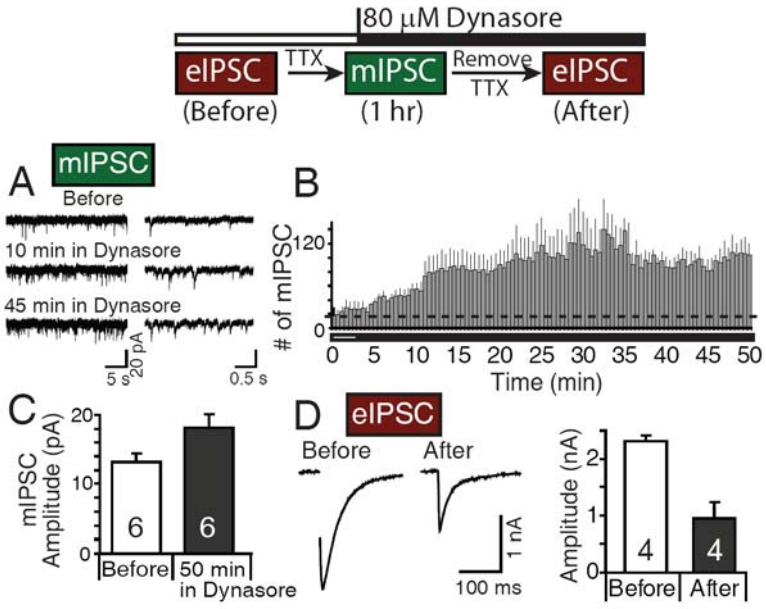

FIGURE 4. 10. Prolonged dynasore application failed to suppress spontaneous neurotransmission.
Miniature IPSC (mIPSC) was measured up to an hour in the presence of 80 μM dynasore. (A) Sample traces at different time points in the presence of 80 μM dynasore. (B) Plot depicts the number of mIPSCs detected per 30 sec period during 1-hour-long recordings. (C) The amplitude of mIPSCs show an increasing trend that did not reach significance (P=0.056, n = 6). (D) Comparison of the amplitudes of eIPSCs detected before and after 1 hour incubation in 80 μM (n = 4). 1-hour incubation in dynasore at rest left 40% of eIPSCs intact. The decay constant of eIPSC before and after prolonged dynasore application was not altered (101±8.8 and 99.45±9 ms before and after dynasore, respectively, n = 4, P>0.4).

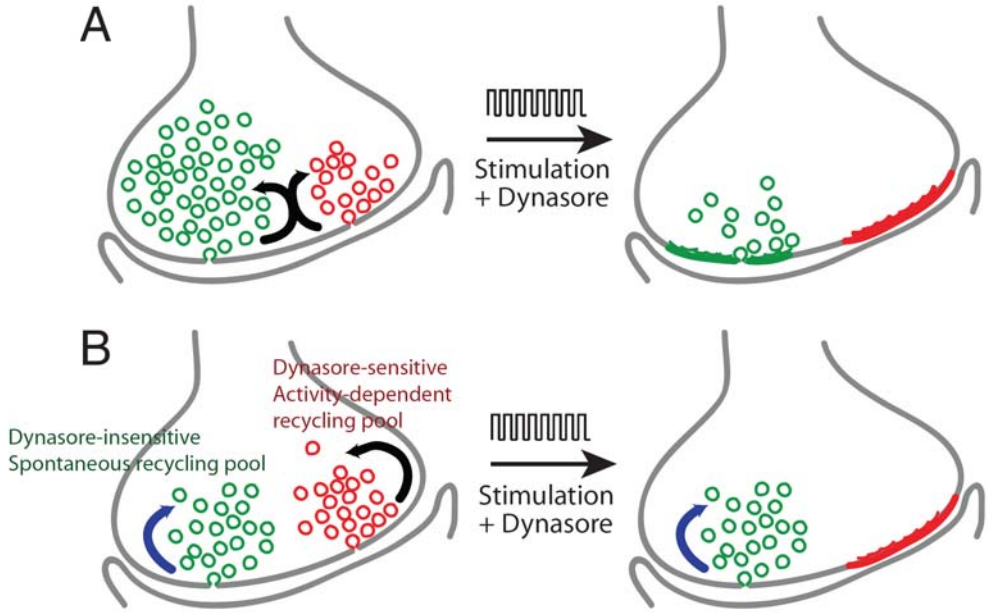

FIGURE 4. 11. Possible scenarios.
(A) Both spontaneous and evoked transmission may share identical recycling pathway for their maintenance but spontaneous recycling synaptic vesicles may originate from an extremely large pool, thereby does not require recycling to maintain transmission for hours. (B) Synaptic terminals may operate a separate recycling pathway to maintain spontaneous neurotransmission, which is dynasore-insensitive. This form of recycling might be dynamin-independent, or, alternatively, it may require a dynamin isoform that is not sensitive to dynasore (e.g. dynamin 3).

Discussion

Major observations on contribution of dynamin to synaptic vesicle endocytosis

In the present study, I made several key observations on how dynamin-mediated synaptic vesicle endocytosis contributes to neurotransmission by taking advantage of dynasore, a reversible small molecule inhibitor of dynamin function. First, in agreement with earlier reports, I verified that dynasore is a bona fide and potent inhibitor of dynamin's GTPase activity (Kirchhausen et al., 2008; Macia et al., 2006). This inhibition of dynamin function, in turn, was correlated with a marked suppression of synaptic vesicle endocytosis during and after synaptic stimulation. Second, dynasore, at concentrations that potently inhibits dynamin activation as well as synaptic vesicle endocytosis, caused use-dependent depression of evoked synaptic transmission at an extremely rapid time scale (~1 s). This finding indicates that neurotransmission during repetitive stimulation requires rapid reuse of synaptic vesicles endocytosed in a dynamin-dependent manner (Ertunc et al., 2007; Harata et al., 2006; Pyle et al., 2000; Sara et al., 2002). Third, under the same settings acute inhibition of dynamin affects synchronous as well as asynchronous release suggesting that both forms of release relies on dynamin-dependent synaptic vesicle recycling. Finally, the experiments presented here suggest that spontaneous neurotransmission is consistently resilient to acute inhibition of dynamin. In contrast to the strong impact of acute dynamin inhibition on evoked synaptic vesicle recycling, dynasore treatment did not significantly affect spontaneous neurotransmission and caused partial decrease in hypertonic sucrose triggered release. Once synaptic vesicles responsive to Ca^{2+}-evoked release were depleted via elevated potassium stimulation in the presence of dynasore hypertonicity-induced release showed a marked reduction (~ 40% of control) but spontaneous release was left largely intact. As the magnitude and duration of high potassium stimulation used in these experiments is sufficient to

mobilize nearly all actively recycling vesicles in a synapse (Groemer and Klingauf, 2007; Kavalali et al., 1999b; Klingauf et al., 1998; Sara et al., 2005), it is rather unexpected that at least 40% of the vesicle pool mobilized by hypertonic sucrose and almost all spontaneous neurotransmission was left intact by this maneuver. These findings contrast the earlier observations that both hypertonic sucrose driven release and spontaneous neurotransmission rely on synaptic vesicle reuse as they can be swiftly suppressed in response to application of vacuolar ATPase inhibitors such as folimycin (e.g. Ertunc et al., 2007).

Insights for composition of synaptic vesicle pools

Taken together, these results can be reconciled with a model where spontaneous release is sustained by a vesicle pool, which reluctantly responds to activity and partly overlaps with the pool that fuses in response to hypertonic stimulation (Figure 4.6). Moreover, although these vesicles can be recruited to fuse during strong stimulation, they do not require dynamin activation for recycling. This proposal is consistent with recent studies in dorsal root ganglion neurons and in the calyx of Held which have shown that neurotransmission can be partly maintained by a pool of vesicles recycling in a dynamin-independent fashion (Xu et al., 2008; Zhang et al., 2004). Furthermore, spontaneous neurotransmission can be maintained after cholesterol depletion, which selectively impairs evoked release as well as clathrin-mediated endocytosis (Subtil et al., 1999; Wasser et al., 2007; Zamir and Charlton, 2006). Interestingly, cholesterol depletion causes a substantial increase in the rate of spontaneous transmission although most vesicles that carry out evoked neurotransmission are either depleted or impaired to fuse (Zamir and Charlton, 2006; Wasser et al., 2007). This finding is reminiscent of the increased spontaneous transmission detected here after prolonged dynamin inhibition at rest (Figure 4.10). The reciprocal interaction between the two forms of neurotransmission may suggest

that once activity-dependent synaptic vesicle recycling is impaired, a secondary pool of vesicles becomes unhindered and augments spontaneous release. This premise agrees well with a recent study at the calyx of Held where after depletion of dynamin-dependent vesicle recycling, an auxiliary vesicle pool was recruited to maintain release independent of GTP hydrolysis (Xu et al., 2008).

The findings described here are consistent with earlier work from manipulation of dynamin function using dominant negative or genetic knockout approaches. Studies on the *Drosophila* temperature sensitive dynamin mutant *shibire* have provided strong support for the hypothesis that endocytosed vesicles are reused rapidly to maintain neurotransmission during activity (Kawasaki et al., 2000). Kinetic analysis of synaptic depression in *shibire* flies suggests a recycling rate of one to two vesicles per second per release site (Delgado et al., 2000). In addition, a recent study on a mouse knockout of dynamin-1 also revealed a similar rapid synaptic depression as our observations due to loss of vesicle endocytosis occurring during synaptic stimulation as well as inhibition of synaptopHluorin trafficking during activity (Ferguson et al., 2007).

Alternative scenarios for role of dynamin in synaptic vesicle retrieval

In the model outlined above, I cannot exclude the possibility that the residual dynamin activity uninhibited by dynasore or a dynasore-insensitive isoform of dynamin (such as dynamin 3) may still be sufficient to sustain spontaneous neurotransmission. Nevertheless, this alternative explanation would suggest that the two forms of vesicle recycling are segregated by their reliance on two markedly distinct levels of dynamin activity or different dynamin isoforms rather then their dependence on dynamin *per se* (Figure 4.11). In agreement with this proposal, in the *Drosophila* neuromuscular junction, temperature sensitive *shibire* mutants show suppression of evoked as well as spontaneous transmission after strong stimulation indicating that the two forms of transmission are

dynamin-dependent. However, in this system recovery of spontaneous transmission after relief of dynamin inhibition requires repopulation of the total vesicle pool, whereas evoked release recovers once the readily releasable pool is repopulated with vesicles (Koenig and Ikeda, 1996, 1999). One caveat of the *shibire* system is the dominant negative nature of the mutation, which may interfere with other trafficking pathways that may act in parallel with the dynamin-dependent trafficking pathway. This caveat of the *shibire* system is supported by the recently characterized phenotype of mouse deficient in dynamin 1, which shows a highly selective suppression of evoked synaptic vesicle trafficking (Ferguson et al., 2007).

The other possibility could be that both synaptic transmission requires dynamin for its maintenance, however, spontaneously recycling synaptic vesicles are originated from extremely large pool of vesicles, thus does not require recycling for up to an hour (Figure 4.10 and 4.11).

In summary, the results presented here bring further insight into the complexity of synaptic vesicle trafficking within individual nerve terminals. Furthermore, spontaneous neurotransmission operates independent of canonical dynamin-mediated synaptic vesicle endocytosis or may have only marginal dependence on dynamin function (Kramer and Kavalali, 2008; Xu et al., 2008) (Figure 4.11). This provides the first evidence of difference at molecular machinery level in mediating evoked versus spontaneous transmission.

Future studies will need to address the molecular mechanism that underlie spontaneous synaptic vesicle endocytosis and identify the machinery required to trigger synaptic vesicle fission independent of dynamin.

CHAPTER FIVE
DISTINCT MODES OF SYNAPTIC VESICLE RETRIEVAL AT REST

Background

Spontaneous neurotransmitter release is a common feature of synapses throughout the nervous system and has, thus, been widely studied, though most often as a simpler proxy for the more complicated action potential–driven synchronized release of neurotransmitters. Spontaneous neurotransmitter release had been considered as synaptic noise or a simple error in tight regulation of fusion, thus, little interest had been invested to its 'raison d'être' for a long time. Recently, however a growing body of literature has examined spontaneous neurotransmission for its own sake. It has been shown that a single vesicle fusion can be sufficient for communication between cortical neurons (Stevens and Wang, 1995) and may contribute to set the inhibitory tone of postsynaptic neurons (Lu and Trussell, 2000). Spontaneous release events may trigger action potential firing in cells with high membrane resistance (Carter and Regehr, 2002; Sharma and Vijayaraghavan, 2003) and may also play a role in the maturation of synapses (Murphy et al., 1994). A series of studies showed that spontaneous neurotransmitter release, rather than evoked neurotransmission, is a specific regulator of postsynaptic sensitivity to neurotransmitters—by suppressing the dendritic protein translation machinery locally and thereby maintaining receptor composition at synapses (Sutton et al., 2006; Sutton et al., 2007; Sutton et al., 2004). A recent study suggests that it may use the same Ca^{2+} sensor as evoked release but with a different sensitivity (Xu et al., 2009), indicating that

spontaneous release may share the exo- and endocytosis machineries with evoked transmission but may make different use of them.

In the previous chapter, I accumulated quite convincing evidence to suggest that separate recycling pathways contribute to selectively maintain spontaneous and evoked transmission. These results suggest that the maintenance of evoked synchronous or asynchronous release strictly depends on dynamin function at a rapid time scale, whereas spontaneous release does not require dynamin activation for up to 1 hour. Spontaneous neurotransmission can be maintained at normal levels even after complete depletion of vesicle pools that sustain Ca^{2+}-evoked neurotransmission.

Chapter 4 strongly suggests that spontaneous and evoked forms of neurotransmission originate from two vesicle pools that can be distinguished by their reliance of dynamin function. This premise is consistent with an earlier report from our laboratory, which suggested that spontaneous and activity-dependent vesicle recycling originate from distinct pools with limited cross-talk (Sara et al., 2005). In contrast, a recent study suggested that the two forms of release originate from the same set of vesicles that recycle upon activity by simultaneous monitoring of two populations of synaptic vesicles (Groemer and Klingauf, 2007).

Both studies employed FM dyes for the fluorescent probes to track synaptic vesicle trafficking (Groemer and Klingauf, 2007; Sara et al., 2005). FM dyes are modified styryl dyes, which fluoresce when inserted into lipid membranes while are quenched in polar environment such as water (Gaffield and Betz, 2006; Grinvald et al., 1988). The length of the lipophilic carbon tail determines the incorporation and departition rate from the plasma membrane in commercially available FM dye derivatives (Figure 5.1).

Throughout this chapter, I used a 90 seconds long, 47 mM K^+ mediated depolarization in the presence of FM dye to label the actively recycling pool of

synaptic vesicles, or synaptic vesicles responsive to depolarization. To selectively label spontaneously recycling synaptic vesicles, a10 minute long incubation was used in the presence of 1 μM TTX and FM dye. Departition or destaining of FM dyes was achieved by application of 90 mM K^+ solution as a challenge with depolarization. Then, I measured 1) the amount of dye uptake (F(0), measured prior to destaining or induction of dye release), which provides a quantity-wise estimation of synaptic vesicles responsive to depolarization or spontaneously fusing, 2) the amount of dye release (ΔF, measured during destaining), which is a measure of the size of synaptic vesicles responsive to depolarization (in the case of depolarization-induced loading, this will be the size of RRP), 3) the release kinetics (τ_{fast}), which provides information on how responsive synaptic vesicles are to a given stimulation (i.e. depolarization).

This chapter aimed to gain new insight into this discrepancy by taking advantage of the differential dynamin-dependence of the two forms of synaptic vesicle trafficking. Earlier work is revisited, which proposed that the spontaneous and evoked forms of release originate from the same set of vesicles that recycle upon activity (Groemer and Klingauf, 2007). Using confocal imaging with meta-detector, I monitored simultaneous release of a pair of green (FM2-10) and red (FM5-95) dyes following their spontaneous or activity-dependent uptake. It was found that the dye release kinetics depends heavily on their mode of uptake, whereas release kinetics of the more hydrophobic dye FM1-43 (used by Groemer and Klingauf) was not sensitive to its mode of uptake.

The difference between FM1-43 (used by Groemer and colleagues) and FM2-10 (used by Sara and colleagues) lies in the length of the lipophilic carbon tail (http://www.probes.invitrogen.com/resources/spectraviewer). FM2-10 (and also FM5-95) has a shorter tail compared to FM1-43, and thus leaves the plasma membrane faster (Figure 5.1) (Gaffield and Betz, 2006).

In addition, I took advantage of differential dynamin dependence between spontaneous and activity-dependent recycling synaptic vesicle pools to delineate synaptic vesicle recycling pathways that operate in parallel by employing FM dyes. Further experiments showed that the discrepancy between the two dyes originated from selective dynasore-sensitive uptake of FM1-43 by a slow asynchronous form of endocytosis that followed strong bouts of network activity present in these dissociated cultures, while FM2-10 application at rest solely tracked canonical spontaneous synaptic vesicle trafficking which is detached from prior activity and insensitive to dynamin inhibition. Thus the previous disagreements seem to stem from analysis limited in their entire reliance on one kind of FM dyes.

How long do the two pools of synaptic vesicles maintain their identity? The stability of synaptic vesicles was investigated and furthermore it was determined whether the two pools of synaptic vesicles are interchangeable at a given synaptic terminal. Delay up to 6 hours between exposure to FM dye and reuse upon depolarization showed minimal FM dye loss during delay, suggesting that synaptic vesicles responsive to depolarization are reluctant to fuse spontaneously for up to 6 hours at room temperature or are not likely replaced by other ‘awakening synaptic vesicles’ belonging to the ‘dormant’ or reserve pool (RP).

Recent independent studies provide further support to the idea of isolated spontaneous exo- and endocytosis operating in parallel (Fredj and Burrone, 2009; Xu et al., 2009). Therefore, the present study proposes that spontaneous recycling operates independent of evoked recycling machinery without a strict requirement for dynamin activation and spontaneously recycling synaptic vesicles are mobilized from an isolated pool of synaptic vesicles.

Materials and Methods

Dissociated hippocampal culture

Dissociated hippocampal cultures were prepared from postnatal Sprague-Dawley rats or floxed CdK5 mice (gift from Dr. J. A. Bibb)as previously described (Kavalali et al., 1999a). Unless stated otherwise, all experiments were carried out after 14 days *in vitro* (DIV) when synapses reach maturity (Mozhayeva et al., 2002).

Fluorescence imaging

A Modified Tyrode's solution containing 2 mM Ca^{2+}, 10 μM CNQX and 50 μM AP-5 was used in all experiments. Synaptic boutons were loaded with 400 μM FM2-10 or 8-16 μM FM1-43 (Molecular Probes, Eugene, OR) under conditions described in the Results section. The modified Tyrode's solution used in all experiments contained (in mM): 150 NaCl, 4 KCl, 2 $MgCl_2$, 10 glucose, 10 HEPES, and 2 $CaCl_2$, (pH 7.4, ≈ 310 mOsm). High K^+ solutions contained equimolar substitution of KCl (90 mM) for NaCl. All staining and washing protocols were performed with 10 μM 6-cyano-7-nitroquinoxaline-2, 3-dione (CNQX) and 50 μM aminophosphonopentanoic acid (AP-5) to prevent recurrent activity.

Maximal loading of the total recycling pool was performed by incubating cultures in a 47 mM K^+ solution for 90 s, which labels all of the recycling vesicle pool in a given synapse (Harata et al., 2001).

To load spontaneously recycling vesicles, cultures were incubated in a modified Tyrode's solution containing 1 μM TTX for 10 min, which inhibits action potentials induced by network activity inherent in the culture. In a typical experiment, high potassium challenge was applied at least three times (for 60-90 s each separated by 60 s interval washes with modified Tyrode's solution) to release all of the dye trapped in presynaptic terminals. Images were taken after

10-minute washes in dye-free solution in nominal Ca^{2+} to minimize spontaneous dye loss. In all experiments isolated boutons were selected (1 μm^2) for analysis and apparent synaptic clusters were avoided (Kavalali et al., 1999b). Baseline images were obtained every second for 30 seconds and cultures were stimulated with field stimulation. Images were obtained by a cooled-intensified digital CCD camera (Roper Scientific, Trenton, NJ) during illumination at 480 ± 20 nm (505 DCLP, 535 ± 25 BP) via an optical switch (Sutter Instruments, Novato, CA). Images were acquired and analyzed using Metafluor Software (Universal Imaging, Auburn Hills, MI).

Spectral imaging experiments

Images were obtained by a Zeiss LSM 510 META laser-scanning microscope equipped with LSM 510 Laser module (Carl Zeiss, Jena, Germany). To optimize image acquisition settings, the spectral signature of each dye was obtained when nerve terminals were labeled with either dye alone or both dyes together.

For dual labeling experiments, spontaneously recycling vesicles were labeled with either FM dye for 10 minutes in the presence of 1 μM TTX, 10 μM CNQX and 50 μM AP-5. After 5-minute perfusion with dye-free solution, neurons were incubated with the other FM dye during high K^+ challenge for 90 seconds. Cells were subsequently excited with lasers both at 488 nm and 543 nm, and the kinetics of fluorescence decrease for both FM dyes was simultaneously monitored (0.5 Hz acquisition rate) during 90 mM K^+ depolarization.

The bleed-through of fluorescence emission from FM 2-10 to red emission of FM 5-95 was approximately 15% whereas the bleed-through of FM 5-95 emission to green was ~3%.

All the experiments were performed at room temperature unless indicated otherwise.

Lentivirus production

HEK 293 cells were transfected with the Fugene 6 transfection system (Roche Molecular Biochemicals) with the expression plasmid and two helper plasmids, which are delta 8.9 and vesicular stomatitis virus G protein (3 μg of each DNA per 75 cm^2 flask of HEK cells) (Dittgen et al., 2004). After incubation of HEK cells at 37 °C for 48 hr, lentivirus containing culture medium was harvested and filtered at a 0.45 μm pore size prior to use for infection. Floxed CdK5 mice cultures were infected with Cre-GFP or GFP at 4 DIV by adding 300 μl of viral suspension to each well.

Data analysis

To quantify FM dye destaining kinetics ~100 synapses per experiment were selected and fluorescence values were normalized to the average baseline fluorescence at onset (F(0)) without subtracting background fluorescence to avoid distortion in destaining profiles that may not reach a "true" baseline (Groemer and Klingauf, 2007). The time constants (τ_{fast} and τ_{slow}) were calculated by fitting the destaining profiles with a double exponential function starting at stimulation onset. Two-tailed unpaired t-test was used for all statistical comparisons and values are given as mean ± SEM.

Results

Different detecting potential at rest between FM1-43 and FM2-10

FM1-43 labels a larger pool of synaptic vesicles at rest compared to FM2-10

Initially, earlier results were revisited in which hippocampal synapses were labeled by the spontaneous uptake of FM2-10 (400 μM) or FM1-43 (8 μM). Spontaneous uptake was measured in the presence of a Tyrode solution containing activity blockers (CNQX, AP-5 and TTX) for 10 minutes. After removal of excess dye (~ 10 min), synapses were challenged with 90 mM K^+ solution repeatedly to mobilize all releasable synaptic vesicles. After 10 minutes of rest the same set of synapses were loaded with FM2-10 or FM1-43 in depolarizing 47 mM K^+ solution to induce activity-dependent dye uptake and subsequently were repeatedly challenged with a 90 mM K^+ containing solution to trigger dye release (Figure 5.2). Under these conditions synapses spontaneously labeled with FM2-10 showed significantly slower destaining upon 90 mM K^+ stimulation in agreement with our earlier report (Figure 5.2.A and C) (Sara et al., 2005), while synapses that took up FM1-43 under resting conditions showed robust dye loss upon 90 mM K^+ stimulation, as reported by Groemer and Klingauf (2007) (Figure 5.2.B and D).

Why do spontaneously recycling synaptic vesicles behave differently depending on employed FM dyes? In order to examine whether FM1-43 and FM2-10 labeled the same fraction of vesicles that recycle spontaneously, the ratio of the amount of spontaneous dye uptake (ΔF (Spon)) to the amount of dye taken up in response to 47 mM K^+ depolarization (ΔF (47mM K^+)) was quantified (Figure 5.2.E). In the case of FM2-10, the ratio was approximately 24%, whereas spontaneous uptake of FM1-43 labeled a significantly larger fraction of vesicles approaching 62% (Figure 5.2.E). Thus, this analysis suggests that the number of

vesicles labeled by FM2-10 and FM1-43 under resting conditions shows only partial overlap.

Simultaneous measurement of synaptic vesicle trafficking using spectrally separable styryl dyes

Vesicles labeled with FM2-10 and FM5-95 at rest are reluctant to reuse upon depolarization

In order to verify the premise that FM2-10 uptake accurately reports the properties of spontaneous synaptic vesicle trafficking, its behavior was compared to the red shifted styryl dye FM5-95. For this purpose, the destaining profiles of the two dyes were acquired simultaneously after spontaneous or stimulation-dependent uptake. To optimize image acquisition settings, the spectral signature of each dye was obtained when nerve terminals were labeled with either dye alone or both dyes together. Figure 5.3 depicts the spectral signature of FM2-10 when excited at 488 nm and FM5-95 after excitation at 543 nm. FM2-10's emission peak was at 570 nm with a second peak at 528 nm, where as FM5-95 showed a strong emission peak near 660 nm (Figure 5.3). The emission peaks of both dyes did not show a significant shift when synapses were labeled with both dyes at the same time. To compare the mobilization kinetics of vesicles recycling spontaneously or in response to activity, I used a dye labeling paradigm and image acquisition setting akin to earlier work by Groemer and Klingauf (2007) (Figure 5.3).

To label activity-dependent recycling vesicles, a 90 seconds long, 47 mM K^+ mediated depolarization was used in the presence of FM2-10 (green) or FM5-95 (red) and after 5 min perfusion with dye free solution, neurons were exposed to the FM dye with the other color for 10 minutes in the presence of 1 μM TTX to label spontaneously recycling synaptic vesicles. Once excess dye was washed out (~10 min), dye destaining profiles were monitored upon 90 mM K^+ application by

exciting both dyes simultaneously at 488 nm and at 543 nm (for example, in Figure 5.4). The destaining profiles emerging from individual synapses were collected at maximum emission windows for each dye (FM2-10: 500-530 nm; FM5-95: 650-710 nm, Figure 5.3.B) and their kinetics were fitted to a double exponential decay function with fast and slow time constants (τ_{fast} and τ_{slow}).

When both FM dyes were taken up in response to 47 mM K^+ depolarization, τ_{fast} of FM2-10 and FM5-95 was largely comparable (Figure 5.4.D and G). However, when FM2-10 was labeled for spontaneously recycling vesicles and FM5-95 for synaptic vesicles which are recycling in response to stimulation, τ_{fast} of FM2-10 was slower that τ_{fast} of FM5-95 (Figure 5.4.E and H). When the dyes were exchanged and FM5-95 was used to label the spontaneously recycling vesicle pool, τ_{fast} of FM5-95 became slower compared to τ_{fast} of FM2-10 (Figure 5.4.F and I).

A particular advantage of these experiments stem from the fact the divergent destaining profiles were obtained simultaneously from the same synaptic bouton. Therefore, the destaining kinetics of the two dyes were further compared in a pair wise manner using the ratio of their fast destaining time constants (τ_{fast}) at each synapse. The average ratio of these fast time constants (τ_{fast} of FM2-10/ τ_{fast} of FM5-95, or R(τ))was around 1.04 when both dyes were taken up in response to 47 mM K^+ depolarization (Figure 5.4.J and K). In agreement with the premise that spontaneous and stimulation-dependent dye uptake selectively labels kinetically separable vesicle pools this ratio was increased to ~2.81 when FM2-10 was used to label vesicles recycling spontaneously (P<0.001) and decreased to ~ 0.52 when FM5-95 was used to mark spontaneous synaptic vesicle recycling (P<0.001, Figure 5.4.J and K).

Synaptic vesicles which take up FM1-43 spontaneously readily respond to depolarization

What about FM1-43? Can a diverse behavior of FM1-43 compared to FM5-95 be detected? Simultaneous spectral imaging experiments were repeated with FM 1-43 and FM5-95 with the same setting (Figure 5.5). As expected, FM1-43 readily released trapped dye upon depolarization when spontaneously loaded as well as when loaded upon depolarization (Figure 5.5.A-B). When FM1-43 was used to label spontaneously recycling pool, the release kinetics of FM1-43 upon depolarization (τ_{fast}) was comparable to of FM5-59 which labeled activity-dependent recycling vesicles (Figure 5.5.D-F). It was also not different from τ_{fast} calculated from Figure 5.5.C ($P>0.5$).

When the ratio of fast destaining time constants (τ_{fast}) at each synapse were compared in a pair wise manner, the average ratio of these fast time constants (τ_{fast} of FM1-43/ τ_{fast} of FM5-95, or R(τ)) was approximately 1.2 when both dyes were taken up in response to 47 mM K^+ depolarization (Figure 5.5.G and H). This ratio remained to ~1.22 when FM1-43 was used to label vesicles recycling spontaneously ($P<0.9$) but decreased to ~ 0.7 when FM5-95 was used to label spontaneous synaptic vesicle recycling ($P<0.001$, Figure 5.5.G and H). Taken together, the opposing observations between FM1-43 and FM2-10 made in simultaneous optical experiments suggest that FM1-43 labels a more loose pool of synaptic vesicles at rest compared to FM2-10.

Manipulation of FM1-43 versus FM2-10 uptake at rest

Why do FM1-43 and FM2-10 display divergent destaining kinetics after spontaneous uptake? These two dyes differ with respect to their relative hydrophobicity. FM1-43 with a longer carbon tail is relatively more hydrophobic, and thus is expected to departition slowly compared to FM2-10 or FM5-95

(Gaffield and Betz, 2006; Klingauf et al., 1998). The next series of experiments extensively explored the possible sources which only can be additionally marked by FM1-43.

Bulk membrane retrieval or slow (compensatory) endocytosis has been proposed to operate as a frequent mode of membrane retrieval in central synapses (Clayton et al., 2007; Cousin, 2009). Previous studies have suggested that this form of endocytosis following strong bouts of neuronal activity may selectively trap more hydrophobic FM1-43 but not FM2-10 (Evans and Cousin, 2007; Richards et al., 2000; Richards et al., 2003). Therefore, it was hypothesized that FM1-43 labels an additional membrane source retrieved by bulk endocytosis.

History of network activity level at given synapses determines the detecting potential of FM dyes

Slow endocytosis or bulk endocytosis is proposed to be activity-dependent (Clayton et al., 2009; Clayton et al., 2008; Evans and Cousin, 2007) and the time course of slow endocytosis turns not to be "slow" at all (Clayton et al., 2008). In spite of its artificial nature, dissociated cultures are highly active environment. In the absence of any blockers, synaptic activity alone can label more than 50% of synaptic vesicles belonging to readily releasable pool (RRP) at a given high density cultured synapses (Sara et al., 2005). In addition, chronic changes in activity levels has been shown to regulate synaptic vesicle trafficking (Virmani et al., 2006). Therefore, it was examined whether the release kinetics of FM1-43 after spontaneous uptake is sensitive to the prior network activity levels in the hippocampal cultures.

To alter the level of background network activity, mature cultures were pre-incubated with 1 μM TTX for 30 min ("pre-silencing") prior to dye uptake and release (Figure 5.6.A-B) or immature hippocampal cultures was used, which typically have lower network activity levels (Figure 5.6.C-D). Under both

conditions, spontaneous uptake of FM1-43 (10 minutes in TTX) resulted in slow dye loss upon subsequent depolarization and the size of the synaptic vesicle pool labeled with FM1-43 showed a significant decrease (Figure 5.6). On the other hand, the conditions did not significantly affect the stimulation dependent uptake and release of FM2-10 (data not shown). This observation strongly suggests that at rest, FM1-43 labeling reflects the history of activity at a given set of synapses, thus contaminated with other endocytic processes operating in parallel.

Temperature regulates the detecting potential of FM dyes

If the history of activity matters, would FM2-10 be able to label more synaptic vesicles as background activity increases? To manipulate overall synaptic activity at cultured synapses, experiments were performed at 37°C. First the effect of temperature on FM dye release was analyzed depending on the type as well as the loading protocol (Figure 5.7). In the case of FM1-43, temperature has minimal effect on FM1-43 uptake during depolarization and at rest as well as the rate of FM1-43 loss upon 90 mM K^+ – induced depolarization (Figure 5.7.E-H, L-M). The slight increase in the RRP size at 37°C (P=0.08) seems to contribute to the decrease in the fraction of vesicles that take up FM1-43 spontaneously because ΔF(spon) remained unchanged at RT and at 37°C (P>0.8).

In contrast, the increase in temperature accelerated the release kinetics of spontaneously labeled FM2-10 in response to depolarization (Figure 5.7.C-D, J). This effect of temperature was selective to spontaneous FM2-10 uptake (Figure 5.7.A-D, I-J). The increase in availability of spontaneously recycling vesicles resulted in an increase of the ratio of the amount of spontaneous dye uptake (ΔF (Spon)) to the amount of dye taken up in response to 47 mM K^+ depolarization (ΔF (47mM K^+)) (Figure 5.7.K). However, this set of experiments was performed in different synapses due to the technical limitation of rapid exchange between

25°C and 37°C. Therefore, I switched to a meta-detector optic system and simultaneously monitored the behavior of double-labeled synaptic vesicles.

Synapses were incubated with FM 5-95 during 47 mM K^+–induced depolarization as a reference (reference loading), and after a brief wash, were loaded with FM1-43 at rest for 10 min or during depolarization at 37°C. As summarized in Figure 5.8, at elevated temperature, spontaneously loaded FM2-10 exhibited relatively faster dye release upon depolarization consistent with previous analysis (Figure 5.8.A-D). A pair wise analysis of the ratio of τ_{fast} measurements at individual synapses reveals that at 37°C, the kinetic difference in the ratio of τ_{fast} ($R(\tau)$) of FM2-10 depending on loading condition disappeared at 37°C (P>0.8) (Figure 5.8.E-F). In other words, FM2-10 exhibited faster destaining kinetics in response to depolarization at 37°C even when spontaneously loaded.

Inhibition of PI3K activity failed to limit FM1-43 uptake at rest

Previously, it was hypothesized that bulk endocytosis or slow endocytosis might contaminate the FM1-43 uptake at rest from labeling "true" spontaneously recycling vesicles. Given that network activity can regulate synaptic vesicle trafficking (Virmani et al., 2006), it was observed that the background network activity level limits FM1-43 uptake at rest(Figure 5.6). This observation suggests that slow endocytosis at rest might contribute to additional membrane source sensitive to FM1-43. Although molecular mechanism required for bulk endocytosis is largely unknown, phosphoinositides (Cremona and De Camilli, 2001; Osborne et al., 2001) and actin (Gad et al., 2000; Qualmann et al., 2000) have been implicated to play a role in bulk membrane retrieval or compensatory endocytosis at synapses. More recently, it has been shown that bulk endocytosis requires the activity of phosphatidylinositol 3-kinase (PI3K) and actin polymerization but not small vesicle endocytosis at bipolar cells (Holt et al.,

2003). In neurons, depolarization-induced Ca^{2+} influx can activate PI3K (Crowder and Freeman, 1999; Ikegami and Koike, 2000). In addition, Ca^{2+} has been shown to regulate actin filament in bipolar synapses (Job and Lagnado, 1998). Therefore, it was examined whether inhibition of PI3K and/or interruption in actin polymerization would limit the additional uptake by FM1-43 at rest.

Hippocampal synapses were loaded with FM 5-95 during 47 mM K^+–induced depolarization as a reference (reference loading), and after a brief wash, incubated with 50 μM 2-(4-morpholinyl)-8-phenyl-4H-1-benzopyran-4-one (LY294002), a selective inhibitor of PI3K for 15 min, then loaded with FM1-43 at rest for 10 min or during depolarization (Vlahos et al., 1994) (Figure 5.9). The amount of dye uptake (F(0)), and the size of the vesicle fraction responsive to depolarization (ΔF) was comparable in both loading conditions in the absence and presence of LY294002, in agreement with no involvement of PI3K in exocytosis or endocytosis of small synaptic vesicles (Holt et al., 2003) (Figure 5.9.D). However, unlike in bipolar cells, inhibition of PI3K had little effect on FM 1-43 release kinetics of spontaneously loaded synaptic vesicles (τ_{fast} in Figure 5.9.C and 5.9.E-F). A counterpart compound with little effect on PI3K activity, 2-piperazinyl-8-phenyl-4H-1-benzopyran-4-one (LY303511, 50 μM) also has no effect in FM1-43 uptake and release regardless of loading condition.

Next, the effect of cytochalasin D (Casella et al., 1981), a potent inhibitor of action filament polymerization was tested on FM1-43 uptake at rest (Figure 5.10). Hippocampal cultures were loaded with FM1-43 at rest in the presence of 20 μM cytochalasin D or 0.1% DMSO after 15 min incubation with cytochalasin D or vehicle (Figure 5.10). Acute inhibition of actin polymerization also failed to limit the labeling by FM1-43 to "true" spontaneously recycling synaptic vesicles, suggesting that bulk membrane retrieval by formation of a large vacuole might not be the likely source of extra FM1-43 uptake at resting condition.

Interruption of CdK5 activity failed to limit FM1-43 uptake at rest

I continued to purse the possibility that other mechanisms implicated in bulk endocytosis contributed to non-specific FM1-43 labeling at rest. The proceeding set of experiments examined the role of cyclin-dependent kinase 5 (CdK5) in bulk membrane retrieval and promiscuous FM1-43 uptake at rest.

CdK5 is a proline-directed serine/threonine kinase, which is presynaptically abundant in mature synapses (Tomizawa et al., 2002). It has been shown that CdK5 has a number of substrates that mediate or regulate exo- and endocytosis including dynamin 1 (Tomizawa et al., 2003). More recently, CdK5 has been shown to regulate activity-dependent bulk membrane retrieval at small synapses (Evans and Cousin, 2007).

A Cre–inducible conditional Cdk5 knockout animal was utilized (floxed CdK5 mice, fCdK5 –/–) (Hawasli et al., 2007) in combination with viral expression of Cre recombinases, hoping to identify additional membrane retrieval mechanisms at rest. Hippocampal cultures obtained from fCdK5-/- mice were infected with Lentiviral Cre-recombinase or GFP at 4DIV. Because Cre-recombinase expression is generally limited to cell bodies, I employed not only red FM dye, FM5-95 but also green FM dyes, FM1-43 and FM2-10. Cultures were loaded with FM dyes during 47 mM K^+–induced depolarization for 90 seconds and challenged with depolarization after removal of excessive dye (Figure 5.11). The FM dye experiment quantifies both exo- and endocytosis during the loading procedure but limits the detection to mainly exocytosis events during the destaining step. If vesicle endocytosis –both slow and fast– rather than exocytosis is regulated by acute inhibition of CdK5 activity, the amount of dye uptake than release kinetics will be a useful indicator to see the effect of CdK5 loss upon endocytosis. However, CdK5 deficient synapses exhibited similar

amount of dye uptake (F(0)), size of RRP (ΔF) as well as release kinetics of FM dyes with all FM dyes employed (Figure 5.11).

CdK5 is known to play an important role in neuronal development and migration (Dhariwala and Rajadhyaksha, 2008; Paglini and Caceres, 2001). Since the expression of CdK5 is knocked-down at early 4DIV, the present results could be due to mal-development of neuronal processes. In addition, synapses were maintained in a cultured environment lacking of CdK5 activity for extended period (for 10-12 days), therefore it is possible that chronic blockade of CdK5 has a different effect on vesicle endocytosis or, was somehow compensated for in culture system.

To acutely inhibit CdK5 activity at mature synapses, a pharmacological approach was employed which utilized roscovitine, a potent antagonist of a range of CdKs including CdK5. In order to address whether CdK5 –dependent membrane retrieval is sensitive to FM1-43 uptake at rest, synaptic vesicles were labeled with FM dyes before and after roscovitine treatment. By taking advantage of dual color imaging apparatus, the destaining patterns of two colors of FM dyes were simultaneously monitored at individual synapses.

Mature hippocampal synapses were loaded with FM 5-95 during 47 mM K^+–induced depolarization as a reference (reference loading), and incubated with 50 μM roscovitine for 15 min prior to spontaneous FM1-43 loading or depolarization –induced FM1-43 uptake (Figure 5.12). However roscovitine showed little effect on FM dye release kinetics of spontaneously loaded synaptic vesicles (τ_{fast} in Figure 5.12.C and 5.12.E-F). The amount of dye uptake (F(0)), and the size of the vesicle fraction responsive to depolarization (ΔF) was comparable in both loading conditions (Figure 5.12.D).

Dynamin inhibition limits the detecting potential of FM1-43

The observations described in chapter four suggest that acute inhibition of dynamin function with dynasore selectively suppresses evoked but not spontaneous synaptic vesicle trafficking. On the other hand, a recent study suggested that interaction between dynamin and syndapin activates bulk endocytosis in an activity-dependent manner (Clayton et al., 2009). These results together with previous observations predict that FM1-43 uptake under resting conditions should be sensitive to dynasore as the degree of spontaneous FM1-43 labeling is sensitive to prior activity. To test this prediction, cells were exposed to FM1-43 in the presence of 80 μM dynasore or 1% DMSO for 10 min under resting conditions (in TTX without "pre-silencing") and subsequently stimulated with 90 mM K^+ after dye removal (Figure 5.13.A-B). Under these conditions, I found that dynasore application indeed decreased the extent of spontaneous FM1-43 uptake and slowed its release kinetics in response to 90 mM K^+ challenge ($P<0.05$, Figure 5.13.A-B). This effect of dynasore was specific to FM1-43 as spontaneous trafficking of FM2-10 was unaffected by the presence of dynasore during dye uptake (Figure 5.13.C-D).

Taken together, these results suggest that under standard conditions spontaneous uptake and release of FM2-10 is a selective reporter for genuine spontaneous synaptic vesicle trafficking, which in turn gives rise to spontaneous neurotransmission. FM1-43, on the other hand, labels two endocytic processes one that overlaps with spontaneous synaptic vesicle trafficking and the other an asynchronous form of endocytosis that follows strong bouts of activity with a delay and requires dynamin function.

Long-term stability of synaptic vesicle pools

So far, these observations support the idea that selective recycling pathways operate in hippocampal synaptic terminals. This begs the question, how long do the two pools of synaptic vesicles maintain their unique identities? The stability of

synaptic vesicles was investigated and whether two pools of synaptic vesicles are interchangeable at a given synaptic terminal. To observe the maintenance of activity-dependent recycling synaptic vesicles, 8 μM FM1-43 was loaded for this pool of synaptic vesicles during depolarization (47 mM K^+) for 90 seconds, and varied wash time from 1 to 6 hours prior to challenge with 90 mM K^+ application to release FM dye. During an extended wash time, Ca^{2+}-free solution was constantly perfused at room temperature. The same synapses were loaded again and challenged with depolarization after a 10 min-long wash. 10 min of rest was allowed in between. The double loading protocol allows us to compare the kinetics and the amount of dye uptake (F(0)) as well as the size of RRP (ΔF) at the same synapses, and also to evaluate the condition of neurons after prolonged incubation at room temperature in Ca^{2+}-free solution (Figure 5.1.4).

If vesicles from the recycling pool are replaced by vesicles from the RP during these washes or vesicles fuse spontaneously during the extended delay, a decrease in the amount of releasable dye (ΔF) should be observed due to the replacement of unloaded vesicles or due to spontaneous loss of loaded vesicles. However, no difference in release kinetics (Figure 5.14.B-E) or the size of pool of synaptic vesicles responsive to depolarization was observed up to 6 hours (Figure 5.14.F-I) compared to after a short wash in the same synapses (Figure 5.14). These results suggest that the synaptic vesicles responsive to depolarization can be maintained with high stability without spontaneous loss or replacement with 'fresh' synaptic vesicles for up to 6 hours, however the possibility remains that synaptic activity or usage might regulate the exchange of synaptic vesicles between two pools, and that temperature may influence the dynamic of synaptic vesicle mobilization.

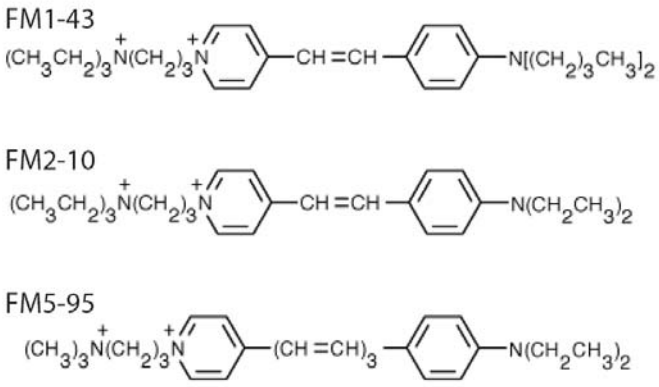

FIGURE 5. 1. Structure of FM dye derivatives
FM dye is composed of a positively charged head group, two aromatic rings containing a different number of double bonds, and carbon tail. The number of double bonds between two aromatic rings determines the emission spectrum and the length of the carbon tail affects the incorporation and departition rate of dye into membranes.

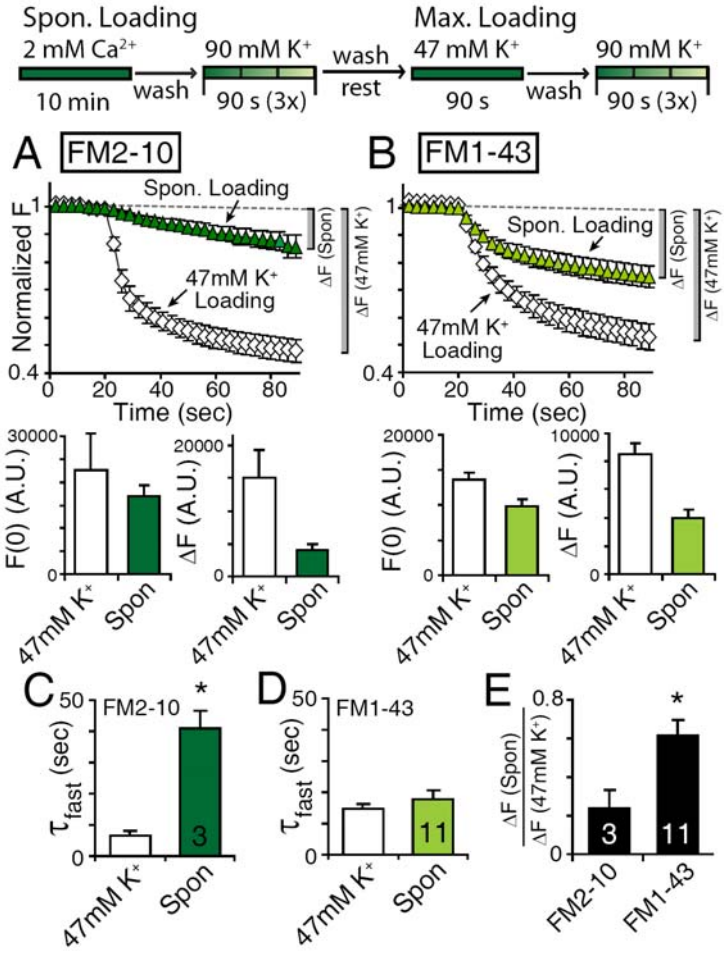

FIGURE 5. 2. Properties of spontaneous synaptic vesicle trafficking reported by FM2-10 and FM1-43 diverge.

The top panel outlines the experimental paradigm used to label vesicles that recycle spontaneously or in response to activity. (A) When FM2-10 was employed to label vesicles at rest (in 2 mM Ca^{2+}, APV, CNQX, and TTX for 10 minutes) or during depolarization (in 47 mM K^+ for 90 seconds) , the kinetics of subsequent dye loss upon 90 mM K^+ stimulation was different depending on the loading protocol. Vesicles labeled with spontaneous dye uptake were refractory to 90 mM K^+ stimulation leading to slow release kinetics. The amount of dye uptake (F(0)) and the size of the synaptic vesicle pool responsive to depolarization (ΔF) were quantified. (B) In contrast, uptake of FM1-43 at rest or in response to depolarization resulted in fast dye loss irrespective of the mode of dye uptake. The amount of dye uptake (F(0)) and the size of the synaptic vesicle pool

responsive to depolarization (ΔF) were quantified. (C) Bar graph depicts the average time constants of dye loss after FM2-10 uptake during activity and at rest (n = 3, 520 synapses for both conditions, P<0.01). (D) Bar graph depicts the average time constants of dye loss after FM1-43 uptake during activity and at rest (n = 11, 1760 synapses for both conditions) (P>0.2). (E) The fraction of vesicles that take up FM1-43 spontaneously is larger than those labeled by FM2-10 at rest with respect to maximal dye uptake induced by 47 mM K^+ stimulation (ΔF (Spontaneous loading protocol)/ΔF (47 mM K^+)) (P<0.05).

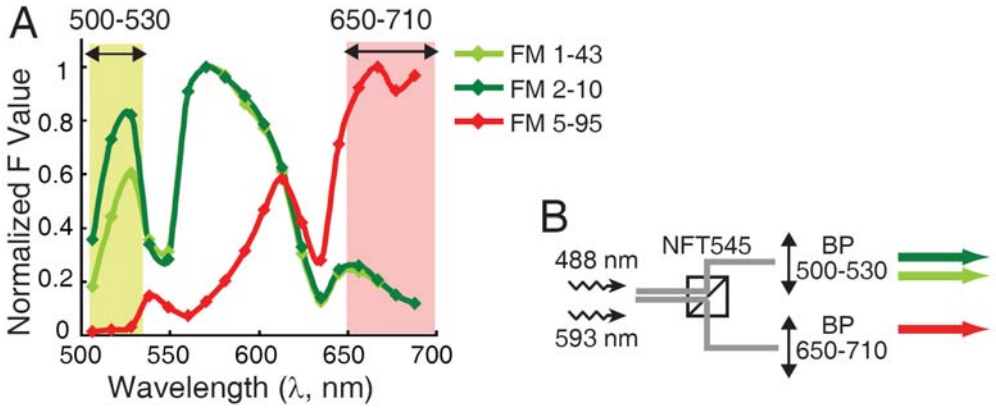

FIGURE 5. 3. Configuration of metadetector to simultaneously monitor spectrally separable FM dyes.
(A) Emission spectra of FM2-10 and FM5-95 during 488 nm and 543 nm excitation. (B) Illustration of confocal configuration for dual color experiments. Samples were excited at both 488 nm and 543 nm. For green signals, the emission passed through the band pass filter 500 – 530 nm was collected. For red signals, the fluorescence emission between 650 – 710 nm was collected.

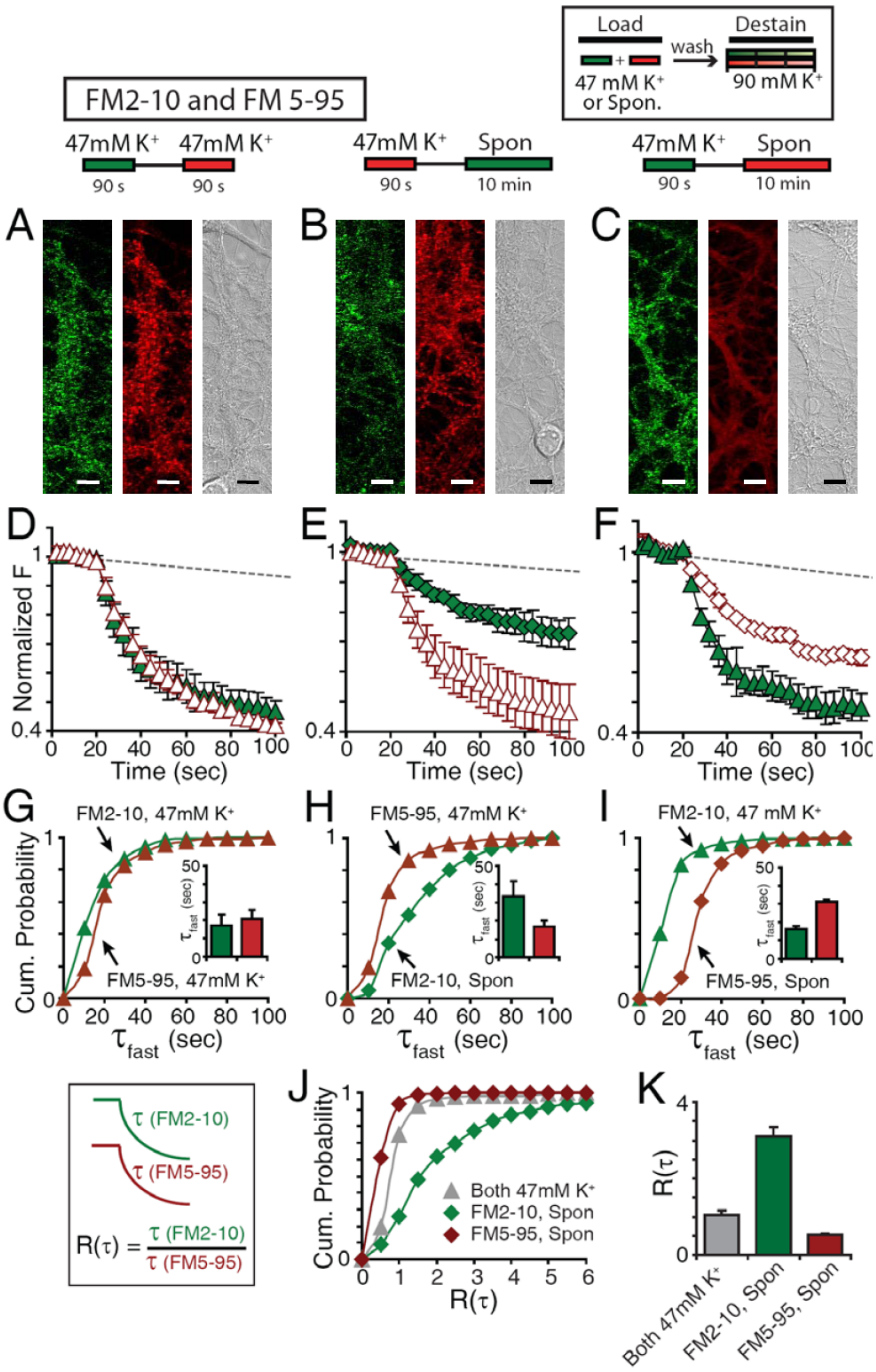
Load
Destain
wash
47 mM K+
or Spon.
90 mM K+
FM2-10 and FM 5-95
47mM K+ 47mM K+
90 s 90 s
47mM K+ Spon
90 s 10 min
47mM K+ Spon
90 s 10 min
A
B
C
D
E
F
Normalized F
Time (sec)
G
H
I
FM2-10, 47mM K+
FM5-95, 47mM K+
FM5-95, 47mM K+
FM2-10, Spon
FM2-10, 47 mM K+
FM5-95, Spon
Cum. Probability
τfast (sec)
τ (FM2-10)
τ (FM5-95)
R(τ) = τ (FM2-10) / τ (FM5-95)
J
K
Both 47mM K+
FM2-10, Spon
FM5-95, Spon
R(τ)

FIGURE 5. 4. Simultaneous monitoring of FM2-10 and FM5-95 release after tandem spontaneous or stimulation-dependent dye uptake shows that spontaneously trafficking vesicles are refractory to activity.
Cultures were incubated with a FM dye in the presence of 47 mM K^+ for 90 sec and after 5 min perfusion with dye free solution. The same neurons were incubated for 10 min with the other color of FM dye at rest (1μM TTX). After dye removal cells were challenged with 90 mM K^+ for 90 seconds for three consecutive rounds and the fluorescence change in both green and red emission windows was simultaneously monitored. (A-C) Representative images of synaptic boutons under each condition are shown. The dye loading condition for each panel is illustrated at the top. (D-F) The graphs depict the average FM dye destaining kinetics from all experiments (n = 3-4, 330-470 synapses under each condition). FM2-10 and FM5-95 behave in a very similar manner when loaded in the presence of 47 mM K^+, presumably due to their similar hydrophobicities (stemming from the lengths of their hydrocarbon tails). After spontaneous uptake, however, both FM2-10 and FM5-95 exhibited slower dye loss in response to depolarization (FM2-10 in E and FM5-95 in F). (G-I) Analysis of the fast time constants of destaining (τ_{fast}) for FM2-10 and FM5-95 at individual synapses. (G) When both dyes were used for activity-dependent labeling, τ_{fast} of FM2-10 and of FM5-95 was comparable (330 synapses from 3 experiments, P>0.6). The total amount of dye uptake (F(0)) as well as the size of the synaptic vesicle pool responsive to depolarization (ΔF) were also comparable in both cases (P>0.2). (H) When FM2-10 was used for spontaneous labeling, τ_{fast} of FM2-10 was slower than that of FM5-95. (320 synapses from 4 experiments, P<0.05). (I) When FM5-95 was used for spontaneous labeling, τ_{fast} of FM5-95 was slower than that of FM2-10 (340 synapses from 4 experiments, P<0.01). (J-K) Analysis of the ratio of τ_{fast} measurements at individual synapses. The τ_{fast} ratio (R(τ)) was defined as τ_{fast} (FM2-10)/ τ_{fast} (FM5-95). The distribution as well as the mean R(τ)s were different depending on the manner in which dyes were taken up.

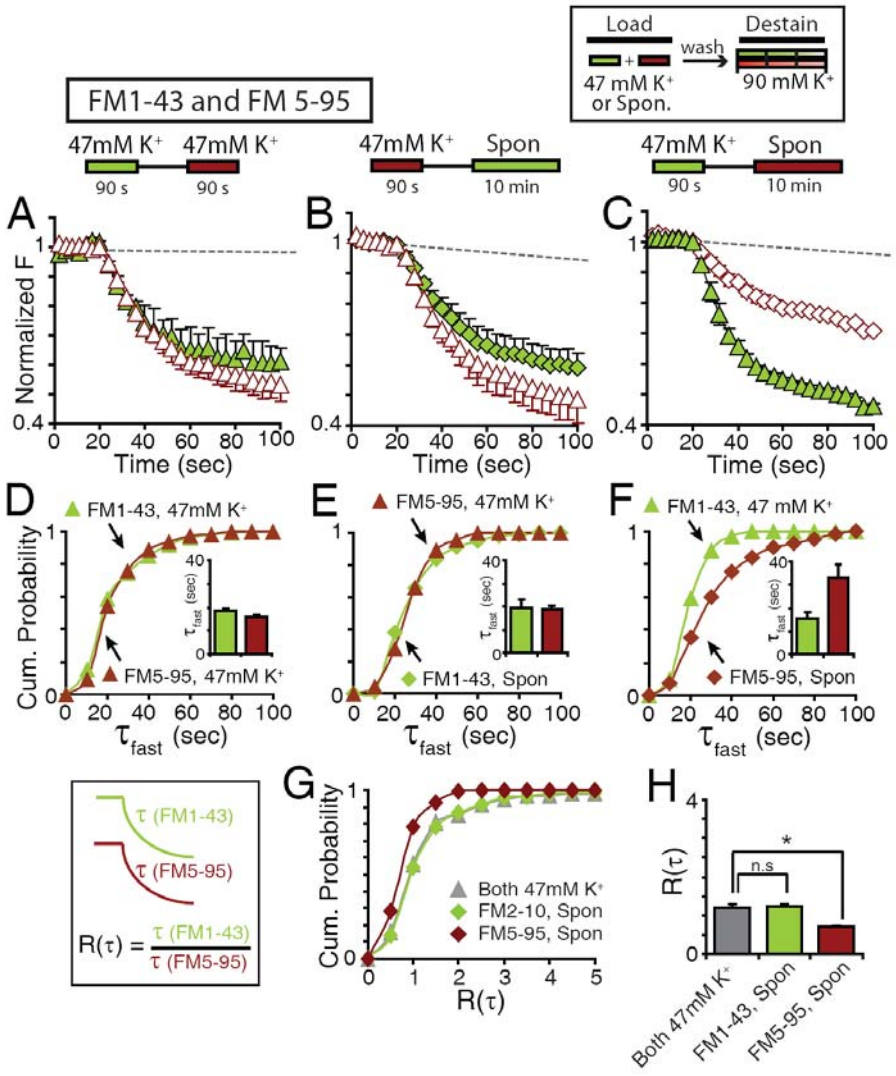

FIGURE 5. 5. Simultaneous monitoring of FM1-43 and FM5-95 release after tandem spontaneous or stimulation-dependent dye uptake shows that spontaneous vesicle trafficking reported by FM1-43 exhibited different behavior upon activity. Experiments were performed as described in FIGURE 5.4. (A-B) The graphs depict the average FM dye destaining kinetics from all experiments (n=2-4, 175-380 synapses under each condition). The dye loading condition for each panel is illustrated at the top. FM1-43 and FM5-95 exhibited prompt release of FM dye upon 90 mM K^+ solution application. After spontaneous uptake, however, FM1-43 exhibited faster dye loss in response to

depolarization whereas FM5-95 showed slower dye loss as in FIGURE 5.4. (FM1-43 in B and FM5-95 in C). (D-F) Analysis of time constants of destaining (τ_{fast}) for FM1-43 and FM5-95 at an individual synapses. (D) When both dyes were used to label the activity-dependent recycling pool, τ_{fast} of FM1-43 and of FM5-95 was comparable (175 synapses from 3 experiments, $P>0.1$). The total amount of dye uptake (F(0)) as well as the fraction responsive to depolarization (ΔF) were also comparable in both cases ($P>0.4$). (E) When FM1-43 was used for spontaneous labeling, τ_{fast} of FM1-43 was comparable to that of FM5-95. (310 synapses from 3 experiments, $P>0.7$). (F) When FM5-95 was used for spontaneous labeling, τ_{fast} of FM5-95 was slower than that of FM1-43 (380 synapses from 4 experiments, $P<0.05$). (G-H) A pair wise analysis of the ratio of τ_{fast} measurements at individual synapses. The distribution as well as the mean R(τ)s were different depending on the manner in which dyes were taken up when FM5-95 was used for spontaneous labeling of synaptic vesicles (*$P<0.001$) but not when FM1-43 was used for labeling of spontaneously recycling synaptic vesicles ($P>0.7$).

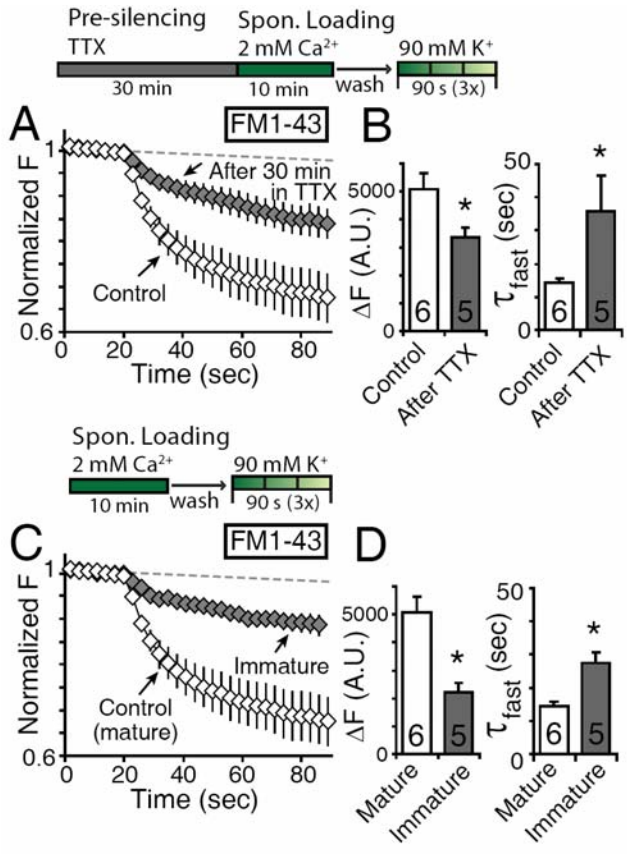

FIGURE 5. 6. FM1-43 labeled synaptic vesicles at rest reflect the history of activity in a given set of synapses.

(A, B) Cells were pre-incubated with 1 μM TTX for 30 min prior to exposure to FM1-43 at rest (in 2 mM Ca^{2+}, APV, CNQX, and TTX for 10 minutes). Inhibition of neuronal network activity for 30 min in TTX reduced the size of the synaptic vesicle pool responsive to depolarization (ΔF, $P<0.05$) and slowed the rate of subsequent dye loss upon depolarization (τ_{fast}, $P<0.05$, 1025 synapses from 6 experiments for control, and 950 synapses from 5 experiments for TTX-treated group). (C, D) In immature synapses (10-12 DIV), FM1-43 labeled a smaller pool of synaptic vesicles at rest (ΔF, $P<0.001$) which were mobilized with a relatively slow rate upon 90 mM K^+ application (τ_{fast}, $P<0.001$, 1025 mature synapses from 6 experiments, 420 immature synapses from 5 experiments).

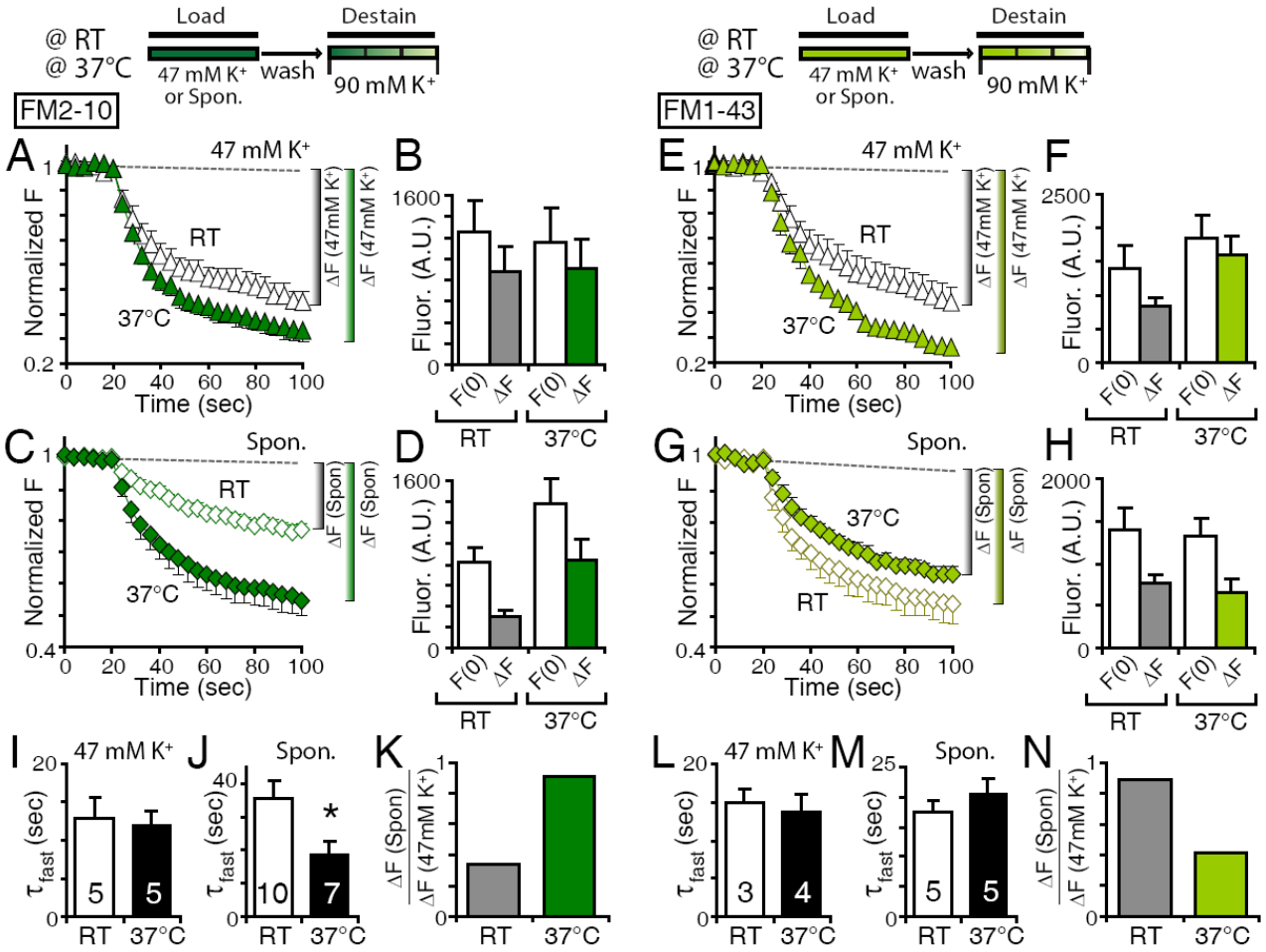
@ RT
@ 37°C
Load
47 mM K+
or Spon.
wash
Destain
90 mM K+
FM2-10
FM1-43
A
B
C
D
E
F
G
H
I
J
K
L
M
N
47 mM K+
Spon.
RT
37°C
Normalized F
Time (sec)
ΔF (47mM K+)
ΔF (Spon)
Fluor. (A.U.)
F(0)
ΔF
τfast (sec)
ΔF (Spon) / ΔF (47mM K+)

FIGURE 5. 7. At elevated temperature, FM2-10 labels a non-specific pool of synaptic vesicles at rest.

Top panels outline the experimental paradigm used to label vesicles that recycle spontaneously or in response to activity at different temperatures. (A, B) When FM2-10 was employed to label vesicle during depolarization (in 47 mM K^+ for 90 seconds), the kinetics of subsequent dye loss upon 90 mM K^+ stimulation was not different depending on the temperature. The amount of dye uptake (F(0)) and the size of the synaptic vesicle pool responsive to depolarization (ΔF) remained unchanged (P>0.8). (C, D) When FM2-10 was employed to label vesicles at rest (in TTX for 10 minutes), the kinetics of subsequent dye loss upon 90 mM K^+ stimulation was different depending on the temperature. Elevated temperature shifted refractory release of FM2-10 labeled vesicles to rapid release upon depolarization. (E-H) In contrast, uptake of FM1-43 at rest or in response to depolarization resulted in fast dye loss irrespective of the mode of dye uptake as well as of temperature. F(0) and ΔF remained unchanged between temperatures (P>0.3) except the size of RRP tends to be larger at 37°C (P=0.08). (I) Bar graph depicts the average time constants of dye loss after FM2-10 uptake during activity at different temperatures (n =5 at each temperature, P>0.7). (J) At 37°C, the time constant of FM2-10 release decreased when loaded at rest (n =7-10 at each temperature, P<0.05), thus is comparable τ_{fast} of FM2-10 loss when loaded during depolarization shown in panel I (P>0.1). (K) The fraction of vesicles that take up FM2-10 spontaneously at 37°C on average, increased compared to at room temperature with respect to maximal dye uptake induced by 47 mM K^+ stimulation (ΔF (Spontaneous loading protocol)/ΔF (47 mM K^+)) Note that this analysis is not done with the same set of synapses due to the technical challenge of rapid control of the temperature. (L, M) Bar graph depicts the average time constants of dye loss after FM1-43 uptake during activity and at rest (n = 11, 1760 synapses for both conditions) (P>0.2). (N) The fraction of vesicles that take up FM1-43 spontaneously at 37°C decreased due to the relative increase in RRP size. ΔF upon depolarization was not changed depending on loading protocol at 37°C (P>0.3).

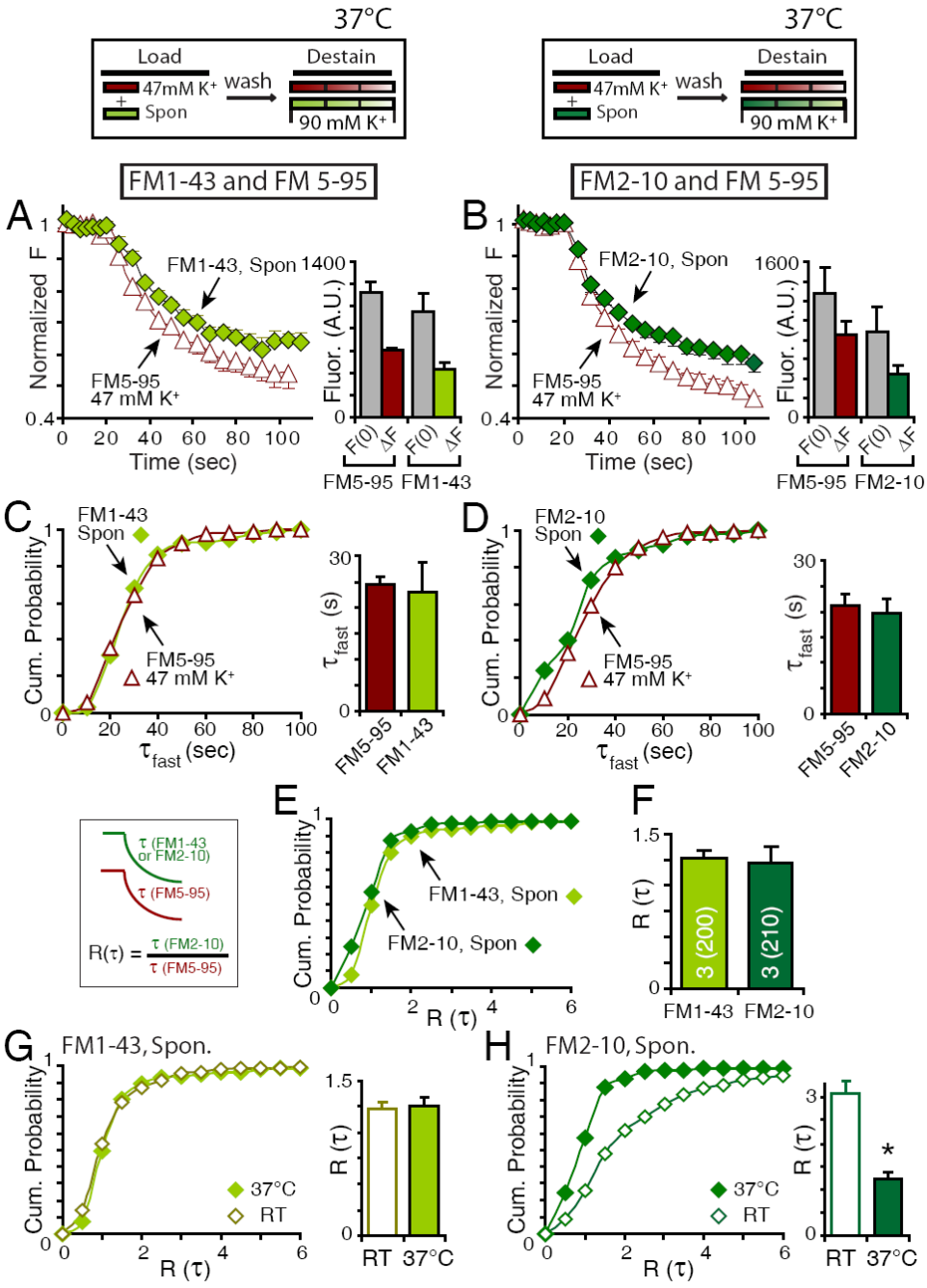
37°C
Load
47mM K+
Spon
wash
Destain
90 mM K+
FM1-43 and FM 5-95
FM2-10 and FM 5-95
A
B
Normalized F
FM1-43, Spon
FM2-10, Spon
FM5-95
47 mM K+
Time (sec)
Fluor. (A.U.)
F(0)
ΔF
FM5-95
FM1-43
FM2-10
C
D
Cum. Probability
τfast (sec)
τfast (s)
E
F
R (τ)
3 (200)
3 (210)
τ (FM1-43 or FM2-10)
τ (FM5-95)
R(τ) = τ (FM2-10) / τ (FM5-95)
G
H
FM1-43, Spon.
FM2-10, Spon.
37°C
RT
*

FIGURE 5. 8. Synaptic vesicles labeled by FM2-10 at rest at 37°C become responsive to depolarization.
Cultures were incubated with FM5-95 in the presence of 47 mM K^+ for 90 sec (reference loading) and after 5 min perfusion with dye free solution, the same neurons were incubated for 10 min with FM1-43 or FM2-10 at rest at 37°C. (A-B) The graphs depict the average FM dye destaining kinetics from all experiments (n = 3, 200-210 synapses under each condition). Both FM143 and FM2-10 behave in a very similar manner in response to depolarization. (C-D) Analysis of the fast time constants of destaining (τ_{fast}) at an individual synapses. FM1-43 and FM2-10 showed comparable τ_{fast} to FM5-95 (P>0.7 and P>0.6, respectively). (E, F) A pair wise analysis of the ratio of τ_{fast} measurements at individual synapses reveals that at 37°C, the difference observed at room temperature disappeared (P>0.8). (G-H) The distribution of the ratio of τ_{fast}, R(τ) measured at 37°C are represented in combination with at room temperature (shown in FIGURE 5.4 and 5.5) for comparison purpose (P>0.7 for FM1-43, P<0.001 for FM2-10).

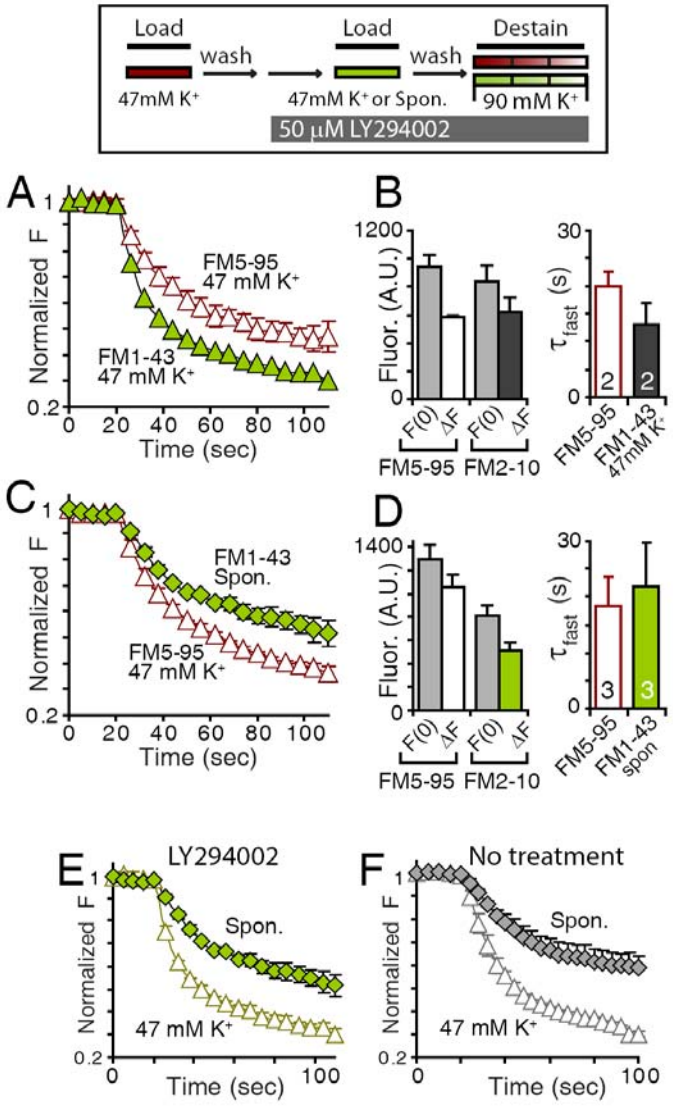

FIGURE 5. 9. Acute inhibition of PI3K activity fails to limit promiscuous labeling of FM1-43 at rest.

After FM5-95 labeling of the readily releasable pool (reference loading), cells were incubated with 50 μM LY294002, a PI3K inhibitor for 15 min prior to the second exposure to FM1-43. FM1-43 was used to label synaptic vesicles belonging to either RRP (in 47 mM K^+ for 90 seconds) or spontaneously recycling pool (in TTX for 10 minutes). (A, B) No difference in release kinetics (τ_{fast} , P>0.3) as well as the amount of dye uptake

(F(0), measuring balance between exo- and endocytosis during 47 mM K^+ depolarization, $P>0.5$) and the size of RRP (ΔF, $P>0.7$) was observed between FM1-43 loading in the presence of LY294002 and reference loading, FM5-95 (200 synapses from 2 coverslips). (C) FMl-43 labeling at rest in the presence of LY294002 showed comparable release kinetics to reference loading, FM5-95 (τ_{fast} , $P>0.7$, 315 synapses from 3 coverslips). (E-F) FM1-43 release curves are represented here for comparison's sake. Note that there is no difference in terms of τ_{fast}, F(0) and ΔF of FM1-43 in both labeling conditions in the presence of LY294002 (shown in current FIGURE panel A and C), compared to tandem loading of FM1-43 (shown in FIGURE 5.5 B and C).

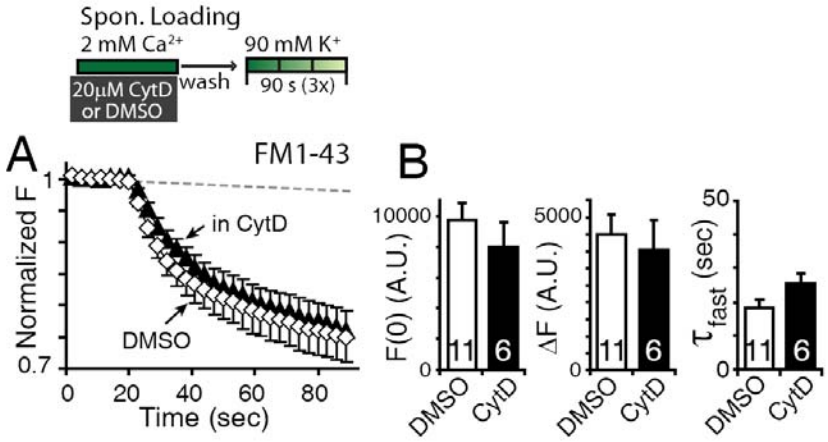

FIGURE 5. 10. Acute interruption of actin polymerization fails to limit promiscuous labeling of FM1-43 at rest.

Cells were incubated with 20 μM cytochalsin D (CytD), an actin filament polymerization inhibitor, or vehicle (0.1% DMSO) for 15 min prior to exposure to FM1-43 at rest (in 2 mM Ca^{2+}, APV, CNQX, and TTX for 10 minutes). (A, B) FMl-43 labeling at rest in the presence of cytochalsin D showed comparable release kinetics (τ_{fast} , P>0.1) as well as the amount of dye uptake (F(0), P>0.3) and the size of the synaptic vesicle pool responsive to depolarization (ΔF, P>0.6) to DMSO control group (600-1700 synapses from 6-11 coverslips).

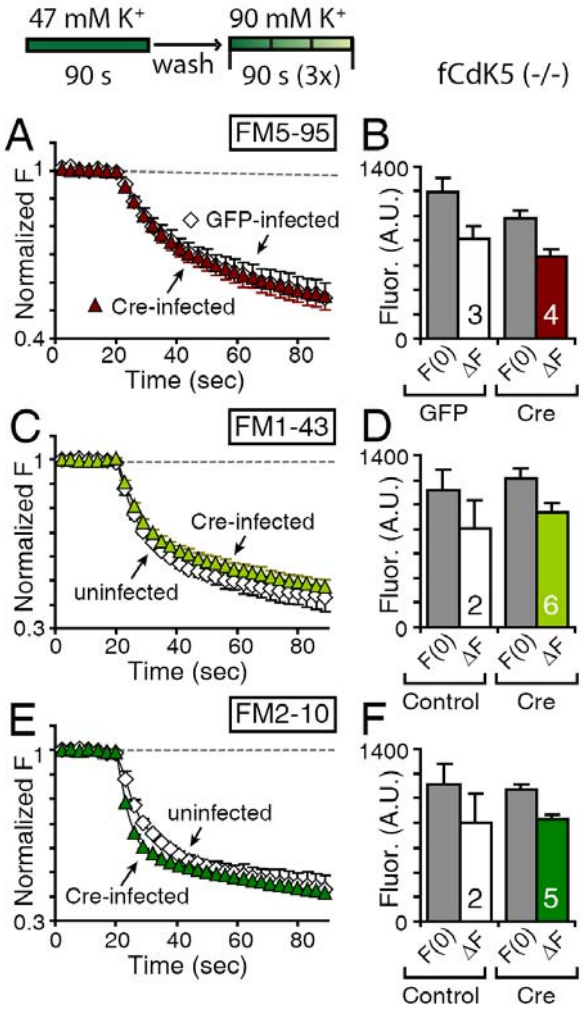

FIGURE 5. 11. CdK5 deficiency has little effect on synaptic vesicle fusion and retrieval.

Hippocampal cultures obtained from floxed CdK5 mice were infected with either GFP- or Cre recombinase conjugated with GFP lentivirus at 4 DIV and analyzed after 14 DIV. Different types of FM dyes were employed to examine synaptic vesicle trafficking at CdK5-deficient synapses and no significant changes in release kinetics, amount of dye uptake (F(0)) or the size of RRP (ΔF). (A-B: FM5-59, n=3-5, *P*>0.1, C-D: FM1-43, n=2-6, *P*>0.4, E-F: FM2-10, n=2-5, *P*>0.7)

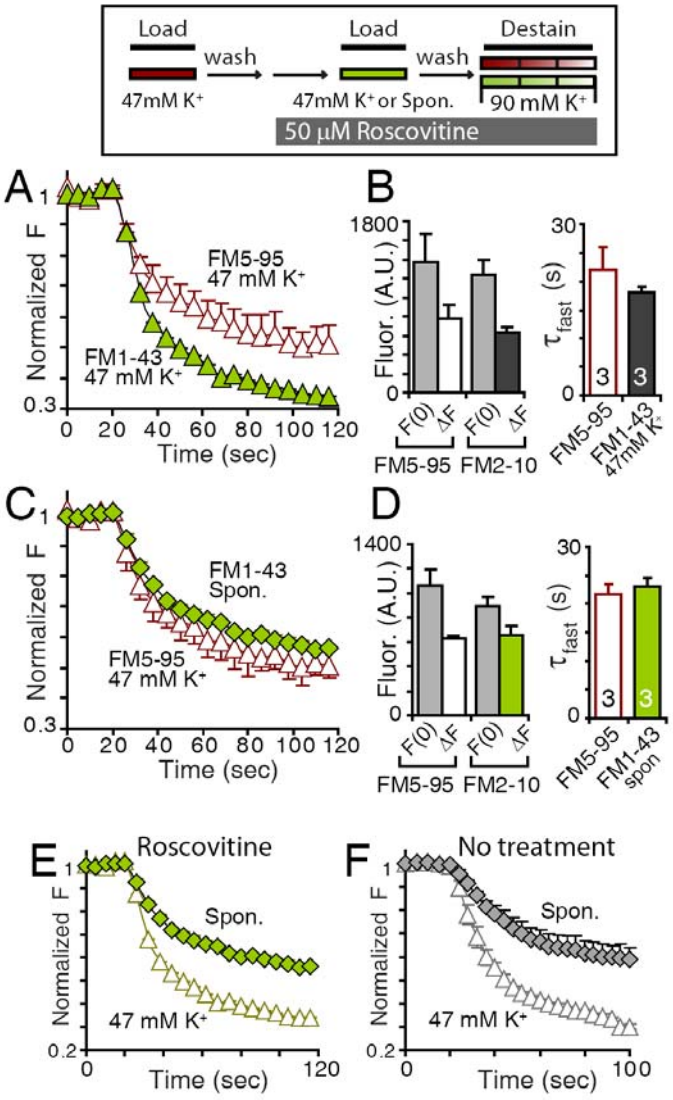

FIGURE 5. 12. CdK activity is not responsible for extra –labeling of FM1-43 at rest. After FM5-95 labeling of RRP (reference loading), cells were incubated with 50 μM roscovitine, a CdK5 inhibitor for 15 min prior to the second exposure to FM1-43. FM1-43 was used to label synaptic vesicles belonging to either RRP (in 47 mM K^+ for 90 seconds) or spontaneously recycling pool (in TTX for 10 minutes). (A, B) No difference in release kinetics (τ_{fast} , P>0.4) as well as the amount of dye uptake (F(0), measuring

exo- and endocytosis during 47 mM K^+ depolarization, $P>0.3$) or the size of RRP (ΔF, $P>0.7$) were observed between FM1-43 loading in the presence of roscovitine and reference loading, FM5-95 (270 synapses from 3 coverslips). (C) FMl-43 labeling at rest in the presence of roscovitine showed comparable release kinetics (τ_{fast} , $P>0.5$), amount of dye uptake (F(0), $P>0.7$) and the size of the synaptic vesicle pool responsive to depolarization (ΔF, $P>0.4$) to reference loading, FM5-95 (220 synapses from 3 coverslips). (E-F) FM1-43 release curves are represented here for comparison's sake. Note that there is no difference in terms of τ_{fast}, F(0) and ΔF of FM1-43 in both labeling conditions in the presence of roscovitine (shown in current FIGURE panel A and C), compared to tandem loading of FM1-43 (shown in FIGURE 5.5 B and C).

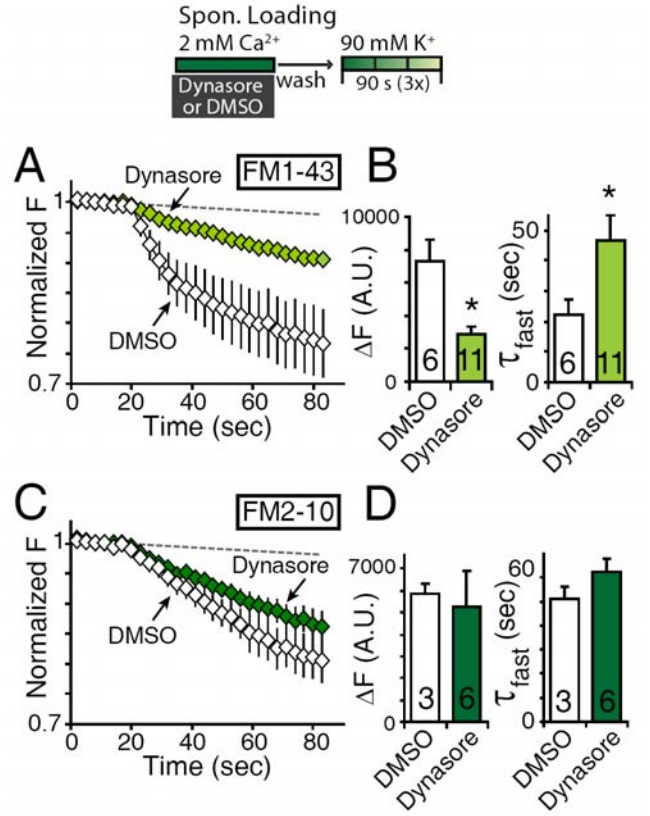

FIGURE 5. 13. Inhibition of dynamin allows for selective detection of spontaneous transmission at central synapses.

(A, B) The presence of 80 μM dynasore caused a significant decrease in the extent of spontaneous FM1-43 uptake at rest (P<0.001) and in the τ_{fast} of destaining kinetics (P<0.05, 490 synapses from 6 experiments for DMSO, 1000 synapses from 11 experiments for dynasore). (C, D) However, in the case of FM2-10, dynasore application failed to alter the extent of spontaneous dye uptake or subsequent dye mobilization, suggesting that FM2-10 solely reports spontaneously recycling synaptic vesicles in the absence of dynamin inhibition (P>0.2, 280 synapses from 3 experiments for DMSO, 550 synapses from 6 experiments for dynasore).

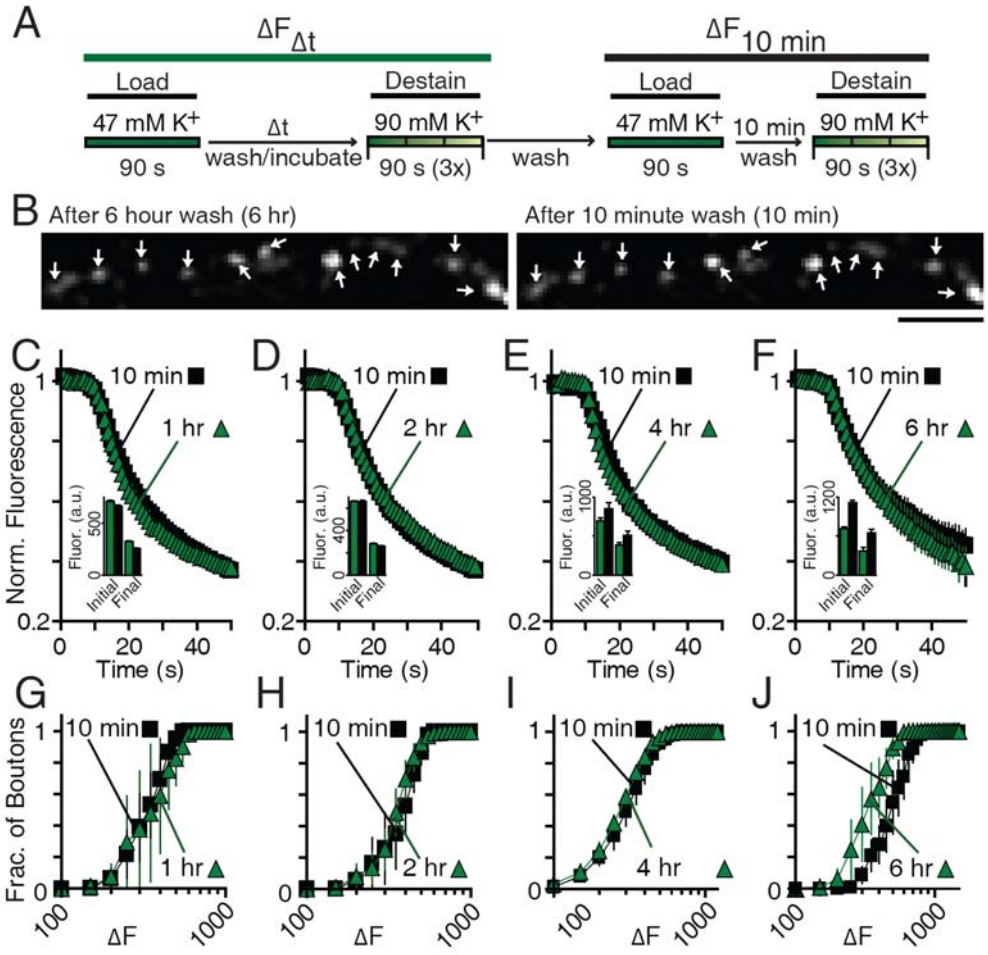

FIGURE 5. 14. The identity of synaptic vesicles which recycle in an activity-dependent manner can be maintained up to 6 hours.
(A) Experimental procedure (B) Sample fluorescent images of boutons at 6 hours after FM dye uptake (left) and the same synapses re-exposed to FM1-43 prior to a 10 minute wash (right). (C-F) Average normalized fluorescence values during destaining and the average initial and final fluorescence values (inset) after the 1-6 hr wash (Δt, green triangles) and after the subsequent 10-minute wash (10 min, black circles). Note that there are no significant differences between any of the curves for each incubation time. (G-J) Average cumulative distribution of the total pool size available after the 1-6 hr wash ($\Delta F_{\Delta t}$) and the total recycling pool after the 10-minute wash (ΔF_{10min}) showing no significant difference in the total pool size after the extended washes compared to the 10-minute wash until 6 hours. (C, G) 1-hr wash, n=3 coverslips (180 boutons total), (D, H)

2-hr wash, n=4 (275), (E, I) 4-hr wash, n=3 (300) (F, J) 6-hr wash, n=3 (180) (A.U. arbitrary fluorescence units, scale bar= 2 μm) (in collaboration with Catherine Wasser).

Discussion

Different detecting potentials of FM dyes at rest

In this chapter, I took advantage of the differential dynamin-dependence of spontaneous and evoked forms of synaptic vesicle trafficking and gained new insight into earlier opposing proposals on whether the two forms of release, evoked and spontaneous release, originate from the same set of vesicles (Groemer and Klingauf, 2007; Sara et al., 2005). I could replicate the original finding that release kinetics of the styryl dye FM2-10 was extremely sensitive to its mode of uptake into nerve terminals. After stimulation triggered dye retrieval, FM2-10 labeled vesicles showed rapid destaining, however, following spontaneous dye uptake their fluorescence loss was refractory to strong depolarization. In contrast, FM1-43 release showed a robust destaining component regardless of its mode of uptake. These observations were also verified by simultaneously monitoring release of a pair of green (FM2-10) and red (FM5-95) dyes simultaneously following their spontaneous or activity-dependent uptake. It was found that the release kinetics of the two dyes depend heavily on the way they were retrieved. Subsequent experiments showed that the discrepancy between FM2-10 and FM1-43 originated from selective dynasore-sensitive uptake of FM1-43 by a slow asynchronous form of endocytosis that followed strong bouts of network activity present in these dissociated cultures. This result is consistent with earlier reports that certain forms of endocytosis triggered after sustained neuronal activity selectively traps more hydrophobic FM1-43 but not FM2-10 (Evans and Cousin, 2007; Richards et al., 2000; Richards et al., 2003). Thus the previous disagreements seem to stem from a limited analysis which is entirely reliant on one kind of FM dye.

These findings indicate that under resting conditions FM2-10 uptake solely labels canonical spontaneous synaptic vesicle trafficking, which is detached

from prior activity and insensitive to dynamin inhibition. These experiments also uncover a slow form of endocytosis that occurs at rest but is still coupled to previous activity that selectively traps FM1-43. These results help reconcile the difference between the earlier findings from our group and those of Groemer and Klingauf (2007) by indicating that the different observations originate from the reliance on distinct dye species that label only partially overlapping vesicular compartments.

Additional membrane retrieval in operation at rest

The relative size of the spontaneously recycling vesicle pool labeled by FM1-43 was significantly larger than the size reported by FM2-10 (Figure 5.2.E), therefore, I hypothesized that FM1-43 might selectively detect the activity-dependent, bulk membrane retrieval at rest. Various methodologies known to interfere with this compensatory endocytosis were employed to limit FM1-43 uptake at rest, including inhibition of PI3K activity and interruption of action polymerization, and suppression or deletion of CdK5 activity by genetic and pharmacologic methods. However, a minimal effect of these maneuvers in FM dye uptake at resting condition was observed with our preparation (Figure 5.9-5.12), in contrast to previous observations (Tomizawa et al., 2003) and to the hypothesis. One explanation for these results could be due to the synaptic specificity in operating mechanisms between bipolar and hippocampal synapses (Holt et al., 2003).

Given that a body of literature supports the important role of CdK5 in vesicle endocytosis, it is puzzling why inhibition of CdK5 activity resulted in no effects on FM dye uptake both during depolarization as well as at rest. In fact, CdK5 has been implicated to regulate endocytosis but the output of regulation seems to remain obscure as opposing observations of CdK5 inhibition on FM dye uptake/release kinetics have been documented (Tan et al., 2003; Tomizawa et al.,

2003). One group observed enhanced endocytosis, in other words increased RRP size (increase in ΔF of FM1-43 during depolarization) upon inhibition of CdK5 (Tomizawa et al., 2003), whereas another study showed that blockade of CdK5 activity suppressed subsequent endocytosis (reduced ΔF of FM1-43 at second round of use but not at first round of endocytosis (Tan et al., 2003). Therefore, it should be considered that where the phosphorylation sites are as well as where the equilibrium of dephosphins is at the given time (Nguyen and Bibb, 2003; Samuels and Tsai, 2003). Depending on the equilibrium of CfK5 activity and presumably due to different phosphorylation sites at given synapses could exert the suppressed or enhanced endocytosis.

I showed, however, that dynamin is responsible for the retrieval of extra membrane structures at rest, which are sensitive to FM1-43. Recent studies showed that the interaction of dynamin 1and syndapin 1 triggers vesicle endocytosis, and this interaction is CdK5-dependent and selectively required for bulk endocytosis but not for clathrin –mediated endocytosis (Anggono et al., 2006; Clayton et al., 2009). This study provides a possible link between dynamin activity and CdK5 –dependent bulk endocytosis.

FM2-10, known to fail to detect bulk endocytosis at widely used concentrations is reported to successfully label this endocytic compartment when higher concentrations are used, suggesting that the affinity of the bulk endocytic compartment could be different for FM1-43 and FM2-10 (Clayton and Cousin, 2008). This could explain why a temperature dependence of FM2-10 in labeling compensatory endocytosis was observed.

In addition, I took advantage of the differential dynamin dependence between spontaneous and activity-dependent recycling synaptic vesicle pools to delineate synaptic vesicle recycling pathways that operate in parallel by

employing FM dyes. Further experiments showed that the discrepancy between the two dyes originated from selective dynasore-sensitive uptake of FM1-43 by a slow asynchronous form of endocytosis that followed strong bouts of network activity present in these dissociated cultures, while FM2-10 application at rest solely tracked canonical spontaneous synaptic vesicle trafficking which is detached from prior activity and insensitive to dynamin inhibition.

A separate recycling pathway to selectively maintain spontaneous transmission

What is the benefit of having a separate recycling pathway to maintain spontaneous transmission? The insight for answers to this question can stem from the fact hat there are no transgenic or knock-out approaches reporting a sole lack of spontaneous transmission over evoked transmission. A number of genetic interventions eliminate or largely suppress Ca^{2+}-dependent, action potential – triggered release while sparing its impact on spontaneous release, as if spontaneous transmission is less sensitive to or better protected from genetic disturbance to serve their purposes. Recent studies seeking for a bona fide function of spontaneous transmission might help to answer the question of why synapses make an effort to selectively maintain this mode of transmission.

In summary, I propose that spontaneous recycling operates independently of evoked recycling machinery without a strict requirement for dynamin activation and spontaneously recycling synaptic vesicles are mobilized from an isolated pool of synaptic vesicles. Synaptic vesicles recycling in an activity-dependent manner are quite stable for up to 6 hours at room temperature at rest. Recent independent studies provide further support to the idea of isolated spontaneous exo- and endocytosis operating in parallel (Fredj and Burrone, 2009; Xu et al., 2009) as well as the idea of separate Ca^{2+} sensor to trigger fusion (Xu et al., 2009) . In addition, I performed extensive analysis on properties of FM dyes.

The observations presented in this chapter will help the field to better understand the complexity of fluorescent probes and to provide useful information in optical reporter selection to study questions in synaptic transmission.

Overall, these findings are consistent with the hypothesis that in central synapses two distinct synaptic vesicle trafficking pathways operate in parallel and maintain evoked versus spontaneous forms neurotransmission thus impacting neuronal signaling in a divergent manner (Sutton and Schuman, 2009; Sutton et al., 2007).

CHAPTER SIX
GLUTAMATERGIC REGULATION OF SYNAPTIC VESICLE REUSE

Background

Most secretory system has a certain level of plasticity. Presynaptic terminals are exceptionally dynamic secretory system and short-term synaptic plasticity (milliseconds to minutes) plays an essential role for information processing in central synapses. Short-term synaptic facilitation is generally mediated by accumulated residual Ca^{2+}. The facilitation occurs when stimulation is repeated within a narrow time window (before the Ca^{2+} influx caused by prior stimulation is buffered) at synapses with relatively low release probability. Most synapses experience depression upon repeated stimulations, presumably as the size of available vesicle decreases, voltage-gated Ca^{2+} channel is inactivated, or presynaptic receptors inhibits fusion machinery via such as Gβγ subunit (Kavalali, 2007).

Synapses can cope with the reduction of available vesicles by recruiting vesicles from two sources; one is reserve pool and the other is synaptic vesicles which have undergone fusion. The replenishing mode from the latter source can occur very rapidly, thus sustains synaptic responses during strong stimulation (Pyle et al., 2000; Sara et al., 2002) and contributes to shaping the kinetics of neurotransmitter release during a range of frequencies (Ertunc et al., 2007).

Given that alterations in the dynamics of vesicle trafficking in presynaptic terminals can be the substrates to mediate short-term plasticity, another form of regulation may operate depending on the concentration of glutamate at the

synaptic cleft or depending on the level of ambient glutamate. This chapter explores the possibilities whether the amount of glutamate released upon action potentials or chronic increase of glutamate in synaptic milieu, in turn, regulates synaptic vesicle reuse and functions as a local feedback mechanism in given synapses.

Materials and Methods

Dissociated hippocampal cultures

Dissociated hippocampal cultures were prepared from postnatal Sprague-Dawley rats (P0-P2) as previously described (Kavalali et al., 1999a). Dissociated cells were plated on zero thickness 12-mm glass coverslips and stored at 37°C with 5% CO_2 in a humidified incubator until use. All experiments were carried out after 14 days *in vitro* (DIV).

Slice preparation

Transverse hippocampal slices (400 μM) were prepared from 12- to 21- day old Sprague–Dawley rats after Nembutal (20 mg kg−1; Abbott Laboratories, IL, USA) anesthesia, and incubated in oxygenated solution containing in mM: 124 NaCl, 5 KCl, 12 NaH_2PO_4, 26 $NaHCO_3$, 10 D-Glucose, 2 $CaCl_2$ and 1 $MgCl_2$ at room temperature (24-27°C). For electrophysiological experiments, after making a cut between CA1 and CA3 regions, individual slices were transferred to the recording chamber that was mounted on the stage of an upright microscope (Nikon E600FN, Tokyo, Japan). During experiments, slices were submerged and extracellular solution was continuously exchanged with a flow rate of 1-3ml/min. All experiments were performed at room temperature. All the handling and killing procedures for animals were approved by the Institutional Animal Care and Use Committee of U.T. Southwestern Medical Center.

Lentivirus production

The synaptophysin-pHluorin (sypHy) construct was a generous gift of Drs. Y. Zhu and C.F. Stevens (The Salk Institute, La Jolla, CA). The vesicular glutamate transporter 1 construct was a generous gift of Dr. R.H. Edwards (UCSF, San Francisco, CA). Lentivirus was produced in HEK 293 cells with the expression plasmid, two helper plasmids, which are delta 8.9 and vesicular stomatitis virus G

protein by using the Fugene 6 transfection system (Roche Molecular Biochemicals). Hippocampal cultures were infected with sypHy at 4 DIV by adding 300 -400 µl of viral suspension to each well, and imaging experiments were carried out during14-21 DIV.

Electrophysiology

Dissociated cultures: Pyramidal neurons were voltage-clamped to −70 mV using an Axopatch 200B amplifier and Clampex 8.0 software (Molecular Devices, Sunnyvale, CA), filtered at 2 kHz and sampled at 5 kHz at room temperature. The pipette solution contained (in mM): 115 Cs-$MeSO_3$, 10 CsCl, 5 NaCl, 10 HEPES, 0.6 EGTA, 20 tetraethylammonium chloride, 4 Mg-ATP, 0.3 Na_2GTP, 10 QX-314 (lidocaine N-ethyl bromide), pH 7.35, 300 mOsm (Sigma, St. Louis, MO). A modified Tyrode solution used as the extracellular solution contained (in mM): 150 NaCl, 4 KCl, 2 $MgCl_2$, 10 glucose, 10 HEPES, and 2 $CaCl_2$, pH 7.4, 310 mOsm. The exchange between extracellular solutions was achieved by direct perfusion of solutions onto the field of interest by gravity.

Hippocampal slices: Electrophysiological recordings were carried out in the whole-cell voltage-clamp configuration on the neurons in the pyramidal cell layer of area CA1. Patch pipettes had resistance of 3-6 MΩ when filled with pipette solution containing (in mM): 110 K-gluconate, 20 KCl, 10 NaCl, 10 HEPES , 0.6 EGTA, 4 Mg-ATP, 0.3 GTP, 10 QX-314 and buffered to pH 7.2-7.3 with CsOH (280-290 mOsm). Recordings were obtained with an Axopatch-200B patch-clamp amplifier (Molecular Devices, Union City, CA, USA). eEPSCs were evoked by stimulation (200 µs duration, 10-80µA amplitude) of Schaffer Collateral afferents using concentric bipolar tungsten electrodes through a stimulus isolation unit. Signals were low-pass filtered at 2 kHz and digitized at 10 kHz.

Fluorescence imaging

Hippocampal cultures were infected with lentivirus expressing the synaptophysin-pHluorin construct or vGluT1-pHluroin construct at 4 DIV. All imaging

experiments were carried out after 14 DIV at room temperature. A Modified Tyrode's solution containing 2 mM Ca^{2+}, 10 μM CNQX and 50 μM AP-5 was used in all experiments. Images were obtained by a cooled-intensified digital CCD camera (Roper Scientific, Trenton, NJ) during illumination at 480 ± 20 nm (505 DCLP, 535 ± 25 BP) via an optical switch (Sutter Instruments, Novato, CA). Images were acquired and analyzed using Metafluor Software (Universal Imaging, Auburn Hills, MI).

Results

The effect of vGlut 1 overexpression in fast synaptic reuse

Previous studies showed that synaptic vesicles are, in fact, not full at rest and thus, the quantal size can be increased by expressing more copies of vesicular transporters (Moechars et al., 2006). To test whether the acute and focal increase in the amount of glutamate released upon action potentials impact short-term synaptic plasticity, the properties of synaptic transmission were examined in the cultured hippocampal synapses where vesicular glutamate transporter 1 (vGlut) is overexpressed.

The overexpression of vGlut1 indeed increased the amplitude of AMPAR –dependent mEPSCs but not the frequency compared to neurons infected with GFP (Figure 6.1.A-C), indicating that synaptic vesicles are not necessarily full after refilling process. This observation suggests the quantal size could be regulated, perhaps, by synaptic activities, and therefore, may be susceptible for plastic changes. The overexpression of vGlut1 has little effect on inhibitory transmission (Figure 6.1.E-F), suggesting that increase of glutamate quntal size was not compensated in means of inhibitory synaptic transmission.

It was further investigated whether the increase of glutamate contents in each synaptic vesicles have impact on short-term synaptic plasticity. I measured paired-pulse ratio (PPR) as well as synaptic depression rate upon 10-20Hz stimulation in GFP– or vGlut1 –infected neurons. The overexpression of vGlut1 did not change the paired-pulse ratio (PPR) (Figure 6.2.A), suggesting that release probability (Pr) of overladen synaptic vesicles remain unchanged. In addition, no significant alterations in short-term depression rate upon 10 and 20 Hz stimulation (Figure 6.2.C-D). The amplitude of first eEPSC was increased in vGlut1 –infected neurons (Figure 6.2.B), indicating the glutamate contents are indeed increased and these observations are not due to the failure in overexpression.

Regulation of vesicle recycling by increase in ambient glutatmate concentration

Previous experiments examined the effect of the focal and transient glutamate concentration in the proximity of active zone. Does the change in ambient glutamate concentration have an effect on synaptic vesicle recycling? To address this question, we measured synaptic vesicle recycling by monitoring the trafficking of pHluorin-tagged synaptic vesicle proteins before and after adding 1-10 μM of glutamate in the bath. The behavior of pHluorin was analyzed in the same set of synapses and, to our surprise, the increase of ambient glutamate concentration was observed to impair synaptic vesicle endocytosis (Figure 6.3).

mGluR1, as a detector of glutamate concentration at synaptic cleft

To dissect which cellular pathway is responsible for this observation, it was hypothesized the effect of bath-applied glutamate might be mediated by Gq – coupled group 1 metabotrophic glutamate receptors (mGluR1). mGluR1 is a convincing candidate for two reasons. First, previous experiments (shown in Figure 6.3) were preformed in the presence of blockers of ionotrophic glutamate receptor, APV and CNQX. Second, bath-applied glutamate is expected to activate peri-synaptic receptors as well.

Thus, the effect of DHPG, a well-known mGluR1 agonist was tested on vesicle endocytosis (Figure 6.4.A). 100 μM DHPG indeed slowered the decay of pHluorin signal, suggesting that the activation of mGluR1 has an effect akin to low concentration of glutamate.

To further examine whether the effect of glutamate and DHPG shares the same cellular mechanisms impacting vesicle endocytosis, cells were pre-treated with mGluR1 –specific antagonist, LY367385 prior to glutamate bath-application.

The inhibition of mGluR1 activation blocks the effect of 1 μM glutamate on vesicle trafficking (Figure 6.4.B), suggesting that the activation of mGluR1 mediates the effect of ambient glutamate on synaptic vesicle reuse.

In parallel with this observation, Mert Ertunc, a former member of the lab, performed patch recordings from acute hippocampal slices and he found that 100 μM DHPG accelerates the rate of short-term synaptic depression in an activity – dependent manner, implying that Gq –coupled mGluR1 impacts synaptic vesicle reuse.

The effect of eCB1R on synaptic vesicle reuse

The activation of postsynaptic mGluR1 can generate endocannabinoids (eCBs). Endocannabinoid receptor 1 (CB_1R) is another Gq-coupled receptors enriched in presynaptic terminal (Chevaleyre et al., 2006). Thus, it was tested whether the presynaptic CB receptors participate in mGluR1-mediated regulation and contribute to the delayed synaptic vesicle reuse. PHluorin-tagged synaptophysin was monitored in the absence and presence of CB_1R and CB_2R agonist, WIN55,212 and CP55,940. As shown in Figure 6.5, the activation of CB_1R decreased the size of fluorescence increase, as implicated in their primary role in synaptic transmission (Figure 6.5). Moreover, the decay phase of pHluorin signal was not affected by the activation of CB_1 and CB_2 receptors, ruling out the possibility that presynaptic CB_1R mediates glutamate –dependent inhibition of fast synaptic reuse.

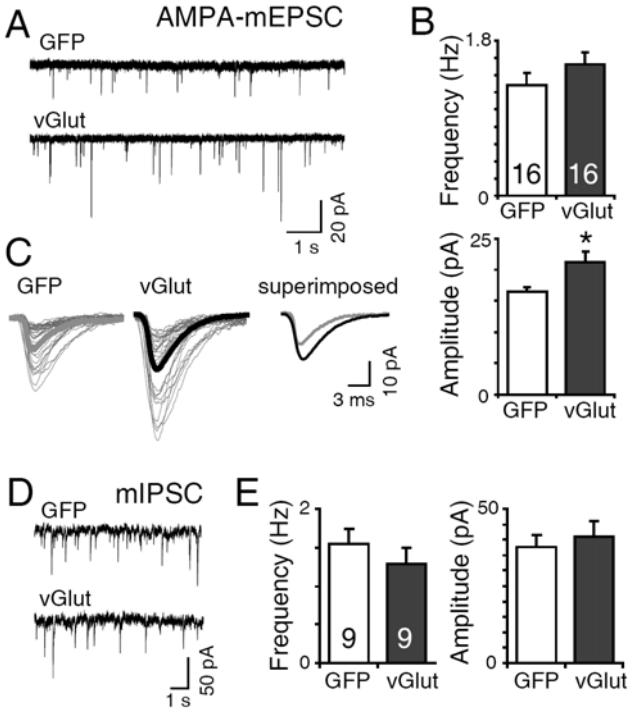

FIGURE 6. 1. The overexpression of vGlut1 increased excitatory quantal size. (A-C: AMPA-mEPSC) (A) Sample recordings of AMPA-mEPSCs in GFP- or vGlut1-infected neurons. (B) The overexpression of vGlut1 selectively increased the amplitude of AMPAR-mediated mEPSCs ($P<0.05$) but not the frequency ($P>0.2$, n=16 each). (C) Individual unitary events show the increase of amplitude in AMPA-mEPSCs. (D-E: mIPSC) (D) Sample recordings of mIPSCs in GFP- or vGlut1- infected neurons.(E) The overexpression of vGlut1 did not alter inhibitory transmission ($P>0.3$, n=9 each).

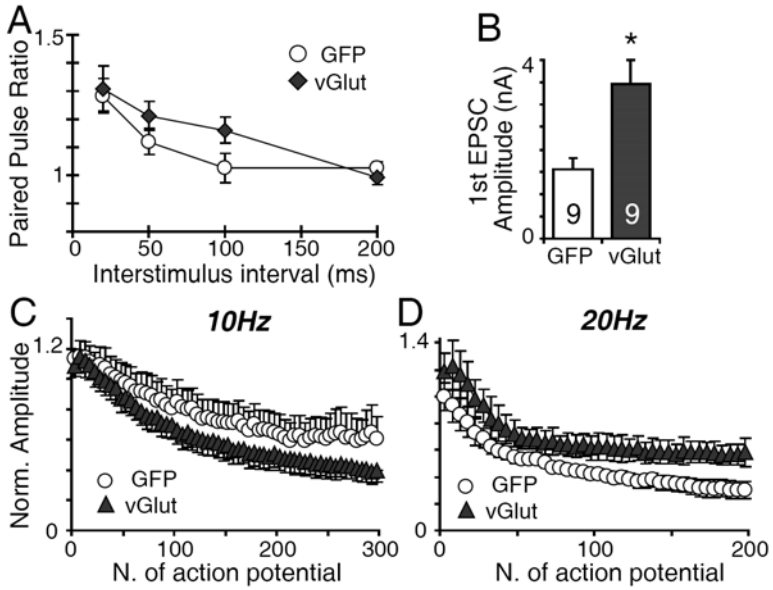

FIGURE 6. 2. The overexpression of vGlut1 has little impact on short-term synaptic plasticity.

(A) The paired pulse ratio in overladen synaptic vesicles by overexpression of vGlut1 was not altered compared to the control (n=11-14, $P>0.05$) (B) The overexpression of vGlut1 significantly augment the synaptic responses, measured as the amplitude of first evoked EPSC ($P<0.01$). (C-D) The rate of short-term synaptic depression during 10 and 20 Hz stimulation was not altered by the increase in glutamate quantal size (n=3-7, $P>0.05$).

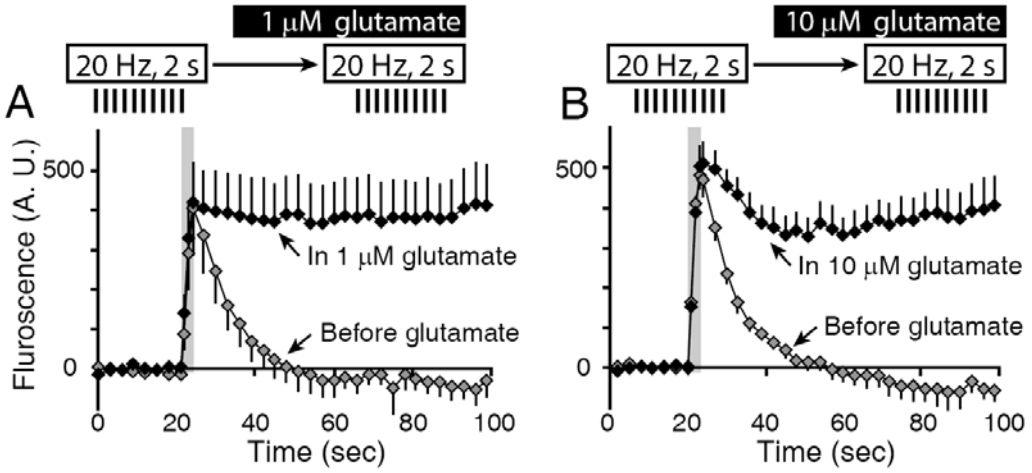

FIGURE 6. 3. Acute application of 1 or 10 μM glutamate impairs synaptic vesicle endocytosis.
Dissociated hippocampal cultures infected with lenti-viral sypHy were briefly stimulated (20Hz for 2 seconds) and 1 or 10 μM glutamate was bath-applied for 3 minutes prior to second stimulation. The fluorescence change was compared in the same set of synaptic boutons before and after addition of glutamate. In this setting, fluorescence increase was not followed by prompt decay after the termination of electrical stimulation. All the experiments were done in the presence of AMPA/NMDA receptor blockers.
(n=400 -450 synapses from 4 coverslips)

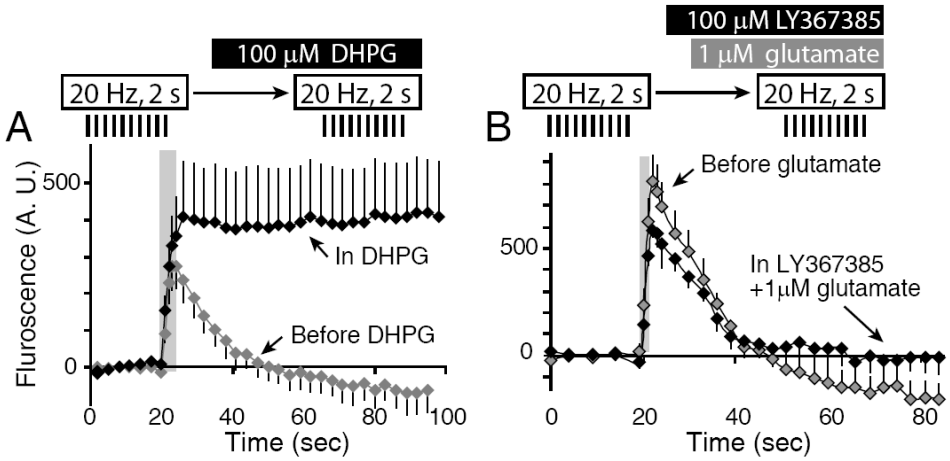

FIGURE 6. 4. mGluR1 mediates the effect of ambient glutamate concentration increase on synaptic vesicle endocytosis.
(A) Dissociated hippocampal cultures infected with sypHy, was briefly stimulated and applied 100 μM DHPG for 3-5 min prior to second stimulation. DHPG revealed further increase during 20Hz stimulation as well as delayed decrease of fluorescence after the stimulation akin to glutamate (n=365 synapses from 4 coverslips). (B) The blockade of mGluR1 activation by 100 μM LY367385, a mGluR1 antagonist abolished the effect of 1 μM glutamate.

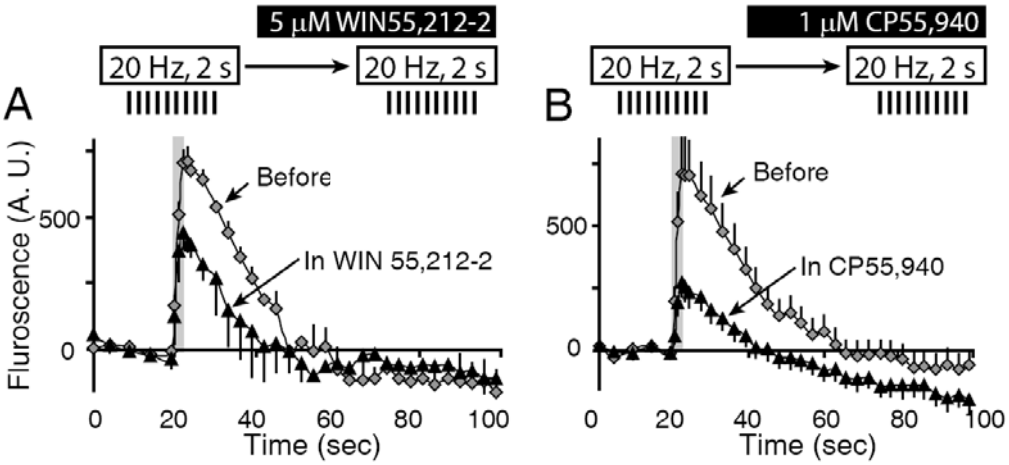

FIGURE 6. 5. The activation of eCB1R is not responsible for the effect of ambient glutamate on synaptic vesicle endocytosis.
(A, B) Both eCB1R agonist, WIN55,212-2 and CP55,940 depressed synaptic responses but had little effect on the decay of fluorescence.

Discussion

This chapter aimed to elucidate the physiological glutamatergic signaling cascades that impact synaptic depression by chronic and acute glutamatergic regulation of vesicle trafficking. It was hypothesized that glutamate release exerts feedback regulation on the kinetics of synaptic vesicle recycling and synaptic depression via activation of Gq –coupled signaling. Chronic activation of mGluRs by ambient glutamate levels may lead to tonic desensitization of downstream signaling cascades and turn the acute negative feedback regulation of synaptic depression and vesicle recycling into a chronic positive feedback regulation and thereby augment synaptic output.

As an effort to elucidate the underlying mechanisms, the acute effects of pharmacological manipulations of signaling elements in this pathway such as PKC and PLCβ were tested on exo-endocytosis coupling and short-term synaptic depression. Mert Ertunc performed electrophysiological recordings in acute hippocampal slice preparation and he found that the presynaptic PKC signaling is responsible for the glutamate –mediated inhibition of fast synaptic reuse. As detailed introduction, dynamin 1 is a substrate of PKC. By activating or inhibiting presynaptic PKC pathway, the balance of phosphorylated and dephosphrylated forms of dynamin might be interrupted. And this interruption may determine which synaptic vesicle reuse mechanism will be dominated at a given synapse. The presynaptic PKC signaling cascade may expedite or impair the recruitment of synaptic vesicles previously undergone exocytosis to RRP and thereby impacts the rate of synaptic vesicle replenishment and short-term synaptic plasticity. Although the molecular mechanisms underlying this rapid local re-use of synaptic vesicles are unknown, the link between PKC –dependent phosphorylation of

dynamin 1 and synaptic vesicle endocytosis is anticipated to provide insight for molecular machinery responsible for rapid synaptic vesicle reuse.

CHAPATER SEVEN
CONCLUSIONS AND FUTURE DIRECTIONS

The composition and trafficking of synaptic vesicles in presynaptic terminals seems much more complex than what has been envisioned. The experiments and observations described in the previous chapters contribute to understanding the complexity of synaptic transmission and yet raise intriguing new questions to be answered.

Kiss and run mode of synaptic vesicle trafficking

Among the three modes of synaptic vesicle trafficking, the 'kiss-and-run' mode is the most controversial. This hypothesis has been extensively challenged probably due to its conceptual convenience as well as its nature (transient pore opening and closure), which is difficult to detect. There is little direct evidence or examples to support the presence of the 'kiss-and-run' type of fusion in central synapses where this particular type of neurotransmitter release would be particularly appreciated (But see; (He et al., 2006; Zhang et al., 2009).

One of the most exciting findings from my work is the re-discovery of La^{3+} as a powerful secretagogue. I thoroughly evaluated La^{3+} -driven synaptic vesicle trafficking by measuring the changes in synaptic activity upon La^{3+} application by whole cell patch clamp recordings and optical imaging techniques using pHluorin and FM dyes in dissociated hippocampal cultures. Based on the discrepancy depending on detection methods, I propose La^{3+} as a novel secretagogue which preferentially triggers the 'kiss-and-run' type of vesicle fusion and retrieval.

I designed resourceful analysis by monitoring of FM dye-labeled vesicles and pHluorin-tagged vesicles and compared the kinetic changes of both fluorescent probes upon concurrent stimulation. PHluorin has better resolution to detect small fusion pore openings and closures compared to FM dyes, and thus pHluorin exhibits a similar fluorescence increase comparable to neurotransmitter release detected by electrophysiology during La^{3+} application. This analysis was used to analyze synaptic responses elicited by stimuli trains (chapter three). I found that at the onset of stimulation, synaptic transmission is dominated by the 'kiss-and-run' –like fusion events and that this type of fusion became more frequent during stronger stimulation. These features agree with the characteristics of another study of the 'kiss-and-run' mode of fusion (Zhang et al., 2009). Thus, experiments using La^{3+} -triggered transmission contribute to the literature supporting the presence of this particular type of neurotransmitter release in central synapses.

The advantage of La^{3+} -triggered synaptic vesicle fusion, unlike other non-canonical secretagogues, is its strict requirement of synaptobrevin 2 to mediate exocytosis, and thus provides a mean to study fusion events in more physiological circumstances. The action of La^{3+} was not altered in the absence of synaptotagmin 1 (chapter two), in line with the observation that La^{3+}'s action was not affected by Ca^{2+}. This feature makes La^{3+} even more attractive. One of the unanswered questions in the synaptic transmission field is whether Ca^{2+} facilitates or is absolutely required for endocytosis, and if so, can the Ca^{2+} influx for induction of vesicle fusion trigger endocytic processes or is the Ca^{2+} entry through other sources responsible for endocytosis. This question has not been directly addressed largely due to the lack of Ca^{2+} -independent secretagogues. Endocytosis is mainly a secondary event following exocytosis, so Ca^{2+} influx is inevitable in the setting to study endocytosis. In addition, as exo- and endocytosis are so tightly coupled,

the Ca^{2+} influx in a given synaptic terminal can not be removed fast enough before endocytosis occurs. However, La^{3+}'s action is not mediated or accelerated by Ca^{2+}, hence La^{3+} can be an essential tool to answer the question of the role of Ca^{2+} in endocytosis.

Dynamin –independent spontaneous vesicle recycling

The prevailing model of synaptic vesicle fusion assumes that synaptic vesicles have same propensity for action potential –driven fusion and spontaneous fusion. Our group originally proposed that synaptic terminals contain "different" synaptic vesicles, some of which are assigned for spontaneous release and some are specialized for evoked release. This idea sounds too luxurious for synapses to afford, if spontaneous transmission serves no purpose. Why do synapses want to maintain two functionally different pools? As detailed in chapter one, the list of spontaneous transmission's assignments in synaptic function and regulation is currently only growing and thereby provides further support for this idea. In addition, a number of genetic interventions affects spontaneous and evoked neurotransmission to different degrees and sometimes in opposite directions, including synaptic proteins (such as synaptotagmin 1 *vs*. synaptobrevin) (Geppert et al., 1994; Schoch et al., 2001) as well as non-synaptic proteins (such as HDAC1, 2 and MeCP2) (Akhtar et al., 2009; Nelson et al., 2008). The model of two functionally separate vesicles might help reconcile these observations.

Our first observation was challenged by another group who elegantly performed double labeling experiments of synaptic vesicles upon their usage and simultaneously monitored the behavior of each set of synaptic vesicles (Groemer and Klingauf, 2007). This disagreement with our original observation leads us, constructively, to detect another endocytic pathway actively running at rest (chapter five). I performed a series of experiments to elucidate why the two

groups observed the seemingly opposing behaviors of spontaneously recycling vesicles. I found that the type of styryl dye used to detect spontaneous fusion at rest is critical because FM1-43, and not FM2-10, was sensitive to the history of activity at given synapses. This additional activity –dependent endocytosis process was dissected to determine which molecular players participate in this process. With the aid of pharmacological tools, I showed that endocytosis operating at rest requires dynamin activity as proposed in activity –dependent bulk endocytosis. Since our original proposal, a couple of independent studies reached the same conclusions as ours (Fredj and Burrone, 2009; Mathew et al., 2008), lending further support to the idea of two vesicle pools selectively dedicated to evoked or spontaneous transmission at central synapses.

Spontaneous transmission independently of evoked transmission

My work described in chapter four provides convincing evidence of the very first molecular signature distinguishing spontaneous transmission from evoked transmission. The inhibition of dynamin activity only suppresses evoked transmission but largely spares spontaneous release. In fact, spontaneous transmission did not seem to require GTPase activity of dynamin for up to an hour. Moreover, spontaneous transmission in dynamin 1 –deficient synapses appeared to be normal, offering further support to the idea of dynamin –independent spontaneous recycling. This is quite surprising given that a body of literature has suggested that dynamin is essential for a broad range of endocytosis.

If dynamin is not involved in the endocytosis of spontaneously recycling vesicles, how do they undergo the scission reaction and become free? Since the spontaneous recycling pathway is lacking dynamin as a player, some protein-protein interactions which can be achieved through dynamin could be overlooked in this situation. Accordingly, it is possible that spontaneous transmission might employ non-classical, as yet unknown endocytic machinery.

Alternatively another isoform of dynamin may mediate the step of vesicle scission, such as dynamin 3. Dynamin 3 is expressed in the brain and the impaired endocytosis during high frequency stimulation observed in dynamin 1 –deficient mice was restored by overexpression of dynamin 3 but not by dynamin 2. The dynamin inhibitor used in the study, dynasore, interestingly suppress the GTPase activity of dynamin 1 and 2 but not 3. Consequently it is possible that the residual activity of dynamin 3 may contribute to spontaneous recycling. However, this scenario infers that the endocytic machinery between evoked and spontaneous release can be exchangeable as dynamin 3 successfully replaced the role of dynamin 1. More careful examination on the differential role among dynamin isoforms is necessary.

What are the determinants for synaptic vesicle fusion propensity? Are synaptic vesicles homogeneously heterogeneous? Where are spontaneously recycling vesicles in the scheme of synaptic vesicle pools? These are intriguing questions with no conclusive answers yet but I can postulate potential answers to these questions based on the current observations and findings.

Synaptic vesicles appear homogenous in size but their protein or lipid composition might slightly vary between synaptic vesicles. Previously, we observed that lipid composition such as cholesterol present in vesicles, can affect the fusion potency (Wasser et al., 2007) and particularly the evoked release. In addition, deletion of certain synaptic vesicle proteins can have more profound effects on spontaneous transmission and in some of cases, or even opposite effects on spontaneous *vs*. evoked transmission. Therefore, besides dynamin, synaptic vesicles themselves may contain molecular markers which can regulate their fusion process *per se*. After all, spontaneous transmission might be under precise control unlike its name (Maximov et al., 2007).

I have accumulated enough evidence to demonstrate that spontaneously recycling synaptic vesicles do not arise from the RRP. Then, where do they come from? The reserve pool or the resting pool can likely be a source of spontaneously fusing vesicles. As shown in chapter four, not all the recycling vesicles are responsive to action –potential firing as they respond to hypertonic challenge but do not evoke any release upon stimuli train. Therefore, a part of the reserve pool might be resistant to evoked release but still fusion –competent. These reluctant vesicles could contribute to spontaneous release. This speculation could explain why the size of evoked responses decreased upon increases of spontaneous release after prolonged inhibition of dynamin activity. The caveat of this scenario is, though, if two pools of synaptic vesicles share the main reservoir, how do they maintain their fusion propensity throughout the cycles of fusion and retrieval. Or, is the collectively named reserve pool perhaps, heterogeneous in terms of fusion propensity?

An essential question for the future concerns will be the purpose of differential regulation of spontaneous release at central synapses. What are the benefits of having separate vesicles for spontaneous release? Why do synapses generate “different” (for somehow) vesicles for two forms of release? Are there any specific signals conveyed with spontaneously releasing vesicles to post synaptic neurons? Can a postsynaptic neuron distinguish which signals are from spontaneously fusing vesicles or from vesicles fused upon action potentials?

Our group is dedicated to addressing these obviously important and extremely intriguing possibilities and has found that spontaneous and evoked release activates a distinct set of NMDA receptors. This fascinating possibility was supported by computational modeling which assumes NMDA receptors with different open probability are distributed along the PSD in a coordinated way. Therefore, spontaneous fusion may achieve to selectively activate NMDA

receptors with a high open probability by releasing either at the periphery of a given active zone or ectopically. Examining this type of sub-compartmentalization of two forms of release requires currently unavailable technology. Given the pace of advances in high-resolution optical microscopy (Willig et al., 2006) combined with novel fluorescent probes such as quantum dots (Zhang et al., 2007), we will soon be able to delve further into the complexities of synaptic transmission at the nanometer scale. With the help of these new tools, we will gain further insight into the nanomechanics of synaptic vesicle trafficking and undoubtedly face new challenges in our understanding of the workings of synapses.

A more clear understanding of the presynaptic machinery and its postsynaptic counterparts that underlie spontaneous and evoked neurotransmission will provide us with molecular and pharmacological tools that can selectively manipulate the two forms of neurotransmission. Independent analysis of spontaneous and evoked neurotransmission may uncover more surprises in the intricacies of communication within individual synapses.

BIBLIOGRAPHY

Abe, H., Tateyama, M., and Kubo, Y. (2003). Functional identification of Gd3+ binding site of metabotropic glutamate receptor 1alpha. FEBS letters *545*, 233-238.

Achiriloaie, M., Barylko, B., and Albanesi, J.P. (1999). Essential role of the dynamin pleckstrin homology domain in receptor-mediated endocytosis. Mol Cell Biol *19*, 1410-1415.

Akhtar, M.W., Raingo, J., Nelson, E.D., Montgomery, R.L., Olson, E.N., Kavalali, E.T., and Monteggia, L.M. (2009). Histone deacetylases 1 and 2 form a developmental switch that controls excitatory synapse maturation and function. J Neurosci *29*, 8288-8297.

Alnaes, E., and Rahamimoff, R. (1974). Dual action of praseodymium (Pr3+) on transmitter release at the frog neuromuscular synapse. Nature *247*, 478-479.

Andjus, P.R., Stevic-Marinkovic, Z., and Cherubini, E. (1997). Immunoglobulins from motoneurone disease patients enhance glutamate release from rat hippocampal neurones in culture. The Journal of physiology *504 (Pt 1)*, 103-112.

Anggono, V., and Robinson, P.J. (2007). Syndapin I and endophilin I bind overlapping proline-rich regions of dynamin I: role in synaptic vesicle endocytosis. Journal of neurochemistry *102*, 931-943.

Anggono, V., Smillie, K.J., Graham, M.E., Valova, V.A., Cousin, M.A., and Robinson, P.J. (2006). Syndapin I is the phosphorylation-regulated dynamin I partner in synaptic vesicle endocytosis. Nature neuroscience *9*, 752-760.

Aravanis, A.M., Pyle, J.L., and Tsien, R.W. (2003). Single synaptic vesicles fusing transiently and successively without loss of identity. Nature *423*, 643-647.

Atasoy, D., Ertunc, M., Moulder, K.L., Blackwell, J., Chung, C., Su, J., and Kavalali, E.T. (2008). Spontaneous and evoked glutamate release activates two populations of NMDA receptors with limited overlap. J Neurosci *28*, 10151-10166.

Auger, C., and Marty, A. (1997). Heterogeneity of functional synaptic parameters among single release sites. Neuron *19*, 139-150.

Barylko, B., Binns, D., Lin, K.M., Atkinson, M.A., Jameson, D.M., Yin, H.L., and Albanesi, J.P. (1998). Synergistic activation of dynamin GTPase by Grb2 and phosphoinositides. J Biol Chem *273*, 3791-3797.

Barylko, B., Binns, D.D., and Albanesi, J.P. (2001). Activation of dynamin GTPase activity by phosphoinositides and SH3 domain-containing proteins. Methods Enzymol *329*, 486-496.

Becher, A., Drenckhahn, A., Pahner, I., Margittai, M., Jahn, R., and Ahnert-Hilger, G. (1999). The synaptophysin-synaptobrevin complex: a hallmark of synaptic vesicle maturation. J Neurosci *19*, 1922-1931.

Bevan, S., and Wendon, L.M. (1984). A study of the action of tetanus toxin at rat soleus neuromuscular junctions. The Journal of physiology *348*, 1-17.

Borisovska, M., Zhao, Y., Tsytsyura, Y., Glyvuk, N., Takamori, S., Matti, U., Rettig, J., Sudhof, T., and Bruns, D. (2005). v-SNAREs control exocytosis of vesicles from priming to fusion. The EMBO journal *24*, 2114-2126.

Bowen, J.M. (1972). Effects of rare earths and yttrium on striated muscle and the neuromuscular junction. Can J Physiol Pharmacol *50*, 603-611.

Breitwieser, G.E., Miedlich, S.U., and Zhang, M. (2004). Calcium sensing receptors as integrators of multiple metabolic signals. Cell Calcium *35*, 209-216.

Cao, H., Garcia, F., and McNiven, M.A. (1998). Differential distribution of dynamin isoforms in mammalian cells. Molecular biology of the cell *9*, 2595-2609.

Carter, A.G., and Regehr, W.G. (2002). Quantal events shape cerebellar interneuron firing. Nature neuroscience *5*, 1309-1318.

Casella, J.F., Flanagan, M.D., and Lin, S. (1981). Cytochalasin D inhibits actin polymerization and induces depolymerization of actin filaments formed during platelet shape change. Nature *293*, 302-305.

Ceccarelli, B., Hurlbut, W.P., and Mauro, A. (1972). Depletion of vesicles from frog neuromuscular junctions by prolonged tetanic stimulation. The Journal of cell biology *54*, 30-38.

Ceccarelli, B., Hurlbut, W.P., and Mauro, A. (1973). Turnover of transmitter and synaptic vesicles at the frog neuromuscular junction. The Journal of cell biology *57*, 499-524.

Cheng, Y., Liu, M., Li, R., Wang, C., Bai, C., and Wang, K. (1999). Gadolinium induces domain and pore formation of human erythrocyte membrane: an atomic force microscopic study. Biochimica et biophysica acta *1421*, 249-260.

Chevaleyre, V., Takahashi, K.A., and Castillo, P.E. (2006). Endocannabinoid-mediated synaptic plasticity in the CNS. Annual review of neuroscience *29*, 37-76.

Choi, S., Klingauf, J., and Tsien, R.W. (2000). Postfusional regulation of cleft glutamate concentration during LTP at 'silent synapses'. Nature neuroscience *3*, 330-336.

Chung, C., Deak, F., and Kavalali, E.T. (2008). Molecular substrates mediating lanthanide-evoked neurotransmitter release in central synapses. J Neurophysiol *100*, 2089-2100.

Chung, Y.H., Sun Ahn, H., Kim, D., Hoon Shin, D., Su Kim, S., Yong Kim, K., Bok Lee, W., and Ik Cha, C. (2006). Immunohistochemical study on the distribution of TRPC channels in the rat hippocampus. Brain research *1085*, 132-137.

Clayton, E.L., Anggono, V., Smillie, K.J., Chau, N., Robinson, P.J., and Cousin, M.A. (2009). The phospho-dependent dynamin-syndapin interaction triggers activity-dependent bulk endocytosis of synaptic vesicles. J Neurosci *29*, 7706-7717.

Clayton, E.L., and Cousin, M.A. (2008). Differential labelling of bulk endocytosis in nerve terminals by FM dyes. Neurochemistry international *53*, 51-55.

Clayton, E.L., Evans, G.J., and Cousin, M.A. (2007). Activity-dependent control of bulk endocytosis by protein dephosphorylation in central nerve terminals. J Physiol *585*, 687-691.

Clayton, E.L., Evans, G.J., and Cousin, M.A. (2008). Bulk synaptic vesicle endocytosis is rapidly triggered during strong stimulation. J Neurosci *28*, 6627-6632.

Cousin, M.A. (2009). Activity-dependent bulk synaptic vesicle endocytosis--a fast, high capacity membrane retrieval mechanism. Molecular neurobiology *39*, 185-189.

Cousin, M.A., and Robinson, P.J. (2001). The dephosphins: dephosphorylation by calcineurin triggers synaptic vesicle endocytosis. Trends in neurosciences *24*, 659-665.

Cremona, O., and De Camilli, P. (1997). Synaptic vesicle endocytosis. Current opinion in neurobiology *7*, 323-330.

Cremona, O., and De Camilli, P. (2001). Phosphoinositides in membrane traffic at the synapse. Journal of cell science *114*, 1041-1052.

Cremona, O., Di Paolo, G., Wenk, M.R., Luthi, A., Kim, W.T., Takei, K., Daniell, L., Nemoto, Y., Shears, S.B., Flavell, R.A., *et al.* (1999). Essential role of phosphoinositide metabolism in synaptic vesicle recycling. Cell *99*, 179-188.

Crowder, R.J., and Freeman, R.S. (1999). The survival of sympathetic neurons promoted by potassium depolarization, but not by cyclic AMP, requires phosphatidylinositol 3-kinase and Akt. Journal of neurochemistry *73*, 466-475.

Curtis, M.J., Quastel, D.M., and Saint, D.A. (1986). Lanthanum as a surrogate for calcium in transmitter release at mouse motor nerve terminals. The Journal of physiology *373*, 243-260.

de Heuvel, E., Bell, A.W., Ramjaun, A.R., Wong, K., Sossin, W.S., and McPherson, P.S. (1997). Identification of the major synaptojanin-binding proteins in brain. J Biol Chem *272*, 8710-8716.

de Lange, R.P., de Roos, A.D., and Borst, J.G. (2003). Two modes of vesicle recycling in the rat calyx of Held. J Neurosci *23*, 10164-10173.

Deak, F., Liu, X., Khvotchev, M., Li, G., Kavalali, E.T., Sugita, S., and Sudhof, T.C. (2009). Alpha-latrotoxin stimulates a novel Pathway of Ca2+-dependent synaptic exocytosis independent of the classical synaptic fusion machinery. J Neurosci *29*, 8639-8648.

Deak, F., Schoch, S., Liu, X., Sudhof, T.C., and Kavalali, E.T. (2004). Synaptobrevin is essential for fast synaptic-vesicle endocytosis. Nat Cell Biol *6*, 1102-1108.

Deak, F., Shin, O.H., Kavalali, E.T., and Sudhof, T.C. (2006a). Structural determinants of synaptobrevin 2 function in synaptic vesicle fusion. J Neurosci *26*, 6668-6676.

Deak, F., Shin, O.H., Tang, J., Hanson, P., Ubach, J., Jahn, R., Rizo, J., Kavalali, E.T., and Sudhof, T.C. (2006b). Rabphilin regulates SNARE-dependent re-priming of synaptic vesicles for fusion. The EMBO journal *25*, 2856-2866.

Deitcher, D.L., Ueda, A., Stewart, B.A., Burgess, R.W., Kidokoro, Y., and Schwarz, T.L. (1998). Distinct requirements for evoked and spontaneous release of neurotransmitter are revealed by mutations in the Drosophila gene neuronal-synaptobrevin. J Neurosci *18*, 2028-2039.

Dekhuijzen, A.J., Iezzi, N., and Hurlbut, W.P. (1989). A re-examination of the effects of lanthanum on the frog neuromuscular junction. Pflugers Arch *414*, 683-689.

Delgado, R., Maureira, C., Oliva, C., Kidokoro, Y., and Labarca, P. (2000). Size of vesicle pools, rates of mobilization, and recycling at neuromuscular synapses of a Drosophila mutant, shibire. Neuron *28*, 941-953.

Dhariwala, F.A., and Rajadhyaksha, M.S. (2008). An unusual member of the Cdk family: Cdk5. Cellular and molecular neurobiology *28*, 351-369.

Dittgen, T., Nimmerjahn, A., Komai, S., Licznerski, P., Waters, J., Margrie, T.W., Helmchen, F., Denk, W., Brecht, M., and Osten, P. (2004). Lentivirus-based genetic manipulations of cortical neurons and their optical and electrophysiological monitoring in vivo. Proc Natl Acad Sci U S A *101*, 18206-18211.

Drose, S., and Altendorf, K. (1997). Bafilomycins and concanamycins as inhibitors of V-ATPases and P-ATPases. The Journal of experimental biology *200*, 1-8.

Edelmann, L., Hanson, P.I., Chapman, E.R., and Jahn, R. (1995). Synaptobrevin binding to synaptophysin: a potential mechanism for controlling the exocytotic fusion machine. The EMBO journal *14*, 224-231.

Ertunc, M., Sara, Y., Chung, C., Atasoy, D., Virmani, T., and Kavalali, E.T. (2007). Fast synaptic vesicle reuse slows the rate of synaptic depression in the CA1 region of hippocampus. J Neurosci *27*, 341-354.

Evans, G.J., and Cousin, M.A. (2007). Activity-dependent control of slow synaptic vesicle endocytosis by cyclin-dependent kinase 5. J Neurosci *27*, 401-411.

Farsad, K., Ringstad, N., Takei, K., Floyd, S.R., Rose, K., and De Camilli, P. (2001). Generation of high curvature membranes mediated by direct endophilin bilayer interactions. The Journal of cell biology *155*, 193-200.

Fatt, P., and Katz, B. (1952). Spontaneous subthreshold activity at motor nerve endings. The Journal of physiology *117*, 109-128.

Feng, L., Xiao, H., He, X., Li, Z., Li, F., Liu, N., Chai, Z., Zhao, Y., and Zhang, Z. (2006a). Long-term effects of lanthanum intake on the neurobehavioral development of the rat. Neurotoxicol Teratol *28*, 119-124.

Feng, L., Xiao, H., He, X., Li, Z., Li, F., Liu, N., Zhao, Y., Huang, Y., Zhang, Z., and Chai, Z. (2006b). Neurotoxicological consequence of long-term exposure to lanthanum. Toxicology letters *165*, 112-120.

Ferguson, S.M., Brasnjo, G., Hayashi, M., Wolfel, M., Collesi, C., Giovedi, S., Raimondi, A., Gong, L.W., Ariel, P., Paradise, S., *et al.* (2007). A selective activity-dependent requirement for dynamin 1 in synaptic vesicle endocytosis. Science *316*, 570-574.

Fernandez-Alfonso, T., and Ryan, T.A. (2004). The kinetics of synaptic vesicle pool depletion at CNS synaptic terminals. Neuron *41*, 943-953.

Fesce, R., Grohovaz, F., Valtorta, F., and Meldolesi, J. (1994). Neurotransmitter release: fusion or 'kiss-and-run'? Trends in cell biology *4*, 1-4.

Fesce, R., Segal, J.R., Ceccarelli, B., and Hurlbut, W.P. (1986). Effects of black widow spider venom and Ca2+ on quantal secretion at the frog neuromuscular junction. The Journal of general physiology *88*, 59-81.

Finn, W.F. (2006). Lanthanum carbonate versus standard therapy for the treatment of hyperphosphatemia: safety and efficacy in chronic maintenance hemodialysis patients. Clin Nephrol *65*, 191-202.

Fredj, N.B., and Burrone, J. (2009). A resting pool of vesicles is responsible for spontaneous vesicle fusion at the synapse. Nature neuroscience.

Gad, H., Ringstad, N., Low, P., Kjaerulff, O., Gustafsson, J., Wenk, M., Di Paolo, G., Nemoto, Y., Crun, J., Ellisman, M.H., *et al.* (2000). Fission and uncoating of synaptic clathrin-coated vesicles are perturbed by disruption of interactions with the SH3 domain of endophilin. Neuron *27*, 301-312.

Gaffield, M.A., and Betz, W.J. (2006). Imaging synaptic vesicle exocytosis and endocytosis with FM dyes. Nature protocols *1*, 2916-2921.

Gandhi, S.P., and Stevens, C.F. (2003). Three modes of synaptic vesicular recycling revealed by single-vesicle imaging. Nature *423*, 607-613.

Gennaro, J.F., Jr., Nastuk, W.L., and Rutherford, D.T. (1978). Reversible depletion of synaptic vesicles induced by application of high external potassium to the frog neuromuscular junction. J Physiol *280*, 237-247.

Geppert, M., Goda, Y., Hammer, R.E., Li, C., Rosahl, T.W., Stevens, C.F., and Sudhof, T.C. (1994). Synaptotagmin I: a major Ca2+ sensor for transmitter release at a central synapse. Cell *79*, 717-727.

Gerachshenko, T., Blackmer, T., Yoon, E.J., Bartleson, C., Hamm, H.E., and Alford, S. (2005). Gbetagamma acts at the C terminus of SNAP-25 to mediate presynaptic inhibition. Nature neuroscience *8*, 597-605.

Goda, Y., and Sudhof, T.C. (1997). Calcium regulation of neurotransmitter release: reliably unreliable? Current opinion in cell biology *9*, 513-518.

Grabs, D., Slepnev, V.I., Songyang, Z., David, C., Lynch, M., Cantley, L.C., and De Camilli, P. (1997). The SH3 domain of amphiphysin binds the proline-rich domain of dynamin at a single site that defines a new SH3 binding consensus sequence. J Biol Chem *272*, 13419-13425.

Granseth, B., Odermatt, B., Royle, S.J., and Lagnado, L. (2007). Clathrin-mediated endocytosis: the physiological mechanism of vesicle retrieval at hippocampal synapses. J Physiol *585*, 681-686.

Grinvald, A., Frostig, R.D., Lieke, E., and Hildesheim, R. (1988). Optical imaging of neuronal activity. Physiological reviews *68*, 1285-1366.

Groemer, T.W., and Klingauf, J. (2007). Synaptic vesicles recycling spontaneously and during activity belong to the same vesicle pool. Nature neuroscience *10*, 145-147.

Gundelfinger, E.D., Kessels, M.M., and Qualmann, B. (2003). Temporal and spatial coordination of exocytosis and endocytosis. Nat Rev Mol Cell Biol *4*, 127-139.

Hablitz, J.J., Mathew, S.S., and Pozzo-Miller, L. (2009). GABA vesicles at synapses: are there 2 distinct pools? Neuroscientist *15*, 218-224.

Harata, N., Pyle, J.L., Aravanis, A.M., Mozhayeva, M., Kavalali, E.T., and Tsien, R.W. (2001). Limited numbers of recycling vesicles in small CNS nerve terminals: implications for neural signaling and vesicular cycling. Trends in neurosciences *24*, 637-643.

Harata, N.C., Choi, S., Pyle, J.L., Aravanis, A.M., and Tsien, R.W. (2006). Frequency-dependent kinetics and prevalence of kiss-and-run and reuse at hippocampal synapses studied with novel quenching methods. Neuron *49*, 243-256.

Hawasli, A.H., Benavides, D.R., Nguyen, C., Kansy, J.W., Hayashi, K., Chambon, P., Greengard, P., Powell, C.M., Cooper, D.C., and Bibb, J.A. (2007). Cyclin-dependent kinase 5 governs learning and synaptic plasticity via control of NMDAR degradation. Nature neuroscience *10*, 880-886.

He, L., and Wu, L.G. (2007). The debate on the kiss-and-run fusion at synapses. Trends in neurosciences *30*, 447-455.

He, L., Wu, X.S., Mohan, R., and Wu, L.G. (2006). Two modes of fusion pore opening revealed by cell-attached recordings at a synapse. Nature *444*, 102-105.

Hefft, S., and Jonas, P. (2005). Asynchronous GABA release generates long-lasting inhibition at a hippocampal interneuron-principal neuron synapse. Nature neuroscience *8*, 1319-1328.

Heidelberger, R. (2001). ATP is required at an early step in compensatory endocytosis in synaptic terminals. J Neurosci *21*, 6467-6474.

Herrington, J., Park, Y.B., Babcock, D.F., and Hille, B. (1996). Dominant role of mitochondria in clearance of large Ca2+ loads from rat adrenal chromaffin cells. Neuron *16*, 219-228.

Heuser, J., and Miledi, R. (1971). Effects of lanthanum ions on function and structure of frog neuromuscular junctions. Proc R Soc Lond B Biol Sci *179*, 247-260.

Heuser, J.E. (1989). Review of electron microscopic evidence favouring vesicle exocytosis as the structural basis for quantal release during synaptic transmission. Quarterly journal of experimental physiology (Cambridge, England) *74*, 1051-1069.

Heuser, J.E., and Reese, T.S. (1973). Evidence for recycling of synaptic vesicle membrane during transmitter release at the frog neuromuscular junction. The Journal of cell biology *57*, 315-344.

Higashijima, T., Ferguson, K.M., Smigel, M.D., and Gilman, A.G. (1987). The effect of GTP and Mg2+ on the GTPase activity and the fluorescent properties of Go. The Journal of biological chemistry *262*, 757-761.

Hinshaw, J.E. (2000). Dynamin and its role in membrane fission. Annual review of cell and developmental biology *16*, 483-519.

Hirst, J., and Robinson, M.S. (1998). Clathrin and adaptors. Biochimica et biophysica acta *1404*, 173-193.

Holt, M., Cooke, A., Wu, M.M., and Lagnado, L. (2003). Bulk membrane retrieval in the synaptic terminal of retinal bipolar cells. J Neurosci *23*, 1329-1339.

Ikegami, K., and Koike, T. (2000). Membrane depolarization-mediated survival of sympathetic neurons occurs through both phosphatidylinositol 3-kinase- and CaM kinase II-dependent pathways. Brain research *866*, 218-226.

Itoh, T., Erdmann, K.S., Roux, A., Habermann, B., Werner, H., and De Camilli, P. (2005). Dynamin and the actin cytoskeleton cooperatively regulate plasma membrane invagination by BAR and F-BAR proteins. Developmental cell *9*, 791-804.

Jahn, R., Lang, T., and Sudhof, T.C. (2003). Membrane fusion. Cell *112*, 519-533.

Jarousse, N., and Kelly, R.B. (2001). Endocytotic mechanisms in synapses. Current opinion in cell biology *13*, 461-469.

Job, C., and Lagnado, L. (1998). Calcium and protein kinase C regulate the actin cytoskeleton in the synaptic terminal of retinal bipolar cells. The Journal of cell biology *143*, 1661-1672.

Jockusch, W.J., Praefcke, G.J., McMahon, H.T., and Lagnado, L. (2005). Clathrin-dependent and clathrin-independent retrieval of synaptic vesicles in retinal bipolar cells. Neuron *46*, 869-878.

Jung, S., Muhle, A., Schaefer, M., Strotmann, R., Schultz, G., and Plant, T.D. (2003). Lanthanides potentiate TRPC5 currents by an action at extracellular sites close to the pore mouth. J Biol Chem *278*, 3562-3571.

Kavalali, E.T. (2006). Synaptic vesicle reuse and its implications. Neuroscientist *12*, 57-66.

Kavalali, E.T. (2007). Multiple vesicle recycling pathways in central synapses and their impact on neurotransmission. J Physiol *585*, 669-679.

Kavalali, E.T., Klingauf, J., and Tsien, R.W. (1999a). Activity-dependent regulation of synaptic clustering in a hippocampal culture system. Proceedings of the National Academy of Sciences of the United States of America *96*, 12893-12900.

Kavalali, E.T., Klingauf, J., and Tsien, R.W. (1999b). Properties of fast endocytosis at hippocampal synapses. Philos Trans R Soc Lond B Biol Sci *354*, 337-346.

Kawasaki, F., Hazen, M., and Ordway, R.W. (2000). Fast synaptic fatigue in shibire mutants reveals a rapid requirement for dynamin in synaptic vesicle membrane trafficking. Nature neuroscience *3*, 859-860.

Kirchhausen, T., Macia, E., and Pelish, H.E. (2008). Use of dynasore, the small molecule inhibitor of dynamin, in the regulation of endocytosis. Methods Enzymol *438*, 77-93.

Klingauf, J., Kavalali, E.T., and Tsien, R.W. (1998). Kinetics and regulation of fast endocytosis at hippocampal synapses. Nature *394*, 581-585.

Koenig, J.H., and Ikeda, K. (1996). Synaptic vesicles have two distinct recycling pathways. J Cell Biol *135*, 797-808.

Koenig, J.H., and Ikeda, K. (1999). Contribution of active zone subpopulation of vesicles to evoked and spontaneous release. Journal of neurophysiology *81*, 1495-1505.

Kramer, H., and Kavalali, E.T. (2008). Dynamin-independent synaptic vesicle retrieval? Nature neuroscience *11*, 6-8.

Kuromi, H., Honda, A., and Kidokoro, Y. (2004). Ca2+ influx through distinct routes controls exocytosis and endocytosis at drosophila presynaptic terminals. Neuron *41*, 101-111.

Lansman, J.B. (1990). Blockade of current through single calcium channels by trivalent lanthanide cations. Effect of ionic radius on the rates of ion entry and exit. The Journal of general physiology *95*, 679-696.

Lansman, J.B., Hess, P., and Tsien, R.W. (1986). Blockade of current through single calcium channels by Cd2+, Mg2+, and Ca2+. Voltage and concentration dependence of calcium entry into the pore. The Journal of general physiology *88*, 321-347.

Lettvin, J.Y., Pickard, W.F., McCulloch, W.S., and Pitts, W. (1964). A Theory of Passive Ion Flux through Axon Membranes. Nature *202*, 1338-1339.

Li, Z., Burrone, J., Tyler, W.J., Hartman, K.N., Albeanu, D.F., and Murthy, V.N. (2005). Synaptic vesicle recycling studied in transgenic mice expressing synaptopHluorin. Proceedings of the National Academy of Sciences of the United States of America *102*, 6131-6136.

Lin, M.Y., Teng, H., and Wilkinson, R.S. (2005). Vesicles in snake motor terminals comprise one functional pool and utilize a single recycling strategy at all stimulus frequencies. The Journal of physiology *568*, 413-421.

Liu, F., Ma, X.H., Ule, J., Bibb, J.A., Nishi, A., DeMaggio, A.J., Yan, Z., Nairn, A.C., and Greengard, P. (2001). Regulation of cyclin-dependent kinase 5 and casein kinase 1 by metabotropic glutamate receptors. Proc Natl Acad Sci U S A *98*, 11062-11068.

Lopatina, L.P., Vasim, T.V., Fedorovich, S.V., and Konev, S.V. (2005). [Lanthanides induce neurotransmitter release from the vesicular pool in rat brain synaptosomes]. Biofizika *50*, 1120-1124.

Lou, X., Scheuss, V., and Schneggenburger, R. (2005). Allosteric modulation of the presynaptic Ca2+ sensor for vesicle fusion. Nature *435*, 497-501.

Lu, T., and Trussell, L.O. (2000). Inhibitory transmission mediated by asynchronous transmitter release. Neuron *26*, 683-694.

Macia, E., Ehrlich, M., Massol, R., Boucrot, E., Brunner, C., and Kirchhausen, T. (2006). Dynasore, a cell-permeable inhibitor of dynamin. Dev Cell *10*, 839-850.

Marks, B., Stowell, M.H., Vallis, Y., Mills, I.G., Gibson, A., Hopkins, C.R., and McMahon, H.T. (2001). GTPase activity of dynamin and resulting conformation change are essential for endocytosis. Nature *410*, 231-235.

Mathew, S.S., Pozzo-Miller, L., and Hablitz, J.J. (2008). Kainate modulates presynaptic GABA release from two vesicle pools. J Neurosci *28*, 725-731.

Matsubara, M., Kusubata, M., Ishiguro, K., Uchida, T., Titani, K., and Taniguchi, H. (1996). Site-specific phosphorylation of synapsin I by mitogen-activated protein kinase and Cdk5 and its effects on physiological functions. J Biol Chem *271*, 21108-21113.

Matthies, H.J., Palfrey, H.C., Hirning, L.D., and Miller, R.J. (1987). Down regulation of protein kinase C in neuronal cells: effects on neurotransmitter release. J Neurosci *7*, 1198-1206.

Maximov, A., Shin, O.H., Liu, X., and Sudhof, T.C. (2007). Synaptotagmin-12, a synaptic vesicle phosphoprotein that modulates spontaneous neurotransmitter release. The Journal of cell biology *176*, 113-124.

Maximov, A., and Sudhof, T.C. (2005). Autonomous function of synaptotagmin 1 in triggering synchronous release independent of asynchronous release. Neuron *48*, 547-554.

McMahon, H.T., Missler, M., Li, C., and Sudhof, T.C. (1995). Complexins: cytosolic proteins that regulate SNAP receptor function. Cell *83*, 111-119.

Mela, L. (1969a). Inhibition and activation of calcium transport in mitochondria. Effect of lanthanides and local anesthetic drugs. Biochemistry *8*, 2481-2486.

Mela, L. (1969b). Reaction of lanthanides with mitochondrial membranes. Ann N Y Acad Sci *147*, 824-828.

Mellman, I. (1996). Endocytosis and molecular sorting. Annual review of cell and developmental biology *12*, 575-625.

Metral, S., Bonneton, C., Hort-Legrand, C., and Reynes, J. (1978). Dual action of erbium on transmitter release at the frog neuromuscular synapse. Nature *271*, 773-775.

Miesenbock, G., De Angelis, D.A., and Rothman, J.E. (1998). Visualizing secretion and synaptic transmission with pH-sensitive green fluorescent proteins. Nature *394*, 192-195.

Miledi, R. (1971). Lanthanum ions abolish the "calcium response" of nerve terminals. Nature *229*, 410-411.

Moechars, D., Weston, M.C., Leo, S., Callaerts-Vegh, Z., Goris, I., Daneels, G., Buist, A., Cik, M., van der Spek, P., Kass, S., *et al.* (2006). Vesicular glutamate transporter VGLUT2 expression levels control quantal size and neuropathic pain. J Neurosci *26*, 12055-12066.

Molgo, J., del Pozo, E., Banos, J.E., and Angaut-Petit, D. (1991). Changes of quantal transmitter release caused by gadolinium ions at the frog neuromuscular junction. Br J Pharmacol *104*, 133-138.

Moulder, K.L., Jiang, X., Taylor, A.A., Shin, W., Gillis, K.D., and Mennerick, S. (2007). Vesicle pool heterogeneity at hippocampal glutamate and GABA synapses. J Neurosci *27*, 9846-9854.

Moulder, K.L., and Mennerick, S. (2005). Reluctant vesicles contribute to the total readily releasable pool in glutamatergic hippocampal neurons. J Neurosci *25*, 3842-3850.

Mozhayeva, M.G., Sara, Y., Liu, X., and Kavalali, E.T. (2002). Development of vesicle pools during maturation of hippocampal synapses. J Neurosci *22*, 654-665.

Mundigl, O., and De Camilli, P. (1994). Formation of synaptic vesicles. Current opinion in cell biology *6*, 561-567.

Murphy, T.H., Blatter, L.A., Bhat, R.V., Fiore, R.S., Wier, W.G., and Baraban, J.M. (1994). Differential regulation of calcium/calmodulin-dependent protein kinase II and p42 MAP kinase activity by synaptic transmission. J Neurosci *14*, 1320-1331.

Murthy, V.N., and Stevens, C.F. (1999). Reversal of synaptic vesicle docking at central synapses. Nature neuroscience *2*, 503-507.

Neher, E., and Sakaba, T. (2008). Multiple roles of calcium ions in the regulation of neurotransmitter release. Neuron *59*, 861-872.

Nelson, E.D., Kavalali, E.T., and Monteggia, L.M. (2008). Activity-dependent suppression of miniature neurotransmission through the regulation of DNA methylation. J Neurosci *28*, 395-406.

Neves, G., and Lagnado, L. (1999). The kinetics of exocytosis and endocytosis in the synaptic terminal of goldfish retinal bipolar cells. J Physiol *515 (Pt 1)*, 181-202.

Newton, A.J., Kirchhausen, T., and Murthy, V.N. (2006). Inhibition of dynamin completely blocks compensatory synaptic vesicle endocytosis. Proceedings of the National Academy of Sciences of the United States of America *103*, 17955-17960.

Nguyen, C., and Bibb, J.A. (2003). Cdk5 and the mystery of synaptic vesicle endocytosis. The Journal of cell biology *163*, 697-699.

Osborne, S.L., Meunier, F.A., and Schiavo, G. (2001). Phosphoinositides as key regulators of synaptic function. Neuron *32*, 9-12.

Otis, T.S., Staley, K.J., and Mody, I. (1991). Perpetual inhibitory activity in mammalian brain slices generated by spontaneous GABA release. Brain research *545*, 142-150.

Otsu, Y., and Murphy, T.H. (2004). Optical postsynaptic measurement of vesicle release rates for hippocampal synapses undergoing asynchronous release during train stimulation. J Neurosci *24*, 9076-9086.

Otsu, Y., Shahrezaei, V., Li, B., Raymond, L.A., Delaney, K.R., and Murphy, T.H. (2004). Competition between phasic and asynchronous release for recovered synaptic vesicles at developing hippocampal autaptic synapses. J Neurosci *24*, 420-433.

Otto, H., Hanson, P.I., and Jahn, R. (1997). Assembly and disassembly of a ternary complex of synaptobrevin, syntaxin, and SNAP-25 in the membrane of synaptic vesicles. Proceedings of the National Academy of Sciences of the United States of America *94*, 6197-6201.

Paglini, G., and Caceres, A. (2001). The role of the Cdk5--p35 kinase in neuronal development. European journal of biochemistry / FEBS *268*, 1528-1533.

Pare, D., Lang, E.J., and Destexhe, A. (1998). Inhibitory control of somatodendritic interactions underlying action potentials in neocortical pyramidal neurons in vivo: an intracellular and computational study. Neuroscience *84*, 377-402.

Parnas, H., and Parnas, I. (2007). The chemical synapse goes electric: Ca2+- and voltage-sensitive GPCRs control neurotransmitter release. Trends in neurosciences *30*, 54-61.

Pecot-Dechavassine, M. (1983). Morphological evidence for tracer uptake at the active zones of stimulated frog neuromuscular junction. Experientia *39*, 752-753.

Peter, B.J., Kent, H.M., Mills, I.G., Vallis, Y., Butler, P.J., Evans, P.R., and McMahon, H.T. (2004). BAR domains as sensors of membrane curvature: the amphiphysin BAR structure. Science *303*, 495-499.

Photowala, H., Blackmer, T., Schwartz, E., Hamm, H.E., and Alford, S. (2006). G protein betagamma-subunits activated by serotonin mediate presynaptic inhibition by regulating vesicle fusion properties. Proceedings of the National Academy of Sciences of the United States of America *103*, 4281-4286.

Piedras-Renteria, E.S., Pyle, J.L., Diehn, M., Glickfeld, L.L., Harata, N.C., Cao, Y., Kavalali, E.T., Brown, P.O., and Tsien, R.W. (2004). Presynaptic homeostasis at CNS nerve terminals compensates for lack of a key Ca2+ entry pathway. Proceedings of the National Academy of Sciences of the United States of America *101*, 3609-3614.

Powis, D.A., Clark, C.L., and O'Brien, K.J. (1994). Lanthanum can be transported by the sodium-calcium exchange pathway and directly triggers catecholamine release from bovine chromaffin cells. Cell Calcium *16*, 377-390.

Praefcke, G.J., and McMahon, H.T. (2004). The dynamin superfamily: universal membrane tubulation and fission molecules? Nat Rev Mol Cell Biol *5*, 133-147.

Pyle, J.L., Kavalali, E.T., Piedras-Renteria, E.S., and Tsien, R.W. (2000). Rapid reuse of readily releasable pool vesicles at hippocampal synapses. Neuron *28*, 221-231.

Qualmann, B., Kessels, M.M., and Kelly, R.B. (2000). Molecular links between endocytosis and the actin cytoskeleton. The Journal of cell biology *150*, F111-116.

Qualmann, B., Roos, J., DiGregorio, P.J., and Kelly, R.B. (1999). Syndapin I, a synaptic dynamin-binding protein that associates with the neural Wiskott-Aldrich syndrome protein. Molecular biology of the cell *10*, 501-513.

Reeves, J.P., and Condrescu, M. (2003). Lanthanum is transported by the sodium/calcium exchanger and regulates its activity. Am J Physiol Cell Physiol *285*, C763-770.

Reichling, D.B., and MacDermott, A.B. (1991). Lanthanum actions on excitatory amino acid-gated currents and voltage-gated calcium currents in rat dorsal horn neurons. The Journal of physiology *441*, 199-218.

Richards, D.A., Guatimosim, C., and Betz, W.J. (2000). Two endocytic recycling routes selectively fill two vesicle pools in frog motor nerve terminals. Neuron *27*, 551-559.

Richards, D.A., Guatimosim, C., Rizzoli, S.O., and Betz, W.J. (2003). Synaptic vesicle pools at the frog neuromuscular junction. Neuron *39*, 529-541.

Ringstad, N., Gad, H., Low, P., Di Paolo, G., Brodin, L., Shupliakov, O., and De Camilli, P. (1999). Endophilin/SH3p4 is required for the transition from early to late stages in clathrin-mediated synaptic vesicle endocytosis. Neuron *24*, 143-154.

Ringstad, N., Nemoto, Y., and De Camilli, P. (1997). The SH3p4/Sh3p8/SH3p13 protein family: binding partners for synaptojanin and dynamin via a Grb2-like Src homology 3 domain. Proc Natl Acad Sci U S A *94*, 8569-8574.

Rizzoli, S.O., and Betz, W.J. (2004). The structural organization of the readily releasable pool of synaptic vesicles. Science *303*, 2037-2039.

Rizzoli, S.O., and Betz, W.J. (2005). Synaptic vesicle pools. Nature reviews *6*, 57-69.

Rizzoli, S.O., and Jahn, R. (2007). Kiss-and-run, collapse and 'readily retrievable' vesicles. Traffic (Copenhagen, Denmark) *8*, 1137-1144.

Rosenmund, C., and Stevens, C.F. (1996). Definition of the readily releasable pool of vesicles at hippocampal synapses. Neuron *16*, 1197-1207.

Roux, A., Uyhazi, K., Frost, A., and De Camilli, P. (2006). GTP-dependent twisting of dynamin implicates constriction and tension in membrane fission. Nature *441*, 528-531.

Royle, S.J., and Lagnado, L. (2003). Endocytosis at the synaptic terminal. J Physiol *553*, 345-355.

Sabatini, B.L., and Regehr, W.G. (1996). Timing of neurotransmission at fast synapses in the mammalian brain. Nature *384*, 170-172.

Saitoe, M., Schwarz, T.L., Umbach, J.A., Gundersen, C.B., and Kidokoro, Y. (2001). Absence of junctional glutamate receptor clusters in Drosophila mutants lacking spontaneous transmitter release. Science *293*, 514-517.

Samuels, B.A., and Tsai, L.H. (2003). Cdk5 is a dynamo at the synapse. Nat Cell Biol *5*, 689-690.

Sankaranarayanan, S., and Ryan, T.A. (2001). Calcium accelerates endocytosis of vSNAREs at hippocampal synapses. Nature neuroscience *4*, 129-136.

Sara, Y., Mozhayeva, M.G., Liu, X., and Kavalali, E.T. (2002). Fast vesicle recycling supports neurotransmission during sustained stimulation at hippocampal synapses. J Neurosci *22*, 1608-1617.

Sara, Y., Virmani, T., Deak, F., Liu, X., and Kavalali, E.T. (2005). An isolated pool of vesicles recycles at rest and drives spontaneous neurotransmission. Neuron *45*, 563-573.

Schneggenburger, R., Meyer, A.C., and Neher, E. (1999). Released fraction and total size of a pool of immediately available transmitter quanta at a calyx synapse. Neuron *23*, 399-409.

Schoch, S., Deak, F., Konigstorfer, A., Mozhayeva, M., Sara, Y., Sudhof, T.C., and Kavalali, E.T. (2001). SNARE function analyzed in synaptobrevin/VAMP knockout mice. Science *294*, 1117-1122.

Schuman, E.M., and Murase, S. (2003). Cadherins and synaptic plasticity: activity-dependent cyclin-dependent kinase 5 regulation of synaptic beta-catenin-cadherin interactions. Philosophical transactions of the Royal Society of London *358*, 749-756.

Segal, J.R., Ceccarelli, B., Fesce, R., and Hurlbut, W.P. (1985). Miniature endplate potential frequency and amplitude determined by an extension of Campbell's theorem. Biophysical journal *47*, 183-202.

Sharma, G., and Vijayaraghavan, S. (2003). Modulation of presynaptic store calcium induces release of glutamate and postsynaptic firing. Neuron *38*, 929-939.

Shimizu, H., Borin, M.L., and Blaustein, M.P. (1997). Use of La3+ to distinguish activity of the plasmalemmal Ca2+ pump from Na+/Ca2+ exchange in arterial myocytes. Cell Calcium *21*, 31-41.

Shuang, R., Zhang, L., Fletcher, A., Groblewski, G.E., Pevsner, J., and Stuenkel, E.L. (1998). Regulation of Munc-18/syntaxin 1A interaction by cyclin-dependent kinase 5 in nerve endings. J Biol Chem *273*, 4957-4966.

Shupliakov, O., Low, P., Grabs, D., Gad, H., Chen, H., David, C., Takei, K., De Camilli, P., and Brodin, L. (1997). Synaptic vesicle endocytosis impaired by disruption of dynamin-SH3 domain interactions. Science *276*, 259-263.

Sillren, L.S., and Martell, A.E. (1971). Stability Constants of Metal-Ion Complexes, Supplement No. 1 (London: Chemical Society).

Slutsky, I., Wess, J., Gomeza, J., Dudel, J., Parnas, I., and Parnas, H. (2003). Use of knockout mice reveals involvement of M2-muscarinic receptors in control of the kinetics of acetylcholine release. Journal of neurophysiology *89*, 1954-1967.

Smith, S.M., Bergsman, J.B., Harata, N.C., Scheller, R.H., and Tsien, R.W. (2004). Recordings from single neocortical nerve terminals reveal a nonselective cation channel activated by decreases in extracellular calcium. Neuron *41*, 243-256.

Smith, S.M., Renden, R., and von Gersdorff, H. (2008). Synaptic vesicle endocytosis: fast and slow modes of membrane retrieval. Trends in neurosciences *31*, 559-568.

Sollner, T., Whiteheart, S.W., Brunner, M., Erdjument-Bromage, H., Geromanos, S., Tempst, P., and Rothman, J.E. (1993). SNAP receptors implicated in vesicle targeting and fusion. Nature *362*, 318-324.

Song, B.D., Yarar, D., and Schmid, S.L. (2004). An assembly-incompetent mutant establishes a requirement for dynamin self-assembly in clathrin-mediated endocytosis in vivo. Mol Biol Cell *15*, 2243-2252.

Stevens, C.F., and Wang, Y. (1995). Facilitation and depression at single central synapses. Neuron *14*, 795-802.

Stevens, C.F., and Wesseling, J.F. (1998). Activity-dependent modulation of the rate at which synaptic vesicles become available to undergo exocytosis. Neuron *21*, 415-424.

Stevens, C.F., and Williams, J.H. (2000). "Kiss and run" exocytosis at hippocampal synapses. Proc Natl Acad Sci U S A *97*, 12828-12833.

Subtil, A., Gaidarov, I., Kobylarz, K., Lampson, M.A., Keen, J.H., and McGraw, T.E. (1999). Acute cholesterol depletion inhibits clathrin-coated pit budding. Proceedings of the National Academy of Sciences of the United States of America *96*, 6775-6780.

Sudhof, T.C. (1995). The synaptic vesicle cycle: a cascade of protein-protein interactions. Nature *375*, 645-653.

Sudhof, T.C. (2000). The synaptic vesicle cycle revisited. Neuron *28*, 317-320.

Sudhof, T.C. (2004). The synaptic vesicle cycle. Annual review of neuroscience *27*, 509-547.

Sun, J., Pang, Z.P., Qin, D., Fahim, A.T., Adachi, R., and Sudhof, T.C. (2007). A dual-Ca2+-sensor model for neurotransmitter release in a central synapse. Nature *450*, 676-682.

Sutton, M.A., Ito, H.T., Cressy, P., Kempf, C., Woo, J.C., and Schuman, E.M. (2006). Miniature neurotransmission stabilizes synaptic function via tonic suppression of local dendritic protein synthesis. Cell *125*, 785-799.

Sutton, M.A., and Schuman, E.M. (2009). Partitioning the synaptic landscape: distinct microdomains for spontaneous and spike-triggered neurotransmission. Science signaling *2*, pe19.

Sutton, M.A., Taylor, A.M., Ito, H.T., Pham, A., and Schuman, E.M. (2007). Postsynaptic decoding of neural activity: eEF2 as a biochemical sensor coupling miniature synaptic transmission to local protein synthesis. Neuron *55*, 648-661.

Sutton, M.A., Wall, N.R., Aakalu, G.N., and Schuman, E.M. (2004). Regulation of dendritic protein synthesis by miniature synaptic events. Science *304*, 1979-1983.

Sutton, R.B., Fasshauer, D., Jahn, R., and Brunger, A.T. (1998). Crystal structure of a SNARE complex involved in synaptic exocytosis at 2.4 A resolution. Nature *395*, 347-353.

Takamori, S., Riedel, D., and Jahn, R. (2000). Immunoisolation of GABA-specific synaptic vesicles defines a functionally distinct subset of synaptic vesicles. J Neurosci *20*, 4904-4911.

Takei, K., and Haucke, V. (2001). Clathrin-mediated endocytosis: membrane factors pull the trigger. Trends in cell biology *11*, 385-391.

Takei, K., Yoshida, Y., and Yamada, H. (2005). Regulatory mechanisms of dynamin-dependent endocytosis. J Biochem *137*, 243-247.

Tan, T.C., Valova, V.A., Malladi, C.S., Graham, M.E., Berven, L.A., Jupp, O.J., Hansra, G., McClure, S.J., Sarcevic, B., Boadle, R.A., *et al.* (2003). Cdk5 is essential for synaptic vesicle endocytosis. Nat Cell Biol *5*, 701-710.

Tomizawa, K., Ohta, J., Matsushita, M., Moriwaki, A., Li, S.T., Takei, K., and Matsui, H. (2002). Cdk5/p35 regulates neurotransmitter release through

phosphorylation and downregulation of P/Q-type voltage-dependent calcium channel activity. J Neurosci *22*, 2590-2597.

Tomizawa, K., Sunada, S., Lu, Y.F., Oda, Y., Kinuta, M., Ohshima, T., Saito, T., Wei, F.Y., Matsushita, M., Li, S.T., *et al.* (2003). Cophosphorylation of amphiphysin I and dynamin I by Cdk5 regulates clathrin-mediated endocytosis of synaptic vesicles. The Journal of cell biology *163*, 813-824.

Ushkaryov, Y.A., Petrenko, A.G., Geppert, M., and Sudhof, T.C. (1992). Neurexins: synaptic cell surface proteins related to the alpha-latrotoxin receptor and laminin. Science *257*, 50-56.

Verstraeten, S.V., Nogueira, L.V., Schreier, S., and Oteiza, P.I. (1997). Effect of trivalent metal ions on phase separation and membrane lipid packing: role in lipid peroxidation. Arch Biochem Biophys *338*, 121-127.

Verstreken, P., Koh, T.W., Schulze, K.L., Zhai, R.G., Hiesinger, P.R., Zhou, Y., Mehta, S.Q., Cao, Y., Roos, J., and Bellen, H.J. (2003). Synaptojanin is recruited by endophilin to promote synaptic vesicle uncoating. Neuron *40*, 733-748.

Virmani, T., Atasoy, D., and Kavalali, E.T. (2006). Synaptic vesicle recycling adapts to chronic changes in activity. J Neurosci *26*, 2197-2206.

Vlahos, C.J., Matter, W.F., Hui, K.Y., and Brown, R.F. (1994). A specific inhibitor of phosphatidylinositol 3-kinase, 2-(4-morpholinyl)-8-phenyl-4H-1-benzopyran-4-one (LY294002). J Biol Chem *269*, 5241-5248.

Wadel, K., Neher, E., and Sakaba, T. (2007). The coupling between synaptic vesicles and Ca2+ channels determines fast neurotransmitter release. Neuron *53*, 563-575.

Wang, L.Y., and Kaczmarek, L.K. (1998). High-frequency firing helps replenish the readily releasable pool of synaptic vesicles. Nature *394*, 384-388.

Wasser, C.R., Ertunc, M., Liu, X., and Kavalali, E.T. (2007). Cholesterol-dependent balance between evoked and spontaneous synaptic vesicle recycling. J Physiol *579*, 413-429.

Wasser, C.R., and Kavalali, E.T. (2008). Leaky synapses: Regulation of spontaneous neurotransmission in central synapses. Neuroscience.

Weiss, G.B. (1970). On the site of action of lanthanum in frog sartorius muscle. J Pharmacol Exp Ther *174*, 517-526.

Willig, K.I., Rizzoli, S.O., Westphal, V., Jahn, R., and Hell, S.W. (2006). STED microscopy reveals that synaptotagmin remains clustered after synaptic vesicle exocytosis. Nature *440*, 935-939.

Wilson, R.I., and Nicoll, R.A. (2001). Endogenous cannabinoids mediate retrograde signalling at hippocampal synapses. Nature *410*, 588-592.

Wilson, R.I., and Nicoll, R.A. (2002). Endocannabinoid signaling in the brain. Science *296*, 678-682.

Wolfel, M., Lou, X., and Schneggenburger, R. (2007). A mechanism intrinsic to the vesicle fusion machinery determines fast and slow transmitter release at a large CNS synapse. J Neurosci *27*, 3198-3210.

Wu, L.G., and Borst, J.G. (1999). The reduced release probability of releasable vesicles during recovery from short-term synaptic depression. Neuron *23*, 821-832.

Wu, L.G., Ryan, T.A., and Lagnado, L. (2007). Modes of vesicle retrieval at ribbon synapses, calyx-type synapses, and small central synapses. J Neurosci *27*, 11793-11802.

Xu, J., McNeil, B., Wu, W., Nees, D., Bai, L., and Wu, L.G. (2008). GTP-independent rapid and slow endocytosis at a central synapse. Nature neuroscience *11*, 45-53.

Xu, J., Pang, Z.P., Shin, O.H., and Sudhof, T.C. (2009). Synaptotagmin-1 functions as a Ca(2+) sensor for spontaneous release. Nature neuroscience.

Yamashita, T., Hige, T., and Takahashi, T. (2005). Vesicle endocytosis requires dynamin-dependent GTP hydrolysis at a fast CNS synapse. Science *307*, 124-127.

Ye, W., and Lafer, E.M. (1995). Bacterially expressed F1-20/AP-3 assembles clathrin into cages with a narrow size distribution: implications for the regulation of quantal size during neurotransmission. J Neurosci Res *41*, 15-26.

Zamir, O., and Charlton, M.P. (2006). Cholesterol and synaptic transmitter release at crayfish neuromuscular junctions. The Journal of physiology *571*, 83-99.

Zhang, C., Xiong, W., Zheng, H., Wang, L., Lu, B., and Zhou, Z. (2004). Calcium- and dynamin-independent endocytosis in dorsal root ganglion neurons. Neuron *42*, 225-236.

Zhang, Q., Cao, Y.Q., and Tsien, R.W. (2007). Quantum dots provide an optical signal specific to full collapse fusion of synaptic vesicles. Proc Natl Acad Sci U S A *104*, 17843-17848.

Zhang, Q., Li, Y., and Tsien, R.W. (2009). The dynamic control of kiss-and-run and vesicular reuse probed with single nanoparticles. Science *323*, 1448-1453.

Zucker, R.S., and Regehr, W.G. (2002). Short-term synaptic plasticity. Annual review of physiology *64*, 355-405.